CA^{2+} REGULATED ANTIBIOTIC RESISTANCE

IN

PSEUDOMONAS AERUGINOSA

By

SHARMILY S KHANAM

Master of Science in
Molecular Medical Microbiology
University of Nottingham
Nottingham, UK
2009

Submitted to the Faculty of the
Graduate College of the
Oklahoma State University
in partial fulfillment of the requirements for the Degree of
DOCTOR OF PHILOSOPHY
July 2017

CA^{2+} REGULATED ANTIBIOTIC RESISTANCE

IN

PSEUDOMONAS AERUGINOSA

Dissertation Approved:

Dr. Marianna A. Patrauchan

Dissertation Adviser

Dr. Rolf A. Prade

Dr. Jeffrey A. Hadwiger

Dr. Erika I. Lutter

Dr. Guolong (Glenn) Zhang

ACKNOWLEDGEMENTS

At first I would like to acknowledge the blissful and enriching five years of graduate life at the department of Microbiology and Molecular Genetics, Oklahoma State University. This journey of mine would not have been possible without the very support of many people who has provided me immense encouragement and motivation to strengthen my confidence.

Foremost, I would like to express my deepest appreciation to my PI and PhD committee chair Dr. Marianna Patrauchan for accepting me as a graduate student and being a steady source of guidance and support. Thank you Marianna, for embracing me by treating me as an essential part of 'Patrauchan lab' family. I believe with time our relationship has grown beyond mentor- disciple relationship. Besides your boundless valuable academic advices, continuous encouragement and motivation as well as your strong belief in my strength and abilities as a student provided a unique and incomparable support for my success as a graduate researcher. I would like to take the opportunity to mention my admiration at your strength as a woman in science. Your personal and professional philosophies have influenced my research viewpoint for betterment for sure. It is my joy to express my sincerest gratitude to you for your support for the academic achievements and

scholarships I have applied or obtained at OSU. Thank you for teaching me scientific writing, critical thinking and scientific communication. Every day in past five years of my graduate life, you have taught me to become a skilled researcher, dedicated mentor and a strong woman in science. It would not be possible to attain my graduate research goal accomplished without your expert advice and invaluable moral and financial support. Above all, I am forever in debt to you for your kind support during the period of my pregnancy and post-partum recovery while wrapping up my graduate research work.

It is my pleasure to recognize all of my astute committee members, Dr. Rolf Prade, Dr. Jeffrey Hadwiger, Dr. Erika Lutter and Dr. Glenn Zhang for their helpful inputs, critical review and guidance with my research. Your valuable advices and constructive criticisms were absolute necessities for the materialization of my thesis. I would like to thank Dr. Prade and Dr. Erika lutter for their expertise and valuable suggestions involving the molecular cloning in *P. aeruginosa*. A Special thanks to you all for your collegial attitude and for providing me with an interactive atmosphere in my committee meetings and beyond. Heartfelt thanks for your valuable time to review my dissertation.

I would like to thank the department of Microbiology and Molecular genetics for giving me the opportunity to pursue my research work. I am morally indebted to the department for the financial assistance for my graduate study and endorse me for various awards during this time. I am deeply grateful to faculty members, staff members and colleagues at the department for their unconditional supports. A special thanks to the current department chair, Dr. Conway for his support and nomination for several awards I have applied or received from OSU. Your support definitely heightened my confidence as a student researcher and motivated me to excel. My special thanks to the past and present staff members of the department office, Sallie, Latecia, Karli, Terressa, Alice and Becky for taking care of all my due paper works and helping me to carry on my graduate research with full attention. A special thanks to Connie Budd and Dr. Gary Marley for allowing me to use their lab instruments many times during my graduate years.

I express sincere appreciations to my lab family. Special thanks to my former colleagues and friends and Manita and Shalaka for welcoming me to the lab and helping me with a smooth transition into the graduate life. I appreciate my current colleagues, Michelle and Biraj for their continuous support and encouragements; specially during past one year when I was working toward wrapping up my graduate research work while being pregnant. My earnest thanks to Ryan, Amber,

Nitu, Tammi, Treyon, Hannah, Afom, Rendi, Erin, Chelsea and Mandi. Thank you all for your loving and caring friendship. Over the past five years, I have been fortunate to work with many scholarly undergraduate students. I thank Laurel, Carlee, Stasha, Caty, Allison, Danci, Kelly, Marysa, Chase, Tanner, Emily and Daniel for their amazing hard work and contribution to my research. You all have helped me to grow both as a researcher and as a mentor.

I express my sincerest gratitude to all the scientists whose support was the key to the accelerated and effective outcome of my research. I would like to thank Dr. Kangmin Duan at University of Manitoba, Winnipeg, Canada and Dr. Meng Meng Dong at the college of Life Science, Northwest University, Shaanxi, China for sharing several promoter activity reporter plasmids. Thanks to Dr. Paul Williams at University of Nottingham, Nottingham, UK and Dr. Keith Poole, Queen's University, Ontario, Canada for sharing the deletion mutants for my research. I would also like to thank Chris Wood at the RT-qPCR core facility at the OSU Department of Botany for training me to how use the RT-qPCR machine and allowing me to use the machine for my research. A special thanks to Dr. Shaw and Brandon Ludetke at OSU and Kerry Williamson at Montana State University, Bozeman, Montana for sharing their experties on RNA extraction with me.

Most importantly, I would like to thank my family for always being by my side. My deepest appreciation goes to my husband, Saki Khan for his absolute support and encouragement. Saki, thank you for sharing all the ups and downs of life with me. As we always say it, “it is a team effort”. Yes, thank you for being a wonderful teammate in finishing up both of our graduate degree and raising two wonderful and smart kids together. I would like to thank my daughter for her presence in my life which has been the eternal source of my strength to face any obstacle in life. I also thank my new born son, for bringing joy in my life. I hope someday both my kids will be proud and inspired by their mother as a woman in science and carry on the passion. I thank my mother for her patience, perseverance and encouragement throughout this long journey filled with challenges. Especially, her support during last one year of my graduate studies had been vital for my overall success in obtaining my research goal. I would like to remember my late father Sohrab Hossain Khan, for I know he would have been very proud of me. Thank you abbu for teaching me the life skills that brought me here today. I would also like to thank my mother in law for being by my side during this journey.

Finally, I would like to thank everyone who has directly or indirectly contributed, supported or motivated me to accomplish my graduate research goal.

Name: SHARMILY S KHANAM
Date of Degree: MAY, 2017
Title of Study: CA^{2+} REGULATED ANTIBIOTIC RESISTANCE IN *PSEUDOMONAS AERUGINOSA*
Major Field: MICROBIOLOGY AND MOLECULAR GENETICS

Abstract: *Pseudomonas aeruginosa*, an opportunistic pathogen, causes life threatening infections in cystic fibrosis (CF) patients. Due to increased abundance of Ca^{2+} in CF lung, *P. aeruginosa* is surrounded with elevated Ca^{2+} that could be recognized by the bacterium as a cue for adaptation in this environment. Previous research by our group and others identified Ca^{2+} responsive regulators and defined their role in Ca^{2+}-dependent virulence factor production. In addition, tightly maintained intracellular Ca^{2+} ($[Ca^{2+}]_{in}$) homeostasis suggests the signaling role of Ca^{2+} in *P. aeruginosa*. Our current study report that growth at 5 mM/ 10 mM Ca^{2+} increases the antibiotic resistance of PAO1 more than 10 fold. Here, our main goal was to elucidate the regulatory role of Ca^{2+} in adaptive antimicrobial resistance and virulence of PAO1. We identified several of the RND superfamily efflux pumps involved in Ca^{2+}-regulated tobramycin resistance, plant infectivity and $[Ca^{2+}]_{in}$ homeostasis maintenance. We have established that Ca^{2+} transcriptionally regulates five of the six efflux pumps involved in Ca^{2+}-induced tobramycin resistance in a growth phase dependent manner. Ca^{2+} reliant tobramycin resistance and increase transcription of *mexAB-oprM*, one of the efflux pumps involved in Ca^{2+}-induced tobramycin resistance, requires intact Ca^{2+} homeostasis. We have also identified a putative calcium channel in PAO1, homologous to the pH-sensitive Ca^{2+} leak channel, BsYetJ in *Bacillus subtilis*. This channel is essential for PAO1 to generate transient changes in $[Ca^{2+}]_{in}$. Disruption of this gene affects the Ca^{2+} regulated global transcription of many virulence and adaptation associated genes in PAO1. The lack of intact $[Ca^{2+}]_{in}$ transients also resulted into reduction in Ca^{2+} regulated virulence of this organism. Previously our lab identified calmodulin-like EF hand protein (EfhP), Ca^{2+}-regulated two-component system (CarSR), Ca^{2+} binding protein (CarP), and Ca^{2+}-regulated OB-fold protein, which contribute to Ca^{2+}-regulated virulence in PAO1. Here, we established that Ca^{2+} regulated transcription of *calC* is dependent on CarSR, CarP and EfhP. Finally, we also identified three hypothetical proteins involved in Ca^{2+}-induced polymyxin B resistance of PAO1. Overall, the findings of this research identifies the genes involved in Ca^{2+} regulatory cascade of *P.* aeruginosa and how they contribute to Ca^{2+} regulated antibiotic resistance and virulence of this pathogen.

TABLE OF CONTENTS

LIST OF TABLES

TABLE OF FIGURES

PREFACE

OVERVIEW OF THE DISSERTATION

CHAPTER ONE. A Brief review on the current knowledge of infection epidemics, virulence, pathogenicity, extent of antimicrobial resistance and the mechanisms involved is depicted in this chapter. An emphasis is given on the different mechanisms of antibiotic resistance in *P. aeruginosa*. A broader discussion on efflux as a mechanism of resistance in bacterium including *P. aeruginosa* is done. An elaboration of each efflux pumps and their clinical relevance in multidrug resistance of *P. aeruginosa* is described. Overall, this signifies the niche of current research putting an emphasis on the urgency to identify novel therapeutic approach to manage *Pseudomonas* infection.

CHAPTER TWO. This chapter focuses on identifying the regulatory role of surrounding Ca^{2+} in antimicrobial resistance of *P. aeruginosa*. By using modern molecular tools, we were able to identify underlying mechanisms of Ca^{2+} regulated tobramycin resistance of this pathogen. We have also established the regulatory role of Ca^{2+} homeostasis in efflux mediated tobramycin resistance of *P. aeruginosa*, PAO1.

CHAPTER THREE. This is a collaborative project where me and my former colleague Dr. Manita Guragain are equal contributing author. Here we have

identified a calcium channel protein which is homologous to the pH sensitive Ca^{2+} leak channel, BsYetJ in Bacillus subtilis. Absence of this channel protein in PAO1 abolished the intracellular Ca^{2+} $[Ca^{2+}]_{in}$ signaling signature as well as Ca^{2+} regulated phenotypes like, pyocyanine production, swarming motility, *etc* in the pathogen. We have used global transcriptomic analysis as well as other molecular techniques to define the regulatory role of $[Ca^{2+}]_{in}$ in genotypic and phenotypic adaptation of *P. aeruginosa* in environment surrounded with increased Ca^{2+}.

CHAPTER FOUR. This section elucidates the investigation and identification of the mechanisms involved in Ca^{2+}- induced polymyxin-B resistance of *P. aeruginosa*, PAO1. Through genetic expression studies as well as mutational studies we have determined that none of the previously known mechanisms of polymyxin-B resistance contribute to Ca^{2+} regulated polymyxin-B resistance in *P. aeruginosa*. Through random mutagenesis we were able to identify three hypothetical proteins, loss of which makes *P. aeruginosa* susceptible to polymyxin-B even when the bacterium was grown at 5mM or 10mM Ca^{2+}. These proteins were never found to be directly or indirectly involved in polymyxin-B ressitance or any polycationic peptide resistance in any bacterium including *P. aeruginosa*.

CHAPTER FIVE. This chapter dissects our understanding of current knowledge on Ca^{2+} as a signaling ion both in prokaryotes and eukaryotes. Here we compare the characteristic features of Ca^{2+} signaling in eukaryotes and prokaryotes and how

P. aeruginosa fit in this scenario. This helped us identifying the significance of our current research in this area.

CHAPTER SIX. In this section three of my either collaborative or individual projects have been discussed under the roof of 'Additional chapters'.

I. This is an additional project in collaboration with my previous colleague, Dr. Manita Guragain. Here I have contributed as a co-author of this project. This section identified the involvement of Ca^{2+} regulated two component system CarSR regulated Ca^{2+} binding proteins CarP and OB-fold protein CarO in Ca^{2+} regulated tobramycin resistance.

II. In collaboration with my former colleague Shalaka lotliker, I have characterized the Ca^{2+} regulated transcriptional profile of three putative carbonic anhydrases in *P. aeruginosa* by RT-qPCR.

III. This chapter describes the approach to establish an animal infectivity model to assess regulatory role of Ca^{2+} on infectivity of *P. aeruginosa*. Here we have used *C. elegans* and Fruit fly (*D. melanogaster*) killing assay and tried to modify the already established animal killing model in order to appropriate our experimental goal. The infection assay protocols were approved by the Biosafety department of OSU to confirm eh safety regulation is maintained during the assay.

CHAPTER SEVEN. This chapter describes in-detail all the materials and methods those have been used for the current study. For commercial kit-based protocols, modifications, if any, were described with the reason why such modifications were performed.

CHAPTER I

LITERATURE REVIEW

Pseudomonas aeruginosa, first isolated from surgical wounds, later identified as a rod shaped Gram-negative bacteria, is a facultative multidrug resistant human pathogen. It causes severe infections in lung airways of cystic fibrosis (CF) patients, burn wounds and intensive care patients, as well as patients with indwelling medical devices, catheters and shunts (1-4). *P. aeruginosa* is also one of the leading causes of infective endocarditis in intravenous drug users, young children, and patients with prosthetic valve replacement (5, 6). The ability of this bacterium to produce an arsenal of virulence associated factors and its multidrug resistant nature makes the infections caused by this pathogen so life threatening (7, 8). Strategic use of different virulence factors is the key component of successful establishment of persistent *P. aeruginosa* infection (9). Also, these combative components combined with extraordinary multidrug resistance is what makes *P. aeruginosa* a "super bug". According to CDC (Center for Disease Control) antibiotic resistance threat report in 2013 (https://www.cdc.gov/drugresistance/threat-report-2013/index.html), *P. aeruginosa* has been considered as a serious threat. World health organization (WHO) has announced *P. aeruginosa* as the second most dangerous pathogen in their report on global priority of antibiotic resistance bacteria (http://www.who.int/medicines/publications/global-priority-list-antibiotic-resistant-bacteria/en/). Among 51,000 of total cases of healthcare associated infections (HAIs), almost 13% are accounted for *P. aeruginosa* infection estimating about 400 deaths per year. Fatality associated with *P. aeruginosa* is

mainly reported for individuals with chronic obstructive pulmonary disease (COPD), infective endocarditis, as well as cancer patients undergoing chemotherapy, and intravenous drug users (6, 10, 11). This impact of *P. aeruginosa infection* is mainly attributed to the combination of virulence associated factors and outstanding antimicrobial resistance of this organism (7, 8). *P. aeruginosa* displays highly flexible genetic features with the ability to alter the genes either by mutation or by uptake of extracellular genetic material (12). Also, multiple mechanisms of intrinsic and adaptive resistance make this pathogen so robust that it can withstand almost all the antimicrobials available for treatments (13) thus making it almost impossible to treat *Pseudomonas* infections.

Antibiotic Resistance of *P. aeruginosa*

The widespread global distribution of *Pseudomonas aeruginosa* in hospital acquired infections is extremely troublesome mainly due to its extraordinary multidrug resistant nature. Although the statistics may vary in different places, *P. aeruginosa* represents a second major cause of hospital acquired infections in intensive care unit (ICU) patients, surgery and burn wound patients, as well as patients with COPD and endocarditis, following the Gram-positive *Staphylococcus* (14). Although scarce in frequency, community acquired infections caused by this pathogen have also been reported globally. Such infections include keratitis, pneumonia, acute conjunctivitis, otitis, and infective endocarditis (15). These

infections, however, once diagnosed, can be treated using multiple groups of antibiotics, in contrast to hospital-acquired infections.

Mechanisms of Antimicrobial resistance

Extreme adaptability of this organisms allows the emergence of pan drug resistant (PDR), extreme drug resistant (XDR) and multidrug resistant strains, particularly during the course of antimicrobial therapy, which leads to re-occurrence and persistence of this infection (16). This development of antibiotic resistance can be attained by the organism through acquisition of genetic materials (plasmids, integrons etc.), mutational alteration of drug targets, enzymatic modification of drugs or by active efflux of a broad range of antibiotics (13, 17). These mechanisms belong to either intrinsic or adaptive mechanisms of antimicrobial resistance of this bacterium.

Intrinsic Mechanisms of Antimicrobial Resistance

P. aeruginosa is intrinsically resistant to many antimicrobials due to its ability to produce antimicrobial modifying enzymes, alteration of membrane permeability as well as active efflux of multiple groups of antibiotics. One of the most remarkable features of *P. aeruginosa* physiology is its membrane barrier. *P. aeruginosa* is impermeable to a large number of toxic chemicals including antimicrobials due to its ability to alter the permeability of outer membrane to these

compounds (18). Porins are channels which allow permeation of different molecules through membrane in a size-dependent manner. This selective mechanism of permeation of hydrophilic molecules excludes many large toxic compounds, thus making *P. aeruginosa* more impermeable and less vulnerable (19). Several examples of outer membrane porins include OprM, OprF, and OprD that are highly abundant and tightly regulated (18, 20). OprD is a major channel for carbapenem uptake and therefore, the inactivation of OprD porin has been identified as a major contributor to carbapenem resistance of this bacterium (21) . Besides the porins, the LPS layer of outer membrane and alteration in lipid A molecules can alter the permeability of membrane to many charged molecules including EDTA, divalent cations like Mg^{2+}, polycationic antimicrobials such as aminoglycosides and polycationic peptides (22-25). *P. aeruginosa* can also protect itself against many membrane permeabilizing molecules by producing proteins such as OprH (H1) to stabilize the electrochemical change of the membrane. These mechanisms are essential for this bacterium to survive in the environment rich in cationic molecules, including the presence of cationic antibiotics such as aminoglycosides, polycationic polypeptides or host immunopeptides (24).

Usually, the wild type *P. aeruginosa* (PAO1) is susceptible to a range of β-lactums, like carboxipenicillins, ureidopenicillins, third and fourth generation cephalosporins as well as carbapenems. On the contrary, the clinically abundant multidrug resistant strains of *P. aeruginosa* display outstanding ability to produce

a variety of β-lactamases and survive against these antibiotics (17). Specifically, cephalosporinase (AmpC β-lactamases), which is encoded by chromosome of many *Enterobacteriacae* including *P. aeruginosa*, is highly inducible (100-1000 times in clinical strains) in *P. aeruginosa*. This enzyme in *P. aeruginosa* is not inactivated by co administration of β-lactamase inhibitors in clinical settings (13, 17). In addition to these chromosomally encoded inducible β-lactamases, the clinical strains of *P. aeruginosa* also have acquired several β-lactamases that are part of either transposable genetic elements or integrons. These include extended spectrum β-lactamase (ESBL) class A and D, carbanicillin hydrolyzing β-lactamases, SHV1 and TEM β-lactamases, all of which confer resistance to a very wide variety of β-lactam antibiotics(12, 13). However, the production of antimicrobial modifying enzymes is not exclusive for β-lactams only. Aminoglycosides modifying enzymes (AMEs) are known to be the major mechanism for the resistance to aminoglycoside antibiotics (gentamycin, amikacin, tobramycin, neomycin, etc.). These antibiotics are one of the most popular choices for *Pseudomonas* infection management and treatment at the hospitals, particularly in CF patients (26, 27). In addition to AMEs, rRNA methylases also contribute to the reistance. These enzymes inactivate aminoglycoside antibiotics by acetylation of the amino groups (aminoglycoside acetyletransferase, AAC), adenylation (aminoglycoside nucleotidyltransferase, ANTs), phosphorylation (aminoglycoside phosphoryle transferase, APHs), or by transferring methyl group to 16SrRNA (methyl transferase, *rmtA-D* genes) (28). *P.*

aeruginosa harbors several variants of these enzymes with an ability to modify amino groups at different positions of different aminoglycoside antibiotics (reviewed in(12)). Such intrinsic ability to readily produce antimicrobial inactivating enzymes provides a fitness benefit and allows this bacterium to persist in clinical settings. Another choice of treatment for *P. aeruginosa* infection is fluoroquinolones, which target DNA gyrase and topoisomerases in bacterium. These enzymes are required to maintain DNA unfolding and supercoiling thus are essential for replication, transcription and translation of the bacterium (12). Mutational changes in these drug targets , DNA gyrase genes (*gyrA* and *gyrB*) as well as topoisomerases (pare and parC) in *P. aeruginosa* has been documented in clinical isolates displaying high ressitance to fluoroquinolone antibiotics (13, 17).

In addition to the production of energetically costly antimicrobial modifying enzymes, *P. aeruginosa* can use a variety of efflux transporters to pump out a wide variety of antibiotics. Five different super families of multidrug efflux pumps have been identified in bacteria. They include ABC (ATP-binding cassette), SMR (small multidrug resistance), MFS (major facilitator superfamily), MATE (multiple antibiotic and toxin extrusion), and RND (Resistance-Nodulation-Division) (29, 30). Among these five groups, the RND family of efflux pumps in *P. aeruginosa* has been recognized as a major contributor to both intrinsic and adaptive resistance of this bacterium to a wide range of antimicrobials. To date *P. aeruginosa* has been shown to possess 12 RND efflux pumps with variable

substrate specificity, MexAB-OprM, MexCD-OprJ, MexEF-OprN, MexPQ-OprM, MexXY-OprM, MexVW-OprM, MexMN-OprJ, MexJK-OprM, TriABC-OpmB, MuxABC-OpmB, MexGHI-OpmD, and CzcCBA-OpmY (13, 31, 32). These pumps are tripartite systems composed of inner membrane RND component, which is driven by H^+ ion gradient and is connected to the outer membrane porin channel through a periplasmic component known as membrane fusion protein (MFS). Together these three components span the membranes and effectively extrude a variety of toxic substrates including antimicrobials from the cytoplasm to outside of the bacteria, enabling their survival in hostile environments including those with high levels of antibiotics (30). In the presence of antimicrobials, the abundance and activity of these pumps is enhanced to serve in extruding drugs (33-37). Among 12 RND pumps identified in *P. aeruginosa*, one can define two large groups: with broad and narrow substrate specificities. MexAB-OprM, MexCD-OprJ, MexXY-OprM, MexVW-OprM and MuxABC-OpmB are known to extrude several antibiotics form chemically diverse groups including β-lactams, fluoroquinolones, cephalosporines, carbapenems, aminoglycosides as well as macrolids (12, 13, 28). On the other hand, MexEF-OprN, MexPQ-oprM, MexJK-OprM, MexMN-oprJ, MexGHI-OpmD as well as TriABC-opmB (13, 32, 38, 39) are known to transport fluoroquinolones, macrolids, chloramphenicol, triclosan and some biocides such as EDTA. A standing alone RND pump is CzcCBA-OpmY, which is the only *P.*

aeruginosa RND efflux pump known to efflux metal ions and protecting the bacterium from toxicity caused by high levels of such ions (40, 41).

RND efflux pumps are integrated into the bacterial physiology and play role in a variety of cellular functions quorum sensing, virulence as well as infectivity of the pathogen (38, 42, 43). For example, TriABC-OpmB enables survival of *P. aeruginosa* in the presence of triclosan and EDTA (32), and is also important for plant infectivity in presence of Ca^{2+} (43). MexCD-OprJ (44) contributes to both antibiotic resistance and virulence of this pathogen. Overexpression of the multidrug efflux pump MexAB-OprM is known to be associated with reduced *lasI* expression.(42) MexEF-OpnN is known to transport the HHQ (4-hydroxy 2-heptyle quinolone) which is an intermediate precursor molecule of PQS(45), thus contributes in PQS associated quorum sensing pathway. Mutant lacking MexGHI-OpmD failed to produce the quorum sensing molecules N-(3-oxododecanoyl)-L-homoserine lactone (3-oxo-C12-HSL) and PQS. This in turn reduced the ability of this mutant to cause infection in both mice and plant model(38) . This pump also transports phenazine molecule that controls the biofilm development by the organism(46) This definitely reflects the importance of this group of efflux pumps for resistance of *P. aeruginosa* as well as it survival in a host environment. The fact that *P. aeruginosa* possess a large number of them further improves the fitness of the bacterium to a variety of environmental settings.

Adaptive Mechanisms of Antimicrobial resistance.

P. aeruginosa is an ubiquitous organism with an outstanding ability to sense and respond to environmental stimuli by modulating its physiology and developing multiple adaptation strategies, ultimately enhancing its survival (47). A manifestation of genomic and physiological plasticity of the organism is its ability to survive host immune response and antimicrobial therapies, persist and establish chronic infection (14, 48). The mechanisms of this plasticity are in the basis of adaptive resistance that has been illustrated in *P. aeruginosa* both *in vivo* and *in vitro* (49-51). One mechanism of adaptive resistance in *P. aeruginosa* involves occurrence of point mutations in genes encoding the targets of antimicrobials, such as *gyrA* and *parC.* DNA gyrase encoded by *gyrA* is the target of fluoroquinolone antibiotics and in clinical strains of *P. aeruginosa*, mutations in the 86 and 87 codon of *gyrA* have been identified and shown to dramatically increase the resistance of the pathogen (52). Another example is mutations occurring in *mexZ, mexR, nfxB, nfxC*, negative regulators of efflux pumps (52). These mutations lead to overexpression of the corresponding efflux pumps, and were observed in a large number of multidrug-resistant clinical isolates. Other examples include mutations leading to overexpression in *ampC* (β-lactamase), efflux pumps *mexAB-oprM, mexXY-oprM*, or downregulation of OprD, observed in clinical *P. aeruginosa* strains isolated from CF and burn patients undergoing aminoglycoside, β-lactamase or carbapenem antimicrobial treatments (21). Daily exposures to antimicrobials in

clinical settings lead to accumulation of such mutations, which enable the bacteria to thrive even when treated with a high dosage of antimicrobials (35, 53-56). All this proves the genetic plasticity of *P. aeruginosa* and the ability of this organism to readily attain multidrug resistance resulting in failure of the drug therapy. Another outstanding adaptation that makes *P. aeruginosa* superior against antimicrobial treatment is its ability to form biofilms. The biofilm acets as a shield and cause reduced drug penetration therefore allows the bacterium to alter genetic behavior. This indeed is an outstanding fitness that supports bacterial survival as well as persistence in a hostile host niche. Therefore biofilm mediated resistance has made this bacterium so robust that it is almost untreatable with available antimicrobials (1, 37, 57). Biofilm mediated antimicrobial resistance is a huge problem, particularly in cases of indwelling catheters, implanted medical devices as well as in burn wounds, the conditions enhancing biofilm formation (58).

Besides the intrinsic and adaptive ressitance mechanisms, P. aeruginosa displayes another way of antimicrobial resistance: acquired ressitance. This bacterium can also acquire antibiotic resistant genes by horizontal gene transfer from the neighboring bacteria using mobile genetic elements, and achieve further increased resistance to antimicrobials. One such example is the transfer of the bla_{imp} integrin from *Serretia mercessance,* which renders resistance to carbapenem group of antibiotics (59) Together, the intrinsic and adaptive features enable *P. aeruginosa* to become multidrug, pan drug or extreme drug resistant.

Finally, resistance to antibiotics can be enhanced in response to host factors serving as a que representing a hostile environment (60). Such cues signal *Pseudomonas* about the environment and may trigger physiological rearrangements. One such crucial decision is a switch from free-swimming to sessile mode of growth. The establishment of biofilms can be initiated or enhanced upon exposure to several host factors as well as antimicrobials; thus protect eh bacterium against the environmental odds (23, 58, 61-63). Calcium (Ca^{2+}) is one of such environmental cue. It is not only abundant in nature, but also serves as an essential secondary messenger regulating many physiological processes in eukaryotic systems. Imbalance in Ca^{2+} homeostasis has been associated with functional disorders in immune responses (64, 65). Furthermore, in CF lungs there is an increased level of Ca^{2+} in the secreted fluids (66-68). So, for *P. aeruginosa* being able to sense the imbalance in Ca^{2+} may be advantageous and help their survival as well as persistence in a host (69-71).

Earlier, Patrauchan's group determined that exposure to increased levels of Ca^{2+} changes the expression profiles of many genes including those encoding for mechanisms of stress response, virulence, transport as well as antimicrobial resistance in *P. aeruginosa* (71-74). Furthermore, it was shown that *P. aeruginosa* is able to maintain a basal intracellular Ca^{2+} concentration at low micromolar level and utilize a variety of Ca^{2+} transporters for balancing this homeostasis (72). These Ca^{2+} transporters also contribute to Ca^{2+} regulated phenotypes such as swarming

and tobramycin resistance. Lack of at least three of these Ca^{2+} transporters reduced the expression of mexAB-oprm at 5 mM Ca^{2+} suggesting the impostance of Ca^{2+} homeostasis in bacterial resistance to efflux mediated tobramycin resistance(43, 72). Such regulatory role of Ca^{2+} however suggests the requirement of Ca^{2+} sensing regulatory component on the membrane, periplasm or cytoplasm to relay the regulatory response. Our lab has also determines two component regulators CarSR, on the outermembrane of *P. aeruginosa* which is highly Ca^{2+} responsive and controls Ca^{2+} regulated physiological features(70). This two component system controls the expression of a downstram β-propeller protein CarP and putative OB-fold protein CarO. CarP contributed to Ca^{2+} regulated tobramycin resistance while CarO is found to be required to protect he cells from Ca^{2+} toxicity(70). Patrauchan lab also has identified calmoduline like Ca^{2+} binding protein, EfhP which is important for maintenance of basal $[Ca^{2+}]_{in}$ in PAO1. Deletion of this gene in both PAO1 and FRD1 strain of *Pseudomonas* aeruginosa reduced the expression of protein abundance of genes belonging to *pvd* operon which is involved in siderophore biosynthesis. Also, Ca^{2+} dependent expression of virulence associated proteins such as proteases or phenazine biosynthesis proteins as well as proteins protecting Pseudomonas from stress were found to be regulated by EfhP in both PAO1 and FRD1. Loss of *efhP* also affected the Ca^{2+} regulated infectivity of *P. aeruginosa* (71). This regulatory role of Ca^{2+} responsive regulators in antibiotic resistance, virulence as well as infectivity of *P. aeruginosa* suggests a possible

signaling role of this molecule in this organism (61, 70, 71). PAO1 displays the potential intracellular signaling role of Ca^{2+} via the transient changes in intracellular Ca^{2+} in response to increased extracellular Ca^{2+} (47). However, the role of intracellular Ca2+ signaling in regulation ofgenotypic and physiological changes in *P. aeruginosa* is yet to be explored. Such knowledge is required to link the external Ca^{2+} sensing ability to the Ca^{2+} response of this bacterium. This will also help in constructing the network of genes which is involved in response and relay of this Ca^{2+} signal.

In my study, I have investigated the regulatory role of Ca^{2+} in antibiotic resistance of *P. aeruginosa*. Upon identifying that growth at elevated level of Ca^{2+} significantly increases PAO1 resistance to tobramycin and polymyxin-B, we have studied and identified contributing Ca^{2+}-regulated mechanisms. These included multidrug efflux pumps from RND superfamily of transporters. Six of the total 12 RND efflux pumps identified in PAO1 are are involved in Ca^{2+} regulated tobramycin resistance. These pumps are either regulated by Ca^{2+} or play role in Ca^{2+} efflux in the bacterium. We have also identified three novel proteins to be involved in Ca^{2+} regulated polymyxin-B ressitance. Furthermore, we have characterized the role of intracellular Ca^{2+} signaling in controlling the antibiotic resistance as well as virulence traits of *P. aeruginosa*. We aimed to initiate identification of the Ca^{2+} regulatory network for better understanding of Ca^{2+} role in regulating the interaction between this pathogen and its host. This knowledge

will help understanding of the mechanisms that *P. aeruginosa* utilizes for recognizing and responding to Ca^{2+}, which is leading to increased adaptation of the pathogen to the hostile host environment and antibiotic therapies. These findings, in future, will enable the development of novel and efficient therapies for preventing or treating *P. aeruginosa* infections.

CHAPTER II

CALCIUM INDUCES TOBRAMYCIN RESISTANCE IN *PSEUDOMONAS AERUGINOSA* BY REGULATING RND EFFLUX PUMPS

This chapter has been published.

"Sharmily Khanam, Manita Guragain, Dirk L. Lenaburg, Ryan Kubat, and Marianna A. Patrauchan. 2017. Calcium induces tobramycin resistance in *Pseudomonas aeruginosa* by regulating RND efflux pumps. *Cell Calcium*, 61, 32-43" and is included in this dissertation with permission from the publisher.

(License number: 4073830180509)

ABSTRACT

Pseudomonas aeruginosa is an opportunistic multidrug resistant pathogen causing severe chronic infections. Our previous studies showed that elevated calcium (Ca^{2+}) enhances production of several virulence factors and plant infectivity of the pathogen. Here we show that Ca^{2+} increases resistance of *P. aeruginosa* PAO1 to tobramycin, antibiotic commonly used to treat *Pseudomonas* infections. LC-MS/MS-based comparative analysis of the membrane proteomes of *P aeruginosa* grown at elevated versus not added Ca^{2+}, determined that the abundances of two RND (resistance-nodulation-cell division) efflux pumps, MexAB-OprM and MexVW-OprM, were increased in the presence of elevated Ca^{2+}. Analysis of twelve transposon mutants with disrupted RND efflux pumps showed that six of them (*mexB*, *muxC*, *mexY, mexJ*, *czcB,* and *mexE)* contribute to Ca^{2+}-induced tobramycin resistance. Transcriptional analyses by promoter activity and RT-qPCR showed that the expression of *mexAB, muxABC*, *mexXY*, *mexJK*, *czcCBA*, and *mexVW* is increased by elevated Ca^{2+}. Disruption of *mexJ*, *mexC*, *mexI*, and *triA* significantly decreased Ca^{2+}-induced plant infectivity of the pathogen. Earlier, our group showed that PAO1 maintains intracellular Ca^{2+} (Ca^{2+}_{in}) homeostasis, which mediates Ca^{2+} regulation of *P. aeruginosa* virulence, and identified four putative Ca^{2+} transporters involved in this process (Guragain, et.al, 2013). Here we show that three of these transporters (PA2435, PA2092, PA4614) play role in Ca^{2+}-induced tobramycin resistance and one of them

(PA2435) contributes to Ca^{2+} regulation of *mexAB-oprM* promoter activity. Furthermore, *mexJ,* c*zcB,* and *mexE* contribute to the maintenance of Ca^{2+}_{in} homeostasis. This provides the first evidence that Ca^{2+}_{in} homeostasis mediates Ca^{2+} regulation of RND transport systems, which contribute to Ca^{2+}-enhanced tobramycin resistance and plant infectivity in *P. aeruginosa.*

INTRODUCTION

Pseudomonas aeruginosa causes severe infections in lung airways of cystic fibrosis (CF) patients, in burn wounds, as well as in intensive care patients and patients with indwelling medical devices, catheters and shunts (3, 4). *P. aeruginosa* is also one of the leading causes of infective endocarditis (5, 6). The high morbidity and mortality of *Pseudomonas* infections is mainly attributed to the combination of multifactorial virulence, outstanding antimicrobial resistance, and physiological adaptability of this organism (7, 8). Besides its ability to undergo genetic alterations, *P. aeruginosa* possesses multiple mechanisms of intrinsic and adaptive resistance, that together make it resistant to most antimicrobials available for treatments. Efflux mediated antibiotic resistance in *P. aeruginosa* has been recognized as one of the major determinants of its intrinsic resistance (7, 30). Among five families of efflux pumps, resistance nodulation division (RND) family of transporters has drawn the most attention in this regard. It is mainly due to the fact that RND transporters effectively pump out a broad range of toxic substances, including antimicrobial drugs (29, 30). So far, 12 efflux pumps have been identified in *P. aeruginosa* PAO1 genome: MexAB-OprM, MexCD-OprJ, MexEF-OprN, MexPQ-OprM, MexXY-OprM, MexVW-OprM, MexMN-OprJ, MexJK-OprM, TriABC-OpmB, MuxABC-OpmB, MexGHI-OpmD, and CzcCBA-OpmY (13).

RND efflux pumps are comprised of three components including inner membrane component (RND), periplasmic membrane fusion protein (MFP) and

outer membrane porin, thus spanning both inner and outer membranes. Their role in *P. aeruginosa* physiology is not limited to efflux, and includes growth control (38), biofilm formation (75), oxidative (76) and nitrosative stress responses (77), as well as transport of signaling molecules involved in cell-cell communication (38, 78, 79). Furthermore, RND efflux pumps play role in host colonization by modulating such mechanisms of pathogen invasion as pyocyanin production and cell motility (78, 80-82).

Calcium (Ca^{2+}) is an essential messenger regulating a great number of vital eukaryotic processes (83, 84). Imbalance in Ca^{2+} homeostasis is associated with many human diseases including those associated with bacterial infections, for example, infective endocarditis and CF (66, 68, 85). There is an elevated level of Ca^{2+} in mitral annulus of endocarditis patients (86), as well as in pulmonary fluids of CF patients (67, 87). Thus, Ca^{2+} likely serves as a host factor triggering physiological adjustments in the invading bacterial pathogens. In agreement, our earlier studies showed that elevated Ca^{2+} enhances *P. aeruginosa* biofilm formation, production of several virulence factors, including pyocyanin, extracellular proteases, and alginate (74, 88). Furthermore, Ca^{2+} and Mg^{2+} modulate antibiotic resistance in *P. aeruginosa* to gentamycin (89), tetracycline, carbenicillin, polymyxin B (69, 90), and chloramphenicol (91). Whereas several resistance mechanisms regulated by low Mg^{2+} have been characterized (22, 23), very little is known about the underlying mechanisms of Ca^{2+} regulation. The roles

of cations in *P. aeruginosa* antimicrobial resistance have been mainly attributed to reduced cell membrane permeability, which consequently reduces the uptake of cationic antibiotics like polycationic polypeptides and aminoglycosides (92, 93). It has been also suggested that *P. aeruginosa* can utilize the outer membrane protein OprH (H1), also cationic in nature, to stabilize the membrane integrity and to reduce the uptake of cationic antibiotics when deficient in magnesium (94). Finally, the multidrug efflux pump MexXY-OprM has been shown to be required for the antagonistic effect of Ca^{2+} and Mg^{2+} on aminoglycosides resistance in *P. aeruginosa* (95) .

Earlier we showed that *P. aeruginosa* maintains intracellular Ca^{2+} homeostasis, and the level of intracellular Ca^{2+} concentration ($[Ca^{2+}_{in}]$) is responsive to changes in extracellular Ca^{2+} (72) as well as to membrane permeabilizers (not published). Furthermore, we identified several putative Ca^{2+} transporters playing role in maintaining Ca^{2+}_{in} homeostasis, whose disruption disturbed Ca^{2+}- induced swarming (72). Here we hypothesize that Ca^{2+}-dependent increase of antibiotic resistance in *P. aeruginosa* is regulated by the transient changes in $[Ca^{2+}_{in}]$, which are generated in response to sudden addition of extracellular Ca^{2+}. This novel perspective is important for understanding the mechanisms of adaptive antibiotic resistance in bacterial pathogens.

This study showed that tobramycin resistance is significantly increased in *P. aeruginosa* grown at elevated Ca^{2+}. To characterize the mechanisms of this induction, we applied a global proteomic approach and identified several RND transporters, whose abundance was affected during growth at elevated Ca^{2+}. Analysis of the corresponding transposon mutants determined that six RND transporters are involved in Ca^{2+}-induced tobramycin resistance. We also determined that Ca^{2+} affects the transcription of several RND transporters, and this effect is mediated by changes in $[Ca^{2+}_{in}]$. Finally, we identified the role of RND transporters in maintaining Ca^{2+}_{in} homeostasis and Ca^{2+}-induced plant infectivity in *P. aeruginosa*. Overall, this is the first report of the regulatory relationship between $[Ca^{2+}_{in}]$ homeostasis and Ca^{2+}-induced antibiotic resistance.

MATERIAL AND METHODS

Bacterial strains, plasmids, and media

P aeruginosa strain PAO1, the non-mucoid sequenced strain was used in the study (96) . Biofilm minimal medium (BMM) (74) contained (per liter): 9.0 mM sodium glutamate, 50 mM glycerol, 0.02 mM $MgSO_4$, 0.15 mM NaH_2PO_4, 0.34 mM K_2HPO_4, 145 mM NaCl, 20 µl trace metals, and 1 ml vitamin solution. Trace metal solution (per liter of 0.83 M HCl): 5.0 g $CuSO_4.5H_2O$, 5.0 g $ZnSO_4.7H_2O$, 5.0 g $FeSO_4.7H_2O$, 2.0 g $MnCl_2.4H_2O$). Vitamins solution (per liter):

0.5 g thiamine, 1 mg biotin. pH of the medium was adjusted to 7.0. Transposon mutants were obtained from the University of Washington transposon mutant library (97) and are listed in table 2.S1. The mutants were generated by ISphoA/hah or ISlacZ/hah insertions and contain tetracycline resistance cassette. The mutations were confirmed by PCR in two steps: first, gene flanking primers were used to verify that the intact gene is disrupted, and second, transposon-specific primers were used to confirm the transposon insertion. The primer sequence is available at www.gs.washington.edu.

The reporter plasmids for promoter activity assay were either received from Dr. Kangmin Duan or constructed (Table 2S1) For this, putative promoter regions of RND operons were amplified and cloned upstream of the promoterless *lux* operon in pMS402.

Table 2.S1: Strains and plasmids used in this study.

Strains/ Plasmids	Description	Ref.
E. coli DH5α	*fhuA2 Δ(argF-lacZ)U169 phoA glnV44 Φ80Δ (lacZ)M15 gyrA96 recA1 relA1 endA1 thi-1 hsdR17*	
P. aeruginosa PAO1	Wild type	(96)
PW1780[a] (*mexB:*Tn5[b])	PA0426 H01::ISlacZ/hah	(98)
PW8752 (*mexC:*Tn5)	PA4599E04::ISlacZ/hah	(98)
PW5233 (*muxC:* Tn5)	PA2526A07::ISlacZ/hah	(98)
PW8386 (*mexV:*Tn5)	PA4374D09::ISlacZ/hah	(98)
PW8137 (*mexI:*Tn5)	PA4207H08::ISlacZ/hah	(98)
PW5180 (*mexE:*Tn5)	PA2493H04::ISlacZ/hah	(98)
PW6963 (*mexQ:*Tn5)	PA3522H12::ISlacZ/hah	(98)
PW7220(*mexJ:*Tn5)	PA3677D11::ISlacZ/hah	(98)
PW4499 (*mexY:*Tn5)	PA2019D05::ISlacZ/hah	(98)
PW3609 (*mexM:*Tn5)	PA1435G06::ISlacZ/hah	(98)
PW1265 (*triA:*Tn5)	PA0156E03::ISlacZ/hah	(98)
PW5224 (*czcB:*Tn5)	PA2521B08::ISlacZ/hah	(98)
PW5099 (*PA2435*:Tn5)	PA2435A02::ISphoA/hah	(98)
PW7626 (*PA3920*:Tn5)	PA3920G01::ISphoA/hah	(98)
PW4602 (*PA2092*:Tn5)	PA2092F01::ISlacZ/hah	(98)

PW4772 (*PA4614*:Tn5)	PA4614B11::ISphoA/hah	(98)
pMS402	Reporter vector, luxCDABE; Kan^R Tmp^R	(82)
pKD-mexA	pMS402 carrying the promoter region of *mexAB-oprM*; Kan^R Tmp^R	(82)
pKD-mexX	pMS402 carrying the promoter region of *mexXY-oprM*; Kan^R Tmp^R	(82)
pKD-czcC	pMS402 carrying the promoter region of *czcCBA*; KanR Tmp^R	(82)
pSK-muxA	pMS402 carrying the promoter region of *muxABC-opmB*; Kan^R Tmp^R	This study
pSK-mexJ	pMS402 carrying the promoter region of *mexJK-oprM*; Kan^R Tmp^R	This study
pSK-mexE	pMS402 carrying the promoter region of *mexEF-oprN*; Kan^R Tmp^R	This study

[a]The mutant identifier from UW transposon mutant library.

[b]The designated name of the mutant strain in this study.

Growth and antibiotic susceptibility assays

For growth studies, cells were inoculated into 3 ml of BMM with no (not added) or 5 mM Ca^{2+} and grown for 12 h at 37 °C and 200 rpm shaking. Thus obtained pre-cultures were normalized to OD_{600} of 0.1 and inoculated into 100 ml of BMM with the corresponding Ca^{2+} concentration at 1:1000 ratio, and OD_{600} was

measured every 2-4 h. Minimum inhibitory concentration (MIC) of tobramycin (aminoglycoside) was determined using both commercially available E-strips (Biomerieux) and conventional serial dilution assay. In brief, cultures were grown in BMM medium at no or 5 mM Ca^{2+} for 18 h and normalized to OD_{600} of 0.1. Then 100 µl of the normalized cultures was spread on BMM agar plates with or without Ca^{2+}. Individual E- strips containing antibiotic gradient were placed onto the inoculated plates, and after 24 h of incubation, the MICs were recorded by determining the concentration of tobramycin on the strip, at which no bacterial growth was detected. For plate dilution assay, middle log cultures grown in BMM with or without added Ca^{2+} were normalized to OD_{600} of 0.3, and inoculated at 1:100 ratio into BMM with the corresponding Ca^{2+} concentration with or without tobramycin. Tobramycin was added at the final concentration of 0.25, 0.5, 0.75, 0.1, 1.5 µg/ml to BMM without added Ca^{2+} and of 1.0, 1.5, 1.75, 2.0, 3.5 µg/ml to BMM supplemented with 5 mM Ca^{2+}. The cultures were incubated with slow (Biotek setting) shaking for 8 h in 96 well plates, and OD_{600} was measured at the 8^{th} h using Synergy Mx Microplate Reader (Biotek). At least three replicates were tested in at least two independent experiments; the mean values of MICs are reported.

Proteomic analysis

Membrane proteins were isolated by carbonate extraction as described in (99) with modifications. Briefly, cell pellets of PAO1 grown at no or elevated [Ca^{2+}] were washed in saline (0.14 M NaCl) and resuspended in TE buffer (10mM Tris/HCl, 1 mM EDTA, pH 8.0), containing Mini Complete protease inhibitor cocktail (1:100 (v/v)). Cells were disrupted by sonication (5 cycles of 30 sec with 1 min interval on ice) using 550 Sonic Dismembrator (Fisher Scientific, Pittsburgh, PA), and then centrifuged at 6,000 g for 10 min at 4 ^{0}C. The procedure was repeated two times. The collected supernatants were combined, diluted with ice-cold 0.1 M sodium carbonate followed by gentle stirring for 1 h, and centrifuged at 100,000 g for 1 h at 4 ^{0}C in a Beckman L8-70M ultracentrifuge. The pellets were collected, washed twice in 50 mM Tris pH 7.3, and subjected to liquid chromatography–tandem mass spectrometry (LC-MS/MS) – based peptide counting. Protein concentration was determined using the 2D Quant kit (GE Healthcare). LC-MS/MS spectrum counting was performed at the OSU Proteomics Facilities. Proteins were identified using Mascot (v2.2.2 from Matrix Science, Boston, MA, USA) and a database generated by *in silico* digestion of the *P. aeruginosa* PAO1 proteome predicted from the genome. Search results were validated using Scaffold 03 (Proteome Software Inc., Portland, OR). Criteria for accepting each ID will conform to the "Paris" guidelines for proteomics results (http://www.mcponline.org/misc/ParisReport_Final.dtl). A set of stringent criteria

for protein identification was used, where only protein probability thresholds greater than 99 % were accepted and at least three peptides needed to be identified, each with 95 % certainty.

RNA isolation and cDNA synthesis

Total RNA was isolated from *P. aeruginosa* PAO1 grown in BMM with no or 5 mM Ca^{2+} using RNeasy Protect Bacteria Mini kit (Qiagen) following the manufacturer's protocol. The purified RNA was eluted with diethylpyrocarbonate (DEPC) treated sterile nanopure water. An additional DNase treatment was performed for eluted RNA sample using turbo DNase (Ambion). The absence of genomic DNA was confirmed by conventional PCR and real time quantitative PCR (RT-qPCR) using *rpoD* primers. RNA yield was measured using NanoDrop spectrophotometer (NanoDrop Technologies Inc.), and the quality of the purified RNA was assessed by Bioanalyzer 2100 (Agilent) and 1% agarose gel electrophoresis. Following the MIQE guidelines (100), only the RNA samples with an OD_{260}/OD_{280} ratio of 1.8-2.0 and an RIN value of ≥ 9.0 were selected for further analyses. RNA samples were stored at -80 °C. Reverse transcription was performed using Transcriptor First Strand cDNA Synthesis Kit (Roche) according to the manufacturer's protocol and stored at -20 °C.

Primers design for RT-qPCR

Primers for 12 RND transporter genes (*triA*, *mexB*, *muxC*, *mexI*, *mexC*, *mexE*, *mexJ*, *mexQ*, *mexV*, *mexX*, *czcB,* and *mexM)* were designed using Primer3Plus (101) or Primer BLAST (102) and listed in Supplementary Table 2S2. Primers were tested *in silico* using OligoAnalyzer (IDT). Their specificity was tested by BLAST alignment against *P. aeruginosa* genome available at www.pseudomonas.com and confirmed by PCR and RT-qPCR melt curve analysis using gDNA as a template. For primer efficiency, RT-qPCR was performed for each primer pair using 10 fold serial dilution of gDNA, and the obtained Cp values were plotted against the concentration of nucleotides. The efficiency was calculated using linear regression analysis. Following the MIQE guidelines (100), the primers with an R^2 value of 0.99 and an efficiency of 97% ± 10 % were selected. Among the four tested housekeeping genes, *rpoD*, *rpoS*, *proC* and *16S rRNA,* which have been previously used in PAO1 RT-qPCR studies (103, 104), the transcription of *rpoD* gene was not affected by Ca^{2+}, and therefore this gene was selected as a control.

Table 2.S2: Primers used in this study

Primer name	Primer sequence (5′ - 3′)	Primer efficiency (%)	Reference
0576_F1	CTCAACTACCAGCGGCAGAA	97	(103)
0576_R1	CGCAGCTCGGTATAGGAAAG		(103)
0156_F1	CTCAACTACCAGCGGCAGAA	93	This study
0156_R1	CGCAGCTCGGTATAGGAAAG		This study
0426_F1	TACGAAAGCTGGTCGATTCC	100	This study
0426_R1	GCGAACTCCACGATGAGAAT		This study
2526_Fiv	AGGAACAGGAAGACCACCAG	100	This study
2526_Riv	TCAAGCTGAACGTGATGGAC		This study
4207 F1	GTCGAACCGAACAAGCTGAT	100	This study
4207 R1	TGTTGCCTTCCTGGGTGTAT		This study
4599_F2	TTCCGAACTCAGCGCCAG	97	This study
4599_R2	ATAGGAAGGATCGGGGCGTT		This study
2493_F1	TGGAACAGTCATCCCACTTC	93	This study
2493_R1	AATTCGTCCCACTCGTTCAG		This study
3677_F3	CGGTAGCTGTTCTGGATGTTC	96	This study
3677_R3	GAGCGGGTAAAGAAGGACCA		This study
3522_F3	CGACGGATAGCCGTTGTAGT	93	This study
3522_R3	TCGCACCTACAAGGTCACTG		This study
2019_F3	TTCTCGACGATCACCCACTC	97	This study
2019_R3	TCAAGGTGGTCAACCCAAAG		This study
4374_F3	AAGGTCTACTCCATCCGTCAG	96	This study
4374_R3	CCGGAAAGGAACAGTACGTC		This study

2521_F2	TGCCCAGTTCGGATTTGAGG	97	This study
2521_R2	CGAGGACGTGGTGTTCGTC		This study
1435_3rt F	GCACCGATCTCCGTAGTCTT	89	This study
1435_3rt R	GGTGGAACTGTCGATCTGGT		This study
muxA- f	AAC**CTCGAG**TTTCAACGGGTC GATCATCT		(82)
muxA- r	CC**GGATCC**ATCACCAGGCCGA TCAC		(82)
mexJ- f	AAA**CTCGAG**GGCGATATTCAG CAGGAC		(82)
mexJ- r	CA**GGATCC**GGTACATGTGACA CCTTC		(82)
mexE- f	AAT**CTCGAG**CATGTTCATCGG CGATCC		(82)
mexE- r	CA**GGATCC**AGGCGCTCAGGAC CAGTA		(82)

*Xho*I and *Bam*HI restriction sites are incorporated (Bold) in the primer to facilitate cloning.

Gene expression analysis

To characterize the transcription profiles of RND genes, RT-qPCR was performed following the manufacturer's protocols (Roche). For this, 5 µl of SYBR green master mix (Roche, Indianapolis, IN), 0.5 µM of each primer and 5 ng of RNA were added to a total volume of 10 µl of reaction mixture. RT-qPCR was run using 384 well plates sealed with LightCycler 480 Sealing Foil (Roche, Indianapolis, IN) in Roche LightCycler 480. At least five technical replicates for each biological replicate and a minimum of three biological replicates for every sample were analyzed. A no-template control was used as a negative control. The cycle included 10 min denaturation at 95 °C followed by 35 cycles of 95 °C for 10 s, 61 °C for 15 s, and 72 °C for 10 s. A fold change in gene transcription was calculated using $2^{-\Delta\Delta Ct}$ method (105). Statistical analysis was performed by using two tailed T-test assuming equal variances.

Promoter activity assay

To characterize the effect of Ca^{2+} on transcription of selected RND transporters during different phases of growth, we assayed their promoter activities in response to Ca^{2+} or tobramycin. For this, putative promoter regions (300-400 bp upstream) of *muxABC*, *mexJK* and *mexEF* were amplified and cloned upstream of

a promoterless *luxCDABE* reporter in pMS402 (82). The vector and promoter constructs for *mexAB-oprM*, *mexXY-oprM*, and *czcCBA-opmY* were generously provided by Drs. Duan and Mengmeng. Promoter constructs were transformed into PAO1 by electroporation as described in (82). The resultant strains were grown for 12 h in BMM, normalized to OD_{600} 0.3, inoculated at 1:100 ratio into fresh BMM with no or 5 mM Ca^{2+}, and grown in 96 well-plate at 37°C with continuous shaking for 10 h. Tobramycin was added to a final concentration of 0.25 - 2.5 μg/ml (Sub inhibitory concentration, SIC, determined by plate dilution assay). Both OD_{600} and luminescence were measured every 30 min using Synergy Mx Microplate Reader. Luminescence measurements were normalized by cell density (OD_{600}) of the corresponding cultures, followed by subtraction of the empty vector normalized luminescence. Finally, ratios between promoter activities determined with and without Ca^{2+} or tobramycin were calculated and averaged over at least three biological replicates. Every experiment was repeated at least twice.

To study the role of intracellular Ca^{2+} homeostasis in Ca^{2+} regulation of RND transcription, the *mexAB-oprM* promoter activity reporter construct was transformed by electroporation into the earlier characterized transposon mutants with disrupted putative Ca^{2+} transporters, *PA2435*:Tn5, *PA2092*:Tn5 and *PA4614*: Tn5 (72). Successful transformants were tested for trimethoprim resistance and light production using Synergy Mx Microplate Reader (Biotek) and used to measure promoter activity as described above.

Virulence assays

To assess the role of RND transporters in *P. aeruginosa* virulence, we used a plant infection model following the modified protocol described in (71, 106). Briefly, organic romaine lettuce leaves were purchased fresh, and healthy looking leaves were detached, washed in 0.1 % bleach and rinsed twice with distilled water and once with nanopure water. Midribs were cut and placed in Petri dish containing Whatman No.1 filter paper soaked in 10 mM $MgSO_4$. *P. aeruginosa* strains grown for 18 h in BMM at no or 5 mM Ca^{2+} were harvested, washed and resuspended in 10 mM $MgSO_4$, containing the same amount of Ca^{2+} as the original culture. The obtained cell suspensions were normalized to an OD_{600} of 0.2 and inoculated into one end of each midrib by injecting 10 µL using a pipette tip. The other end of the midrib was inoculated with $MgSO_4$ containing no or 5 mM Ca^{2+} to be used as a negative control. The Petri dishes were placed in a clear plastic bin, to the bottom of which about 10 ml of water was added to maintain humidity. The bins were incubated at room temperature near a window for six days, and then the developed zones of disease were measured. At least 3 biological replicates were analyzed from the minimum of two independent experiments, and the mean values are reported.

Measurement of intracellular calcium concentration ($[Ca^{2+}]_{in}$)

PAO1 and the transposon mutants with disrupted *mexB*, *mexY*, *muxA*, *mexJ*, *mexE* or *czcB* were transformed with pMMB66EH (courtesy of Dr. Delfina

Dominguez and Dr. Anthony Campbell), carrying aequorin (107) and carbenicillin resistance genes, using a heat shock method described in (108). The transformants were selected on Luria Bertani (LB) agar containing carbenicillin (300 µg/ml) and verified by PCR using aequorin specific primers (For: 5′CTTACATCAGACTTCGACAACCCAAG, Rev: 5′CGTAGAGCTTCTTAGGGCACAG). Aequorin was expressed and reconstituted as described in (72). Luminescence measurements and estimation of free $[Ca^{2+}]_{in}$ was done as described previously (72) with slight modifications. Briefly, mid-log phase cells were induced with IPTG (1 mM) for 2 h for apoaequorin production, and then harvested by centrifugation at 15,000 g for 5 min at 4 ^{0}C. Aequorin was reconstituted by incubating cells in the presence of 2.5 µM coelenterazine for 30 min in the dark. 100 µl of the cells with reconstituted aequorin were equilibrated for 10 min at room temperature in the dark. Luminescence was measured using Synergy Mx Microplate Reader (Biotek). To estimate the basal level of $[Ca^{2+}]_{in}$, the measurements were recorded for 1 min at 5 sec intervals then the cells were challenged with 1 mM Ca^{2+}, mixed for 1 sec, and the luminescence was recorded for 20 min at 5 sec intervals. Injection of buffer alone was used as a negative control, and did not cause any significant fluctuations in $[Ca^{2+}]_{in.}$ $[Ca^{2+}]_{in}$ was calculated by using the formula $pCa= 0.612 (-\log_{10}k) + 3.745$, where k is a rate constant for luminescence decay (s^{-1}) (109). The results were normalized against the total amount of available aequorin as described (72). The discharge was

performed by permeabilizing cells with 2 % Nonidet 40 (NP40) in the presence of 12.5 mM $CaCl_2$. The luminescence released during the discharge was monitored for 10 min at 5 sec intervals. The estimated remaining available aequorin was at least 10 % of the total aequorin. The experimental conditions reported here were optimized to prevent any significant cell lysis.

RESULTS

Ca^{2+} enhances resistance of P. aeruginosa PAO1 to tobramycin

To determine whether Ca^{2+} affects tobramycin resistance in *P. aeruginosa* PAO1, we measured the minimal inhibitory concentration (MIC) of this aminoglycoside antibiotic that is commonly used to treat *P. aeruginosa* infections. For this, PAO1 was grown in BMM at high (5 mM) and low (not added) concentrations of $CaCl_2$, and the MIC of the antibiotic was determined by using both conventional serial dilution approach and E-strips from BioMerieux. Resistance to tobramycin was increased almost 10 fold from 0.38 µg/ml in PAO1 cells grown at no Ca^{2+} to 3.67 µg/ml in cells grown at elevated Ca^{2+}. This level of tobramycin is within the range detected at infection sites (110-113). On the other hand, increased tobramycin resistance is typical for CF clinical isolates of *P. aeruginosa* (114), which may reflect their adaptation to the elevated Ca^{2+} in pulmonary fluids of CF patients (67, 87).

Ca^{2+} alters the production of RND transporters and porins

To identify the molecular mechanisms responsible for Ca^{2+}-induced antibiotic resistance in *P. aeruginosa,* we compared membrane proteomes of cells grown at 5 mM versus not added $CaCl_2$ by using a semi-quantitative LC-MS/MS-based spectrum (peptide) counting approach. This allowed confident identification of about 90 membrane and membrane-associated proteins, differentially expressed during growth at elevated Ca^{2+}. The proteins with a higher number of peptides detected at elevated Ca^{2+} include those representing efflux pumps MexAB-OprM and MexVW-OprM (Table 2.1). Three more efflux pumps (MuxABC-OpmB, MexGHI-OpmD, and TriABC-OpmD) were induced by Ca^{2+} in *P. aeruginosa* FRD1 strain (data not shown). On the contrary, the abundance of CzcA, representing another RND transporter, CzcCBA-OpmY, was reduced in PAO1 in the presence of 5 mM Ca^{2+}. These efflux pumps belong to the RND superfamily of transporters, known for their role in *P. aeruginosa* antibiotic resistance (29, 30). In addition, five porins were induced in the presence of Ca^{2+}, including OprM, which serves as the outer membrane components (OMF) of RND tripartite systems. Together with the inner membrane RND components and the periplasmic membrane fusion proteins (MFS), OMF form functional RND systems (13, 29, 30). OprM can be shared by multiple RNDs, and its overexpression leads to increased multidrug resistance in *P. aeruginosa* (18). Although semi-quantitative, these data

suggest that RND mediated efflux in *P. aeruginosa* is affected by Ca^{2+} and that RND transporters may be involved in Ca^{2+}-induced tobramycin resistance.

Table 2.1: LC-MS/MS analysis of selected P. aeruginosa PAO1 proteins, whose abundance changed during growth at 5 mM Ca2+.

Protein name (PA No.)	Protein description	# of peptides detected at no Ca^{2+}	# of peptides detected at 5 mM Ca^{2+}
RND proteins			
MexB (PA0426)	RND efflux pump MexAB-OprM	15	22
MexV (PA4374)	RND efflux pump MexVW-OprM	3	5
CzcA (PA2520)	RND efflux pump CzcCBA	6	0
Porins			
OprD (PA0958) [a]	Outer membrane porin	1	22
ChtA (PA4675)	TonB dependent porin	9	27
OprF (PA1777)	Outer membrane porin	73	99
OprM (PA0427)	Outer membrane porin	5	8
Opr86 (PA3648)	Outer membrane porin	4	10

[a]Proteins: PA0156 (TriA, which is a part of TriABC-OpmH efflux pump), PA0958 (OprD) was also detected as induced by Ca^{2+} by 2D-PAGE (not shown here).

Several RND transporters are involved in Ca^{2+} regulated tobramycin resistance

To test whether RND transporters play role in Ca^{2+}-induced resistance to tobramycin, we measured the MIC of this antibiotic in the transposon insertion mutants deficient in each of the twelve RND genes encoded in the PAO1 genome. For this, the wild type (WT) PAO1 and transposon mutant strains were grown at 5 mM Ca^{2+} or not added Ca^{2+}, and the MICs were measured by using E-strips and compared. The disruption of *mexB, mexY, muxC, mexE, mexJ* and *czcB* reduced Ca^{2+}-induced tobramycin resistance at least twofold (Fig. 1), whereas the other six RND mutants showed no significant difference in tobramycin resistance (Fig. S1). These observations indicate that six out of twelve *P. aeruginosa* RND systems respond to the presence of Ca^{2+} and contribute to *P. aeruginosa* increased resistance to tobramycin under elevated Ca^{2+} conditions. In addition, the mutants with disrupted *mexB* and *mexY* showed significantly lower resistance to tobramycin when grown without added Ca^{2+} (Fig. 2.1), suggesting that MexAB and MexXY efflux pumps are involved in both Ca^{2+}-induced and Ca^{2+}-independent resistance to tobramycin in the organism. The intriguing difference between the two pumps is that in the *mexB* mutant, elevated Ca^{2+} partially recovers the level of resistance to about 45% of that in the WT, suggesting there is an alternative mechanism of tobramycin resistance that is induced by Ca^{2+} in this mutant as well as the mutants with disrupted *muxC, mexE, mexJ,* and *czcB*. However, in the *mexY* mutant, the addition of Ca^{2+} did not make a difference; supporting previous observations that

MexXY is required for tobramycin resistance (95). To test if the observed differences are not due to possible growth defects in the mutants, we monitored growth of the mutants at elevated Ca^{2+} and detected no significant changes in their growth rates in response to Ca^{2+} (Fig. S2.2).

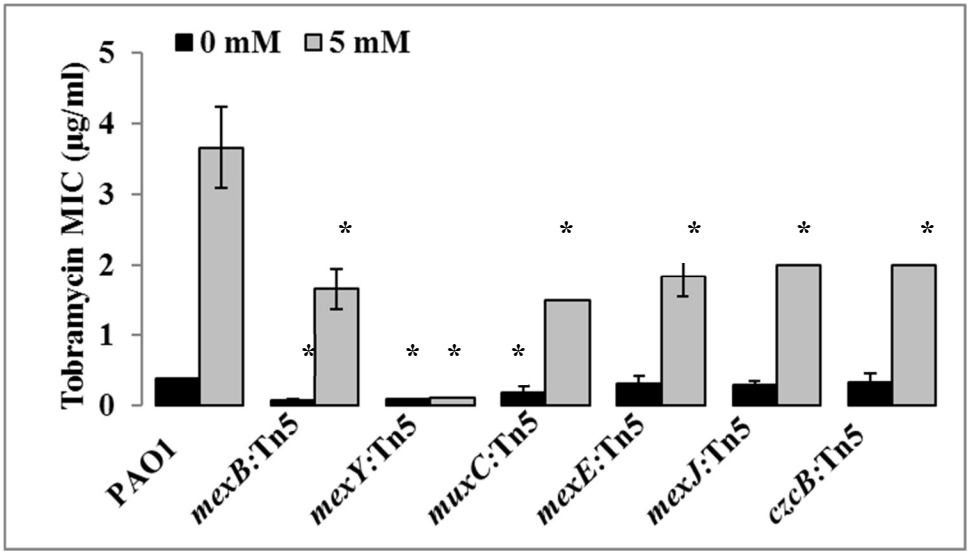

Figure 2.1: MIC of tobramycin for PAO1 and transposon mutants with individually disrupted RND transporters. MIC of tobramycin for PAO1 and transposon mutants with individually disrupted RND transporters. Cells were grown without or with 5 mM Ca^{2+}, normalized to OD600 of 0.1, and plated onto BMM agar plates with the corresponding concentration of Ca^{2+}. E-strips with gradient of tobramycin were placed on the bacterial lawns. MIC was recorded after 24 h incubation. Statistical significance of the difference in MIC between PAO1 and RND mutant strains was calculated using student's T-test. *, $p < 0.05$

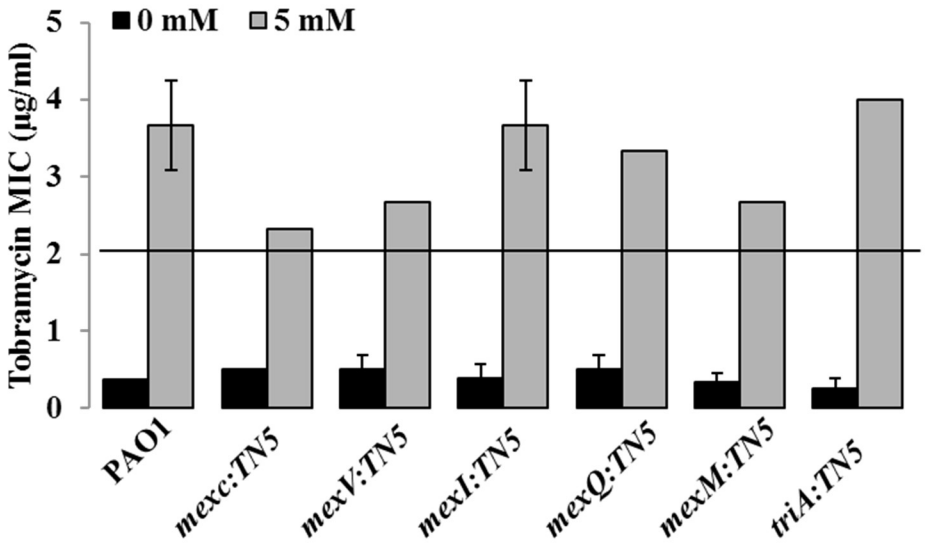

Figure 2.S1: The role of RND transporters in Ca^{2+}- induced tobramycin resistance of PAO1. The cultures were grown without or with 5 mM Ca^{2+}, normalized to OD_{600} of 0.1, and plated onto BMM agar plates with the corresponding concentration of Ca^{2+}. E-strips with gradient of tobramycin were placed on the bacterial lawns. The MIC was recorded after 24 h incubation.

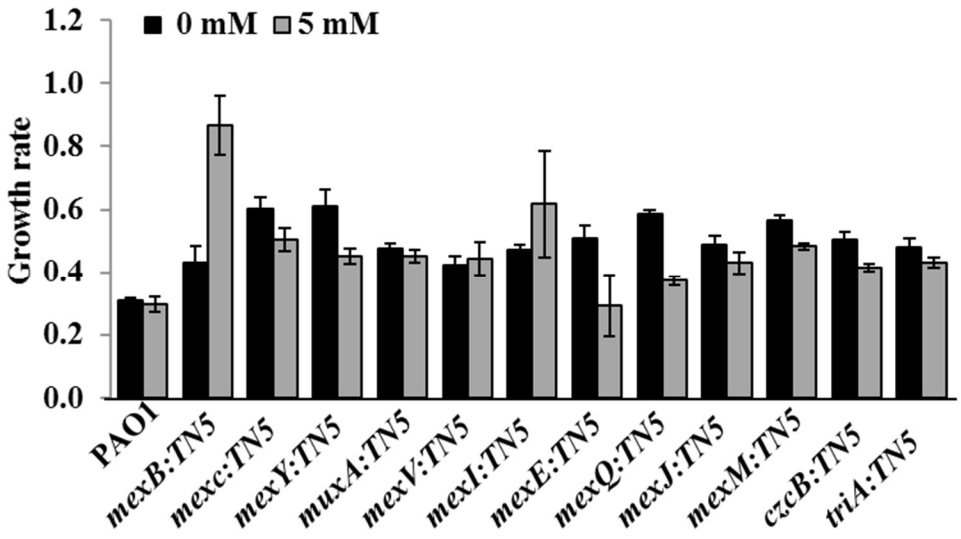

Figure 2.S2: The role of Ca^{2+} on growth rate of PAO1 and RND transporter mutants. The cultures were grown in BMM without or with 5 mM Ca^{2+}, collected, normalized to OD_{600} of 0.1 and inoculated into 100 ml BMM with the corresponding Ca^{2+} concentration at a 1:1000 ratio. The OD_{600} was measured every 4 h. Growth rates were calculated as described in (115).

Ca^{2+} regulates transcription of efflux pumps involved in Ca^{2+}-induced tobramycin resistance

To determine whether Ca^{2+}-dependent involvement of multiple RND systems in tobramycin resistance is mediated by the regulatory effect of Ca^{2+}on the transcription of RND genes, we used RT-qPCR and promoter activity approaches. For RT-qPCR, we tested WT cells grown to mid-log growth phase at elevated and low levels of Ca^{2+}. The analysis revealed that growth at elevated Ca^{2+} affected the expression of four RND genes by at least two fold. Transcripts of *mexV* were twofold more abundant at elevated Ca^{2+}, whereas transcription of *mexX, muxC,* and *mexM* was reduced in response to 5 mM Ca^{2+} (Fig. 2.2). We did not detect the *czcB* transcripts in mid-log PAO1 cells, and the transcription of the other five tested RND systems was not affected by Ca^{2+} (Fig. S2.3). This transcriptional profile did not correlate with the involvement of *mexB, mexY, muxC, mexE, mexJ, czcB,* and *mexX* in Ca^{2+} regulated tobramycin resistance. Therefore, we hypothesized that Ca^{2+} effect on the transcription of the six RND transporters that are involved in Ca^{2+}-induced tobramycin resistance, may be growth-phase-dependent. To test this hypothesis, we monitored the temporal effect of Ca^{2+} on promoter activities of the six RND transporters by using *lux*-based reporter system (Fig. 2.3). We also assayed the activity of the promoters in response to tobramycin at sub-inhibitory concentration. The results confirmed that promoter activities of five RND transporters were transiently increased by Ca^{2+} in a growth-phase-dependent

manner (Fig. 2.3B-F). Interestingly, several spikes of activity were observed, all during transitions between different growth phases. The most significant effect of Ca^{2+} was observed for *mexAB-oprM* promoter, whose activity increased 7 fold after 2 h of growth during the transition to early-log phase (Fig. 2.3 B). At the same time, the promoter responded to the sub-inhibitory concentration of tobramycin. During the mid-log phase (4 h), promoter activities for *mexXY*, *muxABC-opmB*, *mexJK* and *czcCBA-opmY* were moderately (about two-three fold) increased in response to Ca^{2+} (Fig. 2.3 C-F). At the same time, two of these promoters, *mexXY*, *muxABC-opmB,* responded to tobramycin. Further, all the tested promoters responded to tobramycin during the transition to stationary phase (8 h), and all, except for P*mexAB-oprM,* showed about twofold activity increase in response to Ca^{2+} at this point of growth. In agreement with (82), the activity of *mexEF-oprN* promoter was not detected under the tested conditions.

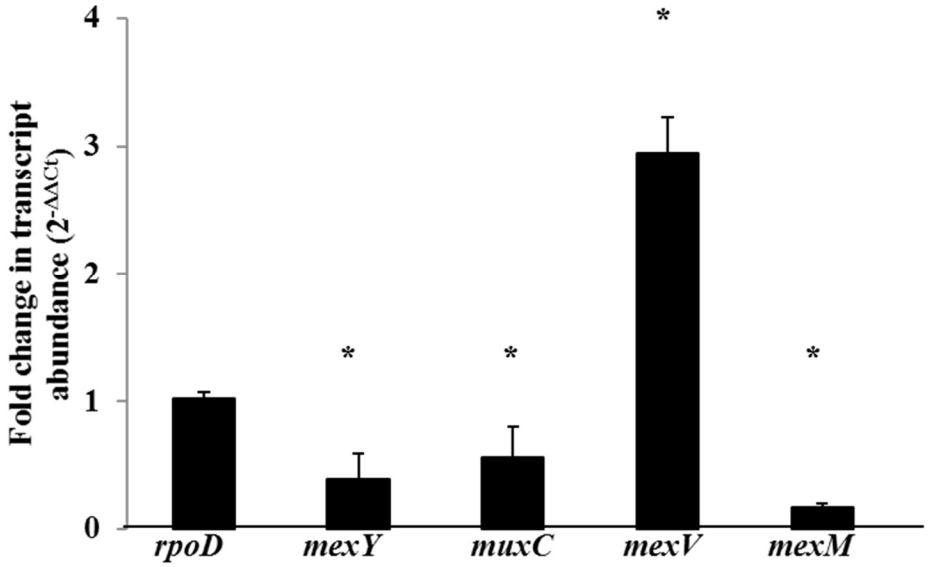

Figure 2.2: The effect of Ca^{2+} on transcript levels of RND genes. RT-qPCR was used to estimate changes in the transcripts levels. PAO1 cells were grown in BMM without or with 5 mM Ca^{2+} until middle log. *rpoD* was used as an internal control. The change in transcript abundance was calculated using $2^{-\Delta\Delta Ct}$ method. Statistical significance of the difference was calculated using t-test for paired samples assuming equal variances. *, $p < 0.05$

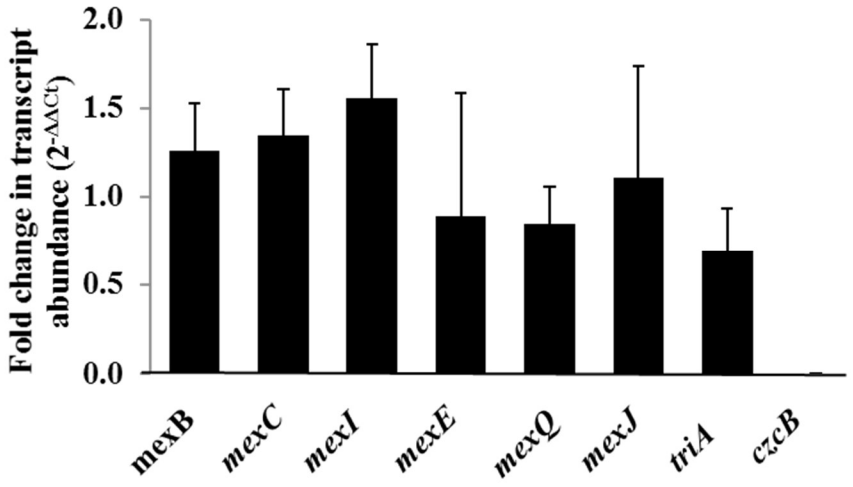

Figure 2.S3: The effect of Ca^{2+} on transcript levels of RND genes. RT-qPCR was used to estimate changes in the abundance of transcripts. PAO1 cultures were grown in BMM without or with 5 mM Ca^{2+} until middle log phase. *rpoD* was used as an internal control. The change in transcript abundance was calculated using $2^{-\Delta\Delta Ct}$ method. Statistical significance of the difference was calculated using t-test for paired samples assuming equal variances. *, $p < 0.05$

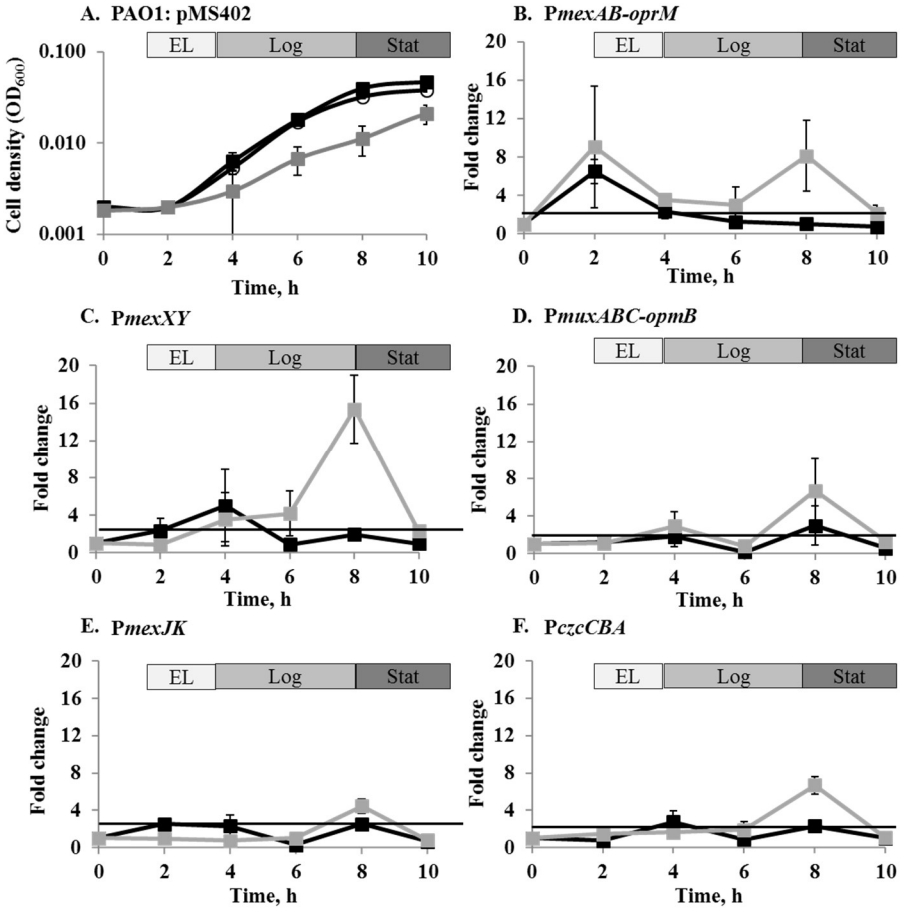

Figure 2.3: Promoter activity analyses of the selected RND transporters. Cells were grown in BMM at 37° C in 96 well clear bottom white plates at fast shaking setting in Synergy Mx microplate reader. A. Growth of PAO1:pMS402 was monitored by absorbance at 600 nm. Black empty circles: 0 mM Ca^{2+}, black squares: 5 mM Ca^{2+}, grey squares: tobramycin. B-F. Fold change in promoter activities for *mexAB-oprM*, *mexXY*, *muxABC-opmB*, *mexJK* and *czcCBA-opmY*. Black squares: effect of Ca^{2+} and grey squares: effect of tobramycin. The horizontal lines across the diagrams show the two fold increase in promoter activity. At least

three biological replicates were included in every experiment. Phases of growth: EL (early logarithmical), Log (logarithmical), and Stat (stationary).

Intracellular Ca^{2+} (Ca^{2+}_{in}) homeostasis mediates Ca^{2+} regulation of mexAB-oprM promoter

Earlier we established that addition of extracellular Ca^{2+} causes transient changes in the intracellular levels of the ion, and suggested that this response likely mediates Ca^{2+} regulation in *P. aeruginosa* (72). Several putative Ca^{2+} transporters were identified and shown to be required for maintaining Ca^{2+}_{in} homeostasis. They include P-type ATPase PA2435, ion exchanger PA2092, and mechanosensitive channel PA4614 (72). We hypothesized that Ca^{2+}_{in} homeostasis is involved in regulating the transcriptional changes detected for several RND efflux pumps. To test this hypothesis, we measured the activity of *mexAB-oprM* promoter in the mutants with disrupted PA2435, PA2092, or PA4614, and therefore disturbed Ca^{2+}_{in} homeostasis. P*mexAB-oprM,* was selected due to its highest response to Ca^{2+} (Fig. 2.3 B). The promoter activity was measured at 5 mM Ca^{2+} or no added Ca^{2+}, and the fold difference was plotted (Fig. 2.4). The most significant reduction of Ca^{2+} induction of P*mexAB-oprM* activity was detected in *PA2435:Tn5* mutant. In this mutant, the activity of P*mexAB-oprM* was increased in response to elevated Ca^{2+} by only two fold (versus 7 fold in PAO1) (Fig. 2.4 B). This suggests that Ca^{2+}_{in} homeostasis regulated by PA2435 mediates Ca^{2+} effect on P*mexAB-oprM* activity.

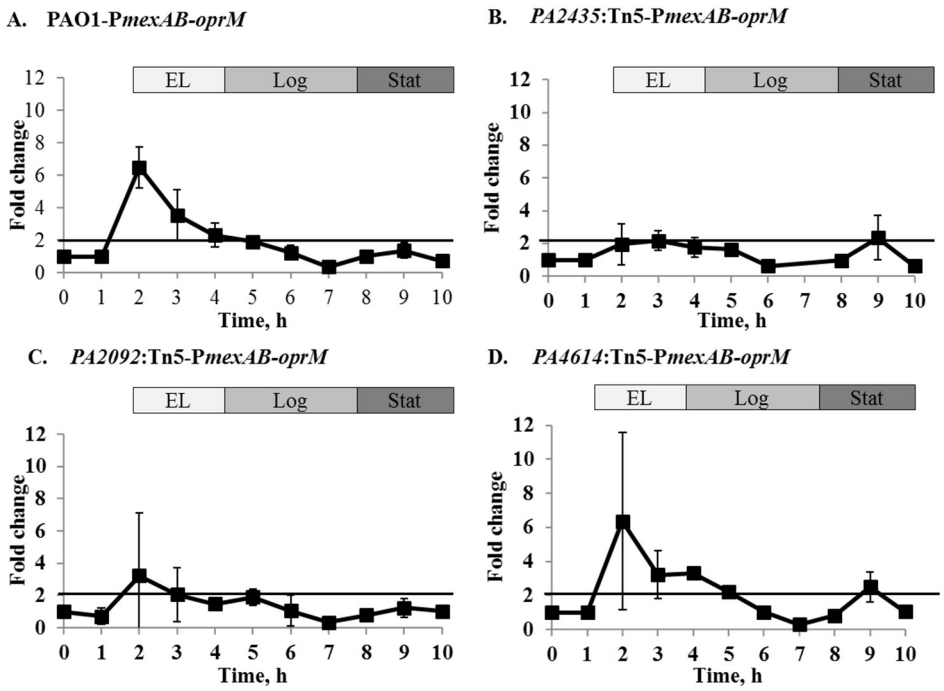

Figure 2.4: Effect of Ca^{2+} on the activity of PmexAB-oprM in *P. aerugionosa* PAO1 and transposon mutants with disrupted PA2435, PA2092, and PA4614. Cells were grown in BMM at 37° C in 96 well clear bottom white plates at fast shaking setting in Synergy Mx microplate reader. A. PAO1 B. PA2435:Tn5 C. PA2092:Tn5 D. PA4614:Tn5 . The horizontal lines across the diagrams show the two fold increase in promoter activity. At least three biological replicates were used for each experiment.

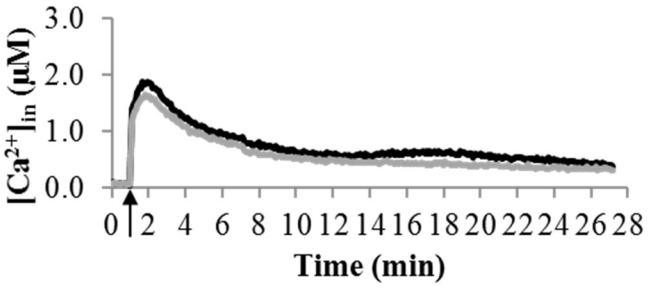

Figure 2.S4: Free $[Ca^{2+}]_{in}$ profiles of *P. aeruginosa* challenged with tobramycin and Ca^{2+}. Black lines represent the response to addition of Ca^{2+} alone and grey lines represent the response to addition of Ca^{2+} together with tobramycin. Compounds were added at the time indicated by the arrow. Changes in free $[Ca^{2+}]_{in}$ were calculated as described in the Methods section. Data shown is representative of at least three biological replicates**.**

We also tested the effect of tobramycin on Ca^{2+}_{in} homeostasis. Sub inhibitory concentration of tobramycin, 0.25 µg/ml (defined for PAO1 growing in BMM) as well as higher levels of the antibiotic: 2.5, 5, 10, and 20 µg/ml were used. However no significant changes in the Ca^{2+}_{in} levels were detected (Fig. S2.4). In case if external source of Ca^{2+} is required for elevating Ca^{2+}_{in}, we added 1 mM extracellular Ca^{2+} either during cell growth or during sample preparation (either 6 min prior to the addition of tobramycin or simultaneously with tobramycin). As above, no effect of tobramycin on Ca^{2+}_{in} levels was detected.

Putative Ca^{2+} transporters contribute to Ca^{2+}-induced tobramycin resistance in PAO1

Since at least one putative Ca^{2+} transporter (PA2435), required for maintaining Ca^{2+}_{in} homeostasis, plays role in Ca^{2+} regulation of *mexAB-oprM* transcription, we tested the role of all four earlier identified putative Ca^{2+} transporters (PA2435, PA2092, PA3920, and PA4614) in Ca^{2+}-induced tobramycin resistance. For this, we measured antibiotic susceptibility of the transposon mutants with individually disrupted PA2435, PA2092, PA3920, and PA4614 by using a dilution assay at high and low Ca^{2+} (Fig.2. 5**).** No significant changes in the tobramycin MIC were detected when the mutants were grown at no added Ca^{2+}. However, when cells of three mutants with disrupted PA2435, PA2092, or PA4614 were grown at 5 mM Ca^{2+}, the MIC was reduced by almost twofold (from 3.5 µg/ml

in PAO1 to 1.75-2.0 µg/ml in the mutants). Considering that in response to extracellular Ca^{2+}, these mutants increase $[Ca^{2+}]_{in}$ to the level of the wild type, but are not able to bring it back to the basal level (72), we propose that this failure of generating a temporally transient elevation of $[Ca^{2+}]_{in}$ reduces their responses to Ca^{2+} regulation and decreases the level of Ca^{2+}-induced tobramycin resistance. These observations support the hypothesis that $Ca^{2+}{}_{in}$ response i.e. a combination of both the amplitude and the duration of $[Ca^{2+}]_{in}$ changes, mediates Ca^{2+} regulation of tobramycin resistance.

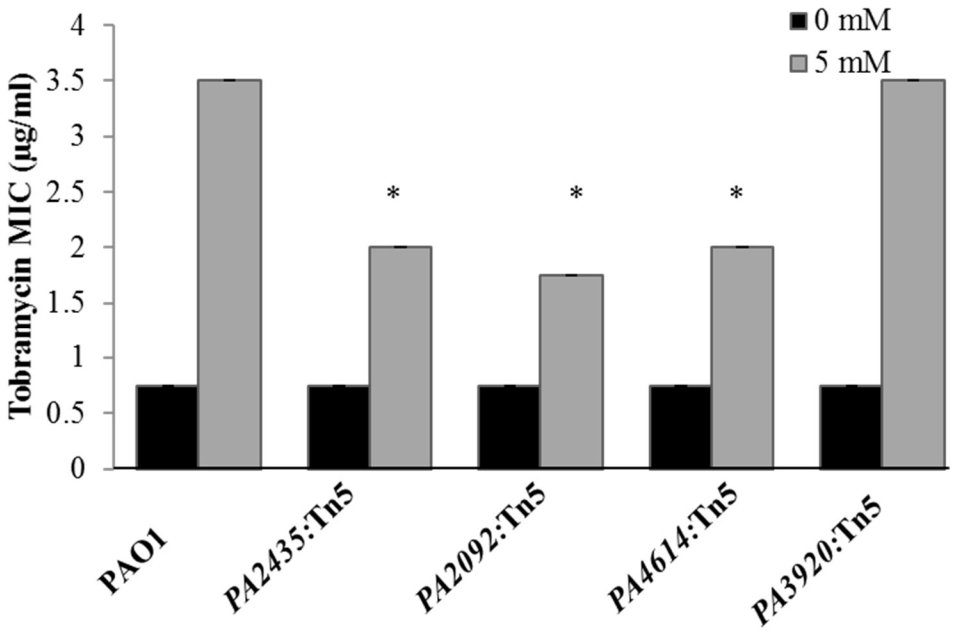

Figure 2.5: MIC of tobramycin measured for PAO1 and transposon mutants with individually disrupted putative Ca^{2+} transporters. The cells were grown in BMM without or with 5 mM Ca^{2+} with serially diluted tobramycin in 96 well plates at 37° C and slow shaking for 8 h. Cell density was measured at 600 nm. At least three biological replicates were used. Statistical significance of the difference in MIC between PAO1 and RND mutant strains was calculated using student's T-test. *, $p < 0.001$

RND efflux pumps are involved in maintenance of intracellular Ca^{2+} homeostasis

Since CzcCBA-OpmY RND system was shown to translocate ions (116), we tested whether the RND pumps involved in Ca^{2+}-induced tobramycin resistance play role in transporting Ca^{2+} and maintaining its intracellular concentration. For this, we monitored [Ca^{2+}_{in}] in the transposon mutants with disrupted *mexB*, *mexY*, *mexJ*, *muxC*, *mexE* or *czcB*. For measuring [Ca^{2+}_{in}], we used a recombinant Ca^{2+}-binding luminescence protein, aequorin. Each strain producing aequorin was cultured without Ca^{2+} or in the presence of 5 mM $CaCl_2$ and challenged with 1 mM $CaCl_2$. We chose 1 mM of Ca^{2+} primarily because in this case the available intracellular aequorin remaining after the completion of the measurements was at least 10% of the total aequorin, enabling accurate estimation of [Ca^{2+}_{in}] (72). When no $CaCl_2$ was added during growth, WT PAO1 maintained 0.3 μM ± 0.09 μM of [Ca^{2+}_{in}], which transiently increased nine fold in response to 1mM $CaCl_2$, followed by slow recovery to 1.1 ± 0.3 μM in 20 min (black line in Fig. 2.6 A-C). Disruption of *mexJ, czcB* (grey lines in Fig. 2.6 A, B), *mexB, mexY* (grey lines in Fig. S5), and *muxC* (not shown) did not affect Ca^{2+}_{in} homeostasis. However, disruption of *mexE* significantly affected the Ca^{2+}_{in} profile in PAO1. This mutant showed 35% lower transient increase of [Ca^{2+}_{in}] than the WT and generated a second transient increase before lowering the level of Ca^{2+}_{in} to the WT level (Fig. 2.6 C). When grown at 5 mM Ca^{2+}, PAO1 maintained [Ca^{2+}_{in}] at 0.3 ± 0.06 μM, which increased in response to the addition of 1 mM extracellular Ca^{2+} by eight fold (black lines in Fig. 2.6 D-

F). Then the level of [Ca^{2+}_{in}] further increased reaching 3.3 ± 0.24 μM after 20 min of monitoring. Similarly, to the cells grown without Ca^{2+}, disruption of *mexB*, *mexY,* and *muxC* (grey lines in Fig. S5) did not affect [Ca^{2+}_{in}] homeostasis in cells grown at elevated Ca^{2+}. However, disruption of *czcB* and *mexE* abolished the ability of PAO1 to maintain [Ca^{2+}_{in}] level, which began to increase rapidly after about 18 min of monitoring (Fig. 6 E, F). Disruption of *mexJ* reduced the response to Ca^{2+}, with 37% less transient increase compared to WT (Fig. 2.6 D). This level remained almost unchanged and reached only about 36% of that of WT after 20 h of monitoring.

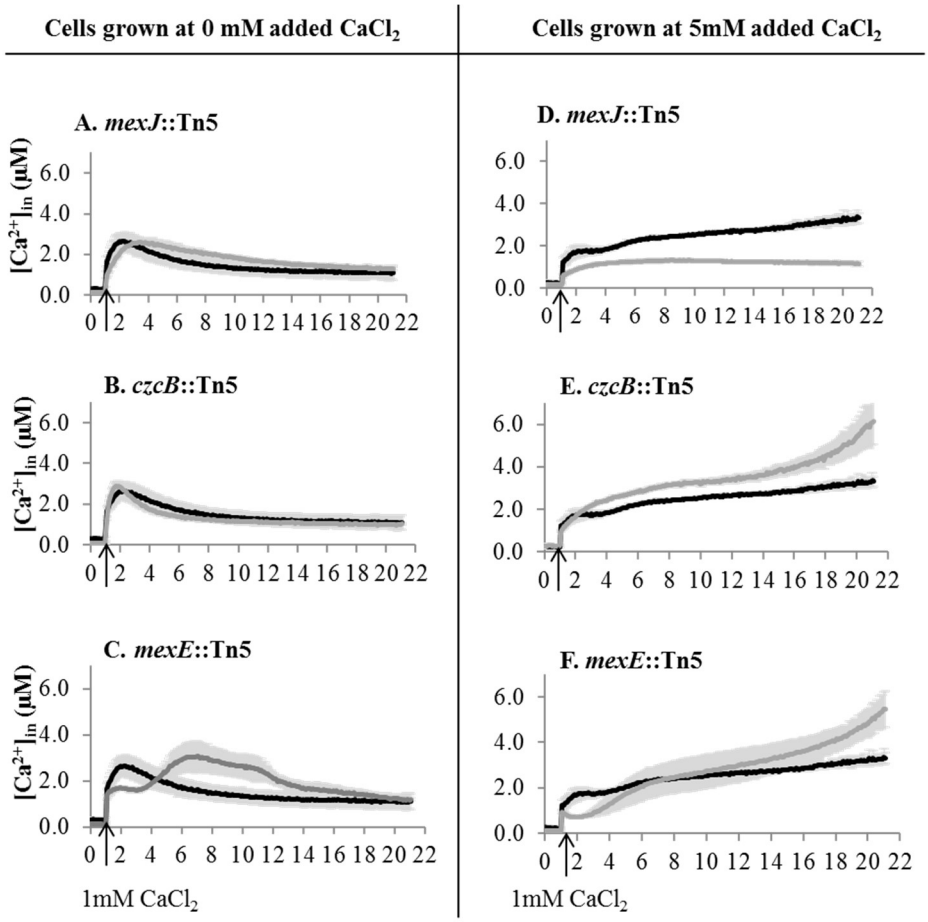

Figure 2.6: $[Ca^{2+}]_{in}$ profiles of *P. aeruginosa* PAO1 (black lines) and mutants (grey lines). **A** and **D**, *mexJ*::Tn5; **B** and **E**, *czcB*::Tn5; **C** and **F**, *mexE*::Tn5. Cells were grown in BMM media without $CaCl_2$ (A, B, and C) or with 5 mM $CaCl_2$ (D, E, and F,). 1 mM $CaCl_2$ was added at the time indicated by the arrows. Changes in free $[Ca^{2+}]_{in}$ were calculated as described in the Methods section. Data show the mean and standard deviation for at least three independent experiments.

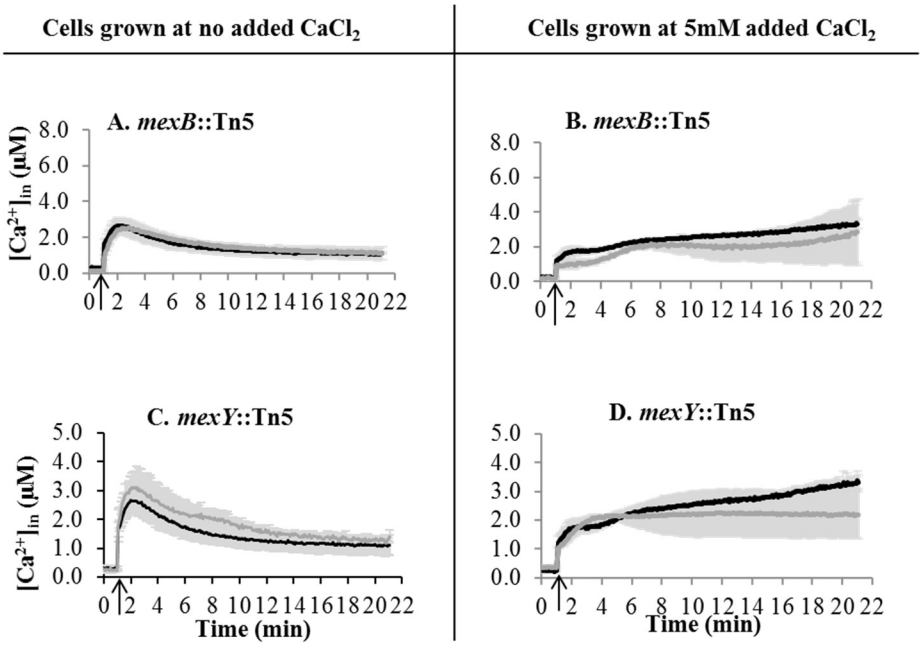

Figure 2.S5. Free $[Ca^{2+}]_{in}$ profiles of *P. aeruginosa* PAO1 (black lines) and transposon mutants (grey lines). *mexB*::Tn5 (**A** and **B**) and *mexY*::Tn5 (**C** and **D**). Cells were grown in BMM media without added $CaCl_2$ (**A** and **C**) or 5 mM $CaCl_2$ (**B** and **D**). Cells were challenged with 1 mM $CaCl_2$ at the time indicated by the arrows. Changes in free $[Ca^{2+}]_{in}$ were calculated as described in the Methods section. Data shown is the mean and standard deviation of at least two independent experiments.

Several RND transporters are involved in Ca^{2+}-induced virulence of P. aeruginosa

Our earlier studies showed that elevated Ca^{2+} induces the production of secreted virulence factors and plant infectivity in *P. aeruginosa* (74). Several RND systems exemplified by MuxABC-OpmB and MexGHI-OpmD were shown to contribute to *P. aeruginosa* virulence (38, 82). Considering the above and the presented here findings that Ca^{2+} regulates the expression of multiple RNDs and that at least three RNDs contribute to maintaining Ca^{2+}_{in} homeostasis, we tested whether any of the 12 RND transporters play role in Ca^{2+}-induced virulence of the pathogen. For this, we used lettuce leaves (*Lactuca sativa*) as an infection model and measured the disease area in the midribs of the leaves infected with PAO1 or RND transposon mutants cells grown at different Ca^{2+} levels. In agreement with our earlier observations, injecting PAO1 cells grown at 5 mM Ca^{2+} caused the disease area at least five fold greater (9 ± 0.2 cm^2) than that caused by injecting cells grown without added Ca^{2+} (1.6 ± 0.6 cm^2) (Fig. 7**).** In contrast, four mutants with disrupted *mexC, mexI, mexJ,* or *triA,* when grown at elevated Ca^{2+}, reduced their ability to cause disease by at least twofold in comparison to PAO1, but showed no significant difference in disease development when grown without added Ca^{2+}. This indicates that the RND systems contribute to Ca^{2+}-induced virulence of the pathogen. Injection of *mexB::Tn5* grown at both low and high Ca^{2+} conditions showed a significant decrease in disease development, indicating Ca^{2+}-independent

role of this transporter in *P. aeruginosa* virulence. Interestingly, mutants with disrupted *mexY, muxC, mexE, mexQ, czcB,* and particularly *mexM* showed significantly greater zones of disease development when grown and injected at no Ca^{2+}, suggesting that the maintenance of these transporters may be energetically costly for the organism and therefore reduces *P. aeruginosa* virulence (Fig. S6).

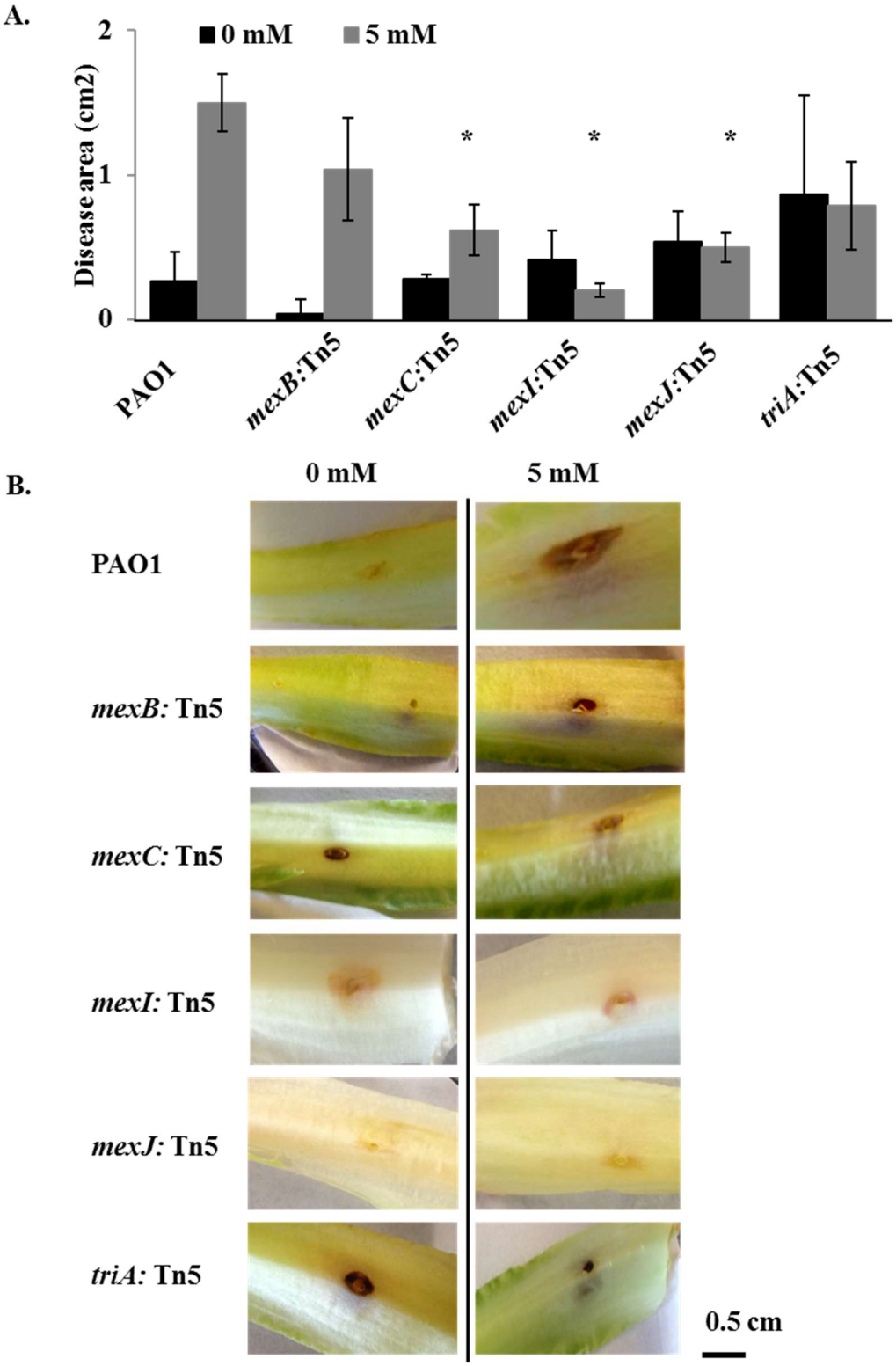
A.
0 mM
5 mM
Disease area (cm2)
2
1
0
*
*
*
PAO1
mexB:Tn5
mexC:Tn5
mexI:Tn5
mexJ:Tn5
triA:Tn5
B.
0 mM
5 mM
PAO1
mexB: Tn5
mexC: Tn5
mexI: Tn5
mexJ: Tn5
triA: Tn5
0.5 cm

Figure 2.7: The role of RND transporters in Ca^{2+}-induced infectivity of *P. aeruginosa*. Cells were grown without or with 5 mM Ca^{2+}, harvested during mid-log, normalized with 10 mM $MgSO_4$ solution without or with 5 mM Ca^{2+}, and injected into sterilized mid ribs of lettuce leaves. $MgSO_4$ with or without Ca^{2+} was injected as a negative control. The disease area was calculated by multiplying the length and width of the zone of apparent necrosis. **A**. The disease area (cm^2) on lettuce leaf midribs caused by PAO1 and the RND transporter mutants. **B**. Representative photographs of the infected lettuce leaves. Statistical significance of the difference in disease area between PAO1 and RND mutant strains grown at 5 mM Ca^{2+} was calculated using student's T-test. *, $p < 0.05$

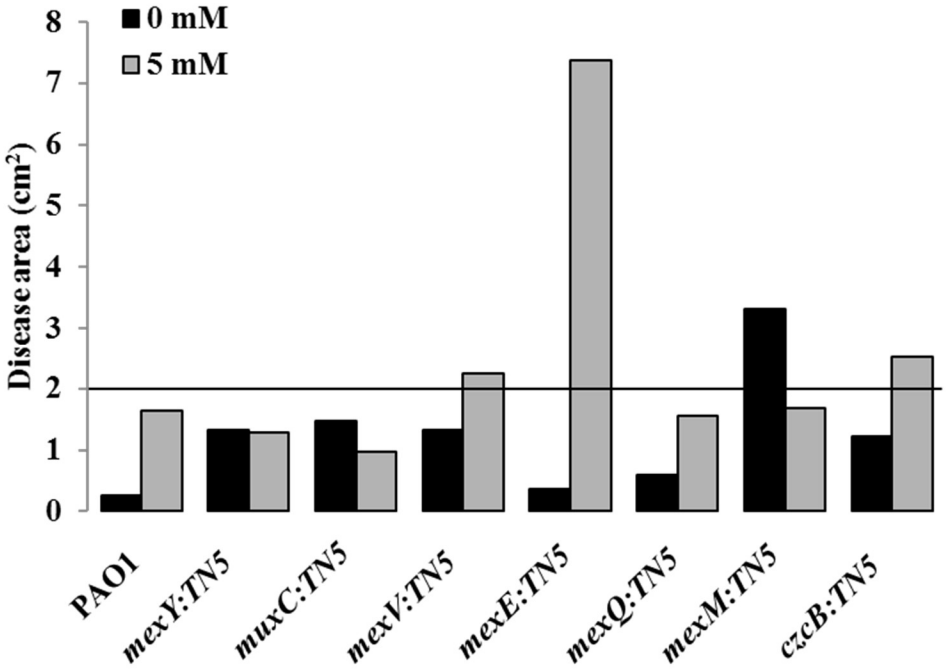

Figure 2.S6: The role of RND transporters in Ca^{2+}- induced plant infectivity of PAO1. The cell cultures were grown without or with 5 mM Ca^{2+}, collected at the middle log phase, normalized to OD600 of 0.1 and injected into sterilized mid ribs of lettuce leaves. $MgSO_4$ with or without Ca^{2+} was injected as a negative control. Disease area was calculated by multiplying the length and width of the apparent necrosis.

DISCUSSION

Pseudomonas is one of the leading causes of severe and life threatening infections in patients with compromised immune system, CF patients, patients with burn wounds, chronic obstructive pulmonary diseases, endocarditis, etc. At present, several types of antibiotics including aminoglycosides are considered to be an effective choice for treating *Pseudomonas* infections (26, 27, 117). However, the increasing resistance of *P. aeruginosa* to most available antimicrobials represents a serious threat and requires a new knowledge of the mechanisms of resistance and their regulation in response to host factors. Here we show that Ca^{2+} at the concentration commonly detected in CF lungs (67, 87), increases *P. aeruginosa* resistance to tobramycin. Proteomic and transcriptomic analyses determined that Ca^{2+} regulates the expression of several RND family efflux pumps, six of which are involved in Ca^{2+}-induced tobramycin resistance. This regulation is mediated *via* transient changes in the intracellular Ca^{2+} levels (summarized in Fig. 2.8). Such response to Ca^{2+}, one of the host factors, exemplifies a successful adaptation strategy that is regulated by Ca^{2+} signaling and leads to the increased resistance and fitness of the pathogen.

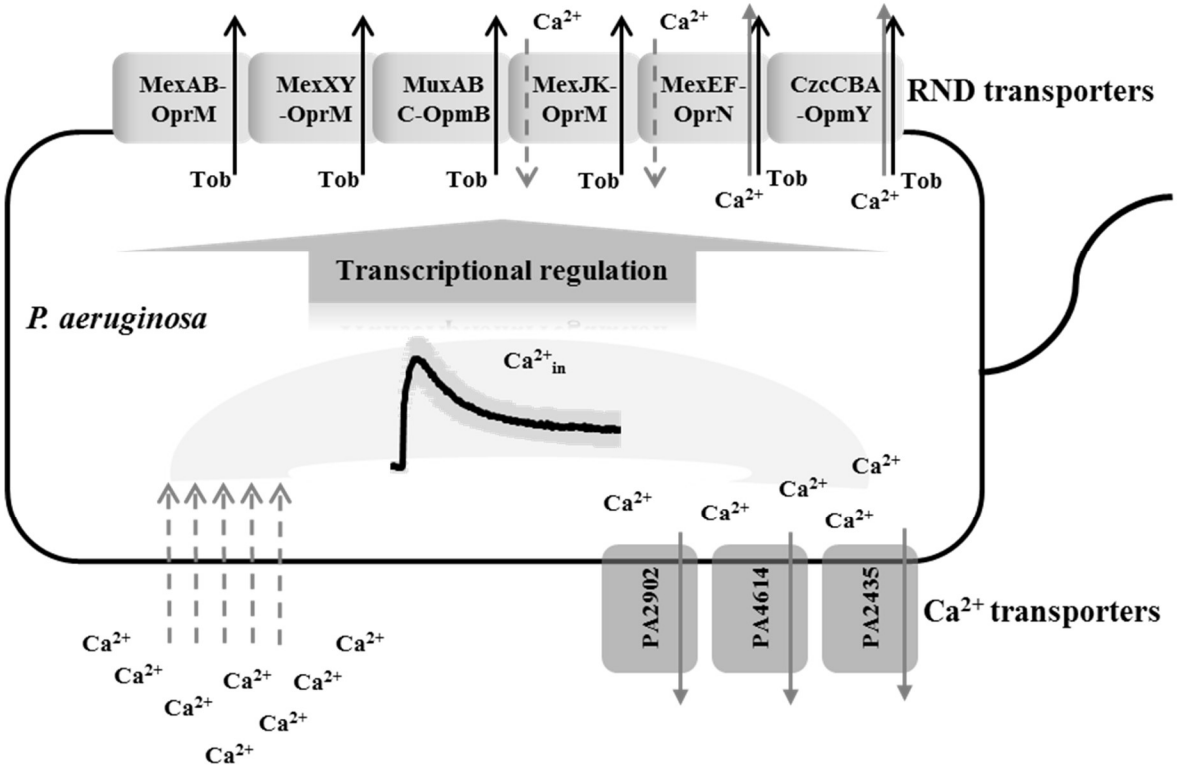

Figure 2.8: The proposed model of Ca^{2+} regulation of tobramycin resistance in *P. aeruginosa.* Elevation of extracellular Ca^{2+} causes a transient spike in $[Ca^{2+}]_{in.}$ Several Ca^{2+} transporters from different families, including PA2902, PA4614, and PA2435 (72), and three RND systems (MexJK-OprM, MexEF-OprN, CzcCBA-OpmY) contribute to the maintenance of $Ca^{2+}{}_{in}$ homeostasis. The intracellular Ca^{2+} signal (both the amplitude and the duration of $[Ca^{2+}]_{in}$ increase) regulates the transcription of several efflux pumps involved in Ca^{2+}-induced tobramycin resistance (MexAB-OprM, MexXY-OprM, MuxABC-OpmB, MexJK-OprM, MexEF-OprN, CzcCBA-OpmY). Black solid arrows: tobramycin efflux, grey solid arrows: Ca^{2+} efflux, grey dashed arrows: Ca^{2+} influx.

Ca^{2+} enhancement of *P. aeruginosa* resistance to aminoglycosides has been shown before (24, 91). Increased efflux and decreased membrane permeability have been suggested as major contributing factors (95). It has been proposed that divalent cations, such as Ca^{2+} and Mg^{2+}, are attracted by the negatively charged binding sites on the outer membrane surface, where cationic antibiotics, including aminoglycosides, would bind. Due to comparatively smaller size of the divalent cations, upon binding, they stabilize the membrane and inhibit the self-promoted uptake of antibiotics (24). It has also been identified that the antagonistic effect of Mg^{2+} and Ca^{2+} on aminoglycoside resistance in *P. aeruginosa* requires the presence of functional MexXY RND transporter (95). Our data confirmed that MexXY-OprM is a major determinant of *P. aeruginosa* aminoglycoside resistance, the lack of which abolishes resistance to tobramycin at both Ca^{2+} conditions. In addition, we detected five other RND systems (MexAB-OprM, MuxABC-OpmB, MexEF-OprN, MexJK-OprM, and CzcCBA) to be involved in Ca^{2+}-induced tobramycin resistance, of which the first two and MexXY-OprM also contribute to tobramycin resistance at low Ca^{2+}. Most of these RND transporters have a broad specificity. For example, MexAB-OprM is known to transport chemically diverse compounds, including cephems, meropenems, fluoroquinolones (18), nalidixic acid (53) tigarcillin (118), ethidium bromide (119) and quorum sensing (QS) signaling molecules (42, 120). MexXY-OprM pumps aminoglycosides, fluoroquinolones, macrolides, and tetracyclines (121-123). MuxABC-OpmB is required for

ampicillin and carbanicillin resistance and was found associated with virulence traits of PAO1, including plant infectivity and twitching motility (82). MexEF-OprN is known to export low levels of ciprofloxacin (39) and a Pseudomonas Quinolone Signal (PQS) precursor, HHQ (4-hydroxy-2-heptylquinoline) (78, 79). MexJK-OprM transports erythromycin and triclosan (124). CzcCBA is the only RND system involved in metal ion efflux, maintaining the heavy metal homeostasis in *P. aeruginosa* and other Gram-negative bacteria (41, 125). However, none of these systems, except for MexXY, have been shown to be associated with Ca^{2+} regulation or Ca^{2+}- regulated processes in bacteria.

Most RND pumps with the exception of *mexAB-oprM,* known to be constitutively expressed in model strains (126), are highly inducible by diverse factors, including antibiotics, (Table 2). Multiple RND systems, such as MexAB-OprM and MexXY, as well as MexEF-OprN and MexJK, can be simultaneously overexpressed in clinical samples from patients undergoing antibiotic treatments (35, 127). Here we report the effect of host levels of Ca^{2+} on the expression of at least seven *P. aeruginosa* RND systems. Although RT-qPCR of mid-log cells only detected elevated transcription of *mexV,* which was not involved in Ca^{2+}-induced resistance, the promoter activities measured over time were increased in a growth-phase-dependent manner for five RND systems, involved in Ca^{2+}-induced tobramycin resistance. The changes were transient and mostly occurring during the transitions between different growth phases, indicating the importance of these

transporters in the growth-related physiological rearrangements of this bacterium. Interestingly, the highest activity increase in response to both Ca^{2+} and tobramycin was observed for the promoter of *mexAB-oprM,* mostly known as constitutively expressed in laboratory strains (126). These data suggest that (1) the involvement of several RND transporters in Ca^{2+}-induced tobramycin resistance is likely due their elevated transcription in response to Ca^{2+}; (2) it is important to measure temporal changes in gene expression for a more accurate characterization of cellular transcriptional profile.

In our and others earlier studies, bacteria were shown to generate intracellular Ca^{2+} transients in response to several environmental and physiological conditions, including extracellular Ca^{2+}, nitrogen starvation, oxidative stress, and carbohydrate metabolism (47, 72). We also showed that changes in Ca^{2+}_{in} level have a regulatory effect on multiple aspects of *P. aeruginosa* physiology (71, 72). Here we explored the role of Ca^{2+}_{in} homeostasis in mediating the regulatory effect of Ca^{2+} on RND transcription. First, we showed that *P. aeruginosa* does not produce any changes in the $[Ca^{2+}]_{in,}$ in response to tobramycin, clarifying that the antibiotic alone does not trigger intracellular Ca^{2+} signaling. Second, we determined that three out of six RND pumps, contributing to Ca^{2+}-induced tobramycin resistance, play role in maintaining Ca^{2+}_{in} homeostasis, particularly in the cells grown at elevated extracellular Ca^{2+}. MexJK is likely involved in Ca^{2+} uptake, CzcCBA – in Ca^{2+} efflux, and MexEF – possibly, in both, This is a novel observation, since

although RND systems are known to efflux chemically diverse substances (Table 2.2), only CzcCBA-OpmY has been shown to maintain flux of several divalent cations, such as copper, cobalt, cadmium, nickel, and zinc, but not Ca^{2+} or Mg^{2+} (41, 128, 129). However, the contribution of this ability of MexJK, MexEF, and CzcCBA to the regulatory role of Ca^{2+}_{in} is not clear and warrants further studies. Third, we showed that the mutants with disrupted putative Ca^{2+} transporters, PA2435, PA2092, PA4614, which, as shown in our earlier studies, fail to recover the elevated [Ca^{2+}_{in}] to the basal level (72), decreased resistance to tobramycin at least twofold. Furthermore, one of them, *PA2435:Tn5,* showed a significantly lower Ca^{2+}-induced *mexAB-oprM* promoter activity. These observations support the hypothesis that the Ca^{2+}_{in} response i.e. a combination of both the amplitude and the duration of $[Ca^{2+}]_{in}$ changes, mediates Ca^{2+} regulation of Ca^{2+}-induced tobramycin resistance.

Table 2.2. Fold change in transcript abundance for *P. aeruginosa* PAO1 RND genes in response to different stimuli.

RND transport system	Gene name	[a]SIC of TOBR in biofilm (37)	[a]SIC of TOBR in planktonic cells (37)	[a]Oxidative stress (130)	[a]Cu^{2+} shock (131)	[a]SIC of AZ (36)	MDR HAI isolates[b] (35)	MDR CF isolates[b] (127)
MexAB-OprM	*mexB*	0.3	1.1	**1.5**	1.2	0.4	6.2	**2**
MexCD-OprJ	*mexC*	**1.9**	**2.5**	0.9	**2.3**	**61**	**83**	
MexXY-OprM	*mexX*	1.4	0.8	**1.8**	**2.3**	**25.7**	**5,880**	**5**
MuxABC-OpmB	*muxC*	0.3	0.9	**1.5**	0.6	1.1		
MexVW-OprM	*mexV*	**1.5**	0.9	1.0	**1.7**	**1.8**	**583**	
MexGHI-OpmD	*mexI*	1.3	**1.9**	1.0	**1.7**	0.1		
MexEF-OprN	*mexE*	**1.5**	**5.0**	**2.7**	0.7	0.7	**35.9**	
MexPQ-OpmE	*mexQ*	1.1	**1.5**	**1.7**	**65.8**	0.3		
MexJK-OprM	*mexJ*	**1.8**	1.1	1.2	**3.0**	**3.9**	4.2	

MexMN-OprM	*mexM*	**1.7**	0.9	1.4	**3.7**	1.1
TriABC-OpmH	*triA*	1.4	0.8	1.2	1.0	0.2
CzcCBA	*czcB*	**1.9**	0.3	1.3	**3.6**	1.4

The increased abundances of transcripts 1.5 fold and above are shown in bold.

[a]The data were collected from the Geo profiles at http://www.ncbi.nlm.nih.gov/geoprofiles.

[b]Fold change in expression compared to that of PAO1. Only the highest fold change in expression level is mentioned.

SIC, Sub-inhibitory concentration. TOBR, Tobramycin. AZ, Azithromycin. MDR, Multidrug resistant. HAI, Hospital acquired infection.

Recently, Mg^{2+}-dependent two-component system ParRS was shown to positively regulate the transcription of two RND efflux pumps MexXY-OprM and MexEF-OprN (132, 133), which we showed to be involved in Ca^{2+} regulated tobramycin resistance. However, disruption of *parR* did not affect Ca^{2+}–induced tobramycin resistance (data not shown). On the other hand, the disruption of two putative Ca^{2+}-binding proteins, CarP and CarO, that play role in the development of intracellular Ca^{2+} responses and whose expression is positively regulated by Ca^{2+}-dependent two-component system CarSR, reduced Ca^{2+} induction of tobramycin resistance (70). This suggests a possible role of Ca^{2+} recognizing two component regulatory system CarSR in regulating Ca^{2+} responses in *P. aeruginosa*, including Ca^{2+}-induced tobramycin resistance.

Finally, we identified that four RNDs: MexCD-OprJ, MexGHI-OpmD, MexJK-OprM, and TriABC-OpmB contribute to Ca^{2+}-induced plant infectivity, of which only MexJK-OprM responded to Ca^{2+} and was involved in Ca^{2+}_{in} homeostasis and tobramycin resistance. The involvement of RND systems in virulence of diverse bacteria has been reported before (134-136), which is mostly due to their role in transporting virulence factors or signaling molecules regulating virulence. In *P. aeruginosa,* several RNDs were shown play role in virulence, including detected here MexCD-OprJ and MexGHI-OpmD (38, 44, 55). The involvement of the RND transporters in Ca^{2+}-enhanced plant infectivity of the

pathogen may be a cumulative result of multiple factors, including Ca^{2+}-regulated transcription of the RND genes or the genes encoding virulence factors.

Overall, as summarized in Fig. 8, elevation of extracellular Ca^{2+} causes a transient increase in $[Ca^{2+}]_{in}$, which regulates the transcription of several efflux pumps involved in Ca^{2+}-induced tobramycin resistance or infectivity. This illustrates a novel mechanism of *P. aeruginosa* adaptive resistance that relies on a large set of RND efflux systems regulated in response to host elevated Ca^{2+}.

ACKNOWLEDGEMENTS

We thank Dr. Steve Hartson and Janet Rogers at the OSU Proteomic Facility for performing MS-based protein identification and analyses. We thank the RT-qPCR core facility at the OSU Department of Botany for support and instrumentation. We also thank Drs. Peter Hoyt and Hong Hwang at the Biochemistry and Molecular Biology Array and Bioinformatics core facility for their help with RNA analyses. We would like to thank Dr. Kangmin Duan at University of Manitoba, Winnipeg, Canada and Dr. Meng Meng Dong at the college of Life Science, Northwest University, Shaanxi, China for sharing several promoter activity reporter plasmids. Undergraduate researchers, Laurel Meysing and Afom Bokre performed PCR-confirmation of the UW transposon mutants and transformation with aequorin encoding plasmid. This work was partially supported

by the Grant-in-Aid from American Heart Association (Award #09BGIA2330036), OCAST (Award #HR12-167) and summer dissertation fellowship, OSU.

CHAPTER III

INTRACELLULAR CALCIUM TRANSIENTS REGULATE ANTIBIOTIC RESISTANCE AND VIRULENCE IN *PSEUDOMONAS AERUGINOSA*

Manita Guragain*, Sharmily Khanam*, Michelle King, Brian Cougar, Hannah Wendelbo, and Marianna A. Patrauchan[#]

Department of Microbiology and Molecular Genetics, Oklahoma State University, Stillwater, OK, US

*Authors have equal contribution

ABSTRACT

Calcium (Ca^{2+}) is a major second messenger regulating essential processes in eukaryotes. However, the regulatory role of intracellular Ca^{2+} in prokaryotes has not been experimentally proven. Our earlier studies established the global effect of elevated Ca^{2+} on gene expression of *Pseudomonas aeruginosa,* a human pathogen causing severe acute and chronic infections. We have also established that *P. aeruginosa* maintains low free intracellular Ca^{2+} level, which transiently increases in response to extracellular Ca^{2+}. These findings suggested that intracellular Ca^{2+} transients play a regulatory role in Ca^{2+} global responses. Here we report identification of a putative Ca^{2+} channel, PA2604, designated as CalC, that is required for the development of transient increases in $[Ca^{2+}]_{in}$ in *P. aeruginosa*. Genome-wide RNA-Seq analysis revealed that PA2604 is involved in Ca^{2+} regulation of at least 800 genes. These genes include those involve in biosynthesis of siderophores, LPS, peptidoglycan, lipid A modification, phosphate metabolism, and global regulators of virulence factors required for the development of the pathogen's chronic infections. Furthermore, disruption of PA2604 abolished regulatory effect of Ca^{2+} on the transcription of multidrug efflux pump *mexAB-oprM* required for Ca^{2+}-induced tobramycin resistance in PAO1. We have also established that Ca^{2+} regulates transcription of PA2604 *via* Ca^{2+} responsive two-component regulator, CarRS, and Ca^{2+}-binding EF hand protein, EfhP. The results provide the first experimental evidence of intracellular Ca^{2+} signaling in

prokaryotes and identify the components of intracellular Ca^{2+} regulatory network controlling the virulence and antibiotic resistance of *P. aeruginosa*.

INTRODUCTION

Calcium ions (Ca^{2+}) represent one of the most essential secondary messengers in eukaryotes, which regulates many vital cellular processes including cell cycle, apoptosis, transport, motility, and metabolism (reviewed in (47)). Therefore, even slight abnormalities in cellular Ca^{2+} homeostasis may cause human diseases, including diseases associated with bacterial infections, such as cystic fibrosis (CF) pulmonary infections and endocarditis (137). As a result of such abnormal Ca^{2+} homeostasis, CF patients accumulate Ca^{2+} in airway epithelia, pulmonary and nasal liquids (67, 138). There is growing evidence suggesting that Ca^{2+} also plays a significant role in the physiology of bacteria by regulating gene expression, providing structural support or activating enzyme activities. The affected processes include maintenance of cell structure, motility, chemotaxis, cell division and differentiation, transport, and spore formation (139-143). It has been shown that extracellular Ca^{2+} regulates expression of a large number of genes involved in such global aspects of bacterial life as general metabolism (electron transport chain, RNA synthesis, protein synthesis/degradation, and carbohydrate metabolism), lifestyle switch and physiological adaptations (spore formation, heterocyst formation, chemotaxis, swarming motility, biofilm formation, iron acquisition, oxidative stress response, and quorum sensing), as well as transport and virulence (T3SS, extracellular proteases, alginate, and toxins) (144-148).

Mechanisms of Ca^{2+} signaling are well studied in eukaryotes. Eukaryotic cells tightly regulate the intracellular calcium concentration $[Ca^{2+}]_{in}$, which transiently changes in response to various stimuli. These transient changes in $[Ca^{2+}]_{in}$ serve as the informational input that is decoded by Ca^{2+}-binding sensors and further transduced *via* protein-protein interactions and post-translational modifications to regulate various cellular processes. Similarly, prokaryotes appear to possess all the prerequisites necessary for using intracellular Ca^{2+} as a mean for informational networking. In addition to the global regulatory effect of fluctuations in environmental Ca^{2+} outlined above, bacteria possess Ca^{2+} transporters, Ca^{2+} storage structures, and calmodulin like Ca^{2+} binding proteins. Furthermore, several bacteria have been shown to maintain $[Ca^{2+}]_{in}$ at sub-micromolar levels produce Ca^{2+} transients in response to environmental and physiological factors (72, 142, 149). Overall, this suggests that bacteria may possess a prototype Ca^{2+} signaling. However, the experimental evidence proving that changes in $[Ca^{2+}]_{in}$ play a regulatory role is still missing.

Pseudomonas aeruginosa is a facultative pathogen and a leading cause of severe nosocomial infections in both immunocompetent and immunocompromised patients (150, 151). *P. aeruginosa* is one of the primary organisms that form biofilms on airway mucosal epithelium of patients with cystic fibrosis (CF) where it contributes to airway blockage and cellular damage. *P. aeruginosa* also causes infective endocarditis and device-related infections with high morbidity and

mortality rates (152-154). *P. aeruginosa* biofilm infections are increasingly difficult to treat with traditional antibiotic therapy, and are often not eradicated by host defense processes (155, 156). Our earlier studies revealed that growth in high Ca^{2+} enhances biofilm formation (146), swarming motility (72), and plant infectivity of *P. aeruginosa* (157). In search of the mechanisms, we showed that Ca^{2+} modulates the expression of a large number of genes including those responsible for production of secreted virulence factors (pyocyanin, rhamnolipid, alginate, extracellular proteases), adaptation to host environment (iron acquisition, oxidative stress response, nitrogen metabolism), antibiotic resistance (multidrug efflux), and quorum sensing signaling (73, 158). We established that *P. aeruginosa* maintains submicromolar level of $[Ca^{2+}]_{in}$, which is transiently increased in response to elevated external Ca^{2+} and identified four putative Ca^{2+} transporters required for $[Ca^{2+}]_{in}$ homeostasis (72). The disruption of these transporters impaired multiple Ca^{2+}-regulated traits, including antibiotic resistance and virulence factor production. Finally, we identified several putative Ca^{2+} binding proteins, including calmodulin like EfhP (157), that mediate Ca^{2+} responses in *P. aeruginosa*. Based on these findings we hypothesized that intracellular Ca^{2+} serves as a second messenger regulating Ca^{2+}-dependent physiology. Here we provide the first direct experimental evidence confirming the regulatory link between the intracellular Ca^{2+} transients and Ca^{2+} response. We identified PA2604, a homolog of *B. subtilis* Ca^{2+} leak channel (159, 160), to be responsible for generating the intracellular Ca^{2+}

transient increase in response to extracellular Ca^{2+}. We designated it CalC, calcium channel, and characterized its role in genome-wide transcriptional response to elevated external Ca^{2+}. We also studied the effect of Ca^{2+} on transcription of PA2604 and the role of several Ca^{2+} responsive regulators in mediating this response. The results support the hypothesis that the transient changes in the intracellular [Ca^{2+}] are required for regulating the physiological response to Ca^{2+} manifested in Ca^{2+}-induced virulence in *P. aeruginosa* and therefore confirm that intracellular Ca^{2+} plays a signaling role in *P. aeruginosa*.

MATERIALS AND METHODS

Bacterial strains, plasmids and media and chemicals.

Strains and plasmids used in this study are listed in **Table 3S1**. *P. aeruginosa* strain PAO1 used in this study is the non-mucoid strain with genome sequence available. Biofilm minimal media (BMM) (146) contained (per liter): 9.0 mM sodium glutamate, 50 mM glycerol, 0.02 mM $MgSO_4$, 0.15 mM NaH_2PO_4, 0.34 mM K_2HPO_4, and 145 mM NaCl, 20 µl trace metals, 1 ml vitamin solution. Trace metal solution (per liter of 0.83 M HCl): 5.0 g $CuSO_4.5H_2O$, 5.0 g $ZnSO_4.7H_2O$, 5.0 g $FeSO_4.7H_2O$, 2.0 g $MnCl_2.4H_2O$). Vitamins solution (per liter): 0.5 g thiamine, 1 mg biotin. The pH of the medium was adjusted to 7.0. Cells were first grown in 5 ml tubes for 16 h (mid-log) and then used to inoculate (0.1%) 100

ml fresh medium in 250 ml flasks. The cultures were grown to mid-log or stationary phase and harvested by centrifugation. Transposon insertion mutants were obtained from the University of Washington Two - Allele library (98) (NIH grant # P30 DK089507) (**Table 3.S1**).

TABLE 3.S1: Strains and plasmids used in this study

Strains/Plasmids	Description	Reference
Strains		
P. aeruginosa PAO1	Wild type sequenced strain	(161)
calC::Tn5	PW5376 PA2604-G04::ISPhoA/hah	(98)
PA5056::Tn5	PW9491 lacZbp03q3G11	(98)
PA5058::Tn5	PW9495 phoAwp10q1D06	(98)
PA5241::Tn5	PW9824 phoAwp03q3A10	(98)
PAO1:pMS402	PAO1 with promoterless pMS402	(82)
PAO1:P*mexAB-oprM*	PAO1 with PmexBA-orM	(82)
calC::Tn5:pMS402	*calC::Tn5* with promoterless pMS402	This study

calC::Tn5: P*mexAB-oprM*	*calC::Tn5* with PmexBA-orM	This study
ladS :: Tn5	PW7727 phoAwp05q1G04	(98)
ladS :: Tn5	PW7726 phoAwp03q1D01	(98)
ΔcarR	PAO1 with deletion of *carS* gene.	(70)
ΔcarP	PAO1 with deletion of *carP* gene.	(70)
ΔcarO	PAO1 with deletion of *carO* gene.	(70)
ΔefhP	PAO1 with deletion of *efhP gene*	(71)
ΔbfmR	PAO1 with deletion of *bfmR* gene.	(162)
ΔlasR (lasR:Gm)	PAO1 with deletion of *lasR* gene	(163)
ladS :: Tn5 / pMS402	*ladS::Tn5* with promoterless pMS402	This study
ladS :: Tn5 / pSK-2604F	*ladS::Tn5* with pSK2604F	This study
ΔcarR / pMS402	*ΔcarS* with promoterless pMS402	This study
ΔcarR / pSK2604F	*ΔcarS* with with pSK2604F	This study
ΔcarP / pMS402	*ΔcarP* with promoterless pMS402	This study
ΔcarP / pSK2604F	*ΔcarP* with with pSK2604F	This study
ΔcarO / pMS402	*ΔcarO* with promoterless pMS402	This study
ΔcarO / pSK2604F	*ΔcarO* with with pSK2604F	This study
ΔefhP / pMS402	*ΔefhP* with promoterless pMS402	This study
ΔefhP / pSK2604F	*ΔefhP* with with pSK2604F	This study
ΔbfmR / pMS402	*ΔbfmR* with promoterless pMS402	This study

ΔbfmR / pSK2604F	*ΔbfmR* with with pSK2604F	This study
ΔlasR / pMS402	*ΔlasR* with promoterless pMS402	This study
ΔlasR / pSK2604F	*ΔlasR* with with pSK2604F	This study
PAO1 / CTX6.1	PAO1 transformed with promoter activity reporter empty plasmid CTX6.1	(164)
PAO1 / CTX-rsmA	PAO1 electroporated with promoter activity reporter construct for *rsmA*	(164)
PAO1 / CTX-rsmZ	PAO1 electroporated with promoter activity reporter construct for *rsmZ*	(164)
calC::Tn5 / CTX6.1	*calC::Tn5* transformed with promoter activity reporter empty plasmid CTX6.1	(164)
calC::Tn5 / CTX-rsmA	*calC::Tn5* electroporated with promoter activity reporter construct for *rsmA*	(164)
calC::Tn5 / CTX-rsmZ	*calC::Tn5* electroporated with promoter activity reporter construct for *rsmZ*	(164)
Plasmids		
pMMB66EH-AEQ	pMMB66EH plasmid containing aequorin gene from *Aequorea Victoria*	(165)
pMS402	Expression reporter plasmid carrying promoterless luxCDABE	(82)

	gene, ori of pRO1615. Kan^R, Tmp^R.	
pSK2604	Promoter region of PA2604 cloned upstream of lux operon on pMS402,	This study
CTX 6.1	Integration plasmid origins of plasmid mini-CTX-*lux*; Tcr	(164)
CTX-*rsmA*	Integration plasmid, CTX6.1 with a fragment of pKD-*rsmY* containing *rsmA* promoter region and *luxCDABE* gene; Kn, Tmp, Tc	(164)
CTX-*rsmZ*	Integration plasmid, CTX6.1 with a fragment of pKD-*rsmY* containing *rsmZ* promoter region and *luxCDABE* gene; Kan^R, Tmp^R, Tc^R.	

The mutants contained ISphoA/hah or ISlacZ/hah insertions with tetracycline resistance cassette that disrupted the genes of interest. The mutations were confirmed by two-step PCR: first, transposon flanking primers were used to verify that the target gene is disrupted, and second, gene-specific primers listed in **Table 3.S2**, were used to confirm the transposon insertion. The primer sequence is available at www.gs.washington.edu. For convenience, the mutants were designated as PA::Tn5, where PA is the identifying number of the disrupted gene from *P. aeruginosa* PAO1 genome (www.pseudomonas.com). Coelenterazine was purchased from Life Technologies (California, USA). Primers were obtained from Integrated DNA technologies.

Table 3.S2: Primers used in this study

Primer name	Sequence (5′- 3′)	Ref.
49172F.f	GGAAGAGTCTCCCCTTCGAC	(98)
49172F.r	TAGAAGAACAGGCGGACGAT	(98)
Aeq-Forward	CTTACATCAGACTTCGACAACCCAAG	(72)
Aeq-reverse	CGTAGAGCTTCTTAGGGCACAG	(72)
PA2604F-F	AAC**CTCGAG**GGTGTGGGTACTCCTTAAC	This study
PA2604F-R	CC**GGATCC**GACCGTTGCCTTAAACC	This study

Enzyme Restriction sites *(Hind*III*, Sac*I*, Xho*I and *Bam*HI) are incorporated (Bold) in the primer to facilitate cloning.

Estimation of Free Intracellular Calcium ($[Ca^{2+}]_{in}$).

PAO1 and mutants were transformed with pMMB66EH (courtesy of Dr. Delfina Dominguez and Dr. Anthony Campbell), carrying aequorin (107) and carbenicillin resistance genes, using a heat shock method described in (108). The transformants were selected on Luria bertani (LB) agar containing carbenicillin (300 µg/ml) and verified by PCR using aequorin specific primers Aeq-Forward and Aeq-Reverse (**Table S2**). Aequorin was expressed and reconstituted as described in (72). Briefly, mid-log phase cells were induced with IPTG (1 mM) for 2 h for apoaequorin production, and then harvested by centrifugation at 5,232 g for 5 min at 4°C. Aequorin was reconstituted by incubating the cells in the presence of 2.5 µM coelenterazine for 30 min.

Luminescence measurements and estimation of free $[Ca^{2+}]_{in}$ were performed as described in (72) with slight modifications. Briefly, 100 µl of cells with reconstituted aequorin were equilibrated for 10 min in the dark at room temperature. Luminescence was measured using Synergy Mx Multi-Mode Microplate Reader (Biotek) at the interval of 5 min. For basal level of $[Ca^{2+}]_{in}$, the measurements were recorded for 1 min, then the cells were challenged with 1 mM Ca^{2+} and the luminescence was recorded for next 20 min. $[Ca^{2+}]_{in}$ was calculated by using the formula $pCa = 0.612(-\log_{10}k)+3.745$, where k is a rate constant for

luminescence decay (s^{-1}) (109). The aequorin standard curve was shared by Dr. Anthony Campbell. The results were normalized against the total amount of available aequorin as described in (72). The discharge was performed by permeabilizing cells with 2% Nonidet 40 (NP40) in the presence of 12.5 mM $CaCl_2$. The luminescence released during the discharge was monitored for 10 min at 5 sec intervals. Injection of buffer alone was used as a negative control, and did not cause any significant fluctuations in $[Ca^{2+}]_{in.}$ The estimated remaining available aequorin was at least 10% of the total aequorin. The experimental conditions reported here were optimized to prevent any significant cell lysis.

Sequence analysis

Sequence homology searches were performed using the NCBI nr database (GenBank release 160.1). Functional domains were predicted using Pfam 31.0. Protein subcellular localization was predicted using pSORTb v3.0 analysis. Predictions of transmembrane helices and signal peptides were performed using TMHMM and SignalP 4.0, respectively. Protein three-dimensional (3D) structure was predicted using iTASSER and SWISS-MODEL and visualized using PyMOL (version 1.8.6.0; Schrödinger, LLC)

Swarming motility assay

Swarming motility was assayed as described in (72). Briefly, PAO1 and mutants were grown in BMM at no added or 5 mM Ca^{2+}. 2 µl of the mid-log cultures normalized to the OD_{600} of 0.3 were spot inoculated onto the surface of BM2 swarm agar (166). After inoculation, the plates were incubated at 37°C for 15 h and the colony diameters were measured. The effect of Ca^{2+} was calculated as a fold difference (ratio) between the diameters of the colonies grown at 5 mM and no added Ca^{2+}.

Pyoverdine assay

Production of pyoverdine was assessed by measuring fluorescence intensity emitted at wavelength of 460 nm following the excitation at 400 nm as described in (55, 167, 168). Mid-log phase bacterial cultures grown in BMM were normalized to OD600 of 0.3. 100 µl of normalized culture was inoculated into 100 mL of BMM and grown at 37°C with shaking 200 rpm until mid-log (12 h) and late stationary phase (24 h). After the OD_{600} of the cultures was measured, cells were pelleted, and the collected supernatants were analyzed for pyoverdine fluorescence. The fluorescence values were normalized by the corresponding cell density measured at OD_{600}.

Antibiotic susceptibility assays

P. aeruginosa resistance to tobramycin and polymyxin B (Pol-B) was assayed as described in (43) . PAO1 and mutants were grown in BMM at no added or 5 mM Ca^{2+}. 100 µl of the mid-log cultures normalized to the OD600 of 0.1 were spread inoculated onto the surface of BMM agar containing no added or 5 mM Ca^{2+}. E-test strips for tobramycin or Pol-B (Biomeurix) were placed on the surface of the inoculated plates and incubated at 37 ^{0}C for 24 h. The minimum inhibitory concentration (MIC) was measured as a point at which the edge of the zone of inhibition crosses the e-test strip. The effect of Ca^{2+} was calculated as a fold difference (ratio) between the MIC at 5mM *vs*. no added Ca^{2+}.

For plate dilution assay, middle log cultures grown in BMM with or without added Ca^{2+} were normalized to OD_{600} of 0.3, and inoculated at 1:100 ratio into BMM with the corresponding Ca^{2+} concentration with or without tobramycin. Considering the earlier established Ca^{2+}-induced tobramycin resistance in *P. aeruginosa* (43), tobramycin was added at the final concentration of 0.25, 0.5, 0.75, 0.1, 1.5 µg/ml to BMM without added Ca^{2+} and of 1.0, 1.5, 1.75, 2.0, 3.5 µg/ml to BMM supplemented with 5 mM Ca^{2+}. The cultures were incubated with slow shaking for 8 h in 96 well plates, and OD_{600} was measured using Synergy Mx Plate reader (Biotek). At least three replicates were tested, and the mean values of MICs were reported.

RNA isolation

Total RNA was isolated from *P. aeruginosa* PAO1 grown in BMM with no or 5 mM Ca^{2+} using RNeasy Protect Bacteria Mini kit (Qiagen) or ZR Fungal/ Bacterial RNA MiniPrep™ (Zymo Research) where cells were processed with 50 µg/ml of lysozyme followed by the manufacturer's protocol for isolation. The purified RNA was eluted with diethylpyrocarbonate (DEPC) treated sterile nanopure water. DNase treatment was performed for eluted RNA sample using turbo DNase (Ambion). The absence of genomic DNA was confirmed by conventional PCR using *rpoD* primers. RNA yield was measured using NanoDrop spectrophotometer (NanoDrop Technologies Inc.), and the quality of the purified RNA was assessed by Bioanalyzer 2100 (Agilent) and 1% agarose gel electrophoresis. Following the MIQE guidelines, only the RNA samples with an OD_{260}/OD_{280} ratio of 1.8-2.0 and an RIN value of ≥ 9.0 and/ or rRNA ratio of 1:2 were selected for further analysis. RNA samples were stored at -80 °C.

Library preparation and RNA Seq

RNA Seq analysis was performed at Vertis Biotechnology AG, Germany. First, RNA samples were assessed by capillary gel electrophoresis using Shimadzu MultiNa microchip and RNA samples with a 16S:23S ratio of 1:1- 1:3 were selected for further analysis. For capable RNA Seq, the RNA samples were enriched by capping the 5′ triphosphorylated RNA with 3′-desthiobiotin-TEG-guanosine 5′

triphosphate (DTBGTP) (NEB). For reversible binding of biotinylated RNA species to streptavidin vaccinia capping enzyme (VCE) (NEB) was used. An elution step was performed to capture the biotinylated species to streptavidin and obtain the 5' fragments of the primary transcripts.

To deplete the ribosomal RNA, RNA samples were treated with Ribo-Zero rRNA kit for bacteria (Illumina). These RNA samples were then used for cDNA library preparation. In brief, the RNA was first poly(A) tailed using poly(A) polymerase. Then the 5′ triphosphate or CAP were removed by pyrophosphatase (Cellsript) and an RNA adapter was ligated to the 5′ monophosphate end of RNAs. cDNA synthesis was performed using the oligo (dT)-adapter primer and M-MLV reverse transcriptase. The resultant cDNA was PCR amplified to yield about 10-20 nm/µl using high fidelity polymerase. The cDNA pool for sequencing was generated by taking equimolar cDNA samples followed by elution of samples to a size range of 200-500 bp from preparative agarose gel. The size fractionation was confirmed by capillary gel electrophoresis. The True-seq primers designed following the Illumina instructions were used for the sequencing. The cDNA pools were sequenced on an Illumina NextSeq 500 system using 75 bp read length.

Promoter activity reporter construction

To study the transcription activation of PA2604, pMS402 with a promoter less *luxCDABE* reporter was used. The vector was generously shared by Drs. Kangmin Duan (Manitoba University, Canada) and Mengmeng (Northwest University, China). The promoter region of PA2604 was predicted by BPROM algorithm. The 139 bp region upstream of PA2604 harboring the predicted promoter was PCR amplified by using *pfx* polymerase kit (Thermo Fischer Scientific) and primers flanking *Bam*HI and *Xho*I restriction sites and cloned upstream of the *luxCDABE* operon. The resultant plasmid was designated pSK-2604F (**Table S1**). The empty vector pMS402 and pSK-2604F were electroporated into PAO1 wild type (WT) and the following mutants *ΔcarR*, *ΔcarP*, *ΔefhP,* and *ΔlasR* (**Table S1**). Successful transformants were selected on LB agar plates containing trimethoprim at 300 µg/ml final concentration. To measure the promoter activities of *rsmA* and *rsmZ*, the integron based promoter activity integron based reporter Empty vector CTX6.1 and promoter activity reporter plasmids CTX-rsmA and CTX rsmZ were generously provided by Dr. Kangmin Duan. These vectors (**Table 3.S1**) were electroporated into PAO1 WT and PA2604:Tn5 mutant. The transformed clones were selected on LB agar plates containing trimethoprim at 300 µg/ml.

Promoter Activity Assay

Strains carrying promoter regions of genes of interest upstream of *luxCDABE* operon were grown in BMM with or without added Ca^{2+} at 37 °C, while shaking at 200 rpm for 12 h. Then OD_{600} of the cultures were measured and normalized to an OD_{600} of 0.3 using BMM with the corresponding Ca^{2+}.The normalized cultures were inoculated into a total volume of 200 µl of BMM at the ratio of 1:100 in 96 well clear bottom plate (Grenier Bio-One) and incubated at fast shaking in Synergy MX plate reader (Biotek). When needed, 5 mM of $CaCl_2$ or sub inhibitory concentration (SIC) of tobramycin defined as two-fold below the experimentally measured MIC 0.25 µg/ ml, were added to BMM. Cell density at OD_{600} as well as luminescence was measured every 30 minute for 10 h. For experiments performed to assess the immediate effect of Ca^{2+} addition on the promoter activity of PA2604, the precultures were grown in 5 ml BMM without added Ca^{2+} for 12 h. Cell density was normalized as described above and 200 µl of the normalized cultures were added to each well of 96 clear bottom plate (Grenier Bio-One). After 5 h of growth in the Synergy MX plate reader (Biotek) at 37 °C and fast shaking, the plate was taken out briefly and Ca^{2+} was added to a final concentration of 5 mM to respective wells. The control wells received the same volume sterile nanopure water.

Luminescence measurements were normalized by cell density (OD_{600}) of the corresponding cultures, followed by subtraction of the empty vector normalized

luminescence. Finally, ratios between promoter activities determined with and without Ca^{2+} or tobramycin were calculated and averaged over at least three biological replicates. Every experiment was repeated at least twice.

RESULTS

In silico search for proteins required for Ca^{2+} uptake in P. aeruginosa PAO1

Previous studies identified two types of Ca^{2+} influx channels in bacteria: PHB-PP, a non-proteinaceous Ca^{2+} influx channel in *E. coli* (109) and BSYetJ, a pH sensitive Ca^{2+} leak channel in *B. subtilis* (159). Sequence analysis of PAO1 genome revealed no closely clustered homologs of PHB-PP synthases. Further, it was shown that *P. aeruginosa* PAO1 produces medium chain length polyhydroxyalkanoate (PHA) (169) and PP. Biosynthesis of PHA requires two PHA synthases: PA5056 and PA5058 (169). The level of PP is determined by the activities of exopolyphosphatase PA5241 and polyphosphate kinase PA5242 (170, 171). We hypothesized that PAO1 produces PHA-PP to serve as Ca^{2+} influx channel and that the proteins involved in PHA-PP synthesis play role in the intracellular Ca^{2+} homeostasis. *In-silico* search for homologs of BSYetJ identified only one homolog PA2604 that shares 23% amino acid sequence identity with BSYetJ in *B. subtilis*. Unlike *bsYetJ* surrounded by genes encoding peptidase, DNA repair proteins, flavin oxidoreductase, and lipoprotein, PA2604 does not occur in

operon-like structure. Further sequence analysis of PA2604 showed that similarly to BSYetJ, this protein contains a Bax Inhibitor-1 (B1-I) domain spanning the entire protein (**Fig 3.1 A**). B1-I containing proteins are conserved membrane spanning proteins that transport Ca^{2+} in and out of the endoplasmic reticulum. The i-TASSER-predicted 3D structure of PA2604 forms seven membrane spanning α-helixes, which is typical for the proteins with B1-I domain (**Fig. 3.1 B**). Based on this analysis, we predicted that PA2604 is a calcium channel and designated it CalC.

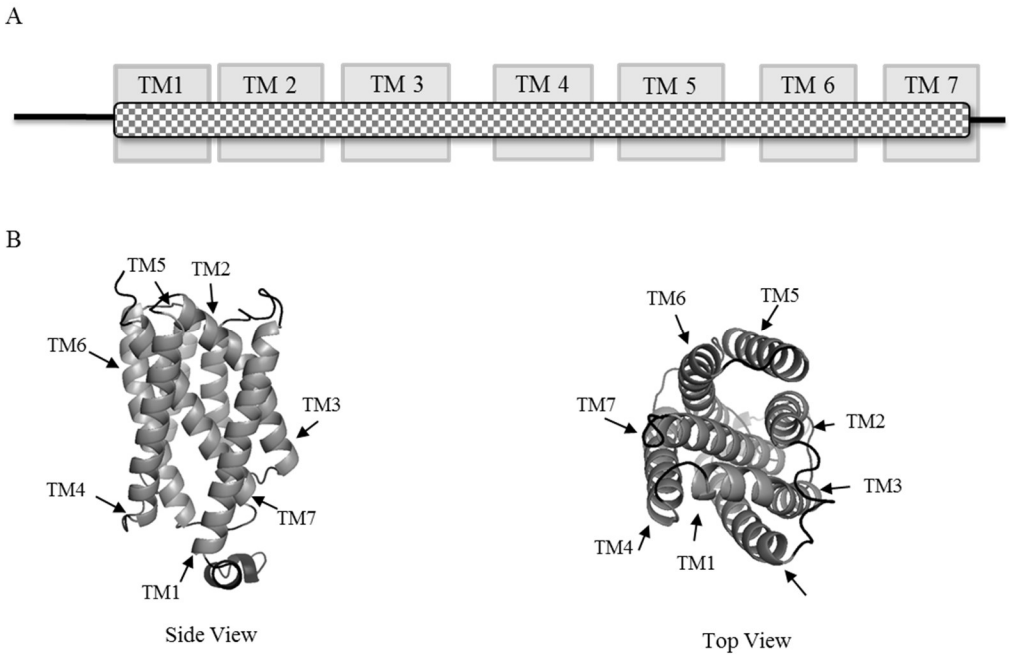

Figure 3.1: Sequence analysis of CalC. A. Schemetic drawing of CalC. Seven transmembrane regions (TM) are shown as light grey boxes. α-helix locations were predicted using TMHMM v. 3.0. The Bax-1 inhibitor domain as predicted by Pfam is indicated by the checkered rectangle. **B.** 3D structure of CalC predicted by iTASSER: side and top view. Transmembrane domains are shown in light grey.

PA2604 is required for generating transient increase in $[Ca^{2+}]_{in}$.

Earlier we showed that *P. aeruginosa* generates transient changes in $[Ca^{2+}]_{in}$ in response to elevated external Ca^{2+}. We hypothesized that proteins responsible for Ca^{2+} uptake would define the transient increase in $[Ca^{2+}]_{in}$ in response to externally added Ca^{2+}. Therefore, four candidates predicted to uptake Ca^{2+}, PA5056, PA5058, *calC*, and PA5241 were tested for their role in $[Ca^{2+}]_{in}$ homeostasis. For this, the corresponding transposon mutants were obtained from the UW mutant library (**Table 3S1**), confirmed by PCR, subjected to measurements of their $[Ca^{2+}]_{in}$ responses to 1 mM Ca^{2+}, and compared to that of the wild type PAO1 cells (**Fig. 3.2 A - D)**.

As established earlier, (72) WT PAO1 maintains $[Ca^{2+}]_{in}$ at the level of 0.3 ± 0.09 μM, which transiently increases nine fold (2.68 ± 0.44 μM) over the period of 0.6 min in response to 1 mM external Ca^{2+}. Disruption of *calC* reduced the basal level of $[Ca^{2+}]_{in}$ by three fold. Further, *calC* mutant showed highly attenuated transient increase $[Ca^{2+}]_{in}$, reaching only 23% of the WT (0.62±0.09 μM) in 0.08 min after addition of 1 mM Ca^{2+} **(Fig.3. 2 A)**. This low increase was not followed by a decline, but instead was followed by a second slow wave of $[Ca^{2+}]_{in}$ increase reaching 3.26 ± 0.27 μM over 9.7 min, and then a slow decline to 2.34±0.37μM, which is two-fold above the recovery level in WT cells. Gene complementation

restored the initial transient increase to WT level, however, did not restore the recovery to the basal level of Ca^{2+}_{in}.

The mutants with disrupted PHA synthases, PA5056, PA5058, or PA5241 did not exhibit a reduction in the initial increase of $[Ca^{2+}]_{in}$ in response to Ca^{2+} addition **(Fig. 3.2 B-D)**. On contrary, all three of them showed a greater $[Ca^{2+}]_{in}$ increase and a significantly reduced (PA5058::Tn5) or abolished (PA5056::Tn5, PA5241::Tn5) recovery to the $[Ca^{2+}]_{in}$ basal level. Thus, over 15 min, the WT cells recovered their $[Ca^{2+}]_{in}$ to 0.15 ± 0.19, whereas the mutants recovered only to 1.18±0.2 μM (PA5058::Tn5), 2.42 ± 0.83 μM (PA5056::Tn5), and 3.24 ± 0.23 μM (PA5241::Tn5).

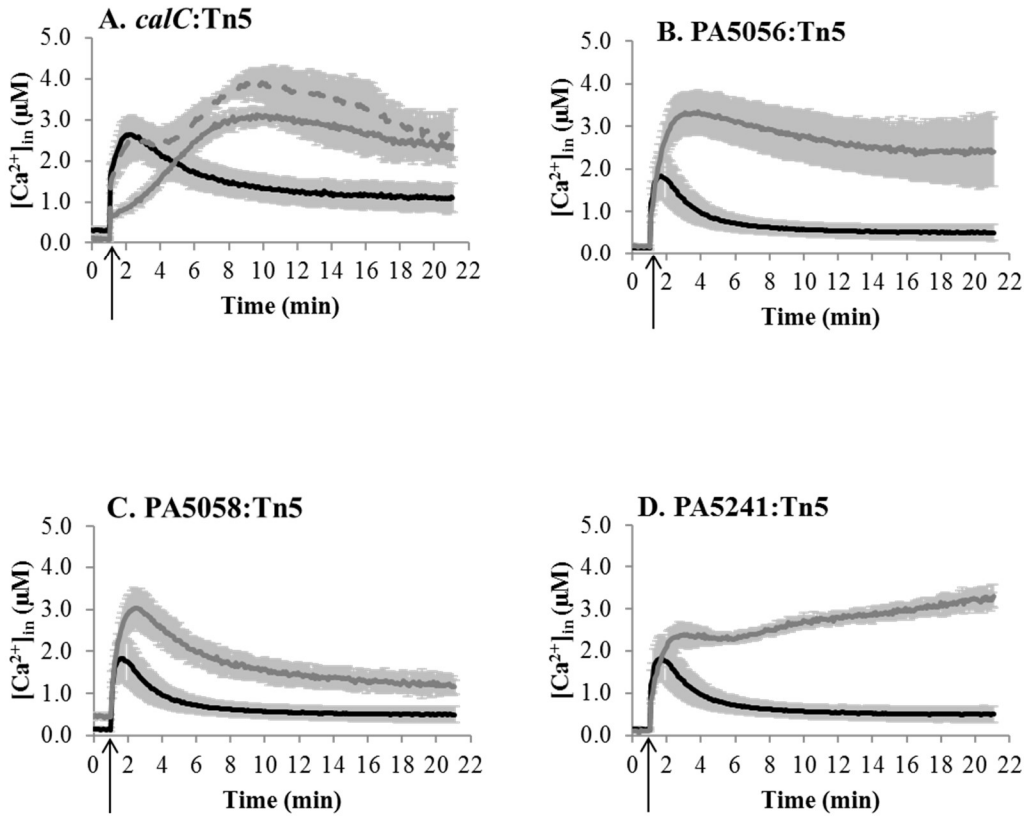

Figure 3.2: **Free $[Ca^{2+}]_{in}$ profiles of transposon mutant with disrupted putative Ca^{2+} channels.** The mutants were obtained from the University of Washington Two-Allele library. Cells were grown in BMM media with no added Ca^{2+}. The basal level of luminescence was monitored for 1 min. 1 mM $CaCl_2$ was added at the time indicated by the arrow, followed by luminescence measurements for 20 min. Changes in free $[Ca^{2+}]_{in}$ were calculated as described in the Methods section. PA numbers represent the open reading frames in PAO1 genome. (A) *calC*::Tn5. (B) PA5056:Tn5. (C) PA5058:Tn5. (D) PA5241:Tn5. Black, PAO1

wild type; grey, transposon mutant; dashed grey, complemented strain. The data is an average of at least three biological replicates.

Ca^{2+} regulates the transcription of calC

The RNA-Seq analysis showed that growth at 5 mM Ca^{2+} increased the transcript abundance of PA2604 by more than two fold (**Fig. 3.3A**). To validate these data and monitor the transcription of *calC* over time during different growth phases, promoter activity assay was used. In cells growing at 5 mM Ca^{2+}, promoter activity of *calC* increased up to 35 fold during early log phase (**Fig. 3.3B**). This increase in promoter activity was until the early stationary phase of growth, at which the effect of Ca^{2+} became negative.

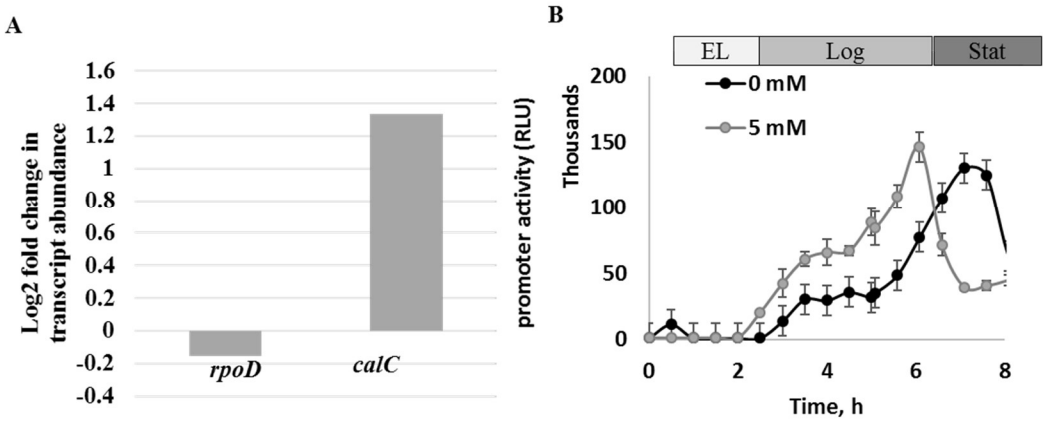

Figure 3.3: Regulatory role of Ca^{2+} on *calC* transcription. A. promoter activity of *calC* at 0 mM (grey circle) and 5 mM Ca^{2+} (black circle). Cells of PAO1, transformed with either the promoterless empty vector or the promoter activity reporter construct of PA2604 (pSK-2604F) were grown in BMM at 37° C in 96 well clear bottom white plates at fast shaking in Synergy Mx microplate reader. The luminescence and cell density (OD_{600}) was measured every two hours **Phases of growth: EL (early log), Log and Stat (stationary).** The data analyses followed the steps: 1) the averaged luminescence reading of non-inoculated controls was subtracted; 2) the luminescence at time 0 was subtracted from subsequent readings. The obtained luminescence readings were 3) normalized by the corresponding cell density and 4) averaged. 5) averaged normalized luminescence of the promoterless vector controls was subtracted from that of the promoter carrying constructs, 6) fold change was calculated versus the condition when no Ca^{2+} or tobramycin were added. At each step of data normalization, any

negative values were replaced by the basal luminescence reading of empty vector at that point. At least 3 biological replicates in each experiment and 2 independent experiments were used. **B.** RNA seq data for Ca^{2+} regulated differential transcription of *calC* in PAO1. RNA polymerase D (*rpoD*) is added as a controle gene that shows no differential expression due to Ca^{2+}.

Ca^{2+} responsive two-component regulator CarRS and putative Ca^{2+} binding proteins CarP and EfhP are involved in Ca^{2+} regulation of calC transcription

In order to identify the mechanism involved in regulating Ca^{2+}-dependent transcription of *calC*, we tested the promoter activity of PA2604 in several mutants lacking earlier identified genes encoding Ca^{2+}-induced two-component system *carRS* and two putative Ca^{2+}-binding proteins CarP and EfhP. In PAO1, PA2604 transcription was dramatically increased by growth at 5 mM Ca^{2+} ($\geq$ 16 fold). On the other hand, in the mutants lacking *carS*, *carP* and *efhP*, this fold change in transcription was significantly low; 3.8 fold, 1.2 and 0.4 fold respectively (**Fig. 3.4)**. We also tested, whether a global quorum sensing regulator *lasR,* is involved in Ca^{2+}-dependent upregulation of PA2604 transcription. However, the *calC* promoter activity in the mutant lacking *lasR* was 30-fold higher than that in PAO1, suggesting a negative regulation, possibly explaining the abrupt decrease of *calC* promoter activity during a stationary phase **(Fig. 3S1).**

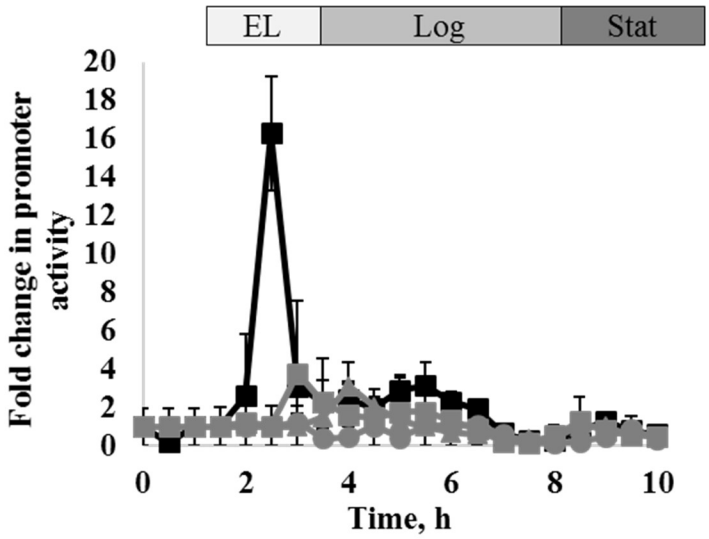

Figure 3.4: Fold change in *calC* promoter activity. Cells of PAO1, *ΔcarR, ΔcarP* and *Δefh* carrying either the promoterless empty vector or the promoter activity reporter construct of *calC* (pSK-2604F) were grown in BMM at 37° C in 96 well clear bottom white plates at fast shaking in Synergy Mx microplate reader. The luminescence and cell density (OD_{600}) was measured every two hours. Phases of growth**: EL (early log), Log and Stat (stationary).** Fold change in PA2604 promoter activity in Black sqare: PAO1, grey square: *ΔcarS* grey triangle: *ΔcarP* and grey circle: *ΔefhP*. The data analysis is same as above. At least 3 biological replicates in each experiment and 2 independent experiments were used.

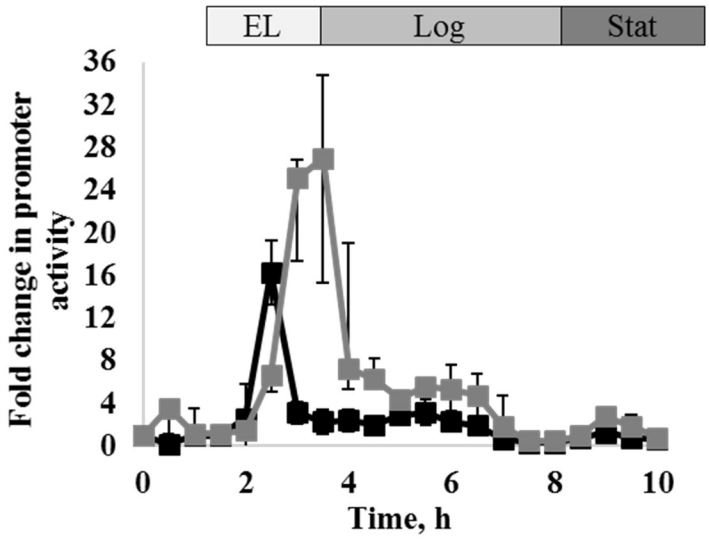

Figure 3.S1: Ca^{2+} regulation of *calC* promoter activity in PAO1 and *ΔlasR* mutant. Cells of PAO1 and *ΔlasR* carrying either the promoterless empty vector or the promoter activity reporter construct of *calC* (pSK-2604F) were grown in BMM at 37° C in 96 well clear bottom white plates at fast shaking in Synergy Mx microplate reader. The luminescence and cell density (OD_{600}) was measured every two hours **Phases of growth: EL (early log), Log and Stat (stationary). Fold change in PA2604 promoter activity in Black sqare: PAO1, grey square: *ΔlasR*.** The data analyses followed the steps: 1) the averaged luminescence reading of non-inoculated controls was subtracted; 2) the luminescence at time 0 was subtracted from subsequent readings. The obtained luminescence readings were 3) normalized by the corresponding cell density and 4) averaged. 5) averaged normalized luminescence of the promoterless vector controls was subtracted from that of the promoter carrying constructs, 6) fold change was calculated versus the

condition when no Ca^{2+} or tobramycin were added. At each steps of data normalization, any negative values were replaced by the basal luminescence reading of empty vector at that point. At least 3 biological replicates in each experiment and 2 independent experiments were used.

CalC regulates Ca^{2+} induced swarming motility, pyoverdin and pyocyanin production

Our previous study showed that *P. aeruginosa* swarming motility is induced by Ca^{2+} (72). To test whether the $[Ca^{2+}]_{in}$ transient increase mediates this regulation, swarming abilities of PAO1 and PA2604:Tn5 were tested at no added or 5 mM Ca^{2+}. Similar to our previous observation, 5 mM Ca^{2+} induced swarming in PAO1. Disruption of PA2604 reduced the swarming diameter by at no added Ca^{2+}. At elevated Ca^{2+}, the mutant's swarming was further reduced by 54% and showed increased branching (**Fig. 3S2 A**).

Earlier, we showed that Ca^{2+} induces pyocyanin production in PAO1 during growth on both liquid and agar media (146). Disruption of PA2604 did not affect the Ca^{2+} induced pyocyanin production while growing on agar, but abolished Ca^{2+} induction of pyocyanin production during growth in liquid (**Fig. 3S2 B**).

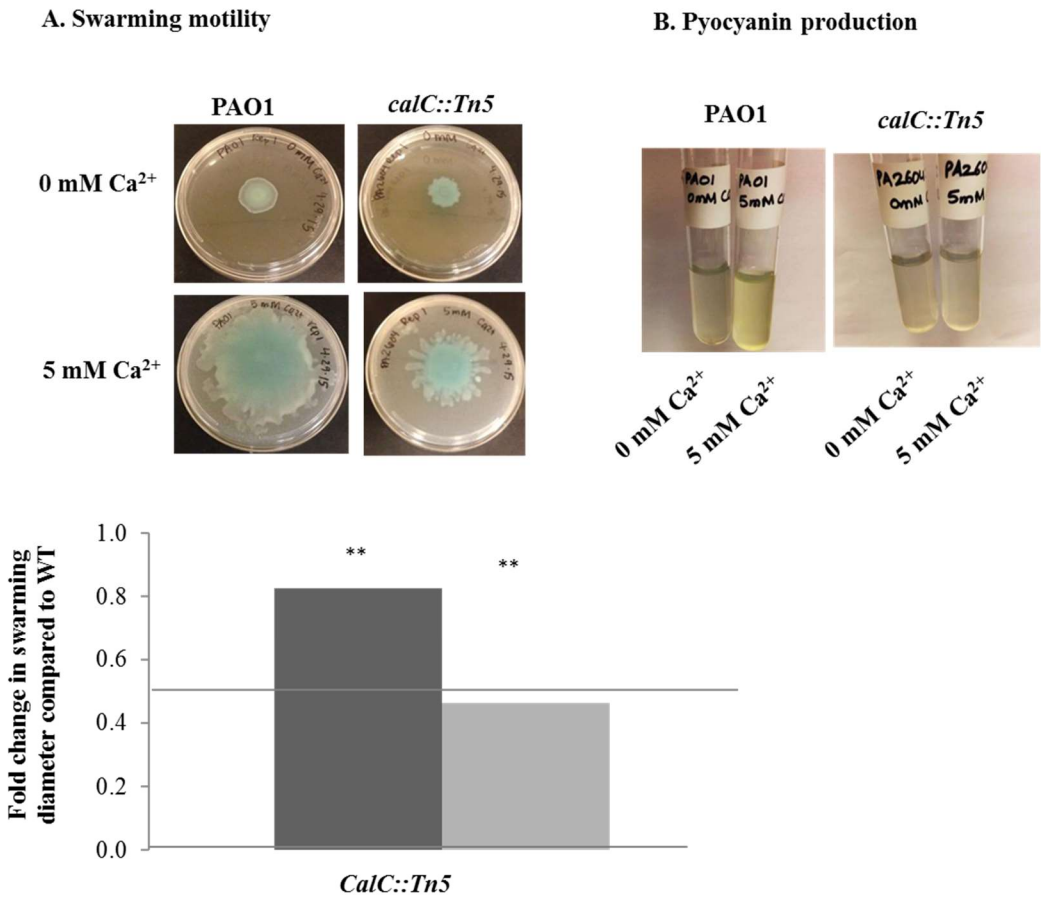

Figure 3.S2: Swarming motility and pycoycanin production. Cells were grown on BM2 swarm agar containing 0 mM or 5 mM Ca^{2+}. (**A**) Growth in swarming agar plates. Colony diameters were measured, and fold differences (5 mM *vs*. 0 mM) were calculated. The averages of at least three biological replicates were used to calculate the fold changes. Significance was calculated using student's T-test. ** $p \leq 0.01$. (**B**) pyocyanin production in liquid media.

PA2604 in involved in Ca^{2+} induced tobramycin resistance by controlling the transcription of multidrug efflux pump

Earlier we showed that elevated Ca^{2+} enhanced PAO1 resistance to tobramycin (Chapter 2) and Pol-B (Chapter 4). Further, the disruption in Ca^{2+}_{in} homeostasis by mutating calcium transporters, PA2435, PA2092, PA3920 and PA4614 affects the efflux mediated tobramycin resistance (43). In order to characterize the role of $[Ca^{2+}]_{in}$ transient increase in Ca^{2+} induction of antibiotic resistance, MICs of tobramycin and Pol-B B for PA2604 mutant were determined. Both E-strip (**Fig.** 3**S3)** and plate dilution assay **(Fig.3.5)** showed that disruption of PA2604 reduced the positive effect of Ca^{2+} on tobramycin resistance by at least 50%. However, no such effect was identified for Pol-B resistance.

To identify the mechanism responsible for this decrease of Ca^{2+} induction, we tested whether disruption of *calC* affects the earlier characterized Ca^{2+}-dependent increase in transcription of *mexAB-oprM* required for tobramycin resistance. In PAO1, growth at 5 mM Ca^{2+} increases by almost 7 fold (**Fig.3.5 B, C**) (43). However, in *calC*:Tn5 mutant, this Ca^{2+} regulated increase of *mexAB-OprM* transcription is inhibited and was only 2.5 fold (**Fig. 3.5 D)**.

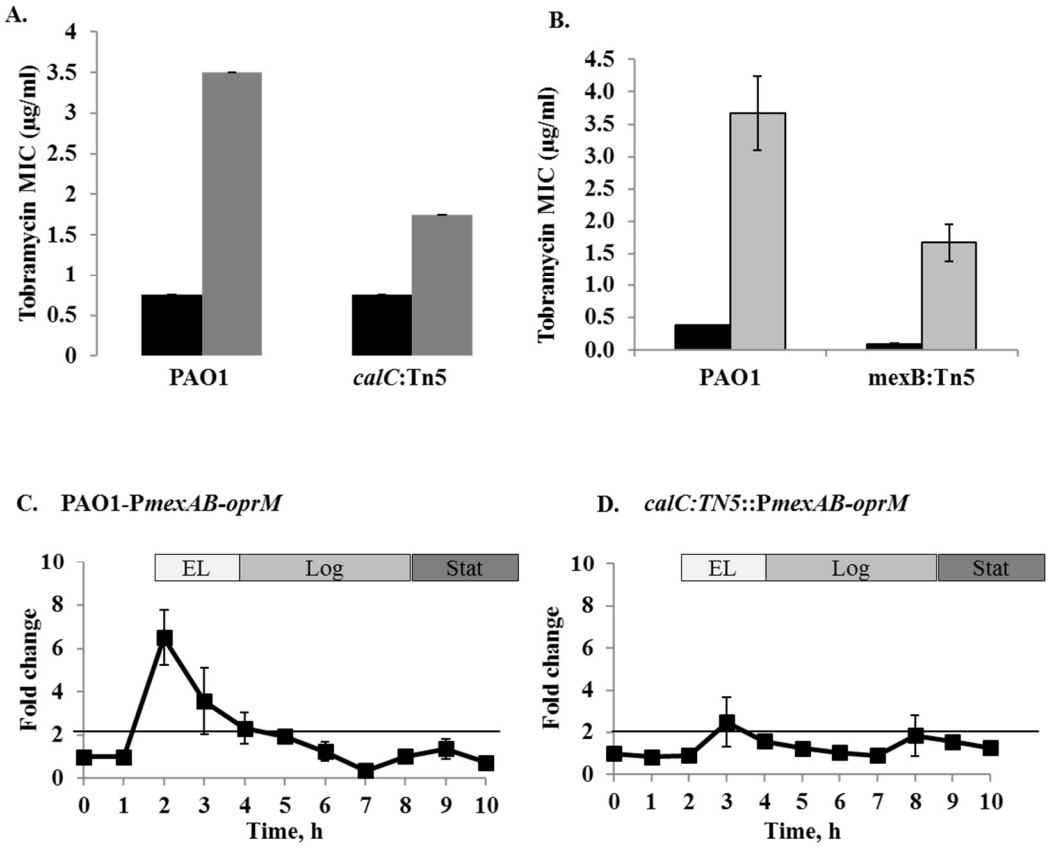

Figure 3.5: Role of *calC* in Ca^{2+} regulated efflux mediated tobramycin resistance in PAO1. A. Tobramycin MIC of PAO1, *calC*:Tn5 and CSK231 by plate dilution assay. 200µl of normalized cultures (OD 0.003) grown in BMM with 0 or 5 mM Ca^{2+} were into each well of clear 96 well-plates with tobramycin Tobramycin was added at the final concentration of 0.25, 0.5, 0.75, 0.1, 1.5 µg/ml to BMM without added Ca^{2+} and of 1.0, 1.5, 1.75, 2.0, 3.5 µg/ml to BMM supplemented with 5 mM Ca^{2+}. No antibiotic control and non-inoculated media controls were added to the wells. The cultures were incubated at 37 °C and slow

shaking for 8 hours before recording the cell density at OD_{600}. The MIC was determined by no growth at the certain tobramycin concentration. At least 3 biological replicates were used. **B.** Tobramycin MIC of PAO1 and *mexB:Tn5* by E-test (43). Cells were grown without or with 5 mM Ca^{2+}, normalized to OD600 of 0.1, and plated onto BMM agar plates with the corresponding concentration of Ca^{2+}. E-strips with gradient of tobramycin were placed on the bacterial lawns. MIC was recorded after 24 h incubation. Statistical significance of the difference in MIC between PAO1 and *mexB:Tn5* mutant was calculated using student's T-test. *, $p < 0.05$. **C, D and E.** Fold change in promoter activity of *mexAB-OprM* in **C.** PAO1 **D.** *calC::*Tn5. Cells of PAO1, *calC::TN5* as well as containing either the promoterless empty vector or the promoters for *mexAB-oprM* were grown in BMM at 37° C in 96 well clear bottom white plates at fast shaking in Synergy Mx microplate reader. The luminescence and cell density (OD_{600}) was measured every two hours Phases of growth: **EL (early log), Log and Stat (stationary).** The data analyses were performed same way as above. At least 3 biological replicates in each experiment and 3 independent experiments were used.

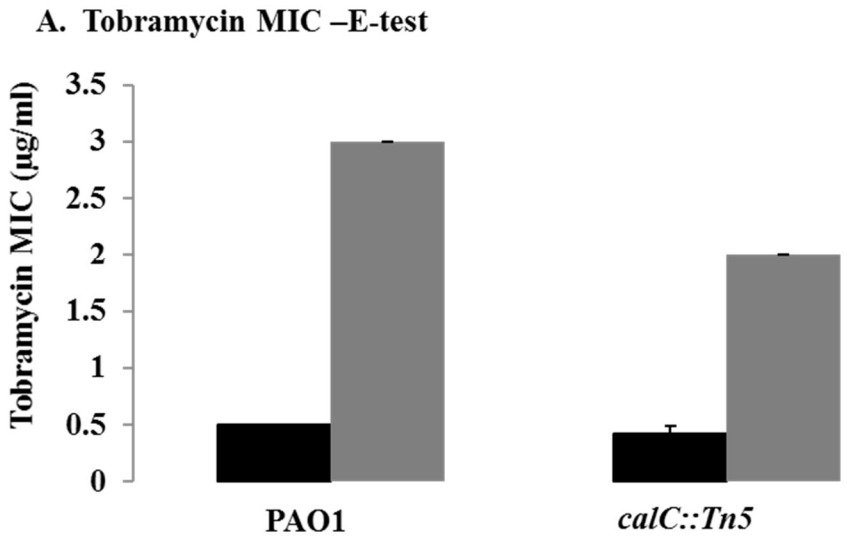

Figure 3.S3: MIC of tobramycin for PAO1 and *calC*::Tn5. Cells were grown without or with 5 mM Ca^{2+}, normalized to OD600 of 0.1, and plated onto BMM agar plates with the corresponding concentration of Ca^{2+}. E-strips with gradient of tobramycin were placed on the bacterial lawns. MIC was recorded after 24 h incubation. Statistical significance of the difference in MIC between PAO1 and *calC*::Tn5 mutant was calculated using student's T-test. *, $p < 0.05$.

PA2604 disruption alters the global regulatory effect of Ca^{2+} on gene expression in P. aeruginosa PAO1

In order to establish the regulatory effect of intracellular Ca^{2+} signaling on global gene transcription, RNA seq analysis was performed in *calC::*Tn5 and PAO1 grown at no added or 5 mM Ca^{2+}. The RNA seq data displayed an overall 95%-97% alignment rate with a number of read ranging from ~18,000- 22,000. Growth at 5 mM Ca^{2+} significantly affected the transcription of at least 1016 genes (≥ 2-fold change in transcription with an *adjP (q) value of ≤ 0.05. The Ca^{2+} regulated transcription of at least 881 genes were identified to be correlated to PA2604. Of these, 342 genes were positively regulated by Ca^{2+} in PAO1 **(Fig. 3.6)**. Transcript abundances of remaining 539 genes, that were down regulated by Ca^{2+} growth in wild type, was increased in the *calC::*Tn5 mutant **(Fig. 3.6)**. Importantly, the transcription of these 881 genes was not affected by the mutation in cells growing without added Ca^{2+}.

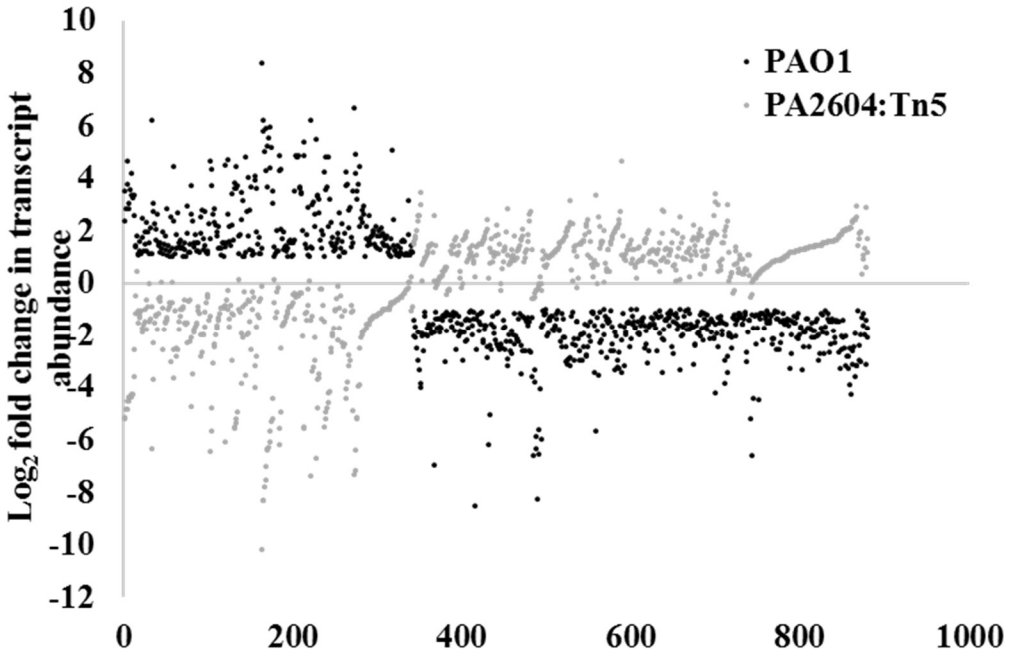

Figure 3.6: Scatter plot of RNA seq data. Differential gene expression in PAO1 and *calC*:Tn5 mutant grown at 5 mM Ca^{2+}. Black circles: PAO1 and grey circles: *calC*:: Tn5. The effect of Ca^{2+} was assessed by comparing the transcript abundance of a gene in bacteria grown at 5 mM Ca^{2+} to that of the same bacteria grown at no added Ca^{2+}. The dots represent the log_2 fold change in transcript abundance of genes which showed significant (≥ 2 fold change in transcript abundance with adjusted P* value (q value) ≤ 0.05) effect of Ca^{2+}.

Table 3.1: RNA seq analyses. These are selected from a total number of 342 genes whose transcription was increased by growth at 5 mM Ca^{2+} in PAO1 but reduced in *calC*::Tn5 mutant grown at 5 mM Ca^{2+}. Also, transcription of these genes was unaffected in the mutant grown without any added Ca^{2+}.

Gene	**PAO1**		***calC*::Tn5**	
	log2Fold Change	padj*	log2Fold Change	padj*
Alginate biosynthesis				
algB	1.22	3.81E-02	-1.20	1.91E-02
clpP	1.13	4.76E-03	-1.07	1.97E-02
cysB	1.59	7.08E-05	-1.29	1.25E-03
Swarming motility				
clpS	1.35	5.30E-03	-0.20	8.35E-01
bswR	1.63	2.74E-04	-0.23	8.00E-01
Biofilm regulation				
bfmR	2.11	1.74E-02	-1.37	4.53E-02
rhlB	1.65	2.38E-02	-0.40	6.92E-01
Chemotaxis				
motA	1.25	1.91E-03	-0.76	9.07E-02
ctpL	2.84	1.56E-03	-1.30	4.93E-02
pctB	1.82	3.58E-05	-1.49	3.36E-04

flagella biosynthesis				
flgC	1.67	4.68E-05	-1.28	2.52E-03
flgF	1.40	1.08E-03	-1.80	9.22E-06
flgG	1.57	3.72E-04	-1.45	6.91E-04
flgH	1.52	4.78E-03	-0.65	2.81E-01
flgM	1.33	1.97E-03	-0.87	5.84E-02
fliD	1.00	1.24E-02	-0.97	3.70E-02
fliE	2.67	1.72E-09	-2.56	1.51E-09
motY	1.30	8.17E-03	-1.51	5.98E-04
Phosphate regulation				
phoA	2.71	3.57E-02	-1.96	2.99E-02
phoB	4.04	2.27E-16	-1.95	1.23E-04
phoR	1.83	9.43E-05	-0.62	2.68E-01
PA4847	1.30	1.54E-03	-0.69	1.51E-01
pstS	2.80	1.44E-11	-1.48	6.08E-04
phnC	3.66	1.11E-03	-2.53	4.95E-04
Pyoverdine biosynthesis/ Transport				
fpvA	4.29	5.75E-13	-7.03	8.25E-23
PA2393	5.91	7.41E-17	-7.53	7.59E-27
PA2403	5.02	1.07E-20	-7.79	4.30E-30
PA2412	8.41	4.02E-47	-10.17	1.10E-59
pvdA	6.22	1.09E-24	-8.33	4.01E-35

pvdE	5.24	8.56E-10	-6.40	1.02E-17
pvdG	5.95	2.48E-08	-6.06	2.44E-15
pvdH	5.54	2.98E-09	-6.29	5.10E-17
pvdJ	3.66	2.39E-08	-6.35	2.11E-17
pvdL	5.17	5.48E-06	-5.30	6.36E-11
pvdN	4.41	1.22E-06	-5.65	6.26E-13
pvdO	3.54	8.44E-05	-5.19	1.89E-10
pvdP	5.78	1.24E-24	-8.30	8.19E-35
pvdQ	3.04	4.21E-03	-4.41	4.63E-07
PA0192	5.37	1.02E-10	-5.53	1.43E-19
tonB2	4.87	6.04E-10	-5.57	4.27E-18
Infection phase regulation				
Small RNA RsmZ	1.06	1.08E-02	-1.52	3.88E-05
Global regulation				
mvaT	1.03	1.62E-02	-1.54	1.42E-04
mvaU	1.91	3.15E-07	-1.53	4.99E-05
Bacteriocin, Phage and antibiotic resistance				
cat	1.22	8.61E-03	-0.62	2.78E-01
pys2	1.11	1.85E-02	-0.04	9.76E-01
armZ	1.53	1.72E-02	-0.63	4.19E-01
Stress response				
ahpC	1.01	2.27E-02	0.08	9.59E-01

obg	1.50	1.46E-03	-1.15	2.04E-02
dps	1.07	1.28E-02	-0.21	8.64E-01
Cell division/ DNA repair				
zipA	1.10	3.57E-03	-0.92	2.26E-02
nusA	1.05	2.24E-02	-0.72	2.26E-01
Sulfar metabolism				
msuE	6.23	3.13E-15	-7.35	8.35E-26
cysD	1.37	2.24E-04	-1.42	2.50E-04
cysI	1.34	9.74E-04	-1.25	1.66E-03
cysP	2.62	3.87E-13	-2.97	2.33E-17
cysT	3.11	2.52E-15	-3.24	1.58E-17
sbp	3.01	9.21E-19	-3.39	1.80E-24
atsA	3.20	3.09E-04	-3.62	1.93E-07
metY	2.18	5.40E-04	-2.09	4.81E-05
msuD	5.50	2.09E-11	-6.69	3.10E-20
Iron homeostasis				
ftnA	1.25	8.14E-03	-1.04	1.94E-02
hitA	1.19	6.89E-03	-1.16	5.20E-03
nitrogen metabolism				
gdhB	2.21	5.65E-06	-1.15	9.93E-03
Oxidative phosphorylation				
atpE	1.84	1.08E-07	-1.09	8.72E-03

cyoA	2.42	6.42E-03	-1.91	3.47E-03
ohr	3.18	3.20E-06	-2.09	1.60E-04
lsfA	3.45	2.13E-22	-3.83	6.56E-32
Transcriptional regulation				
atuR	1.69	2.59E-03	-1.62	8.13E-04
gpuR	1.59	1.55E-02	-0.90	1.41E-01
liuR	1.25	1.57E-02	-1.30	4.89E-03
ohrR	1.98	3.56E-06	-1.55	1.69E-03
alpR	1.38	1.81E-03	-1.44	5.69E-04
prtN	1.42	1.04E-03	-1.24	6.27E-03
vreA	3.53	1.92E-03	-1.37	7.92E-02
Cation transport				
mgtA	4.73	3.80E-13	-0.29	7.29E-01
mgtE	2.66	4.88E-14	-1.00	1.85E-02
mscL	1.11	4.16E-03	-0.60	2.81E-01
ABC transporter				
puuR	3.37	1.82E-17	-3.61	2.56E-23
pstC	1.78	2.76E-05	0.47	4.24E-01
Potassium transport				
kdpA	3.64	7.74E-16	-2.79	5.77E-13
kdpB	1.97	5.00E-04	-1.70	4.61E-04
kdpF	3.91	1.21E-21	-3.19	2.30E-16

Other transporters				
exbB1	4.79	1.62E-17	-4.55	3.93E-22
exbD1	3.21	2.61E-12	-4.15	1.00E-22
oprP	2.33	3.31E-02	-2.47	2.21E-03
Two component systems				
fleQ	1.04	1.33E-02	-0.97	2.22E-02
irlR	1.35	2.07E-02	-0.47	5.55E-01
Protein secretion				
exsB	1.14	2.95E-02	-1.02	7.79E-02
exsA	1.61	3.12E-04	-2.29	3.76E-08
tssA1	1.17	7.88E-03	-2.35	1.87E-09
tssB1	1.20	1.90E-03	-2.46	4.40E-12
amino acid biosynthetic processes				
aruC	2.35	3.42E-09	-1.75	7.17E-06
aruG	1.96	3.92E-04	-0.98	5.26E-02
cysK	1.47	2.65E-03	-1.45	1.84E-03
ilvA2	2.49	1.77E-02	-1.73	2.22E-02
phhA	1.75	4.47E-02	-1.87	4.89E-03
O antigen biosynthesis				
himD	1.65	4.76E-05	-1.18	2.48E-03

peptidoglycan biosynthesis				
pbpG	1.05	3.22E-02	-0.30	7.30E-01
Phospholipid biosynthesis				
psd	1.23	3.24E-02	-0.33	7.12E-01
Metabolic processes				
pcs	1.12	2.96E-02	-0.91	5.76E-02
nadD2	1.64	1.35E-02	-1.24	3.27E-02
ppiB	2.06	1.22E-06	-1.19	9.66E-03
trpG	2.27	7.76E-09	-1.51	1.25E-04
bioA	1.43	1.62E-03	-1.17	8.09E-03
bioB	2.64	3.54E-14	-1.78	5.90E-07
rubA2	1.57	1.56E-03	-0.59	3.38E-01
betT3	2.54	1.30E-05	-3.01	5.10E-10
gshB	2.94	5.56E-10	-2.28	4.41E-08
exaC	1.47	3.57E-02	-2.23	8.34E-05
aruF	2.28	2.42E-08	-1.43	2.50E-04
liuA	1.33	1.74E-02	-1.42	2.91E-03
hdhA	2.83	4.40E-08	-2.43	9.11E-09
pepA	1.72	4.98E-05	-1.27	2.49E-03
tpm	1.03	3.48E-02	-0.92	5.38E-02
nadE	1.42	3.33E-03	-0.85	8.39E-02
pncB1	2.14	3.73E-07	-1.68	1.95E-05

pcnA	3.41	8.17E-17	-2.97	6.83E-16
tal	1.03	4.38E-02	-0.88	7.26E-02
dadA	4.81	9.62E-21	-3.56	1.88E-20
pauD2	1.11	3.31E-02	-0.55	3.63E-01
aspP	1.12	6.55E-03	-0.70	1.35E-01
nrdA	1.02	2.66E-02	0.14	9.05E-01
trxB1	1.40	1.43E-03	-0.71	1.73E-01
accB	1.11	1.65E-02	-1.32	3.47E-03
gloA3	1.26	7.22E-03	-0.33	6.99E-01
mqoA	1.84	1.27E-03	-0.86	1.26E-01
sdhD	2.02	4.61E-06	-1.36	4.95E-03
accD	1.02	1.22E-02	-1.48	9.29E-05
trpE	1.93	2.85E-06	-1.05	1.69E-02
cadA	1.22	1.89E-02	-1.03	3.22E-02
proB	1.17	1.44E-02	-0.88	9.07E-02

*padJ, Adjusted P value/ q value ≤ 0.05.

Among the genes whose gene expression was affected by intracellular Ca^{2+} transients, there were genes responsible for pyoververdine biosynthesis, Pho-regulon, swarming motility, flagella biosynthesis, quorum sensing and biofilm regulation, LPS biosynthesis, peptidoglycan biosynthesis, type 3 and type six

secretion systems, polycationic antimicrobial resistance and manyother genes for transpost and cellular metabolism in general. The most significant positive regulatory effect of $[Ca^{2+}]_{in}$ was found on the genes involved in pyoverdine biosynthesis (≥ 60 fold increase in PAO1; ≥ 250 fold decrease in PA2604:Tn5 mutant) (**Table 3.1)**. Besides pyoverdine, the pho regulon that contributes significantly in regulation of biofilm formation and type 3 secretion system in *P. aeruginosa* (172, 173) as well as the genes involved in positive regulation of biofilm formation, *bfmR*, *rhlB*, alginate biosynthesis genes (*algB*) (174) were highly induced more than two fold in transcription upon exposure to Ca^{2+} in PAO1 and inhibited in the PA2604 mutant at 5 mM Ca^{2+}. On the contrary, negative regulator of biofilm *rsmA*, small RNA RsmZ, genes for type three secretion systems were downregulated in PAO1 but induced in the mutant lacking PA2604 at 5 mM Ca^{2+} **(Table 3.2)**.

Table 3.2: RNA seq analyses. These are selected from a total number of 539 genes whose transcription was decreased by growth at 5 mM Ca^{2+} in PAO1 but increased in *calC*::Tn5 mutant grown at 5 mM Ca^{2+}. Also, transcription of these genes was unaffected in the mutant grown without any added Ca^{2+}.

Gene	**PAO1** log_2Fold Change	padj*	***calC*::Tn5** log_2Fold Change	padj*
ABC transporter				
ccmB	-1.67	7.38E-04	1.83	6.01E-05
modC	-2.05	3.64E-03	1.22	1.11E-01
spuH	-1.43	3.18E-03	1.49	1.58E-03
Other Transporters				
znuB	-1.39	4.07E-02	0.63	5.06E-01
trkH	-1.62	2.62E-03	0.83	2.20E-01
amtB	-2.12	4.28E-07	1.67	1.32E-03
oprL	-1.08	4.45E-03	1.22	5.39E-03
tolA	-1.55	4.89E-05	1.67	7.13E-06
uraA	-1.21	2.88E-02	1.07	4.52E-02
ATP synthesis				
atpA	-1.13	6.71E-03	1.13	2.81E-02
atpC	-2.53	1.89E-08	1.77	1.63E-04
atpD	-1.25	9.66E-03	1.36	7.55E-03
atpF	-1.83	2.17E-06	1.65	3.38E-05
atpG	-1.09	2.31E-02	1.44	3.31E-03
Biofilm formation				
fimX	-2.06	7.59E-06	1.46	1.78E-03
mucR	-1.25	1.74E-02	1.18	2.07E-02
ppkA	-1.94	1.30E-02	0.48	7.73E-01
pppA	-1.81	7.26E-03	0.20	9.29E-01
rsmA	-1.43	5.87E-04	1.88	2.99E-07
tpbA	-2.96	1.56E-03	-0.02	9.99E-01
tpbB	-1.89	3.69E-04	1.67	1.38E-03

wspD	-2.23	4.86E-03	1.75	1.94E-02
Extracellular polysaccharide/ Biofilm regulation				
pelA	-1.83	4.52E-03	0.96	2.13E-01
pelB	-2.71	1.77E-03	1.30	2.17E-01
pelC	-2.60	1.05E-02	0.84	6.14E-01
pelD	-1.99	4.04E-02	0.73	6.33E-01
pelF	-2.23	1.98E-02	0.76	6.23E-01
Flagella biosynthesis				
fgtA	-2.23	3.75E-03	1.33	1.16E-01
flgK	-1.38	9.34E-03	1.29	1.03E-02
flhB	-2.01	3.67E-03	0.91	3.16E-01
fliI	-2.19	4.78E-03	0.98	3.41E-01
fliJ	-3.47	1.74E-05	1.69	7.32E-02
fliP	-1.13	1.66E-02	0.88	1.05E-01
fliQ	-1.17	3.45E-02	1.42	2.69E-03
fliR	-2.14	6.71E-05	1.24	3.56E-02
motC	-2.58	1.95E-08	1.79	1.98E-04
Pili biosynthesis/ motility				
chpA	-2.33	8.18E-05	1.71	3.27E-03
lipB	-1.29	3.41E-03	1.02	2.44E-02
pilC	-1.44	1.55E-03	0.88	9.24E-02
pilD	-1.63	1.90E-04	0.88	8.74E-02
pilE	-1.99	6.14E-04	1.38	1.82E-02
pilF	-1.61	1.11E-05	1.53	9.10E-05
pilH	-1.91	5.44E-07	1.32	8.80E-04
pilJ	-1.82	2.51E-05	1.68	5.62E-05
pilK	-2.58	1.48E-09	2.03	3.00E-06
pilR	-2.50	9.31E-04	1.67	2.81E-02
pilS	-3.07	4.04E-08	1.89	1.50E-03
pilW	-1.92	2.36E-04	0.85	2.05E-01
pilY1	-1.38	1.65E-02	0.92	1.40E-01
Cell signaling				
pqqE	-2.61	9.37E-03	1.23	3.22E-01
braG	-1.92	2.90E-03	1.55	1.13E-02
quiP	-1.25	3.58E-02	1.14	4.02E-02
sahH	-1.29	1.75E-03	1.29	2.13E-03
ppx	-1.06	1.25E-02	0.43	5.18E-01

rhlB	-1.27	1.61E-03	0.87	6.07E-02
Chemotaxis				
chpB	-2.46	3.38E-06	1.88	3.18E-04
motB	-1.12	2.38E-02	1.11	2.07E-02
DNA repair/ Heat-shock/ Stress response protein				
holA	-3.17	1.14E-09	2.86	3.36E-09
mutL	-1.71	8.48E-04	1.22	2.50E-02
nth	-2.24	4.45E-03	1.94	5.94E-03
recJ	-1.39	4.30E-02	0.81	3.17E-01
recR	-1.66	4.76E-03	1.30	2.81E-02
uvrC	-2.58	2.19E-06	1.40	2.21E-02
rnhB	-2.93	4.56E-10	1.10	6.99E-02
groES	-1.32	7.20E-04	1.61	1.39E-05
hscA	-1.45	1.56E-03	2.61	2.08E-11
hslU	-2.65	3.53E-07	2.76	3.62E-09
hslV	-2.59	1.52E-09	2.38	6.03E-09
htpG	-1.62	2.19E-04	1.86	5.30E-06
glnK	-1.10	9.29E-03	1.35	7.98E-03
clpB	-1.65	1.44E-03	1.73	2.26E-04
dnaJ	-1.67	2.20E-03	1.66	8.55E-04
PA0961	-1.17	2.81E-02	0.25	8.35E-01
pcoB	-3.11	1.06E-11	2.24	1.24E-06
recG	-1.54	2.40E-03	0.88	1.24E-01
sspB	-1.70	5.32E-05	1.10	2.27E-02
dnaK	-1.78	1.32E-05	1.89	1.28E-06
groEL	-1.32	2.49E-03	1.03	2.85E-02
Cell cycle/cell division/cell shape regulation				
sss	-2.53	2.72E-03	1.18	2.72E-01
ftsA	-2.17	3.88E-07	1.79	3.46E-05
ftsQ	-2.36	1.80E-07	2.24	4.32E-07
ftsX	-1.28	5.24E-03	0.84	8.77E-02
minE	-1.91	1.31E-06	1.04	2.08E-02
spoOJ	-1.14	9.73E-03	1.11	8.96E-03
surA	-2.32	7.02E-09	2.29	5.83E-09
mrec	-2.13	4.18E-07	1.91	5.74E-06
mreD	-3.46	9.36E-17	2.79	2.94E-11

Antibiotic biosynthesis				
glmM	-1.37	2.05E-03	1.96	5.31E-07
dapB	-2.01	6.18E-05	1.96	3.03E-05
β lactamase resistance				
pbpA	-2.07	3.47E-05	1.68	5.23E-04
mrcB	-1.74	1.29E-05	1.20	5.09E-03
Cationic antimicrobial peptide (CAMP) resistance				
oprH	-6.17	1.84E-48	0.21	8.64E-01
phoQ	-5.02	4.96E-29	0.75	3.86E-01
parS	-1.55	1.71E-02	1.70	1.85E-03
arnA	-5.63	5.07E-19	-0.01	9.99E-01
arnB	-6.53	1.40E-19	-0.11	9.75E-01
arnC	-6.32	1.61E-15	-0.27	9.40E-01
arnD	-5.99	1.78E-08	NA	NA
arnE	-6.58	4.57E-14	-0.58	7.05E-01
arnF	-8.25	1.70E-29	-0.24	9.47E-01
arnT	-5.89	4.12E-13	-0.26	9.42E-01
phoP	-3.78	7.74E-20	-0.54	5.72E-01
pmrA	-3.32	1.98E-09	-0.38	8.27E-01
pmrB	-4.07	3.72E-15	0.24	9.00E-01
LPS biosynthesis				
kdsA	-1.13	8.17E-03	1.57	9.64E-05
lpxA	-1.15	2.42E-02	0.64	3.61E-01
lpxB	-2.05	3.30E-05	0.74	2.83E-01
lpxD	-1.65	2.72E-05	1.23	4.02E-03
msbA	-2.44	1.92E-09	1.61	1.76E-04
murG	-1.31	1.29E-02	1.01	6.89E-02
ostA	-1.04	1.15E-02	1.31	1.53E-03
ptsN	-1.00	2.17E-02	1.07	1.38E-02
waaC	-1.76	8.40E-04	1.39	8.10E-03
waaG	-2.09	6.96E-05	1.74	5.31E-04
wbpG	-2.86	1.28E-10	2.32	5.55E-08
wbpH	-2.89	2.53E-11	2.16	2.84E-07
wbpI	-1.42	2.64E-03	1.01	3.01E-02
wbpK	-1.40	3.35E-03	0.96	4.83E-02
wbpW	-1.27	4.56E-02	1.08	7.47E-02
wbpX	-1.38	4.37E-02	1.28	3.78E-02

wzm	-1.85	3.54E-04	1.57	2.24E-03
wzt	-1.60	7.97E-03	1.19	4.82E-02
wzx	-3.17	8.35E-13	3.15	5.53E-13
O antigen biosynthesis				
waal	-1.63	4.14E-04	1.61	1.80E-04
wzy	-1.96	4.76E-06	2.02	2.25E-06
Peptidoglycan biosynthesis				
glmS	-1.67	4.60E-03	0.96	1.50E-01
ddlB	-2.13	6.93E-05	1.66	1.41E-03
murB	-1.90	3.01E-05	1.15	1.84E-02
murC	-1.53	1.10E-03	1.28	9.01E-03
murE	-1.47	3.43E-03	1.30	6.87E-03
murF	-1.52	2.86E-04	1.47	4.18E-04
murI	-2.42	2.27E-05	1.52	1.35E-02
mltB1	-1.02	4.22E-02	0.79	1.56E-01
PA1689	-1.80	2.43E-04	0.73	2.75E-01
Non-coding RNA				
PA1030.1	-1.64	2.43E-04	0.84	1.12E-01
PA1781.1	-5.64	5.33E-17	3.35	8.37E-07
PA4406.1	-1.14	1.38E-02	0.60	3.98E-01
PA4451.1	-3.41	1.02E-12	0.85	2.22E-01
PA4726.1	-1.09	4.42E-02	0.27	8.43E-01
Oxidative phosphorylation				
atpH	-1.03	9.64E-03	1.59	2.55E-05
ccmE	-1.44	1.24E-03	0.46	4.82E-01
ccmF	-1.36	2.23E-02	1.31	1.60E-02
ccmG	-1.90	2.42E-04	1.99	2.00E-05
ccmH	-2.64	1.90E-07	2.43	5.12E-07
ccoO1	-2.03	2.00E-05	2.10	1.10E-05
ccoP1	-1.68	4.01E-04	1.80	9.31E-05
coIII	-1.59	1.37E-02	2.76	5.36E-08
exaB	-2.88	2.69E-02	0.56	8.17E-01
nuoD	-1.45	5.87E-04	0.44	5.59E-01
nuoE	-3.29	5.39E-16	2.26	1.44E-07
nuoF	-3.33	2.91E-10	1.95	5.34E-04
nuoG	-3.23	1.62E-09	2.16	7.94E-05
nuoH	-2.36	2.22E-07	1.69	8.78E-04

nuoJ	-2.17	6.43E-06	1.08	5.43E-02
nuoK	-1.23	2.90E-02	0.76	2.71E-01
nuoL	-2.61	7.88E-08	1.49	6.08E-03
nuoM	-2.59	2.05E-07	1.92	1.52E-04
nuoN	-2.96	1.20E-09	2.14	1.96E-05
Phospholipid biosynthesis				
acpP	-1.68	2.07E-05	0.60	2.59E-01
cdsA	-1.71	1.48E-03	0.69	3.65E-01
pgpA	-1.01	2.66E-02	0.22	8.33E-01
Regulation of transcription				
glmR	-1.42	1.91E-03	1.28	5.17E-03
greA	-1.77	1.27E-05	1.00	3.62E-02
greB	-1.39	5.91E-03	1.32	5.77E-03
Ribosomal protein				
ffs	-1.52	1.13E-02	0.08	9.65E-01
ftsI	-1.14	4.57E-03	0.84	6.49E-02
rplJ	-1.38	1.84E-04	0.84	1.09E-01
rplQ	-1.03	7.81E-03	1.28	8.70E-04
rpmA	-1.48	6.19E-04	0.69	2.17E-01
rpmE	-1.19	2.80E-02	0.70	3.29E-01
rpmF	-2.68	4.94E-09	2.04	1.10E-05
rpmJ	-2.43	2.98E-09	1.56	1.68E-04
rpsB	-1.13	4.93E-03	1.25	2.62E-03
rpsN	-1.15	1.23E-02	0.51	4.62E-01
rpsU	-1.29	6.57E-03	1.06	3.08E-02
rnt	-1.60	1.59E-03	1.35	8.26E-03
trmA	-1.92	8.77E-04	1.85	3.75E-04
Protein secretion				
xcpU	-1.93	1.50E-02	1.16	1.82E-01
pscU	-2.00	1.77E-02	0.26	9.15E-01
vgrG1	-1.37	1.89E-02	-0.28	8.37E-01
csaA	-1.01	4.41E-02	0.14	9.18E-01
tatC	-1.98	4.18E-05	1.73	2.49E-04
xcpQ	-2.02	5.55E-05	1.56	1.92E-03
xcpX	-1.49	3.49E-02	1.06	1.48E-01
secF	-1.33	1.93E-03	0.80	1.07E-01

Sulfer metabolism				
metZ	-2.33	3.20E-06	1.21	2.48E-02
moeB	-2.39	2.17E-04	1.45	3.54E-02
Two component system				
ansB	-1.51	7.02E-03	0.79	2.66E-01
ccoQ1	-1.51	5.63E-03	1.56	3.57E-03
creC	-1.42	2.69E-02	0.50	6.24E-01
glnD	-2.83	5.29E-06	2.99	1.19E-07
ntrC	-2.98	3.07E-13	1.99	2.78E-06
Urea degradation				
speC	-1.07	4.46E-02	1.46	2.57E-03
ureA	-2.99	3.69E-03	1.68	1.21E-01
ureC	-3.01	1.25E-03	1.98	3.16E-02
ureE	-2.42	2.16E-02	1.91	4.40E-02
ureG	-1.97	2.04E-02	1.98	7.19E-03
TCA cycle/ Acetyle co-A				
aceF	-1.91	9.67E-05	1.78	1.61E-04
eno	-2.03	2.45E-07	2.07	3.68E-07
sdhB	-1.44	1.34E-04	1.63	2.74E-05
sucA	-1.86	4.24E-05	1.91	3.27E-05
hemK	-1.93	2.05E-03	1.48	1.51E-02

*padJ, Adjusted P value/ q value ≤ 0.05

The *pvdAEGLOHQ* genes, which are part of pyoverdine biosynthesis operon, were highly induced in PAO1 grown at 5 mM Ca^{2+}. However, their transcription in *calC* mutant was either reduced or remained unchanged **(Fig. 3.7A)**. To validate this observation, we measured pyoverdine production. In agreement, PAO1 cells grown at 5 mM Ca^{2+} produced almost 140-fold more pyoverdine during both middle log and 78-fold more during stationary phases of growth. However, in

the *calC*::Tn5 mutant, production of pyoverdine synthesis was almost same as that at no added Ca^{2+}. **(Fig. 3.7B and Fig. 3S4),** whereas the mutation alone did not affect the level of pyoverdine produced at no added Ca^{2+}. The transcription of biofilm regulator gene *bfmR*, negative regulator for acute infection, sRNA RsmZ showed a similar trend: induced in PAO1 in the presence of Ca^{2+}, but not induced in the *calC* mutant under the same conditions**.** On the contrary, genes encoding structural or secreted components of type three secretion system *spcS*, *pscU*, and the regulators which upregulate the T3SS in PAO1, PA1629, RsmA were downregulated by Ca^{2+}in PAO1, but either upregulated or remained unchanged in *calC*:Tn5 mutant at 5 mM Ca^{2+} **(Fig. 3.7C)**.

MreB is an actin like cytoskeleton protein which, in association with the peripheral peptidoglycan synthesis proteins, MreC, MreD, RodZ determines the rod shape of bacteria. Upon down regulation of MreB, rod shaped bacterial cells displays a spherical morphology (175, 176). The *mreC* and *mreD* genes were downregulated in PAO1 in response to Ca^{2+} by 11 fold and 4 fold respectively, but upregulated in the *calC* mutant about four fold **(Fig. 3.7D)**. Electron microscopy of the WT and mutant cells grown at elevated Ca^{2+} revealed that PAO1 cells lost their regular rod cell shape in the presence of 10 mM Ca^{2+}, whereas *calC*::Tn5 mutant retained its cell shape **(Fig.3. 7E).**

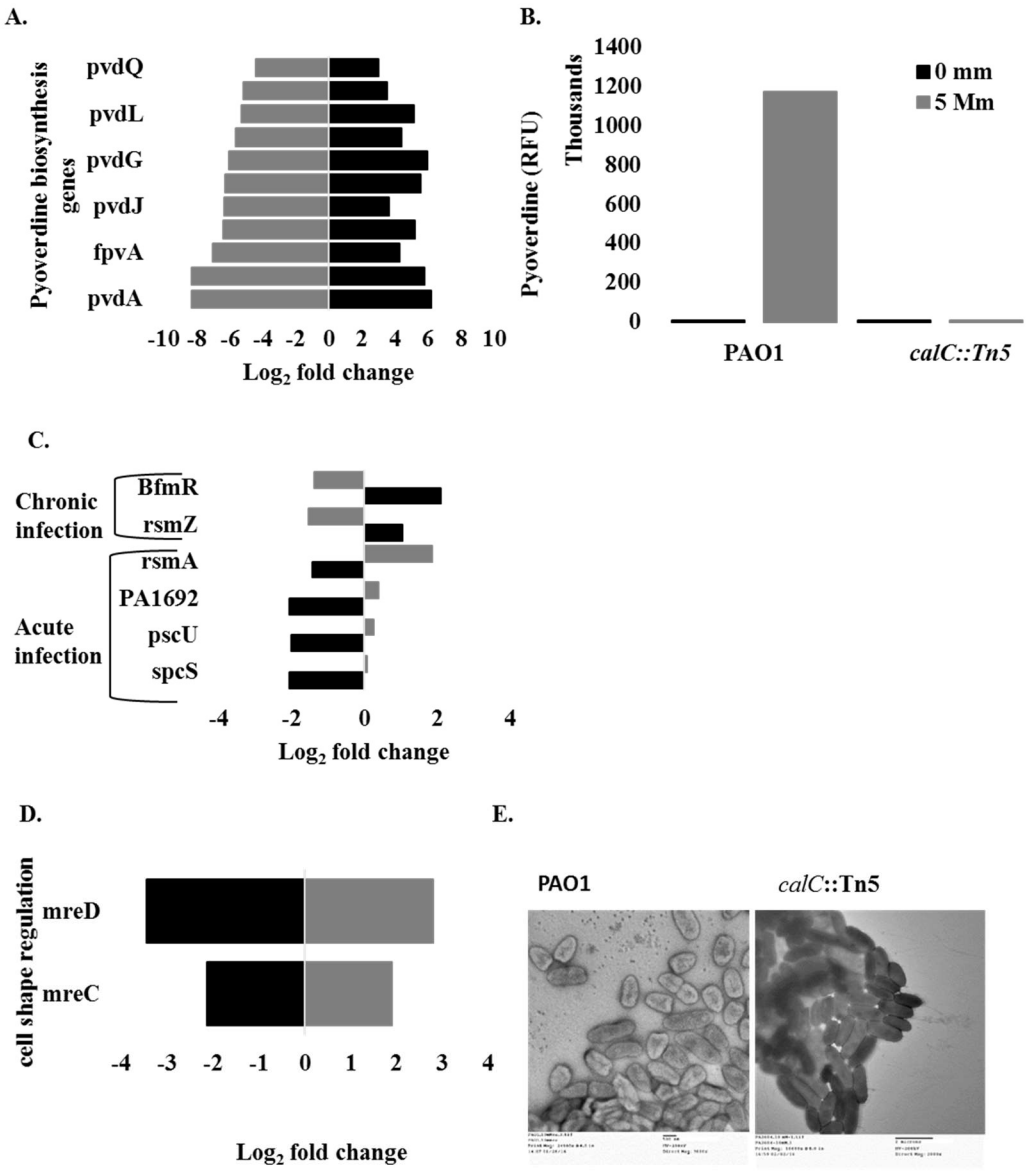

Figure 3.7: The role of *calC*::Tn5 in Ca^{2+}-regulated pathogenicity and virulence of PAO1. A. Effect of 5 mM Ca^{2+} on the transcript abundance of *pvd* genes on pyoverdine biosynthesis operon **B.** Effect of 5 mM Ca^{2+} on pyoverdine biosynthesis in PAO1 during middle log. **C.** Transcript abundance of genes

involved in pathogenic lifestyle switch in PAO1 : Solid black and *calC*::Tn5 : Grey. Adjusted *P value ≤ 0.05. **D.** Transcript abundance of genes involved in cellular shape maintenance in PAO1 : Solid black and *calC*::Tn5 : Grey. Adjusted *P value ≤ 0.0001. **E.** Electron microscopic photograph of PAO1 and *calC*::Tn5 grown in presence of 10 mM Ca^{2+}.

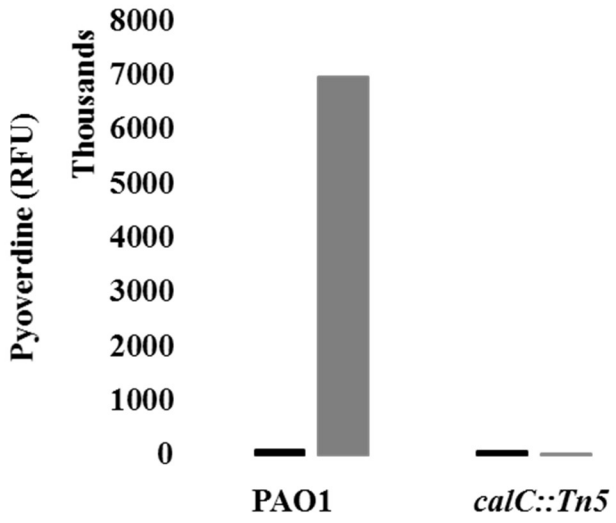

Figure 3.S4: Pyoverdine biosynthesis during stationary phase. Effect of 5 mM Ca^{2+} on pyoverdine biosynthesis in PAO1 and *calC::Tn5* at no added Ca^{2+} (solid black) and 5 mM Ca^{2+} (grey)

DISCUSSION

Earlier research by others and our work in *P. aeruginosa* identified that bacteria, in general, and *P. aeruginosa,* in particular, possess all the components necessary for functional intracellular Ca^{2+} signaling. These components include tightly regulated Ca^{2+}_{in} homeostasis; Ca^{2+} transporters and Ca^{2+} binding proteins maintaining this homeostasis (70-72); generation of transient spikes in $[Ca^{2+}_{in}]$ in response to external Ca^{2+} addition; global regulatory effect of external Ca^{2+} fluctuations on cell physiology; and Ca^{2+} responsive transcriptional regulators (70, 177). However, the experimental evidence supporting the regulatory role of the transient changes in $[Ca^{2+}_{in}]$ was missing. Here we report the identification of the first putative Ca^{2+} channel, CalC, in *P. aeruginosa*, that is required for the development of transient increases in $[Ca^{2+}]_{in}$. We also show that the lack of this protein reduced the effect of external Ca^{2+} on gene expression. The latter was supported by testing several Ca^{2+}-dependent phenotypes, such as antibiotic resistance and production of virulence factors. These results provide the first experimental evidence of Ca^{2+}_{in} signaling in prokaryotes and identify novel components of Ca^{2+}_{in} regulatory network controlling the virulence and antibiotic resistance of this pathogen.

Our first goal was to identify mechanisms responsible for generating the intracellular Ca^{2+} transient in response to extracellular Ca^{2+}. By using a bioinformatic approach we identified PA2604, a homologue of BsYetJ, the Ca^{2+}

leak channel in *B. subtilis* (159, 160). Based on the predicted domain and structure similarity with BsYetJ and the observation of significantly reduced Ca^{2+}_{in} transients in the mutant with disrupted PA2604, we predicted it to be a functional $\underline{Ca}^{2+}$ channel and designated it CalC. Another homologue of BsYetJ, human Bax inhibitor-1 (HbI-1) protein, is highly conserved and widely distributed transmembrane proteins on cellular organelles enabling the stored Ca^{2+} to release into the cytoplasm and generate cytoplasmic Ca^{2+} transients recognized as a signal. These channels are driven by concentration gradient and can passively transport Ca^{2+} in or out of cytoplasm or cellular membrane bound organelles(178). We have previously established that *P. aeruginosa* maintains its resting intracellular Ca^{2+} at 90 - 190 nM. When 1 mM external Ca^{2+} is added, this generates almost 10,000 fold gradient of Ca^{2+} across the cell wall, and causes $[Ca^{2+}]_{in}$ to be increased about 13 fold transiently followed by almost a full recovery back to the basal level (72). If the gradient is removed by chelating external Ca^{2+}, the resting level of $[Ca^{2+}]_{in}$ is fully recovered (not published). Measuring the $[Ca^{2+}]_{in}$ in *calC::*Tn5 revealed that CalC is primarily involved in influx of Ca^{2+}. However, it also showed that the loss of CalC resulted in reduced resting level of $[Ca^{2+}]_{in}$ and a partial loss of Ca^{2+} efflux enabling recovery back to basal $[Ca^{2+}]_{in}$ level. The former suggests that CalC is involved in maintaining Ca^{2+}_{in} homeostasis at low external Ca^{2+} levels as well. The latter may indicate a more complex role of CalC and its interactions with proteins involved in Ca^{2+} efflux. For the purpose of this study, we took advantage of the fact

that disruption of *calC* significantly reduced the initial increase of $[Ca^{2+}]_{in}$ in response to external Ca^{2+}. Since we hypothesized that *P. aeruginosa* has a functional $Ca^{2+}{}_{in,}$ the $[Ca^{2+}]_{in}$ transient would serve as a second messenger. Then its amplitude should be recognized as a signal and trigger the changes in gene expression shaping the global response to external Ca^{2+}. Therefore, the *calC* mutant with significantly impaired $[Ca^{2+}]_{in}$ should lack Ca^{2+}-regulated gene expression and the earlier observed phenotypic response to Ca^{2+}. Thus, the mutant provided us with a tool to generate a direct evidences confirming the signaling role of intracellular Ca^{2+} in *P. aeruginosa*.

The effect of $Ca^{2+}{}_{in}$ in global gene transcription has been a key piece in our study that establishes the impact of $Ca^{2+}{}_{in}$ transients in adaptive genetic modulation. Among the 1016 Ca^{2+} regulated genes in PAO1, 881 are dependent on the generation of $Ca^{2+}{}_{in}$ transients. We also report here that $Ca^{2+}{}_{in}$ transients positively regulates 342 genes and negatively regulates 539 which includes the genes. The genes whose transcription is affected by loss of $Ca^{2+}{}_{in}$ transients are, genes for pyoververdine biosynthesis, Pho-regulon, swarming motility, flagella biosynthesis, quorum sensing, biofilm regulation, LPS biosynthesis, peptidoglycan biosynthesis, type 3 and type six secretion systems, polycationic antimicrobial resistance and manyother genes for transpost and cellular metabolism in general. The most significant positive regulatory effect of $Ca^{2+}{}_{in}$ transients is observed for pyoverdine biosynthesis. Pyoverdine is a siderophore molecule and one of the major virulence

factors in *P. aeruginosa*(179). Primarily the iron chelating properties of pyoverdine serves in the pathogen for sequestering iron from host. This molecule also actively regulates the cell-cell communication as well as virulence of *P. aeruginosa* (180, 181). The phenotypic assay confirmed this regulatory effect of Ca^{2+}_{in} on the biosynthesis of pyoverdine. The Ca^{2+} regulation of increase in pyoverdine biosynthesis in PAO1 was completely abolishes in the *calC*::Tn5 mutant during both middle log as well as stationary phase of growth. Similarly, reduction in Ca^{2+} regulated transcript abundance for *PhoABR, bfmR*, *rhlB* in *calc*::Tn5 mutant is displayed. The pho regulon in *P. aeruginosa*, which is involved in phosphate metabolism, also contributes significantly in regulation of biofilm formation type 3 secretion system in *P. aeruginosa* (172, 173). BfmR, RhlB also controls the alginate biosynthesis genes (*algB*) and contributes in biofilm formation of *P. aeruginosa* (174). This may reflect a validation of regulatory role of Ca^{2+} on formation of robust biofilm formation in *P. aeruginosa* (74) at the transcriptional level. Simultaneouly, the negative regulation of the *rsmA*, small RNA RsmZ, (174) genes for type three secretion systems, *pscU*, *spcS* (61, 164) further supporta that Ca^{2+}_{in} transients positively regulate the biofilm formation, therefore promotes chronic infection caused by *P. aeruginosa*. Divalent cations are known to interrupt the cellular integrity for *P. aeruginosa* (24, 182).

However, most of the studies on cell membrane alteration is focused on the impact of polycationic polypeptides like host immune peptides or polycationic

antibiotics. Therefore mainly reflects the involvement of underlying mechanisms involved in resistance to such cationic compounds (24, 183, 184). Here we have identified the role of Ca^{2+} on the cellular shape (membrane integrity) maintenance of *P. aeruginosa*. Our transcriptional analysis reveals decrease in transcript abundance of mreC and mreD genes in PAO1 when cells are grown in presence of 5 mM Ca^{2+}. This decrease is however recovered in the *calC*::Tn5 mutants.

merC and *merD* genes are involved in peptidoglycan synthesis pathway and thus contributes to cell shape maintenance of bacteria (176, 185). Although this is an exciting establishment, assessment of role of Ca^{2+} on membrane integrity as well as role of CalC , MreC and MreD is required to further validate such finding.

Finally, our RNA seq analysis reveales at least 219 genes of unknown function whose transcription was differentially regulated by [Ca^{2+}_{in}] at 5 mM Ca^{2+}. Investigating the function of these genes might bring forth new knowledge in Ca^{2+} signaling of PAO1 and help us understand the significance of Ca^{2+} regulation in cellular adaptation as well as pathogenicity.

The finding that exposure to elevated Ca^{2+} increases transcription of *calC* was not anticipated and suggests that CalC is not a part of the mechanisms evolved to protect cells against toxic levels of Ca^{2+}. Here we aimed to identify the mechanisms involved in this regulation and tested a potential role of the previously identified Ca^{2+} responsive two component regulator CarSR (70), sensory kinase,

LadS (61), putative Ca^{2+} binding phytase CarP (70), and putative Ca^{2+} binding EF hand protein EfhP. CarSR is a Ca^{2+} regulated two component system which controls the transcription of two downstream Ca^{2+} regulated genes, *carO* and *carP*. Both CarO and CarP are involved in Ca^{2+} regulated tobramycin resistance. CarP also protects PAO1 from Ca^{2+} toxicity at high Ca^{2+} environment (70). LadS is another inner membrane sensory kinase that responds to external Ca^{2+} and mediates phosphorylation of GacA to turn on GacS-GacA mediated upregulation of chronic infection caused by P. aeruginosa (177). The Ca^{2+} binding calmoduline like EF hand protein EfhP of *P. aeruginosa* contributes to Ca^{2+} homeostasis and Ca^{2+} regulated virylence factor production (71). The identified role of these proteins in mediating Ca^{2+} regulation of *calC* promoter activity in PAO1 will help elucidate the relationship between these Ca^{2+} responsive regulatory proteins and CalC in mediating Ca^{2+} regulated phenotypic changes in this organism. Since, our previous microarray (70) data shows a regulatory role of Ca^{2+} on the genes involved in quorum sensing network, we included *lasR* to investigate the possible connection between Ca^{2+} signaling and quorum sensing in PAO1. We have determined that, CarR, CarP and EfhP are involved in the transcriptional enhancement of *calC* at 5 mM Ca^{2+}. This definitely interconnects these regulatory and functional component of Ca^{2+} signaling together (**Fig. 3.8**).

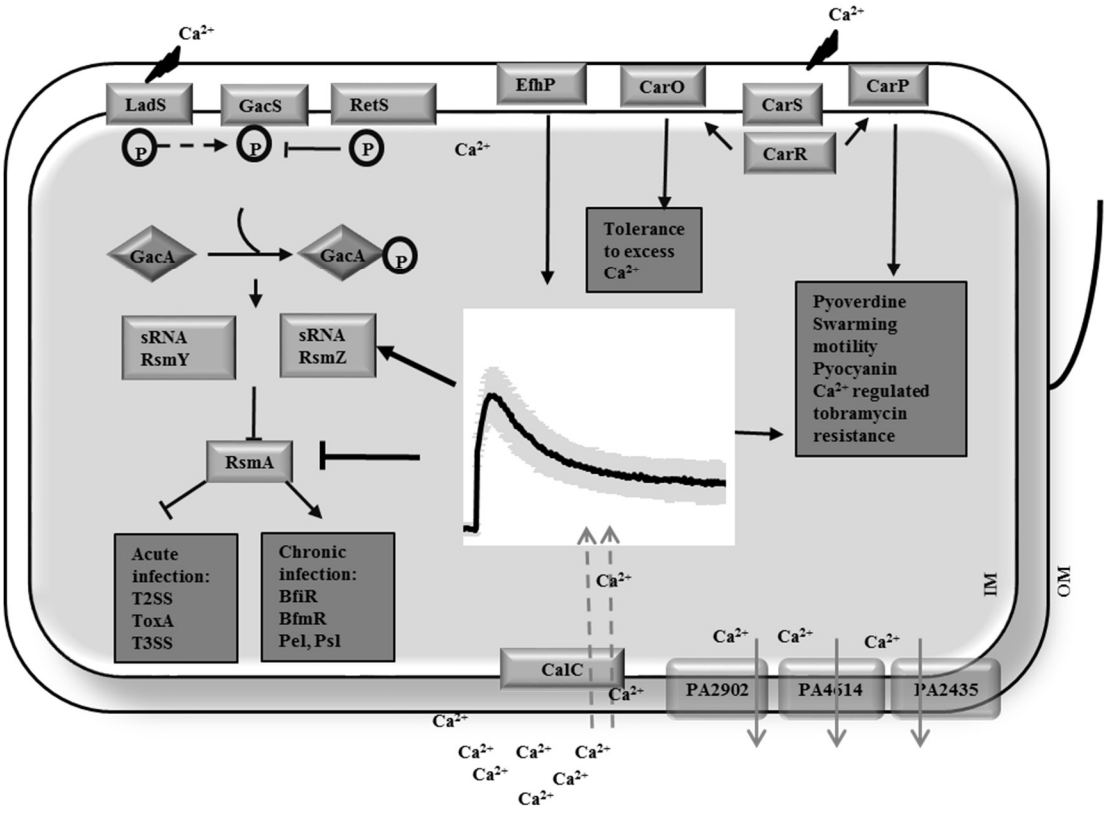

Figure 3.8: Relationship of CalC to other Ca^{2+} responsive regulators.

Earlier we showed that Ca^{2+} regulates efflux mediated tobramycin resistance in PAO1 (43). Here we investigated the role of *calC,* i.e. Ca^{2+}_{in} transients, in mediating this regulation. Disruption of *calC* significantly reduced Ca^{2+} induction of tobramycin resistance in PAO1. The mutant also showed lower level of promoter activity of *mexAB-oprM* genes.

Overall, this study identified intracellular Ca^{2+} as a second messenger in *P. aeruginosa* and established its role in regulating *P. aeruginosa* adaptations to the environments with fluctuating levels Ca^{2+}, one example of which is a human host. This signaling likely enables a recognition of changes in host Ca^{2+} homeostasis and provides a mean for fine tuning of *P. aeruginosa* physiology increasing its fitness and enhancing its chances for survival. Identification of several global regulators, including quorum sensing, responding to $[Ca^{2+}_{in}]$ uncovers another level of complexity in the structure of signaling and regulatory networks in *P. aeruginosa*.

ACKNOWLEDGEMENTS

We thank Dr. Steve Hartson and Janet Rogers at the OSU Proteomic Facility for performing MS-based protein identification and analyses. We also thank Drs. Peter Hoyt and Hong Hwang at the Biochemistry and Molecular Biology Array and Bioinformatics core facility for their help with RNA analyses. We thank Dr. Kangmin Duan at University of Manitoba, Winnipeg, Canada and Dr. MengMeng Dong at the college of Life Science, Northwest University, Shaanxi, China for

sharing reporter plasmid pMS402. We express our thanks to Drs. Tyrrell Conway and Jeremy Jackson at Microbiology and Molecular Genetic department, OSU and Dr. Joe E Grissom from Oklahoma University for their support in RNA Seq analysis. This work was supported by the OCAST (Award #HR12-167).

CHAPTER IV

THREE NOVEL PROTEINS PA2803, PA3237 AND PA5317 CONTRIBUTE TO CA^{2+}- INDUCED POLYMYXIN-B RESISTANCE IN PSEUDOMONAS AERUGINOSA.

Sharmily Khanam[1], Kerry Williamson[2], Dirk L Lenaburg[1], Tanner Onstein[1], Michael J. Franklin[2], and Marianna A. Patrauchan[1#]

[1]Department of Microbiology and Molecular Genetics, Oklahoma State University, Stillwater, OK, US

[2] Department of Microbiology and Immunology, Montana State University, Bozeman, MT, US

ABSTRACT

Calcium (Ca^{2+}) is an essential second messenger in eukaryotes and regulates vital processes in both eukaryotes and bacteria. Ca^{2+} homeostasis is impaired during diseases, which may lead to its elevated levels, as exemplified in mucous and nasal secreted fluids in patients with cystic fibrosis (CF). Our earlier work identified that Ca^{2+} enhances production of several secreted virulence factors and induces tobramycin resistance in *Pseudomonas aeruginosa*, a primary pathogen causing life-threatening antibiotic-resistant infections in CF patients. Here, we have identified that growth in the presence of elevated Ca^{2+} increases *P. aeruginosa* resistance to polymyxin B (Pol-B) more than 30 fold. To investigate the molecular mechanisms of Ca^{2+} induced Pol-B resistance, we performed random mutagenesis and identified three genes, whose products contribute to Ca^{2+}-induced Pol-B resistance of *P. aeruginosa*: PA2803, PA3237, and PA5317. Sequence analysis predicted that PA2803 encodes for a cytoplasmic phosphonoacetaldehyde hydrolase, PA3237 - metal-binding inner membrane protein and PA5317 - peptide-binding periplasmic component of ABC transporter. Genome-wide RNA-Seq analyses determined that transcription of PA2803 and PA3237 is induced at least 3 fold by elevated Ca^{2+}. RNA-Seq analyses also demonstrated the two-component regulators (PhoPQ, PmrAB and ParRS) and their regulatory targets *arnB, arnC,*

arnD, arnT, arnE earlier identified to enable Pol-B resistance, were negatively regulated by Ca^{2+}. In agreement, none of mutants lacking *phoP, pmrB and parR* contributed to Ca^{2+}-induced Pol-B resistance. We have also tested the mutants lacking Ca^{2+} inducible two component regulator CarR for it's involvement in Ca^{2+}-induced Pol-B resistance and determined no contribution of carR in this process.

Further functional characterization of the three proteins will lead to discovery of novel Ca^{2+}-regulated Pol-B resistance mechanisms, providing a better understanding of polycationic polypeptide antibiotics action mechanisms and a basis for developing novel therapeutic approaches to treat *P. aeruginosa* infections.

INTRODUCTION

Pseudomonas aeruginosa is one of the major causes of nosocomial infections in both immunocompromised and immune competent patients in the U.S.A. and worldwide (7, 8). *P. aeruginosa* is known to also infect indwelling medical devices, such as shunts and catheters (186) and cause severe and life-threatening infections in the lung airways of patients with cystic fibrosis (CF) (2). Despite being an opportunistic pathogen, *P. aeruginosa* is often mentioned as one of the deadliest pathogens due to its outstanding ability to adapt to the host environment and persist antimicrobial treatments (187). A vast repertoire of intrinsic, adaptive, and acquired antimicrobial resistance mechanisms allow the bacterium to become remarkably resistant to almost all antibiotics available for treatment (7).

The continuous failure of conventional antimicrobials for treating *Pseudomonas* infections has forced scientists to look for alternative therapeutic approaches. Cationic peptides are antimicrobial molecules naturally produced in a host body, and therefore represent an excellent potential for treating infections. Particularly in immunocompromised patients where the lack of immune response facilitates persistence of pathogens (188). Two polycationic peptides, Pol-B and Pol-E (Colistin), have been used as antimicrobials since their early discovery as an effective drug against *Pseudomonas* infection by Edger and Dickenson (189, 190). Currently, since modern antibiotics fail, and new ones are lagging in the pipeline,

polymyxins made a comeback to treatments plans (190, 191). In fact, polycationic antibiotics are considered as one of the last hope in the treatment of nosocomial infections caused by many gram negative bacteria, including *P. aeruginosa* (22). Among them, Pol-B and Pol-E are the most popular choice due to their high efficacy (191, 192). Although, adaptive resistance mechanisms for these antimicrobials have been studied since 1970 in laboratory strains, resistant strains have been rarely documented in clinical studies (193-195). The known resistance mechanisms include adaptive features protecting the bacteria *via* alterations in membrane permeability, as well as modification of LPS and lipid A molecules (22, 24, 196).

Like in any other Gram-negative bacteria, outer membrane in *P aeruginosa* acts as a protective shield against many environmental stresses, including toxic metals, antibiotics, and host immune responses. In *P. aeruginosa*, lipid A significantly contributes to the virulence of the organism (197, 198). *P. aeruginosa* is able to modify lipid A molecule and generate a variety of lipid A species, particularly during biofilm formation. Some of these changes, for example, the length of the side chain, have been associated with the degree of *P. aeruginosa* virulence (199, 200). Lipid A modifications with added palmitoyl, amino arabinose, or 3- hydroxyl decanoate have been detected in the lung airways of patients with CF (197). Furthermore, acylation of usual penta- or hexa-acylated lipid A has been associated with severe forms of CF infection. This modification also strengthens

the bacterial resistance and persistence in a host (199, 201). Polymyxins are known to target lipid A and thus anchor themselves followed by forceful disruption of the membrane and killing the bacteria. Therefore lipid A modifications disabling the interaction with polymyxins provides a resistance mechanism (25, 202). There are at least 8 enzymes shown to be involved in lipid A modification. ArtnT transfers 4-amino-4-deoxy-l-arabinose to the aminoarabinose moieties, EptA and EptB add phosphoethanolamine). LpxT is responsible for dephosphorylation, PagL and LpxR -deacylation, PagP – acylation, and LpxO - hydroxylation of lipid A molecule (202, 203). The primary research on the enzymatic modifications of lipid A and its effect on polymyxin-B is broadly perfomed using Salmonella sp. However, *P. aeruginosa* carries all the enzymes and is known to use them for the same purpose, except the PagL orthologues which causes deacylation of lipid A (reviewed in (25)). Nonetheless, the deacylation of lipid A has been observed in the polymyxin resistant strains (203, 204). Besides spontaneously occurring lipid A modifications during infections, lipid A modifications can be enhanced in the presence of polymyxin-B or growth at limited Mg^{2+} condition (25, 205, 206), suggesting that lipid A modification is an adaptive mechanism of *P. aeruginosa* regulated in response to its environment.

To date, five two component systems have been identified in *P. aeruginosa* to control lipid A modification based resistance to Pol-B (207) . Among them, PhoPQ and PmrAB both were displayed with *ArnBCDTE* operon mediated L-

Ara4N transfer to lipidA resulting into Pol-B resistance of *P. aeruginosa* (208, 209). Two other two-component systems ParR-ParS and CprR-CprS are induced by a variety of polycationic antibiotics leading to amino arabinose transferase, ArnT by activation of *Arn* operon and the modification of lipid A (22). The latter two-component regulators are induced during growth at limited Mg^{2+} (23) and upregulate the PmrAB responsible for *ArnBCDTE* expression(22, 210). Interestingly, mutation in ParRS is known to cause constitutive expression of this operon independent of PmrAB (207). Although exact mechanism is yet to be disovered, mutants of *colR*/ *colS* two component regulator/ sensor has been reported to enhance the Pol-B resistance of *P. aeruginosa* in mutants lacking *phoQ* (211).

Here we have determined that growth at elevated Ca^{2+} increases resistance of *P. aeruginosa* to Pol-B by more than 30 fold. RNA-Seq analyses showed that none of the known mechanisms of Pol-B resistance contribute to this Ca^{2+} effect. This study aimed to identify the mechanisms of Ca^{2+}-induced Pol-B resistance.

MATERIALS AND METHODS

Bacterial strains, plasmids and media

Strains and plasmids used in this study are listed in **Supplementary table S4.1**. *P. aeruginosa* strain PAO1 used in this study is the non-mucoid strain with genome sequence available. The bacterial strains were maintained on LB agar

containing corresponding antibiotics. For antimicrobial susceptibility and growth analysis Biofilm minimal media (BMM) was used. BMM (146) contained (per liter): 9.0 mM sodium glutamate, 50 mM glycerol, 0.02 mM $MgSO_4$, 0.15 mM NaH_2PO_4, 0.34 mM K_2HPO_4, and 145 mM NaCl, 20 µl trace metals, 1 ml vitamin solution. Trace metal solution (per liter of 0.83 M HCl): 5.0 g $CuSO_4.5H_2O$, 5.0 g $ZnSO_4.7H_2O$, 5.0 g $FeSO_4.7H_2O$, 2.0 g $MnCl_2.4H_2O$). Vitamins solution (per liter): 0.5 g thiamine, 1 mg biotin. The pH of the medium was adjusted to 7.0. For growth analysis cells were first grown in 5 ml tubes for 16 h (mid-log) and then used to inoculate (0.1%) 100 ml fresh medium in 250 ml flasks. This middle log cultures were harvested for transcriptomic analysis. Transposon insertion mutants were obtained from the University of Washington Two - Allele library (98) (NIH grant # P30 DK089507) (**Table S4.1**). The mutants contained ISphoA/hah or ISlacZ/hah insertions with tetracycline resistance cassette that disrupted the genes of interest. The mutations were confirmed by two-step PCR: first, transposon flanking primers were used to verify that the target gene is disrupted, and second, transposon-specific primers were used to confirm the transposon insertion. The primer sequence is available at www.gs.washington.edu. For convenience, the mutants were designated as PA::Tn5, where PA is the identifying number of the disrupted gene from *P. aeruginosa* PAO1 genome (www.pseudomonas.com).

Table 4.S1: Strains and plasmids used in this study.

Strains/ Plasmids	Description	References
E. coli DH5α	*fhuA2 Δ(argF-lacZ)U169 phoA glnV44 Φ80Δ (lacZ)M15 gyrA96 recA1 relA1 endA1 thi-1 hsdR17*	
P. aeruginosa PAO1	Wild type	(96)
PW3128 (*phoP*:Tn5)	PA1179F08::ISlacZ/hah	(98)
PW9024 (*pmrB*:Tn5)	PA4777A09::ISlacZ/hah	(98)
PW4167 (*parR:*Tn5)	PA1799G12::ISlacZ/hah	(98)
ΔcarR:Gm (*ΔPA2657)*	PAO1 with deletion of *carR* by replacing with Gm^R gene.	(70)
PW5693(PA2802:Tn5)	PA2802D02::ISlacZ/hah	(98)
PW5694(PA2803:Tn5)	PA2803A12::ISlacZ/hah	(98)
PW5696(PA2804:Tn5)	PA2804G06::ISlacZ/hah	(98)
PW6426(PA3237:Tn5)	PA3237F01::ISlacZ/hah	(98)
PW6427 (PA3238:Tn5)	PA3238A02::ISlacZ/hah	(98)
PW9960(PA5317:Tn5)	PA5317H12::ISlacZ/hah	(98)
PW5349(PA2590:Tn5)	PA2590H04::ISlacZ/hah	(98)
PAOH26NTG22.3	Selected Polymyxin-B sensitive PAO1 mutant of PAO1	This study
PAOH27NTG22.5	Selected Polymyxin-B sensitive PAO1 mutant of PAO1	This study

PAOH28NTG22.5	Selected Polymyxin-B sensitive PAO1 mutant of PAO1	This study
PAOH29NTG22.17	Selected Polymyxin-B sensitive PAO1 mutant of PAO1	This study
PA2803::pDOH30	PA2803:Tn5 containing pDH30 plasmid with the PA2802-PA2804 region	This study
PA3237:: pDOH31	PA3237:Tn5 containing pDH31 plasmid with the PA3237-PA3238 region	This study
PA5317:: pDOH33	PA5317:Tn5 containing pDH33 plasmid with the PA5317 region	This study
pMF36	A broad host range *trc* expression vector	(212)
pDOH30	pMF36 with PAO1 gene fragments containing part of PA2802- PA2804	This study
pDOH31	pMF36 with PAO1 gene fragments containing part of PA3237- PA3238	This study
pDOH32	pMF36 with PAO1 gene fragments containing part of PA2590	This study
pDOH33	pMF36 with PAO1 gene fragments containing Part of PA5317	This study

Antibiotic susceptibility assays

P. aeruginosa resistance to Pol-B was assayed as described in (43). Briefly, bacterial strains were grown in BMM at no added or 5 mM Ca^{2+}. 100 µl of the mid-log cultures normalized to the OD600 of 0.1 were spread inoculated onto the surface of BMM agar containing no added or 5 mM Ca^{2+}. E-test strips for Pol-B (Biomeurix) were placed on the surface of the inoculated plates and incubated for 24 h. The minimum inhibitory concentration (MIC) was measured as a point at which the edge of the zone of inhibition crosses the e-test strip.

Proteomic analysis

Membrane proteins were isolated by carbonate extraction as described in (99) with modifications. Briefly, cell pellets of PAO1 grown at no or elevated [Ca^{2+}] were washed in saline (0.14 M NaCl) and resuspended in TE buffer (10mM Tris/HCl, 1 mM EDTA, pH 8.0), containing Mini Complete protease inhibitor cocktail (1:100 (v/v)). Cells were disrupted by sonication (5 cycles of 30 s with 1 min interval on ice) using 550 Sonic Dismembrator (Fisher Scientific, Pittsburgh, PA), and then centrifuged at 6,000 g for 10 min at 4 ^{0}C. The procedure was repeated two times. The collected supernatants were combined, diluted with ice-cold 0.1 M sodium carbonate followed by gentle stirring for 1 h, and centrifuged at 100,000 g for 1 h at 4 ^{0}C in a Beckman L8-70M ultracentrifuge. The pellets were collected, washed twice in 50 mM Tris pH 7.3, and subjected to liquid chromatography–

tandem mass spectrometry (LC-MS/MS) – based peptide counting. Protein concentration was determined using the 2D Quant kit (GE Healthcare). LC-MS/MS spectrum counting was performed at the OSU Proteomics Facilities. Proteins were identified using Mascot (v2.2.2 from Matrix Science, Boston, MA, USA) and a database generated by *in silico* digestion of the *P. aeruginosa* PAO1 proteome predicted from the genome. Search results were validated using Scaffold 03 (Proteome Software Inc., Portland, OR). Criteria for accepting each ID will conform to the "Paris" guidelines for proteomics results (http://www.mcponline.org/misc/ParisReport_Final.dtl). A set of stringent criteria for protein identification was used, where only protein probability thresholds greater than 99 % were accepted and at least three peptides needed to be identified, each with 95 % certainty.

Random mutagenesis and selection of Pol-B sensitive mutants at 10 mM Ca^{2+}

Random mutants were generated as described in **(213, 214).** Briefly, PAO1 cells were grown in the presence of NTG (N-methyl N-nitro-N-nitrosoguanidine) in BMM at 37° C for 12 h while shaking at 200 rpm. The cells were collected and washed with 10 mM phosphate buffer (pH 7). Pelleted cells were serially diluted in the buffer and plated on BMM agar at 10 mM Ca^{2+} and incubated at 37° C for 24 h. To select polymyxin-B susceptible mutants at elevated Ca^{2+}, plate dilution MIC assay was used. The individual clones were grown in BMM with no added or 10

mM Ca^{2+} for 12 h, then cultures were normalized to OD_{600} of 0.3. 10 µl of these normalized cultures were added to BMM with the corresponding Ca^{2+} and polymyxin-B added to the media. The clones displaying no or poor growth in BMM supplied with Ca^{2+} and Pol-B were selected from the replica culture and used for complementation and sequencing.

DNA manipulation and sequencing

Genomic DNA from PAO1 was isolated and fragmented by standard procedure. The fragments were cloned into pMF36 to create a PAO1 genome library. Selected random mutants susceptible to Pol-B at high Ca^{2+} were electroporated with the plasmid library. Clones with restored Pol-B resistance at elevated Ca^{2+} selected, their complementing plasmid extracted, transformed into *E. coli* DH5α cells. The *E. coli* transformants were selected on ampicillin LB plates. The plasmids were purified and sequenced using *tac* promoter specific primer.

Bioinformatics analyses

Sequence homology searches for identified genes involved in Ca^{2+} regulated Pol-B ressitance were performed using the NCBI nr database (GenBank release 160.1), Refseq as well as PDB database. Percent identity was calculated over entire length of the protein. Functional domains were predicted using Pfam 31.0. Protein subcellular localization was predicted using pSORTb V3.0 analysis.

Protein three-dimensional (3D) structure was predicted using I-TASSER (215-217) and visualized using PyMOL(218) (version 1.8.6.0; Schrödinger, LLC). To predict the conserved domains CDD database (219) was used. TMHMM 2.0 (220)was used for identifying transmembrane component of the proteins.

RNA isolation

Total RNA was isolated from *P. aeruginosa* PAO1 grown in BMM with no or 5 mM Ca^{2+} using RNeasy Protect Bacteria Mini kit (Qiagen) or ZR Fungal/ Bacterial RNA MiniPrep^{TM} (Zymo Research) where cells were processed with 50µg/ml of lysozyme followed by the manufacturer's protocol for isolation. The purified RNA was eluted with diethylpyrocarbonate (DEPC) treated sterile nanopure water. DNase treatment was performed for eluted RNA sample using turbo DNase (Ambion). The absence of genomic DNA was confirmed by conventional PCR using *rpoD* primers. RNA yield was measured using NanoDrop spectrophotometer (NanoDrop Technologies Inc.), and the quality of the purified RNA was assessed by Bioanalyzer 2100 (Agilent) and 1% agarose gel electrophoresis. Following the MIQE guidelines, only the RNA samples with an OD_{260}/OD_{280} ratio of 1.8-2.0 and an RIN value of ≥ 9.0 and/ or rRNA ratio of 1:2 were selected for further analysis. RNA samples were stored at -80 °C.

Library preparation and RNA seq

RNA seq analysis was performed at Vertis Biotechnology AG, Germany. First, RNA samples were assessed by capillary gel electrophoresis using Shimadzu MultiNa microchip and RNA samples with a 16S/23S ratio of 1:1- 1:3 were selected for further analysis.

For capable RNA seq, first the RNA samples were enriched by capping the 5′ triphosphorylated RNA with 3′-desthiobiotin-TEG-guanosine 5′ triphosphate (DTBGTP) (NEB). For reversible binding of biotinylated RNA species to streptavidin vaccinia capping enzyme (VCE) (NEB) was used. And elution step was performed to capture the biotinylated species to streptavidin and obtain the 5' fragments of the primary transcripts.

Two different aliquots of RNA samples were then treated with Ribo-Zero rRNA kit for bacteria (Illumina) to deplete the ribosomal RNA. These RNA samples were then used for cDNA library preparation. In brief, the RNA sampleas were poly(A) tailed using poly(A) polymerase. The 5′ triphosphate or CAP were then removed by pyrophosphatase (Cellsript) and an RNA adapter was ligated to the 5′ monophosphate end of RNAs. cDNA synthesis was performed using the oligo (dT)-adapter primer and M-MLV reverse transcripase. The resultant cDNA was then PCR amplified by up to 13 cycle to yield about 10-20 nm/µl using high fidelity polymerase. The cDNA pool for Illumina NextSeq sequencing was

generated by taking equimolar cDNA samples followed by elution of samples to a size range of 200-500 bp from preparative agarose gel. The size fractionation was confirmed by capilary gel electrophoresis. The True-seq primers designed following the illumine instructions were used for the sequencing. The cDNA pools were sequenced on an Illumina NextSeq 500 system using 75 bp read length.

RESULTS

Ca^{2+} increases the Pol-B resistance of P. aeruginosa

In agreement with previous studies (221-224), we show that growth at elevated Ca^{2+} increased resistance to Pol-B in *P. aeruginosa*. By using E-strips with gradient of Pol-B, we determined that the MIC for Pol-B in PAO1 increased by 32 fold at 10 mM Ca^{2+} **(Fig. 4.1A**) and 28 fold at 5 mM (**Fig.4.1 C**). We also measured Pol-B susceptibility in planktonic cultures and determined almost 12 fold increase in MIC of PAO1 grown at 10 mM Ca^{2+} (**Fig.4.1B**).

The earlier identified mechanisms of Pol-B resistance do not contribute to Ca^{2+}-regulated polymyxin-B resistance in PAO1

In order to test whether the earlier characterized regulators of Pol-B resistome of PAO1, such as two component systems PhoPQ, PmrAB, and ParRS (22, 23, 210, 225), are also involved in the observed Ca^{2+}-enhanced resistance, we determined Pol-B MIC in the transposon mutants for *phoP*, *pmrB*, and *parR* (Table 4S.1) by using E-strips. We also included a deletion mutant of the earlier identified Ca^{2+} responsive two component regulator *carSR* (70). The antimicrobial susceptibility test showed that none of these mutations had any significant effect on Ca^{2+}-increased Pol-B resistance in *P. aerugi*nosa (**Fig. 4S.1**). In agreement, the proteomic analysis detected that although PhoP, ParR, and PmrB peptides were detected in cells grown at 0 mM Ca^{2+}, they were below detection level at 5 mM Ca^{2+} (Table 4.1). A similar reduction in response to elevated Ca^{2+} was observed for the transcripts of the corresponding genes. Furthermore, the enzymes regulated by the two-component systems and known to be responsible for lipid A modifications enabling resistance to Pol-B: ArnT (8), ArnB (19), ArnC (15), and ArnD (30), were also down-regulated in the cells grown at 5 mM Ca^{2+} both at transcriptional and protein levels (Table 4.1). One exception is WbpM, a protein important for O antigen biosynthesis, membrane permeability as well as peptide susceptibility of *P.*

aeruginosa (226, 227), whose peptide abundance was increased at least threefold at 5 mM Ca^{2+}, but whose transcription was not affected by Ca^{2+} **(Table 4.1)**.

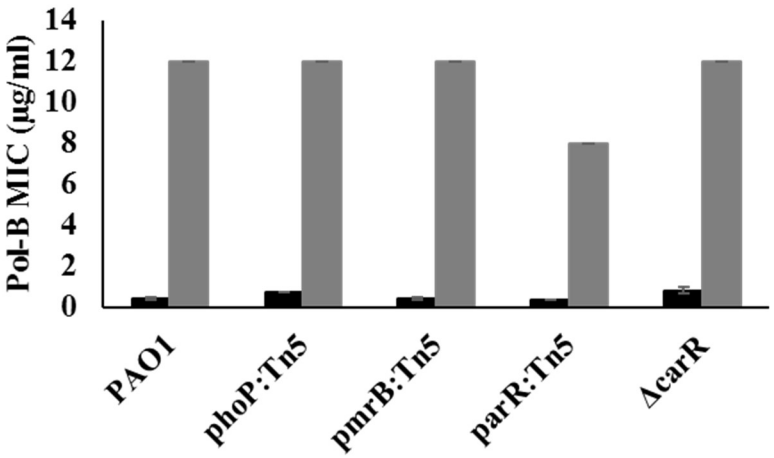

Figure 4.S1: Role of two component systems Ca^{2+} induced Pol-B resistance. Cells were grown without or with 5 mM Ca^{2+}, normalized to OD600 of 0.1, and plated onto BMM agar plates with the corresponding concentration of Ca^{2+}. E-strips with gradient of Pol-B were placed on the bacterial lawns. MIC was recorded after 24 h incubation. Solid Black: no added Ca^{2+}, Solid Grey: 5 mM Ca^{2+}.

Table 4.1. Effect of elevated Ca^{2+} on transcription and translation of selected *P. aeruginosa* PAO1 genes and proteins known to contribute to polymyxin-B resistance in PAO1. assessed by, correspondingly, RNA Seq and LC-MS/MS analyses

Gene name (PA No.)	Protein description	transcript abundance at 5 mM Ca^{2+}		# of peptides detected at no Ca^{2+}	# of peptides detected at 5 mM Ca^{2+}
		Log_2 fold change	padj*		
Two component systems					
phoP(PA1179)	Two-component response regulator	-3.8	7.1E-22	20	ND
pmrB(PA4777)	Two-component response regulator	-4.0	5.7E-17	14	ND
parR(PA1799)	Two-component response regulator	-1.6 (*parS*)	0.003	1	ND
cprR(PA3077)	Two-component response regulator	-1.5	0.57	ND	ND
colR (PA4381)	Two-component response regulator	0.4	0.29E-1	ND	ND
Outer membrane protein					
oprH(PA1178)	Outer membrane protein, H1	-6.2	1.5E-51	20	ND
Lipid A modifying enzymes					

arnT(PA3556)	Inner membrane L-Ara4N transferase	-5.9	8.0E-15	8	ND
arnB(PA3552)	UDP-4-amino-4-deoxy-L-arabinose--oxoglutarate aminotransferase	-6.5	1.3E-21	19	ND
arnC(PA3553)	Glycosyl transferase	-6.3	2.3E-17	15	ND
arnD(PA3554)	4-deoxy-4-formamido-L-arabinose-phosphoundecaprenol deformylase	-6.0	7.0E-10	30	ND
Protein for membrane integrity					
wbpM(PA3141)	Nucleotide sugar epimerase	0.44	0.16	4	13

ND, Not detected.

Three hypothetical proteins of unknown function are involved in Ca^{2+}- induced Pol-B resistance of PAO1

To identify the mechanisms enabling Ca^{2+}-induced Pol-B resistance, we employed genome-wide random chemical mutagenesis followed by Pol-B susceptibility tests of the individual clones. A total number of 20 mutants with increased Pol-B susceptibility at elevated Ca^{2+} were selected. Complementation of these mutants with PAO1 genome library resulted in at least 50% recovery of the wild type resistance in four of the mutants **(Fig.4.1)**. Sequencing of the complementing genome fragment identified several regions of PAO1 genome. Region 1 contained, PA2802, PA2803, PA2804; region 2: PA3237, PA3238; region 3: PA2590; and region 4: PA5317. In order to further determine which of these genes are involved in Ca^{2+} regulated Pol-B resistance, the corresponding transposon mutants with individually disrupted genes of interest were obtained from the University of Washington transposon mutant library (98) and tested their Ca^{2+}-dependent Pol-B susceptibility. This allowed identification of three genes: PA2803, PA3237 and PA5317, the mutation of which reduced Pol-B resistance at elevated Ca^{2+} by more than 50% **(Fig. 4,2)**. The complementation of the mutants with the corresponding genome fragments restored the wild type level of Pol-B **(Fig. 4.2)**.

Interestingly, the disruption of PA3238 resulted in increased Pol-B resistance at 5 mM Ca^{2+} **(Fig. 4S2)**.

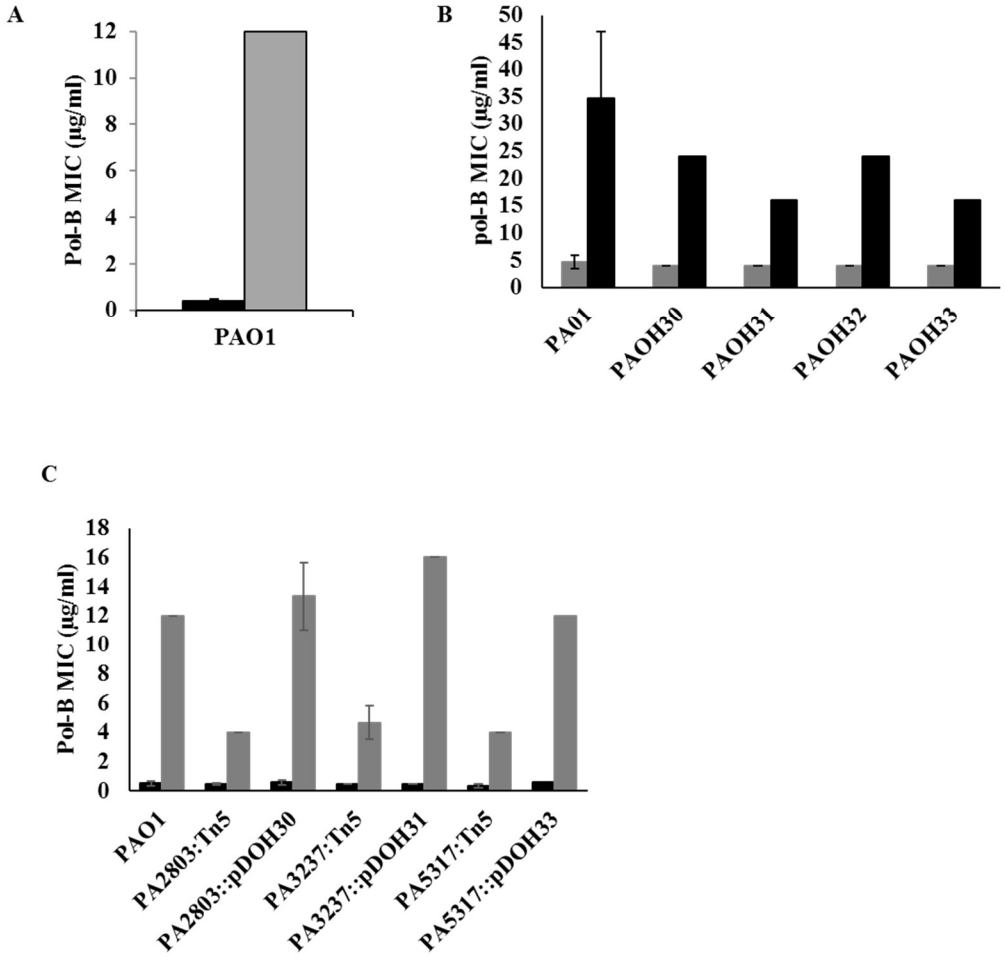

Figure 4.1: Pol-B susceptibility assay. A. E-test for PAO1 Cells were grown without or with 5 mM Ca^{2+}, normalized to OD600 of 0.1, and plated onto BMM agar plates with the corresponding concentration of Ca^{2+}. E-strips with gradient of pol-B were placed on the bacterial lawns. MIC was recorded after 24 h incubation. **B.** Plate dilution assay for PAO1 and selected complemented NTG

mutants. The cultures were grown without or with 10 mM Ca^{2+}, normalized to OD_{600} of 0.3, and normalized cultures were inoculated into corresponding media at 1:100 ratio. 200 µl of this culture were then added to each well of 96 well plate with or without pol-B at different concentration. Plates were incubated at 37° C with fast shaking in Biotek plate reader. The MIC was recorded after 24 h incubation. **C.** E-test for PAO1 and transposon mutants. The MIC assay was performed as described above. Solid Black: no added Ca^{2+}, Solid Grey: 5 mM or 10 mM Ca^{2+}.

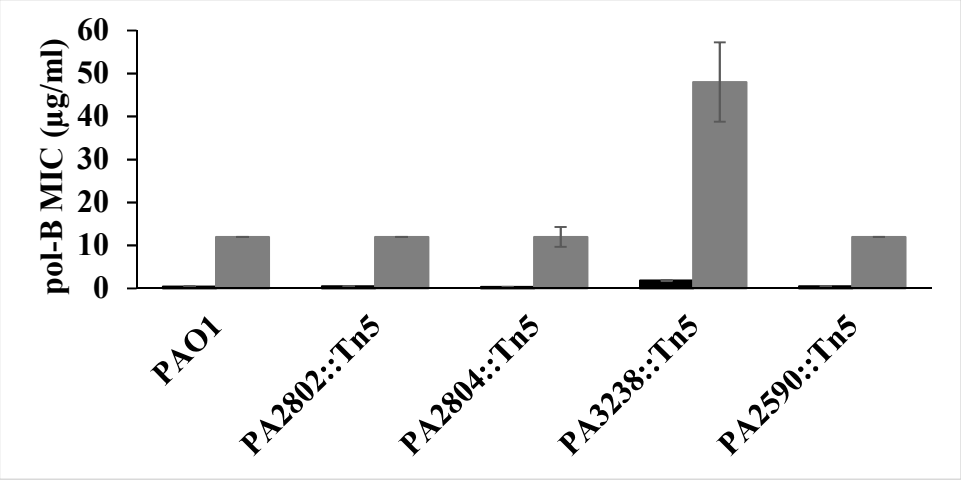

Figure 4.S2: Role of the genes identified by random mutagenesis in Ca^{2+} induced polymyxin-B resistance. Cells were grown without or with 5 mM Ca^{2+}, normalized to OD600 of 0.1, and plated onto BMM agar plates with the corresponding concentration of Ca^{2+}. E-strips with gradient of pol-B were placed on the bacterial lawns. MIC was recorded after 24 h incubation. Solid Black: no added Ca^{2+}, Solid Grey: 5 mM Ca^{2+}.

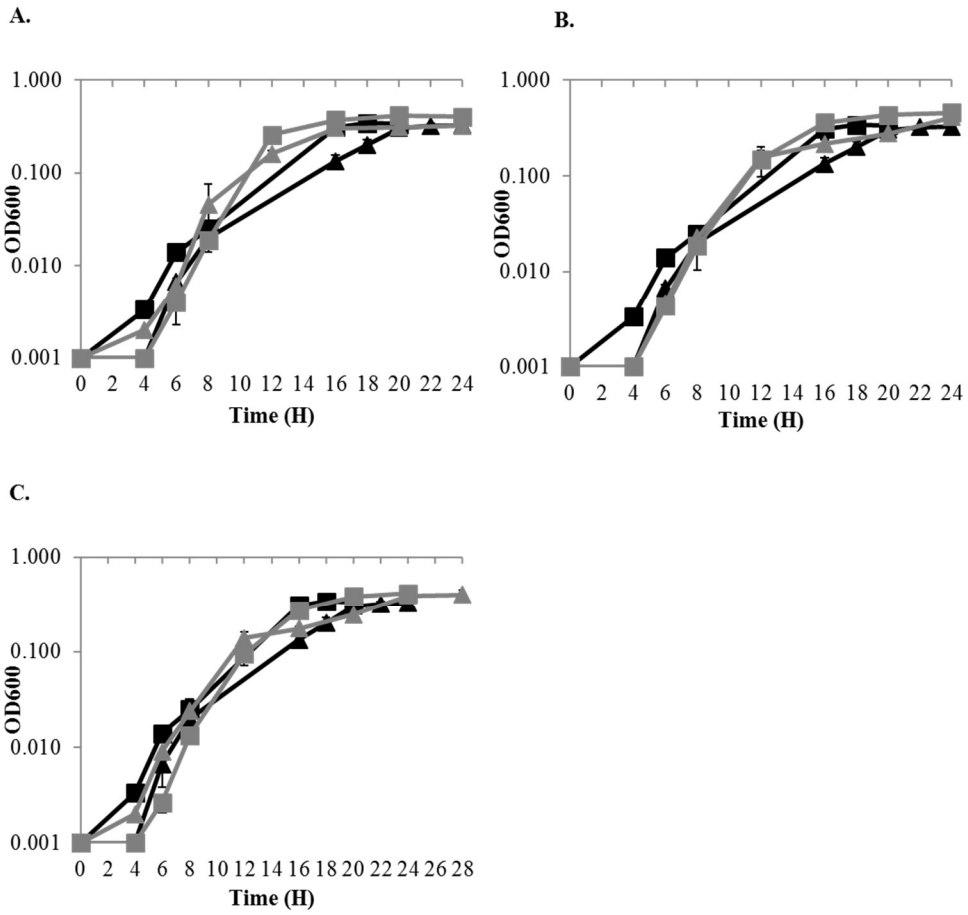

Figure 4.S3: Growth analysis of PAO1 and A. PA2803, B. PA3237 and C. PA5317. Cells were grown without or with 10 mM Ca^{2+}, normalized to OD600 of 0.1, and normalized culture was added to 100 ml of BMM with corresponding Ca^{2+} at 1:1000 ratio. Cell density at 600 nm was measured every 2-4 hours. PAO1: Black and the mutants: Grey. No added Ca^{2+}: square, 10 mM Ca^{2+}: triangle.

Sequence analyses predicted PA2803 to encode a putative phosphonoacetaldehyde hydrolase, PA3237 - a DNA binding protein and PA5317 - a peptide binding component of ABC transporter

Through BLASTP homologue search in non-redundant protein data base PA2803 is found to be conserved among gram negative proteobacteria. Based on 99% amino acid identity over the entire protein length with phosphonoacetaldehyde phosphoglucomutase YcjU from *Enterobacter cloacae*, PA2803 was predicted to encode a phosphonoacetaldehyde hydrolase. Through genome wide sequence homologue searchin E. coli, YcjU has been identified among other haloacid dehalogenase like phosphatases (228). In *E. coli* YcJu catalyzes the conversion of D-glucose 1-phosphate to D-glucose 6-phosphate through the intermediate beta-D-glucose 1,6-bisphosphate (227). According to functional domain prediction in Conserved Domain Database (CDD), PA2803 contains a haloacid dehalogen (HAD)-like domain, which is conserved throughout all kingdoms of life and serves in a wide variety of enzymatic reactions **(Fig. 4.2 A)**. For instance, HAD domain is required for phosphate hydrolysis in SERCA (Sarcoendoplasmic reticulum Ca^{2+}-ATPase) (229). By using PSORTb 3.0 algorithms, PA2803 was predicted to reside in cytoplasm. Further, this protein is conserved among pseudomonads. Among 184 complete sequenced *Pseudomonas* genome, homologue of PA2803 is identified in 40 genomes with a percent identity ranginf from 25% to 63%. In *P. aeruginosa* genome, the closest paralog is PhnX (PA1311), a phosphonoacetaldehyde

hydrolase sharing 25 % amino acid identity. In addition, PA2803 and PhnX have similar genomic environments, including transcriptional regulator (PA2802/PA1309) and phsphonohydrolase/2-aminoethylphosphonate-pyruvate transaminase (PA2804/PA1310) **(Fig. 4.2B)**. According to I-Tasser algorithm and based on structural homology to phoshonoacetaldehyde hydrolase from *Oleispira antarctica*, PA2803 was predicted to form a 3D structure with 10 α-helices and one parallel β-sheet. It was also predicted to bind Ca^{2+} *via* Gly16, Ser18, Ser49, Ala164 residues, but with a moderately low C score (0.33) **(Fig. 4.2C)**.

PA3237 shares 100% amino acid identity with a hypothetical membrane protein in *E. cloacae*, PA3237 which also carries the domain of unknown function (DUF2061) like PA3237.BLASP analysis in Pseudomonas.com database identified homologues of PA3237 in chromosome of *P. stutzeri, P.resinovorus, P. alcaligens, P. mendocina, P. pseudoalcaligens, P. plecoglossicida* and *P. balaerica* with a % identity ranging from 42% to 81%. In P. aeruginosa however, only one paralogue, PA2183 has been detected with DUF2061 domain. By using TMHMM 2.0 algorithm, PA3237 was predicted to have 23 amino acid residues (13-35) embedded into the inner membrane **(Fig. 4.2 A)**. Further analysis with PSORTb 3.0 supported the prediction of PA3237 to be localized within an inner membrane. According to I-Tasser, PA3237 is structurally similar to the archaeal metal-binding protein SS06904 from hyperthermophilic *Sulfolobus solfataricus* **(Fig. 4.2C)**.

Very recently, two *dpp* operons (*dppBCDF* and *dppA1-A5*) have been annotated in PAO1 genome, with PA5317 annotated as *dppA5* (230) . These operons were previously identified by using dipeptide utilization based screening by Pletzer *et al* (231). According to CDD functional domain prediction, PA5317 contains dipeptide binding domain, PBP2-DppA **(Fig. 4.2A)** present in the periplasmic fold of ABC transporters. DppA is a periplasmic dipeptide transporter protein found in *E. coli* that has the identical functional domain as PA5317, DppA5. DppA is a membrane protein that transports peptides, proteins and contributes to peptide chemotaxis (232). Dpp proteins are also known to function as drug receptors (233). Structural prediction by I-Tasser PA5317 modeled a globular structure based on homology to dipeptide binding protein from *Pseudoalteromonas* sp. SM9913, a Gram-negative marine bacterium **(Fig. 4.2C)**.

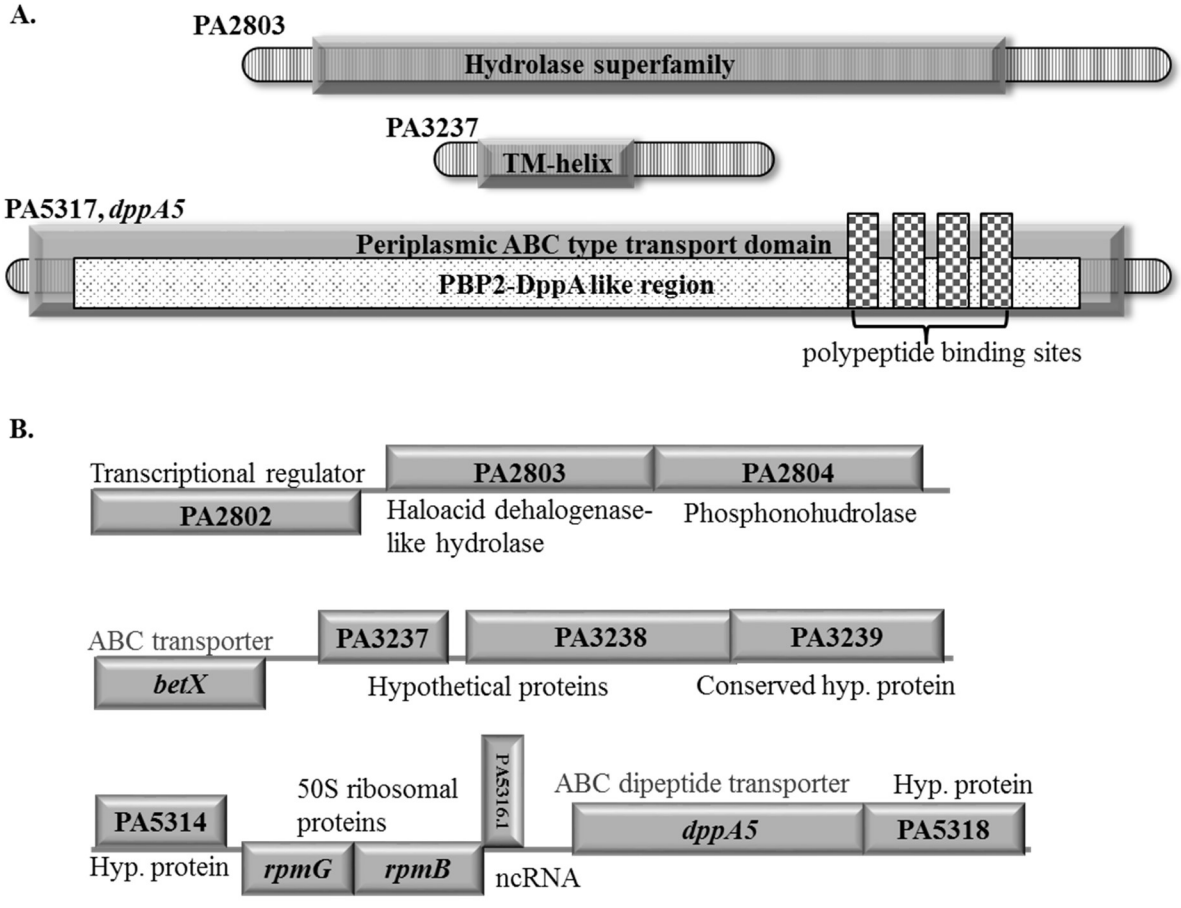
A.
PA2803
Hydrolase superfamily
PA3237
TM-helix
PA5317, dppA5
Periplasmic ABC type transport domain
PBP2-DppA like region
polypeptide binding sites
B.
Transcriptional regulator
PA2802
PA2803
Haloacid dehalogenase-like hydrolase
PA2804
Phosphonohudrolase
ABC transporter
betX
PA3237
Hypothetical proteins
PA3238
PA3239
Conserved hyp. protein
PA5314
Hyp. protein
50S ribosomal proteins
rpmG
rpmB
PA5316.1
ncRNA
ABC dipeptide transporter
dppA5
Hyp. protein
PA5318

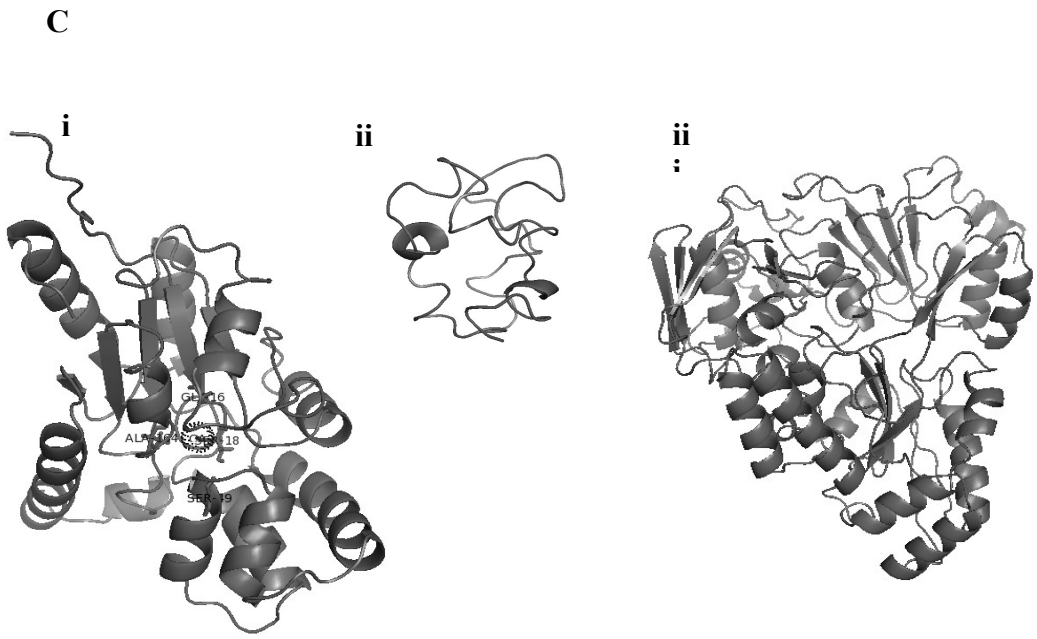

Figure 4.2: **Sequence analysis for PA2803, PA3237 and PA5317. A**. Prediction of functional domains of PA2803, PA3237 and dppA5. Analysis was done using Coserved Domains and Protein Classification (CDD) data base, X ref: Pfam, Iterative Threading Assembly Refinement Algorithm (I-Tasser) and Transmembrane Helices; Hidden Markov Model (TMHMM) 2.0. The HAD domain of PA2803 was predicted by I-Tasser analysis and CDD database. The transmembrane helices of PA3237 was predicted by TMHMM analysis. The PBP2-DppA like conserved domain in PA5317 was identified using CDD, X-ref: P-fam. The peptide binding sites in DppA5; W404, I 408, MGWA 421-424 and D 426, was determined by sequence alignment in CDD database. **B.** Schematic presentation of genomic neighborhood of PA2803, PA3237 and *dppA5*. The gene annotation is as in http://www.pseudomonas.com. C. 3D Structure prediction by I-Tasser for PA2803, PA3237 and DppA5. The modeling was done by PyMOL Version 3.0. PA2803 is predicted to bind Ca^{2+} at the core region surrounded by G16, S18, S49 and A164 with a confidence score (C score) of 0.33 (C score ranges from 0-1, higher C score represents the reliability of prediction).

Ca^{2+} regulates the transcription of PA2803 and PA3237

RNA-Seq transcriptional analysis revealed that Ca^{2+} regulates transcription of PA2803 and PA3237 in *P. aeruginosa* PAO1. The transcript abundance of PA2803 and PA3237 was elevated by almost 7 and 3 fold, respectively during growth at 5 mM Ca^{2+} (**Fig 4.3**). This supported the earlier observation by microarray analysis that PA2803 and PA3237 were up-regulated at least 3 fold in, respectively, planktonic and biofilm cultures of *P. aeruginosa* FRD1 grown at 10 mM Ca^{2+} (**Table 4.2).** These genes were also reported induced in PAO1 in response to subinhibitory concentrations (SIC) of tobramycin (5 µg/ml) and Cu^{2+} shock (10 mM) (37, 131). Response to tobramycin constituted 2-3 fold induction, whereas response to Cu^{2+} shock was about 2 fold for PA2803 and 357 fold for PA3237. Furthermore, when PAO1 cells were grown at 10 mM Cu^{2+}, transcription of all three, PA2803, PA3237 and PA5317, was increased by at least 20 fold (131).

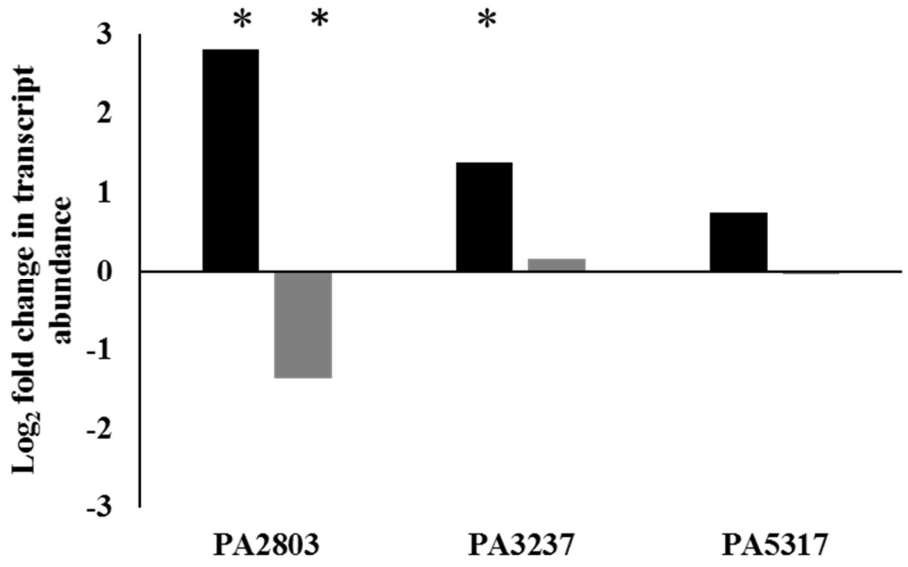

Figure 4.3: RNA-seq analysis: Fold change in transcript abundance of PA2803, PA3237 and PA5317 in PAO1 in response to 5 mM Ca^{2+}. For this RNA was isolated from PAO1 cultures growth in BMM with no added or 5 mM Ca^{2+} till middle log. RNA-seq was performed using Illumina NextSeq sequencing. Adjusted *P value ≤ 0.01.

DISCUSSION

With the current problem of global rise in increasing multidrug resistance, polycationic polypeptides were considered as one of the last line of defense against multidrug resistant bacterial infections (22) and became one of the most popular choices of combinatorial antimicrobial therapy (190, 234, 235). However, resistance to these antibiotics is not unfounded in *P. aeruginosa* (191, 236), and represents a great concern. Here, we showed that the earlier discovered lipid A modification-based mechanism of PolB resistance are not involved in Ca^{2+}-induced pol-B resistance in PAO1, and identified three genes potentially constituting novel mechanisms of resistance to this antibiotic in the presence of the cation.

The involvement of two component systems PhoPQ, PmrAB, ParRS in Pol-B resistance in *P. aeruginosa*, (23, 210, 237) as well as its association to another divalent cation, Mg^{2+} (23) are the major reason we selected these systems to investigate their role in Ca^{2+} regulated Pol-B ressitance. Besides the enzymes which govern the lipidA modification, OprH (H1), a membrane protein, also cationic in nature, can stabilize the membrane integrity to reduce the uptake of cationic antibiotics (94) Interestingly, both the protein abundance and well as transcript abundance of the two component proteins and the the enzymes regulated by them as well as the membrane protein H1 was found un detected or reduced when PAO1 was grown in presence of 5 mM Ca^{2+} compared to that at no added Ca^{2+} (Table 1).

This suggests that there might be some other mechanisms of adaptive Pol-B resistance yet to be discovered. To further confirm the role of the already known mechanisms of Pol-B resistance in the Ca^{2+} regulated pol-B resistance of PAO1, antimicrobial susceptibility assay were performed for the mutants lacking functional individual genes belonging to the two component systems. In addition, we also tested the mutant lacking *carR*, part of Ca^{2+} responsive two component system, CarSR, for its Pol-B susceptibility at 5 mM Ca^{2+}. CarSR is a two component system which can sense the presence of external Ca^{2+} in the environment and regulate many Ca^{2+} regulated phenotypes in *P. aeruginosa* (70). None of the two component regulators showed any involvement in Ca^{2+} regulated Pol-B resistance (Fig. S1), confirming our previous observation through the proteomic and transcriptomic analysis. Therefore, we pursued NTG mediated random mutagenesis to identify the genes involved in Ca^{2+}-induced pol-B resistance.

Through an extensive screening of Pol-B susceptible random mutants at 10 mM Ca^{2+}, we identified three hypothetical proteins whose absence make *P. aeruginosa* susceptible to Pol-B even when 5 mM or 10 mM Ca^{2+} was added to the medium. PA2803 is predicted as a Phosphonoacetaldehyde dehydrolase by BLAST homologue search. Phosphonoacetaldehyde dehydrolases are enzymes involved in hydrolysis of phosphate in the phosphor-molecule biosynthesis (238). PAO1 itself carries another Phosphonoacetaldehyde dehydrolases, PhnX, which hydrolyzes

Aminoethylphosphonic acid to liberate phosphate for the bacterium to utilize (239). The best functionally characterized homologue of PA2803, YcjU, a phosphoglucomutase, is a phosphatase with the HAD domain in *E. coli* which belongs to the glucose metabolism pathway of the bacterium (228). In *E. coli*, loss of *ycjU* has been documented for quinolone and nalidixic acid resistance of the bacterium (240, 241). This protein is also required for the bacterium to survive against oxidative stress (241). However, the *phnX* in PAO1 has never been documented to play role in stress protection or antibiotic resistance of the bacterium. Since, phosphonohydrolase dehydrolases are known enzymes to hydrolyze phosphate intermediates of phosphonolipid, phosphonoprotein and phosphonosugar metabolism (228, 242), it would be plausible to investigate its role in membrane integrity and thus Pol-B resistance of PAO1. Also, since PA2803 displays Ca^{2+} binding potential (Fig. 2 C). An investigation of the protein function in presence of Ca^{2+} may shed light on how this enzyme can be involved in Ca^{2+} regulated Pol-B resistance of PAO1.

Very little knowledge is available on PA3237 as well as its closely related homologues. However, through global gene expression analysis PA3237 has been hound to be regulated positively by PQS, quorum sensing molecule (243). This gene is also highly upregulated at the swarm center of swarming colonies of PAO1(244). Lastly, PA5317, recently annotated as dppA5 (230) is a predicted peptide binding component of an ABC transporter . With the peptide binding ability

predicted by I-Tasser, PA5317 is likely to be involved in transport of molecule which either inactivate Pol-B or inhibit it from binding and disrupting the membrane.

The Pol-B or TLR4 mediated alteration of bacterial outer membrane involves the mechanisms which protect the bacterium from initial attack of the compounds on the membrane (25, 245). Since none of these mechanisms contribute to Ca^{2+} regulated Pol-B resistance, it is likely that Ca^{2+} may protect the bacterium from attack of Pol-B on the inner membrane, which in fact is the lethal effect of the antibiotic (192). Specially, the transcriptional regulation of PA2803 and PA3237 by growth at increased Ca^{2+} **(Fig. 3)** and other stimuli such as Cu^{2+} or tobramycin at sub inhibitory concentration **(Table 4.2)** indicates significance of these genes in adaptive physiological response in *P. aeruginosa*. Therefore, involvement of PA2803, a cytoplasmic protein, PA3237, a cytoplasmic membrane protein and PA5317 a periplasmic peptide binding protein in Ca^{2+} regulated Pol-B resistance may reveal unique mechanisms of adaptive polycationic peptide resistance in PAO1.

Table 4.2: Effect of different stimuli on transcription of PA2803, PA3237, and PA5317 genes in *P. aeruginosa* PAO1.

Gene ID	Gene annotation	Fold change in Gene transcription in response to Ca^{2+}		[c]SIC of TOBR in planktonic cells (37)	[d]Cu^{2+} shock (131)	[e]Adapted Cu^{2+} shock (131)
		[a]Planktonic culture	[b]Biofilm			
PA2803	Probable phosphonohydrolase	1.4	1	**2**	**5**	**89**
PA3237	probable metal binding protein	0.8	1.7	**3**	**357**	**21**
PA5317	Probable periplasmic peptide binding component of ABC transporter	0.8	1	1	1	**20**

The increased abundances of transcripts 2 fold and above are shown in bold.

The data were collected from the Geo profiles at

http://www.ncbi.nlm.nih.gov/geoprofiles.

[a]Microarray was performed using RNA isolated from *P. aeruginosa* FRD1 strain grown in BMM with no added or 10 mM Ca^{2+}.

[b]Microarray was performed using RNA isolated from microsection of Biofilm of *P. aeruginosa* FRD1 strain grown at no added or 10 mM Ca^{2+}

[c] Planktonic cultues were grown in presence of 5 µg/ml of tobramycin and RNA isolated from late exponential phase cultures.(37)

[d] 10 mM $CuSO_4$ was added to PAO1 culture. For Cu^{2+} shock, cells were harvested at middle log and treated with $CuSO_4$ for 4.5 Hrs and for adapted Cu^{2+} shock, $CuSO_4$ was added at the beginning of the growth and the cells were grown in presence of added 10 mM $CuSO_4$ (131)

However, more investigation is required to identify the underlying mechanisms governed by PA2803, PA3237 and PA5317 and determine how these proteins protect *P. aeruginosa* from Pol-B at high Ca^{2+}. In depth bioinformatics analysis to make a relationship tree for each of these proteins will help us predict its true function. Such prediction can be utilized to design and assay the function of the proteins and how they contribute to Ca^{2+} regulated Pol-B resistance of PAO1.

Overall, we identified that there are three novel proteins which are involved in Ca^{2+} regulated Pol-B resistance. This can lead to identification of novel mechanisms which can be utilized by the bacterium to thrive against polycationic polypeptides, either antibiotics or from host. The identification of the function of this proteins in Ca^{2+} regulated Pol-B can direct us toward discovery of alternative treatment therapy to avoid rising antimicrobial resistance toward this antibiotic.

ACKNOWLEDGEMENTS

We thank Dr. Steve Hartson and Janet Rogers at the OSU Proteomic Facility for performing MS-based protein identification and analyses. Undergraduate researchers, Laurel Meysing, Danci Johnston and Kelly Burch performed PCR-confirmation of the UW transposon mutants. This work was partially supported by the Grant-in-Aid from American Heart Association (Award #09BGIA2330036) and OCAST (Award #HR12-167).

CHAPTER V

DISCUSSION

The main goal of this research was to establish the regulatory role of Ca^{2+} on antibiotic resistance of *P. aeruginosa*, specifically tobramycin and polymyxin-B (Pol-B).

Our lab focuses on elucidating the signaling role of Ca^{2+} and determine the Ca^{2+} regulatory network in human pathogen *P. aeruginosa,* PAO1. Previous research in our lab has identified that PAO1 maintains Ca^{2+} homeostasis *via* multiple mechanisms including influx and efflux of Ca^{2+} with the help of several Ca^{2+} transporters (72) and several Ca^{2+}-binding proteins(70, 71) with diverse functions. The global regulatory effect of Ca^{2+} on transcriptomic (70) and proteomic expression (73) including many virulence associated factors (74) suggests that Ca^{2+} may play a role as a second messenger modulating PAO1 physiology. Both in our lab and others have identified Ca^{2+} responsive regulators that can sense the presence of external Ca^{2+} and relay the signal to control virulence and pathogenicity associated regulatory network as well as other physiological responses in *P. aeruginosa*, PAO1 (61, 70, 177, 246). Our current research mainly focuses on the intracellular Ca^{2+} $[Ca^{2+}]_{in}$ signaling in *P. aeruginosa* and its involvement in Ca^{2+} regulated virulence and antibiotic resistance in this pathogen. Here we have determined the regulatory role of Ca^{2+} on tobramycin (aminoglycoside) and polymyxin-B (polycationis polypeptide) resistance of PAO1. We have identified the role of at least six RND efflux pumps in Ca^{2+} regulated tobramycin resistance, three of which also participates in efflux of Ca^{2+} in this

organism (43). We have also identified three novel proteins which contribute to Ca^{2+} regulated polymyxin-B resistance of PAO1. Furthermore, through homologue search we have identified a Ca^{2+} channel protein, PA2604 (designated CalC), which is required for the development of $[Ca^{2+}]_{in}$ transient increases. Lack of functional *calC* disrupted Ca^{2+} regulation of many virulence and cell integrity associated genes in this organism and abolished Ca^{2+} induction of tobramycin resistance. Altogether, these discoveries support our hypothesis that Ca^{2+} regulatory network is involved in regulation of adaptive resistance and virulence of *P. aeruginosa*.

Evolution of Ca^{2+} signaling in living organisms developed as a mean to utilize abundant environmental Ca^{2+} as a resource for survival and adaptation. On the other side, to protect themselves from the toxicity of the environmental Ca^{2+}, living organisms developed mechanisms to maintain a balanced access of Ca^{2+} into their cellular systems and control Ca^{2+}-dependent changes in their physiology (83, 247, 248). Thus, from the very ancestral life form, Ca^{2+} has been established as a powerful first and second messenger controlling a variety of cellular processes (247, 249, 250). The maintenance of basal $[Ca^{2+}]_{in}$ at a very low concentration (nM level) in the presence of a gradient with the extracellular Ca^{2+} (mM level) of more than 100,000 fold requires Ca^{2+} chelating, buffering, extruding in a high rate and efficiency. Such homeostasis is maintained by copious numbers of proteins with selective affinity toward Ca^{2+} that can chelate or bind Ca^{2+} to keep the intracellular and extracellular Ca^{2+} gradient intact. Besides, numbers of transporters, channels

and pumps, have been known to extrude Ca^{2+} with an extraordinarily high speed and efficiency (248). In eukaryotes, the amplitude and frequency of changes $[Ca^{2+}]_{in}$ hold the key feature for $[Ca^{2+}]_{in}$ signaling and is orchestrated by proteins with C2 domains or PIP2 domains, the P-type ATPases, Na^{+}/Ca^{2+} or K^{+}/Ca^{2+} ion exchanger as well as voltage gated channels in eukaryotic cells (251-253). In eukaryotic cells the transient changes in $[Ca^{2+}]_{in}$ level are generated by both acquisition of stored Ca^{2+} (254) *via* voltage-gated channels (248) as well as transporters of extracellular Ca^{2+} across the plasma membrane by transient receptor potential (TRP) ion channels (255). This transient increase in $[Ca^{2+}]_{in}$ allows the signaling initiation. However, increased Ca^{2+} is buffered by Ca^{2+} binding proteins (CaBPs) (256) or extruded out of cytoplasm by sarcoendoplasmic reticulum P-type ATPases (SERCA) into the ER or plasma membrane P-Type ATPases (PMCAs) to outside of the cells very quickly in order to bring back the cytoplasmic level of Ca^{2+} to basal level (248, 252, 253). This synchronized change in $[Ca^{2+}]_{in}$ is the key feature that mediates signaling by Ca^{2+} as both primary and second messenger regulating cellular processes such as cell division, fertilization, muscle contraction, nerve cell stimulation, as well as heart function, regulation of hormone secretion and balance, and immune response (64, 83, 84, 248).

Since evolution of Ca^{2+} signaling is a natural phenomenon happened at the earlier developmental stages of earth, it is likely that the single celled organisms pioneered in adaptation of Ca^{2+} homeostasis and signaling mechanisms. The

experimental evidence of $[Ca^{2+}]_{in}$ homeostasis in prokaryotes dates back to late 1980s (257). This delay reflects the limitation of tools to assess the Ca^{2+} homeostasis in prokaryotes. The structural differences in prokaryotes and eukaryotes as well as the toxicity of the reagents used to measure $[Ca^{2+}]_{in}$ made the use of many $[Ca^{2+}]_{in}$ measurement tools unusable for bacteria (reviewed in (251)). Nonetheless, identifying the ability of prokaryotes to maintain tightly regulated basal $[Ca^{2+}]_{in}$ at a very low level (170-300 nM), which is similar to eukaryotes (100-300 nM), became a big breakthrough in this area of research (257, 258). The construction of aequorin based $[Ca^{2+}]_{in}$ measurement tool (258) allowed to further advance the progress in this area. Although the knowledge on Ca^{2+} signaling in bacteria is at its early phase, many CaBPs as well as Ca^{2+} transporters and channels have been identified in different bacteria starting from the very first discovery of Ca^{2+} signaling potential in *E. coli* in 1987 (257). These proteins, particularly bacterial P-type ATPases share strong similarity to those in eukaryotes. For instance, the P-type ATPase, YloB in *Bacillus subtilis* is similar to the SERCA P-type ATPase on ER of eukaryotic cells (259). Also, many other bacteria have been shown to possess P-type ATPases, such as CaxP in *Streptococcus pneumonia*, PMAI in *Synechocystic sp*., PacL in *Synechococcus sp*, Cda in *Flavobacterium adoratum*, Lmo818 and LMCAI in *Listeria monocytogens*, some of which were shown to be involved in Ca^{2+} transport or Ca^{2+} regulated physiological responses. In addition to P-type ATPases, there are electrochemical potential driven

transporters that also contribute in Ca^{2+} homeostasis maintenance (reviewed in (47)). Among channels, the pH sensitive Ca^{2+} leak channel BsYetJ in *B. subtilis* has been experimentally characterized to transport extracellular Ca^{2+} into cytoplasm and is activated by change in pH of the environment (178). Prokaryotes also encode a large number of proteins with characteristic features indicating their ability to bind Ca^{2+}. Some of these proteins carry Ca^{2+} binding motifs ranging from calmoduline like EF- hand to β-roll, Greek key, Blg domain (47). The discovery of acidocalcisome like Ca^{2+} storage membrane components in *Rhodospirillum rubrum* and *Agrobacterium tumefaciens* is an evidence that bacteria may be able to instigate the changes in $[Ca^{2+}]_{in}$ by storing Ca^{2+} in these compartmentalized Ca^{2+} stores (260, 261). Along with the presence of transporters and other CaBPs, there is a growing evidence of Ca^{2+} regulation of bacterial physiology strongly suggesting the signaling role of Ca^{2+} in bacteria. Binding of Ca^{2+} may provide protein stability which is required for enzymatic activity of that protein. One such example is transglycolase Slt35 in *E. coli* which has EF-hand like Ca^{2+} binding site. Binding of Ca^{2+} to this site stabilizaes the protein to allow enzymatic function, catalyzing intermediates of peptidoglycan biosynthesis (262). Besides this, Ca2+ sensing two component regulators CarR-CarS in Vibrio cholerae has been experimentally established to bind external Ca^{2+} and relay the signal to control biofilm formation (263) Altogether the above knowledge suggests that there may be an intricate

regulatory cascade which actively response and relay the Ca^{2+} signal in bacteria (reviewed in (47).

In our lab, we study the signaling role of Ca^{2+} using the model organism *Pseudomonas aeruginosa*, PAO1. *P. aeruginosa*, though opportunistic in nature, is a notorious pathogen with outstanding multidrug resistance. The study of Ca^{2+} signaling is important for *P. aeruginosa* since the pathogen resides in the lungs of Cystic fibrosis (CF) patients where there is an abundance of free Ca^{2+} (67, 68). Furthermore, due to the aberrations in ion homeostasis in CF lungs, the level of Ca^{2+} is elevated in lung, nasal, and oral liquids (67). Regulatory role of Ca^{2+} in adaptive virulence and pathogenicity traits of *P. aeruginosa* including production of biofilm, extracellular proteases, rhamnolipid, pyocyanin (73, 74) as well as T3SS and T6SS (264, 265) in *P. aeruginosa* raises a fundamental question: whether P. aeruginosa can utilize Ca^{2+} as a signaling ion to modulate it's physiological response. In my research, I have observed a striking spike in antibiotic tolerance of *P. aeruginosa* toward tobramycin (aminoglycoside) and Pol-B (polycationic polypeptide) when grown at elevated Ca^{2+}. Both of these antibiotics are cationic in nature and represent one of the most effective choices for treatment against *P. aeruginosa* infections. Since our main goal is to elucidate the Ca^{2+} regulatory network, we aimed to identify the mechanisms of Ca^{2+}-induced antibiotic resistance. The increase in the MIC for aminoglycosides in the presence of divalent cations has been observed in the clinical isolates of *P. aeruginosa* (266). However,

no underlying mechanisms of Ca^{2+} regulated antibiotic resistance were known. *P. aeruginosa* is an organism capable of using a multitude of mechanisms to obtain antibiotic resistance. Therefore, it was important to first study whether any of the known mechanisms are responsible for Ca^{2+} regulated antibiotic resistance. In order to do so, we used global proteomic and transcriptomic approaches. The former identified several transporters from the RND superfamily of efflux pumps to be significantly more abundant when the bacterium was grown in presence of elevated Ca^{2+}. Efflux pumps are one of the major cause of antimicrobial resistance to multiple antibiotics (30). Interestingly, these transporters play a multi-layered role in many processes such as stress responses (76, 77) , virulence (45, 81), extruding chemically diverse toxic chemicals, biocides (32), cell signaling molecules (38, 78) , toxic metals (41, 267) as well as antibiotics (21, 34, 122). Furthermore, there is a large number of efflux pumps encoded in *P. aeruginosa* genome. Among the twelve efflux pumps identified in *P. aeruginosa* PAO1, six were identified in our research to be involved in Ca^{2+} regulated tobramycin resistance. This is a novel discovery, since prior to our study, MexXY-OprM was the only efflux pump known to contribute to efflux mediated aminoglycoside resistance of *P. aeruginosa* (33, 121, 122, 268). Also, in our data, *mexY* mutant was the only one that showed reduction in tobramycin resistance even when Ca^{2+} was not present in the growth medium (43). However, the other five efflux pumps appear to be involved in tobramycin resistance of this pathogen only at elevated Ca^{2+}. The involvement of six efflux

pumps in Ca^{2+} regulated tobramycin resistance indicates the possibility of more than one type of Ca^{2+} regulation. The pumps' activity could be enhanced upon exposure to external Ca^{2+}. Either the gene expression of this pumps are regulated by Ca^{2+} or tobramycin could be co-effluxed along with the Ca^{2+}. First, we identified that except MexEF-OprN, all five of these pumps are transcriptionally regulated by Ca^{2+}. Second, involvement of MexJK-OprM, MexEF-OprN and CzcCBA in Ca^{2+} efflux indicated that tobramycin resistance by these pumps could be as a result of co-efflux of the tobramycin and Ca^{2+} through the pumps. Interestingly, sequence analysis prediction identifies CzcCBA as a cation transporting pump in *P. aeruginosa* (41, 116), our study is the first experimental evidence that it plays role in Ca^{2+} efflux in this organisms. Besides involvement of several efflux pumps in Ca2+ regulated tobramycin ressitance and plant infectivity requirement of intact Ca^{2+} homeostasis for transcriptional regulation of the efflux pumps indicates possible role of Ca^{2+} signaling in this regulatory effect (72)

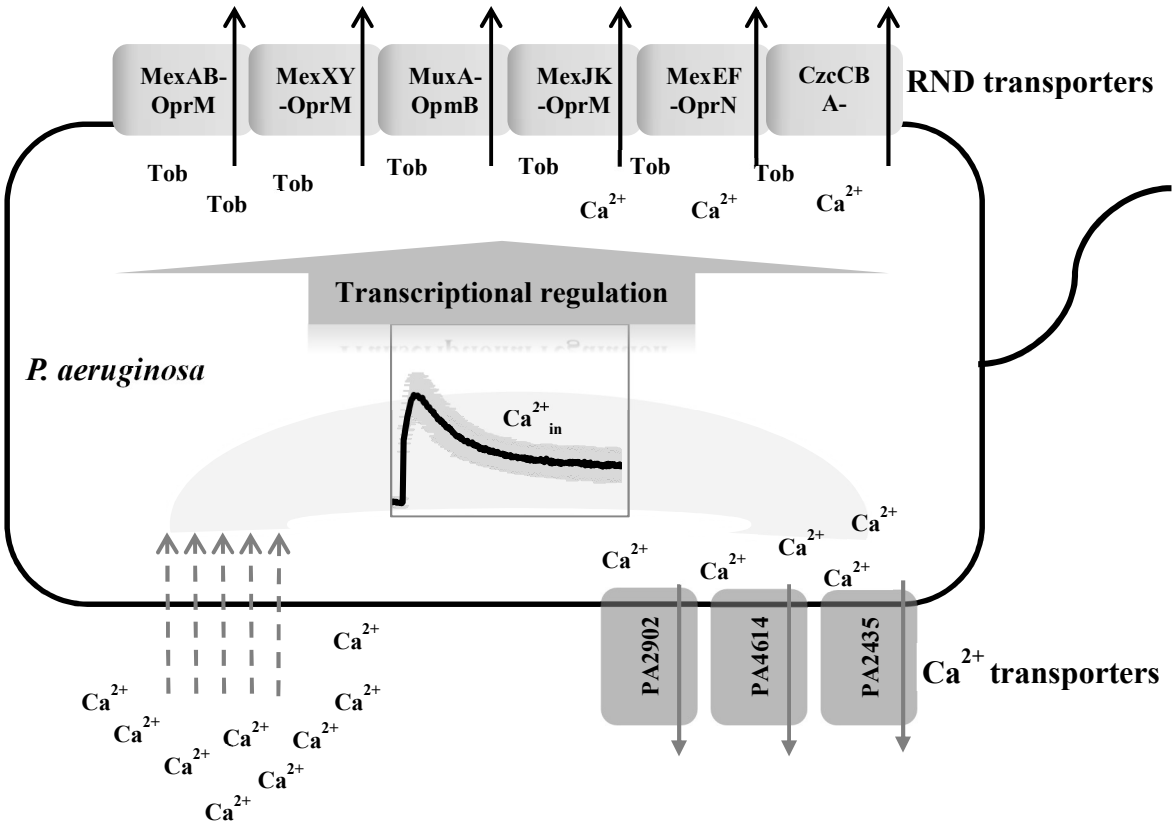

Figure 5.1: The proposed model of Ca^{2+} regulation of tobramycin resistance in *P. aeruginosa.* Elevation of extracellular Ca^{2+} causes a transient spike in $[Ca^{2+}]_{in}$. Several Ca^{2+} transporters from different families, including PA2902, PA4614, and PA2435 [39], and three RND systems (MexJK-OprM, MexEF-OprN, CzcCBA-OpmY) contribute to the maintenance of $Ca^{2+}{}_{in}$ homeostasis. The intracellular Ca^{2+} increase regulates the transcription of several efflux pumps involved in Ca^{2+}-induced tobramycin resistance (MexAB-OprM, MexXY-OprM, MuxABC-OpmB,

MexJK-OprM, MexEF-OprN, CzcCBA-OpmY). Black arrows: tobramycin efflux, grey solid arrows: Ca^{2+} efflux, grey dashed arrows: Ca^{2+} influx.

Loss of Ca^{2+} transporters causes reduction in Ca^{2+}- induced tobramycin resistance as well as Ca^{2+} regulated transcriptional upregulation for the *mexAB-oprM* efflux pump. These findings are summarized in figure 5.1 and support an intriguing possibility that intracellular Ca^{2+} signaling is involved in regulation of Ca^{2+}-enhanced antibiotic resistance and virulence of this pathogen.

In order to determine the role of $[Ca^{2+}]_{in}$ transients in regulating Ca^{2+}-induced antibiotic resistance and virulence of PAO1, our first goal was to identify a channel protein which is required for generating the cytoplasmic $[Ca^{2+}]_{in}$ transients. In eukaryotes, such channels allow the transient entry of Ca^{2+} and generation of a peak in $[Ca^{2+}]_{in}$ followed by buffering or extrusion of the Ca^{2+} out of cytoplasm by CaBPs and Ca^{2+} transporters (248). Poly β hydroxy-bytyrate- poly phosphate (PHB-PP) complexes are kwon to form channel like structure identified in the cell membrane of many bacterium including, *Azotobacter vinelandii, Bacillus subtilis, Haemophilus influenzae, and E. col etc*(269-271). Both $Ca2^{+}$ influx channels and (PHB-PP) channels have been identified in bacteria as involved in generating the transient peak of $[Ca^{2+}]_{in}$ (272). Although homologue search for PHB synthase gene in PAO1 did not identify any protein clusters. However *P. aeruginosa* is known to produce polyhydroxyalkanoate (PHA) which requires the PHA synthesases, PA5056 and PA5058. The polyphosphate (PP) regulation in *P. aeruginosa* involves the exopolyphatase PA5241 and the polyphosphate kinase,

PA5242 (170, 171). Therefore, it is likely that P. aeruginosa uses PHA-PP channels instead of PHB-PP channels to bind to Ca^{2+}. We have also, in our research, identified a homologue of Ca^{2+} channel BsYetJ of *B. subtilis* (178), PA2604 (CalC) in PAO1. Among the PHA synthases, PP regulators and the calcium hannel CalC, CalC is the only one without which the transient changes in $[Ca^{2+}]_{in}$ that potentially holds the '$[Ca^{2+}]_{in}$ signaling signature' was nearly abolished (**chapter 3**). Furthermore, the disruption of *calC* caused the loss of Ca^{2+} regulated pigment production, swarming motility as well as tobramycin resistance. The global transcriptional analysis with RNA–Seq of the mutant with disrupted *calC* revealed the regulatory role of $[Ca^{2+}]_{in}$ transients in transcription of many virulence associated genes as well as genes for transport, cellular metabolism and catabolism, oxidative phosphorylation, phosphate regulation *etc* in response to Ca^{2+}. These most significant effect has been identified for the genes included *pvd* genes whose expression was downregulated in the mutant but was > 200 fold upregulated by Ca^{2+}. Supporting this, we measured pyoverdine production in PAO1 and detected no pyoverdine accumulation in the mutant at 5 mM Ca^{2+}. Considering that CalC is required for generating the $[Ca^{2+}]_{in}$ transients and that its mutation reduced Ca^{2+} effect on global transcription in PAO1, we concluded that $[Ca^{2+}]_{in}$ transients are required to mediate Ca^{2+} regulation in *P. aeruginosa* physiology. This supports our hypothesis that $Ca^{2+}{}_{in}$ plays a signaling role in this organism.

The next task was to determine the relationship between CalC with other Ca^{2+} responsive regulators and Ca^{2+} binding proteins, that were earlier identified to mediate Ca^{2+} regulation in PAO1. One major event of Ca^{2+} signaling in eukaryotes involves binding Ca^{2+} to calmodulin sensors, leading to conformational changes and facilitating binding of calmodulin to other regulatory proteins, thus transducing the Ca^{2+} signal towards regulation of gene expression (248). Previously our lab identified calmodulin-like CaBP in *P. aeruginosa*, EfhP which has Ca^{2+} binding EF hand regions and contributes to Ca^{2+}-regulated virulence (71). We predict that EfhP functions in Ca^{2+} signal transduction. In addition to EfhP, our group identified CarP, an inner membrane anchored periplasmic protein, regulated by Ca^{2+}responsive two component system CarSR and contributes to both Ca^{2+} homeostasis as cellular tolerance to increased surrounding Ca^{2+} (70). The actual mechanism how CarP mediates this function is yet to be discovered. However, based on sequence analyses, it may bind Ca^{2+} and either transduce this signal or activate a putative phytase domain releasing inorganic phosphate and potentially contributing to protecting cells against elevated Ca^{2+}. Another putative periplasmic Ca^{2+}-binding, CarO, is regulated by CarSR in Ca^{2+}-dependent manner and contributes to Ca^{2+} homeostasis in PAO1. CarP and CarO both contribute to Ca^{2+}-regulated tobramycin resistance in *P. aeruginosa*. Besides the CaBP identified in our lab, LadS is a sensor kinase, which is phosphorylated upon exposure to increased external Ca^{2+} and regulates GacA-GacS controlling lifestyle of *P. aeruginosa.* The involvement of all

these proteins in Ca^{2+} regulation is summarized in **Figure. 5.2**. By using promoter activity, we showed a regulatory relationship of *calC* with *carR*, *carP* and *efhP*. The Ca^{2+} regulated increase of *calC* transcription was completely abolished in the mutants of *carR*, *carP*, and *efhP*, thus identifying Ca^{2+} regulatory network. Although the RNA-seq analysis suggested that Ca^{2+} regulated transcription of *rsmA*, which is a GacA-GacS dependent regulator contributing to inhibition of acute infection and promote chronic infection by upregulating the genes involved in this process, , is also dependent on *calC*, further analysis is required to confirm this relationship. Promoter activity of *calC* in the mutant lacking *ladS* as well as the promoter activity of the LadS regulated downstream regulator *rsmA* and sRNA RsmZ (**Figure 5.2**) will help us to build the connection between *calC*- and *ladS*-dependent Ca^{2+} regulon.

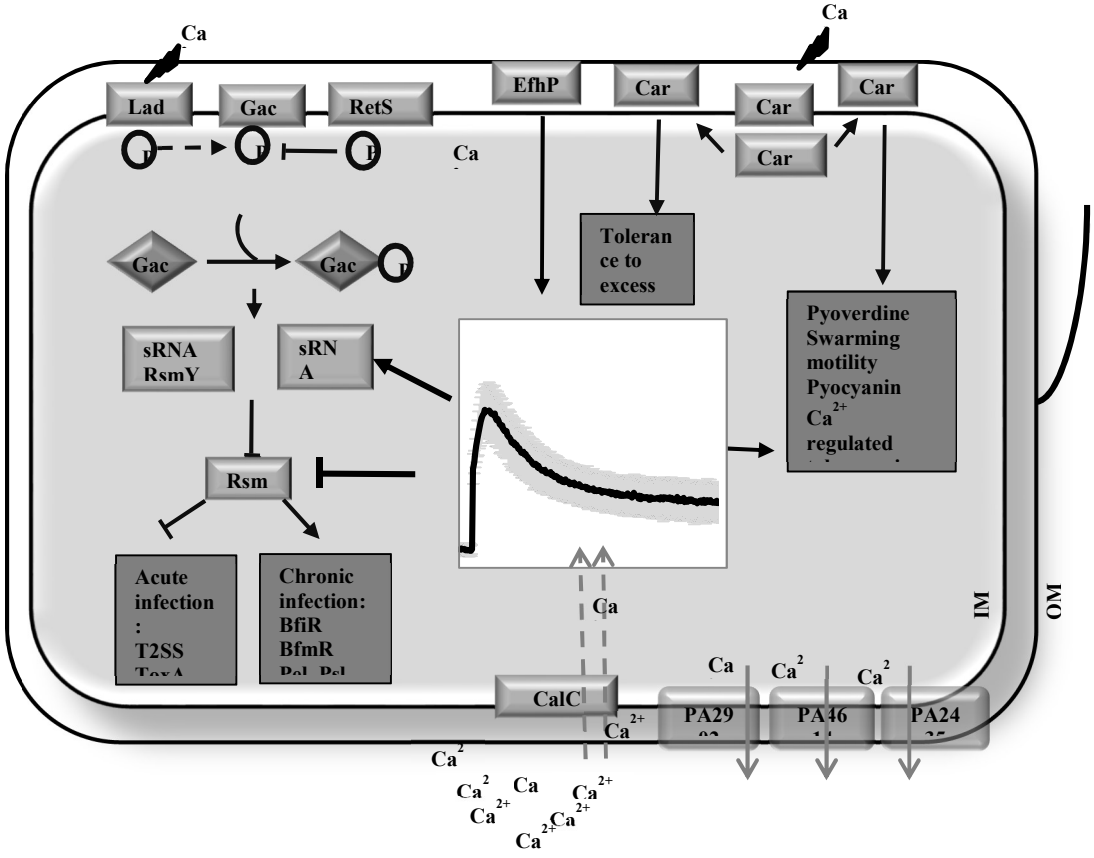

Figure 5.2. Relationship between CalC and other Ca^{2+} responsive regulators, transporters and CaBPs in *P. aeruginosa*.

Finally, we have also investigated the mechanisms of Ca^{2+} -induced Pol-B resistance in *P. aeruginosa*. PhoPQ, PmrAB, ParRS and CprRS-dependent lipid A modifications are the known key resistance mechanisms of Pol-B in Gram-negative bacteria including *P. aeruginosa* (22, 205, 210). These modifications include enzymatic acylation or deacylation of the acyle chains, amino-arabinose, phosphoethanolamine attachment ot the phosphate residues on the glucosamine or KdO of lipid A (22, 23, 225, 236, 273, 274). Interestingly, our global proteomic and transcriptomic (RNA-seq and microarray) analyses supported that none of the known mechanisms of Pol-B-B resistance respond to Ca^{2+}. Further analysis by mutational study confirmed that the two component regulators PhoPQ, PmrAB and ParRS controlling the lipid A modifications mediated Pol-B resistance in *P. aeruginosa* (22, 236) do not contribute to Ca^{2+}-dependent increase in Pol-B resistance of this pathogen. Instead, we have discovered three hypothetical proteins, PA2803, PA3237 and PA5317 which contributes to this phenomenon. While PA3237 is homologous to archaeal metal binding protein and PA5317 is a predicted peptide binding component of ABC transporter, PA2803 shares homology to phosphonoacetaldehyde hydrolase in *Enterobacter cloacae* (**Chapter 4**). Although YcjU, (241) the homologue of PA2803 is known to contribute to bacterial resistance to the antibiotic nalidixic acid , none of the PA2803, PA3237 and PA5317 have ever been identified to be involved in Pol-B resistance. Further

analysis is required to determine the functional roles of these proteins in Ca^{2+} regulated polymyxin-B resistance of *P. aeruginosa*.

Overall, we have identified the mechanisms involved in Ca^{2+} regulated tobramycin resistance and how the $[Ca^{2+}]_{in}$ homeostasis is involved in this process. Further extension of the relationship between Ca^{2+} responsive mechanisms and CalC will allow reconstruction of Ca^{2+} signaling network in *P. aeruginosa*. Such knowledge with provide us with in-depth understanding of how this pathogen can utilize Ca^{2+} as a source of information in an attempt to adapt to its environment. This will further our understanding of adaptive resistance and virulence of *P. aeruginosa* and its interactions with the host and help to come up with better strategies to treat or prevent *Pseudomonas* infections.

CHAPTER VI

CO-AUTHORED PROJECTS

I

ROLE OF THE TWO-COMPONENT REGULATOR, CarSR, IN REGULATING *PSEUDOMONAS AERUGINOSA* CALCIUM-INDUCED ANTIBIOTIC RESISTANCE.

M. Guragain, M. King, K.S. Williamson, A.C. Perez-Osorio, T. Akyama, S. Khanam, M.A. Patrauchan, and M.J. Franklin. 2016, *Journal of Bacteriology*. The *Pseudomonas aeruginosa* PAO1 two-component regulator, CarSR, regulates calcium homeostasis and calcium-induced virulence factor production through its regulatory targets, CarO and CarP.

INTRODUCTION

Pseudomonas aeruginosa, a natural inhabitant of soil and water, is able to infect a variety of hosts, including plants and humans. In humans, it causes severe acute and chronic infections by colonizing respiratory and urinary tracts, burned or wounded epithelia, cornea, and muscles (161, 275, 276). The versatility of *P. aeruginosa* pathogenicity is associated with diverse metabolic capabilities, multiple mechanisms of resistance, a large repertoire of virulence factors, and adaptability, due in part to tightly coordinated regulation of gene expression. A large portion of

the *P. aeruginosa* PAO1 genome, approximately 9.4%, encodes transcriptional regulators (277, 278), including two-component regulators (TCS): 89 response regulators, 55 sensor kinases, and 14 sensor-response regulator hybrids (161). The regulatory targets for most of these regulatory systems are unknown.

Calcium plays an important signaling role in both eukaryotic and prokaryotic cells. In prokaryotes, Ca^{2+} is an essential nutrient, since it is a necessary cofactor for many enzymes. However, Ca^{2+} can be toxic to cells at high concentrations, and therefore bacteria maintain a low sub-micromolar intracellular concentration of Ca^{2+} (279). *P. aeruginosa* may encounter environments where external Ca^{2+} levels are in the milimolar range, varying from 10 mM in soil (280) to 40 mM in hypersaline lakes (281). As a plant and human pathogen, *P. aeruginosa* may be exposed to lower but also varying Ca^{2+} levels. For example, in plants, Ca^{2+} concentration ranges from 0.01 to 1 mM in extracellular spaces (282) and from 1 to 10 mM in apoplasts (283). In a human body, Ca^{2+} levels may reach about 1 - 2 mM in extracellular fluids and saliva (284) (285), and 5 mM in blood (286) and human milk (287). In case of disease, for example, during cystic fibrosis (CF) pulmonary infections, both intracellular and extracellular Ca^{2+} levels fluctuate in response to inflammation (87, 288), and the overall Ca^{2+} levels in nasal secretions and sputum increase at least two fold (285) reaching up to 3-7 mM (289, 290).

In a previous study, we demonstrated that *P. aeruginosa* maintains a sub-micromolar intracellular concentration of Ca^{2+} ($[Ca^{2+}]_{in}$) (279). However, when the cells are exposed to high levels of extracellular Ca^{2+}, characteristic of the environments described above, the cells undergo a transient increase of $[Ca^{2+}]_{in}$. The transient increase is followed by a return to sub-micromolar levels of $[Ca^{2+}]_{in}$ and a maintenance of homeostatic concentration of internal Ca^{2+}, apparently due to the transport of excess Ca^{2+} through Ca^{2+} export pumps. Interestingly, in addition to maintenance of Ca^{2+} homeostasis, *P. aeruginosa* recognizes the external concentration of Ca^{2+} as a physiological signal, and responds through changes in the abundances of intracellular proteins and secreted virulence factors, alginate, pyocyanin, and secreted proteases (146, 291). This Ca^{2+} triggered change in *P. aeruginosa* physiology leads to enhanced plant infectivity (157), biofilm formation, and swarming motility (146, 279, 291). Furthermore, Ca^{2+} alters the abundance of *P. aeruginosa* proteins involved in iron acquisition, quinolone signaling, nitrogen metabolism, and stress responses (146, 291). These observations suggest that Ca^{2+} plays an important regulatory role in *P. aeruginosa* virulence. However, the molecular mechanisms responsible for sensing environmental Ca^{2+} and regulating the Ca^{2+}-induced responses are not known. Therefore, the goals of this study were to identify and characterize Ca^{2+}-mediated molecular responses.

Bacteria use two-component regulatory systems (TCSs) to sense and respond to diverse and continuously changing environmental stimuli, including

changing cation concentrations. TCSs help regulate responses to Na^{+}, Mg^{2+}, and other cations, and therefore are likely involved in Ca^{2+}-dependent regulation. A typical TCS contains a sensor kinase located partially in the cytoplasmic membrane and a cognate response regulator (292). Upon exposure to a stimulus, the sensor kinase autophosphorylates at histidine residues. The consequent conformation change enables the transfer of a phosphate group to the aspartate residue on the cognate response regulator, which typically results in DNA binding to an activator DNA sequence and changes in gene expression (278, 293). *P. aeruginosa* has many TCSs, and some of these have been characterized. For example, PhoPQ and PmrAB regulate resistance to polymyxin B and antimicrobial peptides *via* lipid A modification at low magnesium (Mg^{2+}) concentration (294-297). PhoPQ also regulates aminoglycoside resistance, twitching and swarming motility, surface attachment, and biofilm formation, ultimately contributing to regulation of virulence (298, 299). PmrAB is induced by cationic antimicrobial peptides including polymyxins (295), whereas PhoPQ is induced by polyamines and low [Mg^{2+}] (300). Other TCSs respond to metals, including the CzcRS and CopRS systems that regulate the resistance to zinc and copper, respectively (131, 301). CzcRS also regulates the transcription of CzcrBCA Resistance-Nodulation-Division (RND) efflux pump, which is responsible for carbapenem resistance (301). GacAS and AlgRZ regulate the production of several virulence factors including pyocyanin, cyanide, lipase, and alginate, as well as systemic virulence

and motility (166, 299, 302-305). GacAS also controls the production of the quorum sensing signaling molecule N-butyryl-homoserine lactone (306) and resistance to diverse antibiotics, including the aminoglycosides, gentamicin, and chloramphenicol (299). Transcription of *gacS* is repressed by sub-inhibitory concentrations of tobramycin, ciprofloxacin, and tetracycline (307). AlgRZ also regulates early stages of biofilm formation (308) and the expression of quorum sensing genes (309). Another TCS, FleRS regulates flagella synthesis, adhesion (310), motility, and antibiotic resistance (311). Five TCS response regulators PA1099, PA3702, PA4547, PA4493, and PA5261 are involved in coordinating the interactions of the bacterium with the host lung epithelium (312). However, most other TCS encoded on the *P. aeruginosa* genome remain uncharacterized, with their signals and regulatory targets yet to be identified.

In this study, we used microarray analysis to characterize the global transcriptional response of *P. aeruginosa* to elevated external Ca^{2+}. From these analyses, we identified the TCS, PA2656-PA2657 (here referred to as calcium regulator, *carSR*), whose transcription is highly induced by elevated Ca^{2+} in planktonic cultures of *P. aeruginosa* PAO1. Using deletion mutations and microarray analysis, we identified the regulatory targets of *carSR*, which include the hypothetical proteins PA0320 and PA0327. Further characterization of PA0320 and PA0327 indicate that they play roles in maintaining Ca^{2+} homeostasis. PA0327

also influences production of the virulence factor, pyocyanin, and swarming motility in a Ca^{2+}-dependent manner.

MATERIALS AND METHODS

Bacterial strains, plasmids, and media.

Strains and plasmids used in this study are listed in Table S1. *P. aeruginosa* PAO1 is a non-mucoid strain with the complete genome sequence available (161). The gene PA2657 (*carR*) was deleted from PAO1 using allelic exchange as described previously (146). PAO1 mutants with transposon insertion in PA0320 (PA0320-H07::IS*lacZ*/hah) and PA0327 (PA0327-B11::IS*phoA*/hah) were provide by the University of Washington two-allele library. The sites of transposon insertions were confirmed by two-step PCR, using the primer sequences available at www.gs.washington.edu. For convenience, the transposon mutants were designated as PA::Tn5, where PA is the identifying number of the disrupted gene from the *P. aeruginosa* PAO1 genome (www.pseudomonas.com). Each mutant gene was complemented by cloning the gene behind the arabinose-inducible P_{BAD} promoter in the Tn7 vector, pTJ1 (313) (graciously provided by Dr. Joanna Goldberg). For complementing vectors, PA0320 and PA0327 were amplified using PCR with gene-specific primers listed in Table S1. The PCR products were cloned into TA cloning vectors (Invitrogen). The resulting plasmids were digested with

*Nco*I and *Hind*III, and the bands containing PA0320 and PA0327 were ligated into pTJ1, producing plasmids pTA56 and pTA57, respectively. A Tn7-based construct containing both PA2657 and PA2656 was used to complement the PA2657 mutant, to correct for any possible polar effects due to the disruption of PA2657. PA2656 and PA2657 were amplified separately using Phusion® High-Fidelity DNA polymerase (NEB). After addition of 3' A-overhang by *Taq* DNA polymerase, PCR products were cloned into TA cloning vectors. The *Eco*RI-*Eco*RV fragment containing PA2656 was ligated into pTJ1, followed by ligation of the *Eco*RI fragment containing PA2657. The resulting plasmid was labeled pTA104. The Tn7-based vectors were integrated into the chromosome of the respective *P. aeruginosa* mutant strains using electroporation, along with the Tn7 transposase helper plasmid, pTNS1, with selection for trimethoprim resistance. The trimethoprim resistance marker was then removed using pFLP2 (314). pTNS1 and pFLP2 were graciously provided by Dr. Herbert Schweizer.

Table 6.1.1. Strains and plasmids used in this study

Strains/Plasmids	Description	Reference
Pseudomonas aeruginosa PAO1	Wild type sequenced strain	(161)
Δ*carR:Gm*	PAO1 with deletion of *carR* by replacing with Gm^R gene.	This study
PA0320-H07::ISlacZ/hah	PAO1 with Tn5 disruption in PA0320	(97)
PA0327-B11::ISphoA/hah	PAO1 with Tn5 disruption in PA0327	(97)
Δ*carR:Gm::pBAD-carRS*	Deletion of *carR* complemented with *carRS*	This study
PA0320-H07::ISlacZ/hah/pBADPA0320	Tn5 disruption of PA0320 complemented by pBAD-PA0320	This study
PA0327-B11::ISphoA/hah/pBADPA327	Tn5 disruption of PA0327 complemented by pBAD-PA0327	This study
pTJ1	TN7 ventor containing pBAD promoter , Tmp^R.	

Antibiotic susceptibility assays

Antibiotic susceptibility assays were performed using tobramycin and polymyxin B E-strips (Biomerieux). In brief, strains were cultured in BMM medium with no added $CaCl_2$ or 10 mM $CaCl_2$ for 18 h and normalized to an OD_{600} of 0.1. 100 µl of the normalized cultures was then spread on BMM agar plates with or without added $CaCl_2$. E- Strips with tobramycin and Polymyxin B gradients were placed onto the inoculated plates. After 24 h of incubation at 37°C, the MICs were recorded by determining the concentration of antibiotics on the strip at which no bacterial growth was detected. At least three replicates were tested in at least two independent experiments; the reported MICs are the mean values of the collected measurements. The coefficient of variation between biological replicates was less than 25%.

RESULTS

PA0327 and PA0320 contributes to Ca^{2+} regulated tobramycin resistance in PAO1

To assess the role of PA2657, PA0327 and PA0320 in Ca^{2+}- induced tobramycin and polymyxin-B resistance, antibiotic susceptibility of *ΔPA2657*, *PA0327:IS*, *PA0320:IS* and complemented strains *ΔPA2657:A2657*, *PA0327:IS:PA0327*, *PA0320:IS:PA0320* were performed and compared to that of

PAO1. PAO1, when grown in presence of 10 mM Ca^{2+} had tobramycin MIC of 4 which is 8 fold higher than that of PAO1 grown without any added Ca^{2+} (0.5 µg/ml) (Fig. 6.1). However, both *PA0327:IS*, *PA0320:IS* showed almost 2 fold reduction in MIC for tobramycin when the bacteria was grown in presence of 10 mM Ca^{2+}. This loss of Ca^{2+} regulated tobramycin resistance was further restored to the level of tobramycin susceptibility of PAO1 in the complemented strains, *PA0327:IS:PA0327*, *PA0320:IS:PA0320* (Fig. 6.1.1).

PAO1 grown in BMM without added Ca^{2+} showed 32-fold increase in MIC for polymyxin-B when the bacteria were grown in presence of 10 mM Ca^{2+} (32µg/ml) than that of the bacteria grown without any added Ca^{2+} (1.0 µg/ml). However, PA2657, PA0327 and PA0327 did not show any involvement in Ca^{2+}-induced polymyxin-B resistance of PAO1 (Fig. 6.1.2).

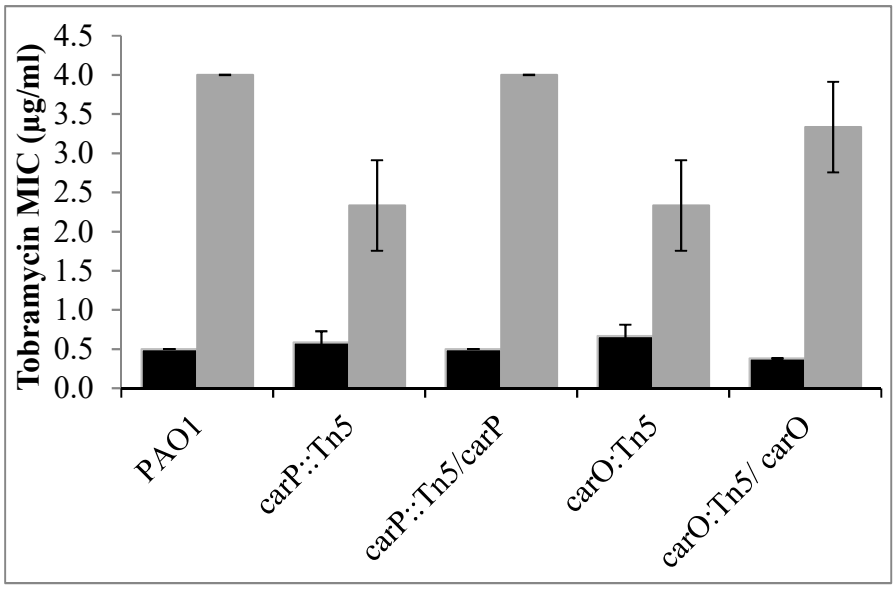

Figure 6.1.1: Minimum inhibitory concentrations (MICs) of tobramycin for *P. aeruginosa* PAO1, mutants *carO::Tn5*, and *carP::Tn5,* and their complemented counterparts *carO::Tn5/carO*, and *carP::Tn5/carP* grown on BMM with 0 mM $CaCl_2$ (dark grey bars) or 10 mM $CaCl_2$ (light grey bars). Cells were grown in BMM without adding $CaCl_2$ until mid-log phase, their OD_{600} were normalized to 0.1, and the aliquots of 100 µL were plated onto BMM agar for MIC measurements. E-strips with tobramycin gradient were placed on the bacterial lawns, and the MICs were recorded after 24 h incubation. The data represent the mean and standard deviations of at least three biological replicates from two independent experiments. Statistical significance of the differences was calculated using Student's T-test. *, $p<0.05$.

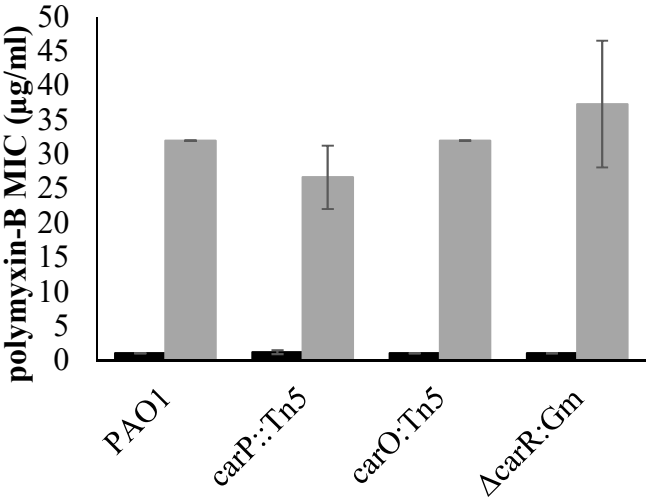

Figure 6.1.2: Minimum inhibitory concentrations (MICs) of polymyxin-B for *P. aeruginosa* PAO1, mutants *carP::Tn5*, and *carO::Tn5,* and *carR::Gm* grown on BMM with 0 mM $CaCl_2$ (dark grey bars) or 10 mM $CaCl_2$ (light grey bars). Cells were grown in BMM without adding $CaCl_2$ until mid-log phase, their OD_{600} were normalized to 0.1, and the aliquots of 100 µL were plated onto BMM agar for MIC measurements. E-strips with polymyxin-B gradient were placed on the bacterial lawns, and the MICs were recorded after 24 h incubation. The data represent the mean and standard deviations of at least three biological replicates from two independent experiments.

DISCUSSION AND CONCLUSION

Global microarray analysis identified two component system CarRS that is highly inducible by growth at 10 mM Ca^{2+} and regulates the expression of two genes encoding for β-propeller protein CarP and OB-fold protein CarO in Ca^{2+} dependent manner. Loss of these proteins abolished many Ca^{2+} regulated phenotypes such as swarming motility, tolerance to Ca^{2+}, and Ca^{2+} regulated pyocyanin production. Since Ca^{2+} upregulates PA2656-PA2657, PA0327 and PA0320, we have investigated their role in Ca^{2+}- induced polymyxin-B and tobramycin resistance. We found that loss of PA2657, PA0327 and PA0320 did not make any effect on Ca^{2+} induced polymyxin-B resistance of PAO1. Lack of PA2657 has no contribution in Ca^{2+}- induced tobramycin resistance as well. On the contrary, lack of functional PA0327 and PA0320 caused two fold reductions in Ca^{2+} regulated increase of tobramycin MIC in PAO1. This was further restored in these mutants complemented with corresponding genes. This suggests, PA0327 and PA0320 contributes in Ca^{2+}- induced tobramycin resistance and it is independent of PA2656-PA2657 mediated regulation of PA0327 and PA0320. This also indicates that, Ca^{2+}- induced tobramycin efflux by six efflux pumps identified (43) could be controlled by PA0327 and PA0320.

Overall these data indicate that CarRS plays a major role in sensing and relaying extracellular Ca^{2+} signaling in *P. aeruginosa*, which controls several

modulates the production of several virulence factors and antibiotic resistance of the pathogen.

II

CALCIUM REGULATES THE TRANSCRIPTION OF THREE BETA-CARBONIC ANHYDRASES IN *PSEUDOMONAS AERUGINOSA*

Part of this project has been included into the dissertation of Shalaka Lotlikar and is part of OSU library materials.

S. R. Lotlikar, S. S. Khanam, B. Kayastha, and M. A. Patrauchan. Beta-Carbonic Anhydrases play role in calcium mineralization and virulence of *Pseudomonas aeruginosa*. (Manuscript in preparation)

INTRODUCTION

Calcium (Ca^{2+}) is one of the key signaling molecules in eukaryotes. Its homeostasis in human cells is essential for a number of cellular processes including innate immune response (315) and is tightly controlled (reviewed in (316). Ca^{2+} cellular concentrations fluctuate in response to diseases. For example, in cystic fibrosis (CF) patients, an elevated level of Ca^{2+} is found in pulmonary fluids and nasal secretions (317, 318). Increased levels of Ca^{2+} are also found in serum of patients with cardiovascular disease (CVD) and hypertension (319, 320). Elevated

Ca^{2+}concentration and scattered Ca^{2+} deposits are characteristic to calcified atherosclerotic lesions of endocarditis patients (321). Imbalance in Ca^{2+} homeostasis has been also implicated in soft tissue calcification, which is commonly associated with chronic kidney disease (322), arteriosclerosis (323), and diseases associated with bacterial infections, for example, late stages of cystic fibrosis (CF) and infective endocarditis (324-326).

Soft tissue calcification is the deposition of Ca^{2+} in the form of phosphates or carbonates in soft tissues of a human body. Most commonly Ca^{2+} deposits contain phosphates or hydroxyapatites, which may disrupt normal processes, cause metastatic calcification, and lead to numerous diseases including hypervitaminosis D, tumoral calcinosis. arteriosclerosis, venous calcifications, or dermatomyositis (327, 328). Ca^{2+} carbonate deposition has been observed in a variety of soft tissues including the cervical spine, and was associated with collagen-vascular diseases (329), gallstones and kidney stones (330). A variety of factors may lead to soft tissue calcification. In addition to aging and injury, the factors may include infection (331), osteoporosis (332), and genetic (333) or autoimmune disorder (334). Ca^{2+} carbonate precipitation (CCP) can be carried out abiotically (335) or triggered by biological factors. The key chemical factors contributing to CCP include the concentrations of Ca^{2+} and carbonate (CO_3^{2-}), saturation index (Ω, where $\Omega > 1$ means system is saturated and precipitation may occur), Ca^{2+}/CO_3^{2-} ratio, and availability of nucleation sites (336, 337). The concentration of CO_3^{2--}

ions is dependent on pH, temperature, and partial pressure of CO_2 (338). Biological factors include the presence of bacterial cell surfaces and metabolic activity of the organisms involved. Bacterial cell surfaces provide negatively charged groups, which bind Ca^{2+} ions and thus may foster nucleation (339-341). The metabolic activities may favor CCP by providing CO_3^{2-} ions and increasing pH (339). Several metabolic pathways were shown to generate CO_3^{2-} and contribute to CCP. They include autotrophic pathways such as photosynthesis, methanogenesis and heterotrophic pathways including nitrogen cycle, urea hydrolysis and sulfate reduction (342, 343) (337). Although several Gram positive and Gram negative species including *Bacillus, Myxococcus,* and *Pseudomonas,* have been shown to be involved in CCP (344-346), the molecular mechanisms of microbially induced CCP are not clearly defined.

Carbonic anhydrases (CAs), EC 4.2.1.1, are metalloenzymes that catalyze the reversible hydration of CO_2 to HCO_3^- ($CO_2 + H_2O \Leftrightarrow HCO_3^- + H^+$). They are present in all three domains of life and involved in different physiological functions including pH homeostasis, CO_2/ HCO_3^- transport, and carbon fixation (reviewed in (347)). Due to the catalytic activity, CAs may drive the formation of $CaCO_3$ under appropriate environmental conditions. *In-vitro* studies with purified bovine CA (eukaryotic CA) have shown the role of CAs in the biocatalytic capture of CO_2 and precipitation of $CaCO_3$ (348). The role of eukaryotic CAs in calcification has been

shown in mollusks shells (349) and fish otoliths (350). Membrane bound α-CAs from coral *Stylophora pistillata* (351) were shown to be involved in CCP. Several prokaryotic CAs including extracellular CA from *Bacillus sp* (352) and β-CA from *Citrobacter freundii* SW3 (353) were suggested to contribute to CCP , however these studies only aimed biotechnological applications associated with CCP. Here we hypothesize that *P. aeruginosa* is capable of $CaCO_3$ deposition, which contributes to the virulence of the organism. Earlier we showed that *P. aeruginosa* PAO1 produces three functional β-CAs designated psCA1, psCA2, and psCA3 (354), which may contribute to the process of Ca^{2+} deposition. In this study, we applied real time quantitative PCR to study the assess the expression profiles of *psCAs.*

MATERIALS AND METHOD

RNA isolation and cDNA synthesis

Total RNA was isolated from *P. aeruginosa* PAO1 grown in BMM with no added or 5mM Ca^{2+} using RNeasy Protect Bacteria Mini kit (Qiagen) following the manufacturer's protocol. PAO1 was grown until middle-log phase (13 h; OD_{600} 0.2), and 15 ml of the culture was used for RNA isolation. DNase treatment was performed using column-based kit (Qiagen) and Turbo DNase treatment (Ambion).

The absence of genomic DNA (gDNA) was confirmed by conventional PCR and real time quantitative PCR (RT-qPCR) using *16SrRNA* primers. RNA yield was measured using NanoDrop spectrophotometer (NanoDrop Technologies Inc.), and the quality of the purified RNA was assessed by Bioanalyzer 2100 (Agilent) and 1% agarose gel electrophoresis. Following the MIQE guidelines (100), only the RNA samples with an OD_{260}/OD_{280} ratio of 1.8-2.0 and an RIN value of ≥ 9.0 was taken for further analyses. A total amount of 6 µg – 20 µg of RNA was purified from each sample. RNA samples were stored at -80 °C. Reverse transcription of total RNA (1 µg) was performed using Transcriptor First Strand cDNA Synthesis Kit (Roche) according to the manufacturer's protocol. The obtained cDNA was quantified by RT-qPCR using *16S rRNA* primers and stored at -20 °C.

Primers design and selection for RT-qPCR

Primers for CA encoding genes, *psCA1* (PA0102), *psCA2* (PA2053) and *psCA3* (PA4676) (Table 6.2.1) were designed using Primer3 Plus (101) and Primer BLAST (102). Primers were tested *in silico* for secondary structure formation using IDT oligoanalyzer. Their specificity was tested by BLAST alignments against *Pseudomonas* genome available at www.pseudomonas.com and confirmed by conventional PCR and RT-qPCR melt curve analysis. Primer efficiency was calculated using linear regression curve analysis. For this, RT-qPCR was performed for each primer pair using 10 fold serial dilution of gDNA, and the obtained Cp

values were plotted. Primers with an R^2 value of 0.99 and an efficiency of 93 (efficiency of the primer for the control gene) ± 10 % were accepted for further work according to the MIQE guidelines (100). The efficiency of the selected primers was: 97 %, (*psCA1*), 93 %, (*psCA2*), and 94 % (*psCA3*). Four housekeeping genes, *rpoD*, *rpoS*, *proC* and *16SrRNA* (103, 104) were selected and tested for their transcriptional response to Ca^{2+}. The transcription of *16SrRNA* gene was not affected by Ca^{2+} and therefore this gene was selected as a control. Due to the low Cp value of *16SrRNA* (≤ 8 for 5 ng of cDNA), transcriptional profiling for this gene was done using 10 fold diluted cDNA.

Table:6.2.1 Primers for RT-qPCR

Name	**Sequence (5' → 3')**	**Ref.**
psCA1-F	AGAGAGCATATGCCAGACCGTATG	This study
psCA1-R	AGAGAGGGATCCTCACGAGCTCAG	This study
psCA2-F	AGAGAGCATATGCGTGACATCATCG	This study
psCA2-R	AGAGAGGGATCCTCAGGCGAC	This study
psCA3-F	AGAGAGCATATGAGCGACTTGCAG	This study
psCA3-R	AGAGAGGGATCCTCAGCAGCAAC	This study

Gene expression analysis

To characterize the transcription profiles of *psCA1*, *psCA2* and *psCA3* genes, RT-qPCR was performed. For this, 5 µl of SYBR green master mix (Roche, Indianapolis, IN), 0.5 µM of each primer and 5 ng of nucleotides were added to a total volume of 10 µl of reaction mixture. RT-qPCR was run using 384 well plates sealed with LightCycler 480 Sealing Foil (Roche, Indianapolis, IN) in Roche LightCycler 480. At least five technical replicates for each biological replicate and a minimum of three biological replicates for every sample were analyzed. A no-template control was used as negative control. The cycle included 10 min denaturation at 95 °C followed by 35 cycles of 95 °C for 10 s, 61 °C for 15 s, and 72 °C for 10 s. A fold change in gene transcription was calculated using $2^{-\Delta\Delta Ct}$ method (105). Statistical analysis was performed by using two tailed T-test assuming equal variances.

RESULTS

Ca^{2+} regulates the expression of at least one β-CA in P. aeruginosa

In the earlier studies, we showed that externally added Ca^{2+} alters both transcription and translation of a number of proteins in *P. aeruginosa*, and increases the expression of several virulence factors including alginate, proteases, and pyocyanin (146). In order to determine the effect of Ca^{2+} on the transcription of the

three *P. aeruginosa* PAO1 β-CAs, we performed RT-qPCR. For this, PAO1 cells were grown at no added or in the presence of 5 mM Ca^{2+} and subjected to RNA extraction and analysis. The transcription of *psCA1* and *psCA3* was increased by about 5 and 11 fold, respectively, in the cells grown at 5 mM Ca^{2+} (Fig. 6.2.1). The *psCA2* transcripts were not detected under the tested conditions.

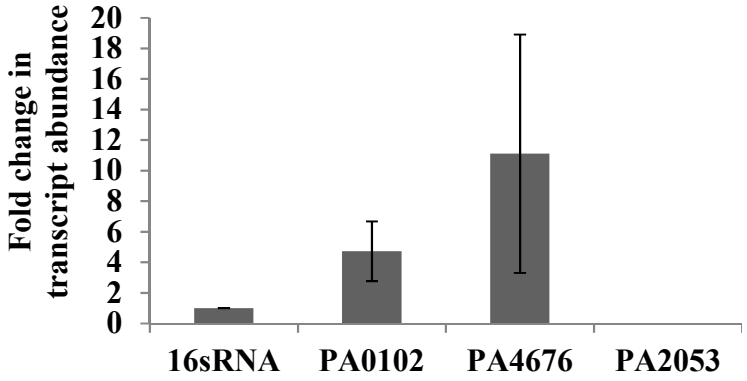

Figure 6.2.1: Effect of Ca^{2+} on transcription of psCAs; *psCA1* (PA0102), *psCA2* (PA2053), and *psCA3* (PA4676) in *P. aeruginosa* PAO1. The fold difference was calculated based on four biological replicates using *16S rRNA* gene as a control. The two-tailed student's t-test was performed, and the *P* values were as follows 0.02 for *psCA1*, 0.08 for *psCA3*. The transcripts of *psCA2* were not detected under either condition. * indicates $P \leq 0.05$.

The comparison of transcriptomic (microarray and RNA-seq) and proteomic analyses (Table 6.2.2) for PAO1 grown in presence of either 5 mM or 10 mM Ca^{2+} revealed that Ca^{2+} positively regulates the expression of *psCA1*. However, the expression of *psCA2* was found unchanged in response to Ca^{2+} in all three sets of analysis. Interestingly, RT-qPCR data shows highest induction of Ca^{2+} on transcription of *psCA3* while microarray, RNA-seq as well as proteomic analysis displays otherwise. The expression of *psCA3* remains unchanged in transcriptomic (microarray and RNA-seq) and proteomic analysis of PAO1 grown in presence of Ca^{2+}. Therefore, RT-qPCR for *psCA3* requires further validation.

Table 6.2.2: Ca^{2+} regulated expression profile of three carbonic anhydrases in *P. aeruginosa*.

Gene name, Gene Identifier.	Log_2fold change in transcript abundance in response to 10 mM Ca^{2+} (Microarray [a]) (70)	Log_2fold change in transcript abundance in response to 5 mM Ca^{2+} (RNA-seq [a])	Fold change in transcript abundance in response to 5 mM Ca^{2+} (RT-qPCR [a])	Fold change in protein abundance in response Ca^{2+} (LC-MS/MS[b])
psCA1, PA0102	2.8	1.08	5 ± 2	3.2
psCA2, PA2053	0.1	-0.06	ND	ND
psCA3, PA4676	0.4	-0.89	11 ± 8	ND

a. RNA was isolated from planktonic culture of PAO1 grown in BMM with or without Ca^{2+} (10 mM/ 5 mM) till middle log.
b. Protein was extracted from planktonic culture of FRD1 strain grown in BMM with or without 10 mM Ca^{2+}.

DISCUSSION AND CONCLUSION

Both *psCA1* and *psCA3* have a moderate to high catalytic activity in contributing to Ca^{2+} deposition. The transcriptional regulation of these enzymes by Ca^{2+} suggests the presence of Ca^{2+} dependent transcriptional regulators which can sense the presence of increased surrounding Ca^{2+} and modulate the $CaCO_3$ deposition. Another possibility is a direct binding of Ca^{2+} to a CA as a co-factor and enhancing the activity of the enzymes. A similar Ca^{2+} dependent regulation was observed for the CmpA, a subunit of the BCT1 HCO_3^- transporter, whose binding to HCO_3^- is dependent on Ca^{2+} (355). The disagreement between the undetectable level of *psCA2* transcripts and the increased abundance of the protein at elevated Ca^{2+} is difficult to explain, but may be due to a short life-time of the transcript and increased stability of the protein in the presence of Ca^{2+}.

Finally, the phenomenon of Ca^{2+}-regulated CAs-mediated $CaCO_3$ precipitation by *P. aeruginosa* may present a mechanism enabling the pathogen to survive, grow and proliferate within a host. It may represent a novel virulence factor increasing the ability of the pathogen to invade a host. In agreement, the transcription of *psCA1* and *psCA2* was induced at least threefold in *P. aeruginosa* isolates from CF lung sputa (GDS2869) (356), the transcription of *psCA1* increased fourfold in burn wound model and nine-fold in *P. aeruginosa* isolates from CF sputum (GDS2869) (357). This suggests a potential role of these proteins in the

ability of *P. aeruginosa* to survive in a host, as it has been shown for β-CAs in *H. pylori* (358), *S.* Typhimurium (359), *S. pneumoniae* (360), and *M. tuberculosis* (361) . Further studies are needed to decipher the role of $CaCO_3$ precipitation in virulence and pathogenicity of *P. aeruginosa* as well as other pathogenic bacteria, many of which contain multiple β-CAs as well as γ-CAs. This knowledge may provide the basis for the development of novel approaches for treating robust bacterial infections.

III

OPTIMIZATION OF INFECTIVITY ASSAY TO ASSESS THE ROLE OF CALCIUM ON INFECTIVITY OF *PSEUDOMONAS AERUGINOSA*.

Sharmily Khanam,* Allison Lawson and Marianna A. Patrauchan

Department of Microbiology and Molecular Genetics,

Oklahoma State University, Stillwater, OK, US

INTRODUCTION

Pseudomonas aeruginosa is a multidrug resistant human pathogen. The infection caused by this pathogen is of a serious concern for the immunocompromised patients, patients with Cystic fibrosis (CF), endocarditis, indwelling medical devices, and burn wounds (15, 113, 186, 362). *P. aeruginosa* associated morbidity and mortality occurs in individual with Chronic obstructive pulmonary disease (COPD), infective endocarditis, cancer patients undergoing chemotherapy, intravenous drug users(6, 10, 11). The high morbidity and mortality of *Pseudomonas* infections is mainly attributed to the combination of virulence

factors and outstanding antimicrobial resistance of this organism (7, 8). Strategic use of different virulence factors is the key component of successful establishment of persistent *P. aeruginosa* infection (9). The remarkable ability of *P. aeruginosa* to adapt to a wide range of environments is reflected in the broad distribution of this organism in diverse niches ranging from terrestrial to freshwater to human body (363). The genus *Pseudomonas* is highly diversified in its symbiotic relationships with a host, including non-pathogenic *P. putida*, nitrogen-fixing symbiont *P. stutzeri*, beneficial for plans *P. fluorescence*, plant pathogen *P. syringe*, and human pathogen *P. aeruginosa* (364). Many studies focused on comparison of genotypic and phenotypic diversity among *P. aeruginosa* isolated from different environmental niches (365) (58). The population of *P. aeruginosa* isolates found in a single niche can display a great amount of heterogeneity in their metabolism . For example the biofilm community of Pseudomonas consist of population of bacterium producing cell signaling molecule as well as the population which do not produce the molecules and rather cheat on their neighbors who does (362).

Among many adaptations in *Pseudomonas* genus, the most dominant mechanism is its ability to alter genetic information by mutations or uptake of extracellular DNA from neighboring bacteria (366). *P. aeruginosa* genome contains many characteristic features that allow *P. aeruginosa* to maintain genetic plasticity (363). Presence of repetitive intergenic palindromic (REP) elements, lineage specific regions (LSR), regions of genetic plasticity (RGP), allow the

adaption to a diverse niche (364). Pathogenicity caused by *P. aeruginosa* involves a broad array of virulence factors, which allow successful entry, invasion and establishment of *P. aeruginosa* infection. For instance, in this organism, lipid A induces mucin production in the lung of CF patients (197, 198). It has been identified that the biofilm community of *P. aeruginosa* contains variety of lipid A species, and the length of the side chain of lipid A molecule is major contributor in the degree of virulence in *P. aeruginosa* (199, 200). Type IV pili are used for twitching motility and are of high importance for entry and dispersion of *P. aeruginosa* in the site of infection (367). In CF patients, the initial entry and establishment of *P. aeruginosa* is facilitated by binding of the pathogen with asialo GM1 by means of pili. This ensures adherence of *P. aeruginosa* and allows the pathogen to exert other virulence traits (368) and biofilm formation. (367). Flagella is a filamentous appendage like structure, which aids in adherence and movement. Due to the immunogenic nature of flagella, *P. aeruginosa* tends to get rid of it at later stages of establishment of infection (48). *P. aeruginosa* produces a mucoid exopolysaccharide which protects the bacteria against hostile reactive oxygen species produced by the host PMNs (polymorphonuclear cells) (369) as well as rhamnolipids molecules which aid in early onset of infection (370, 371). In addition, *P. aeruginosa* possesses 5 different secretory systems among which type II and type III secretion systems are known to secret toxins of high importance (372). Type II secretion system is involved in secretion of extracellular proteases

LasA, LasB, lipases, alkaline phosphatases, phospholipases, exotoxin-A, etc. These secreted virulence factors are essential to break the epithelial barrier of host tissue and enable invasion of *P. aeruginosa* with an attempt to establish a chronic infection (48, 369, 372). Type III secretion system is responsible for secretion of exotoxins, ExoT, ExoU, ExoS and ExoY which play a major role if disruption of immune response and establishment of pathogen in the host body (48, 372). Also, Pyocyanin, another toxin produced by *P. aeruginosa*, is a redox reactive blue-green pigmented toxin (373) and plays a major role in infection establishment by this pathogen.

Ca^{2+} is an important signaling ion which controls a variety of cellular processes in human body including the immune system (65, 374). In CF patients there is an increased Ca^{2+} level present in the pulmonary and nasal secreted fluids (110). Therefore, any positive regulatory effect of elevated Ca^{2+} on *Pseudomonas* virulence can increase the adversity of infection and worsen the prognosis for patients. Dr. Patrauchan's group studies the regulatory role of Ca^{2+} on *P. aeruginosa* physiology and determined that growth at Ca^{2+} increases the production of many virulence factors(74) as well as infectivity of *P. aeruginosa* in plant (lettuce leaf) infection model (43). However, considering that *P. aeruginosa* is a human pathogen, we aimed to study Ca^{2+} regulation of the pathogen's virulence in animal models, such as nematode worm, *Caenorhabditis elegans* and fruit fly, *D. melanogaster*.

Both models, *C. elegans* and fruit fly, have been in use for assessment of P. aeruginosa infectivity and determining the virulence factors associated with the infectivity (375-379). Here we have optimized the established killing assays for both animal models and assessed the role of Ca^{2+} in virulence of *P. aeruginosa* strain PAO1.

MATERIALS AND METHOD

Strains, plasmids and media

P. aeruginosa PAO1, the non-mucoid strain with genome sequence available (www.pseudomonas.com) was used in the study. The *C. elegans* wild type (N2 bristol) and temperature sensitive sterile mutant CF 512 (rrf-3(b26) II; fem-1(hc17) IV) were received from Caerhabditis Genetic Center (CGC) in University of Minnesota and was maintained on Nematode growth medium monoxenic culture with *E coli* OP50. LB medium, modified synthetic cystic fibrosis mimicking medium (mSCFM) (380), biofilm minimal medium (BMM) (146) contained (per liter): 9.0 mM sodium glutamate, 50 mM glycerol, 0.02 mM $MgSO_4$, 0.15 mM NaH_2PO_4, 0.34 mM K_2HPO_4, and 145 mM NaCl, 20 µl trace metals, 1 ml vitamin solution. Trace metal solution (per liter of 0.83 M HCl): 5.0 g $CuSO_4.5H_2O$, 5.0 g $ZnSO_4.7H_2O$, 5.0 g $FeSO_4.7H_2O$, 2.0 g $MnCl_2.4H_2O$). Vitamins solution (per liter): 0.5 g thiamine, 1mg biotin. The pH of the medium was adjusted to 7.0. When

required, $CaCl_2 \cdot 2H_2O$ was added to a final concentration of 5 mM. Nematode growth medium (NGM). Cornmeal agar medium.

PAO1 and mutant cells were grown at no added or 10 mM Ca^{2+}. Middle log cultures grown in 5 ml BMM were inoculated (0.1 %) into 100 ml of fresh BMM (no added or 10 mM Ca^{2+}) and incubated at 37°C, shaking at 200 rpm in a MaxQ 5000 floor-model shaker (Thermo Scientific). Absorbance at 600 nm was recorded every 2-4 h using a Biomate 3 spectrophotometer (Thermo Scientific).

Table 6.3.1. Strains and plasmids used in this study

Strains/Plasmids	Description	Reference
Pseudomonas aeruginosa PAO1	Wild type sequenced strain	(161)
C elegans N2 bristol	Wild type C. elegans	(375, 381)
C. clegans, CF 512 (rrf-3(b26) II; fem-1(hc17) IV)	Temperature sensitive sterile mutant of *C. elegans*	(375)

Maintenance of C. elegans and fruit fly

Both *C. elegans* worms and fruit flies were grown and maintained in lab for animal infectivity assays. For regular maintenance of worms, permanent stock preparation and worm synchronization prior to the assay was performed according to the procedure described in the worm book (http://www.wormbook.org/chapters/www_strainmaintain/strainmaintain.html).

C elegans N2 bristol and temperature sensitive sterile mutant CF 512 were received on a NGM plates. Worms were fed on E coli OP50 strain. The worms were maintained on NGM plates with E. coli OP50 as food for the worm (381). Briefly, the bacteria from the monoxenic (containg only E. coli, OP50 cells on plate) C elegans culture were streaked onto an LB plate and one single clone was inoculated into LB broth overnight culture. 100 µl of the overnight culture was inoculated (seeded) onto NGM plates and grown overnight at 37°C. Prior to inoculation, the plates were dried by incubation in 37°C incubator for about 15 min. Then the bacterial inoculation was performed and paltes were incubated at 37° C for 24 hours. Chunk of agar from the original NGM plates containing the worms were cut and transferred to the new plates containing E. coli OP50 lawn. Plates were incubated at room temperature (upside-up position) for the spread and growth of C elegans worms. Since the L1 and L2 stage of larvae are metabolically the best

one to keep at -80°C freezer for longer period, the worms to be stocked were age synchronized and collected at these stages of their growth. For synchronization, the gravid (worms with eggs) worms were collected by washing with M9W media and worms were collected by spinning down in a clinical centrifuge at 1,000 rpm for 5 min. The eggs were released by adding 1:4 ratio of 5N NaOH and household bleach at a total volume of 500 µl and spinning down the mixture at 4,500 rpm in a clinical centrifuge for 5 min. The pelleted eggs were washed with M9W media at least twice before adding a final of 5 ml of M9W into the tubes. The tubes were incubated at room temperature at slow shaking for about 12 h before inoculating the eggs onto fresh NGM plates with E coli OP50 cells. Once the L1, L2 larvae of C. elegans were hatched, they were collected from NGM plates. The plates were rinsed superficially with M9W buffer (0.3% (w/v) KH2PO4, 0.6% (w/v) Na2HPO4, and 0.5% (w/v) NaCl in sterilized nanopure water. Autoclave at 121°C for 30 min, cool to 60°C, and add filtersterilized 1 mM MgSO4.), and the solute were collected into cryovials at a 1:1 ratio of 30 % glycerol and worms in M9W buffer. The cryovials then were placed into container box inside a Styrofoam box. The Styrofoam box was kept in -80 ^{0}C to allow gradual freezing. The container box was taken out of the Styrofoam box after 7 days and kept in -80^{0} C freezer.

The fruit flies were maintained in cornmeal agar for daily maintenance as described in (382). *D. melanogaster* OR flies were maintained in plastic 250 mL Erlenmeyer flasks (VWR) capped with a foam plug (VWR) containing cornmeal

agar. Standard cornmeal fly medium (28 g dried brewer's yeast, 77 g cornmeal (Sigma), 27 g sucrose, 53 g glucose, 3.5 mL propionic acid, 0.3 mL 85 % phosphoric acid and 6 g select agar (Invitrogen) per liter) was used for regular maintenance. The flies were transferred from old maintenance flasks to new ones on a regular basis and maintained at room temperature. The medium was monitored for possible contamination with indigenous mold population carried by the flies. For the infectivity assay, flies were transferred from maintenance vials to empty vials first in a cold room and sedated by placing them on a cold surface (tile placed directly on ice in a foam container). For feeding assays, the synchronized flies separated and collected as above, were transferred to fly vials containing 6 mL of sucrose agar (1.2 g Bacto-agar (Difco), 14 mL 20% sucrose and 41 mL sterile distilled water).

C. elegans and fruit fly killing assay optimization

There are two different *C. elegans* killing assay previously been established to characterize the effect of Pseudomonas infection in this worm (375). The fast killing assay is performed on brain heart infusion media BHI medium where mostly toxin secreted by Pseudomonas pathogenic strains can kill C. elegans within as quickly as 4 hours- 24. On the contrary the slow killing assay is performed on NGM plates where the PA14 strains killd the C. elegans over the period of 2-3 days (375). FTo assess the effect of Ca^{2+} on killing of *C. elegans* by *P. aeruginosa*, slow killing

assay was selected over the fast killing assay. It was mainly because BHI medium contains an undefined Ca^{2+}. On the other hand, NGM medium is defined, and the level of Ca^{2+} could be controlled to the final concentration of 5 mM.

In order to determine the effect of Ca^{2+} regulated pseudomonas infection on the death of fruitflies, 5 mM Ca^{2+} was added to the sucrose agar medium. Also, the pelleted bacterium was resuspended into sucrose containing 5 mM Ca^{2+} prior to adding these suspensions to the sucrose agar medium assay vials. as well as the bacteria to be added to the media as a food source. Three different media, LB (Luria Bertani), BMM (Biofilm minimal media) and SCFM (Synthestic Cystic Fibrosis Mimicking media) were assessed to finalize the one that shows regulatory (negative/positive) effect of Ca^{2+}on the infectivity of *P.* aeruginosa. For this, *P. aeruginosa* was grown in those media containing no added or added 5 mM Ca^{2+} prior to the assay.

C. elegans slow killing assay

Modified slow killing assay was performed using *Caenorhabditis elegans* wild type N2 bristol strain and temperature sensitive sterile mutant CF-512 (fer-15(b26) II (CGC). In order to identify the role of Ca^{2+} in virulence of *P. aeruginosa* PAO1, bacterial lawn was grown on NGM agar plates with no added Ca^{2+} or 5 mM Ca^{2+}. Previously well grown adult gravid worms were used for worm synchronization. Gravid worms were removed from the worm plate with M9W

buffer followed by disruption of worms to release eggs by adding 5 N NaOH and household bleach at 1:4 ratio. The mixture was vigorously vortexed for no more than 4 min and 14ml of M9W buffer was added. The eggs were washed three times with M9W buffer and resuspended into 5 ml of M9W buffer. The 15 ml falcon tubes containing the eggs were placed in a shaker at 200 rpm and room temperature (25°C) for 12 hours. Synchronized L1 stage larvae were transferred to NGM agar plates provided with *E coli* OP50. The worms were grown for 34 h until they reach the young adult stage. 30-40 young adult worms were then seeded in to the slow killing assay plates: NGM agar with bacterial lawn on it at 0mM or 5mM Ca^{2+}. Dead worms were displaying no movements on the plate were scored using dissection microscopy every 12 hours.

Fruit fly assay

D. melanogaster (OR) flies were maintained in foam plugged plastic 250 mL Erlenmeyer flasks (VWR). Standard cornmeal fly medium (28 g dried brewer's yeast, 77 g cornmeal (Sigma), 27 g sucrose, 53 g glucose, 3.5 mL propionic acid, 0.3 mL 85 % phosphoric acid and 6 g select agar (VWR) per liter) was used for regular maintenance of the fly. For fly feeding assays, sucrose agar (1.2 g Bacto-agar (Difco), 14 mL 20% sucrose and 41 mL sterile distilled water) was used. Fly synchronization was done prior to each feeding assay. In brief, the adult flies from fly maintenance vial were transferred at least twice at two days' interval and the

same age larvae were grown. Two- day-old synchronized flies were finally transferred to a new fly maintenance vial and left overnight. The flies were separated into polystyrene fly vials (Applied Scientific) and starved for 6 h before separating the male flies from the female flies and transferring the synchronized male flies to the assay vials. Simultaneously, 16 h bacterial precultures were harvested, and adjusted to the OD_{600} of 3.0 by resuspending the bacterial pellet in 200 µl of 5% sucrose with or without added 5 mM Ca^{2+}, in which the bacteria were grown. The normalized culture was then inoculated into the fly vials containing 2.3 cm whatman filter disk placed on top of sucrose agar (5% sucrose and 2.2% select agar). The assay vials inoculated with 5% sucrose alone were used as negative controls. Starved synchronized male flies were transferred to the sucrose feeding vials containing the bacterial suspensions and incubated at 25ºC. Dead flies were scored daily for 14 days.

RESULTS

Growth at BMM showed greater lethal effect of P. aeruginosa compared to growth at LB or SCFM

At first, we have investigated the effect of different bacterial growth media on *Pseudomonas* infectivity in *D. melanogaster* (fruit flies). For this, PAO1 was grown in either LB, BMM, or SCFM before inoculating into the sucrose agar vials

for the infectivity assay. After 14 days of incubation it was determined that growth of PAO1in BMM showed the highest mortality rate compared to that of LB or SCFM. 50% of the flies dies out of *Pseudomoans* infection within 7 days when the bacterium was grown in BMM medium (LT_{50}, 7days). On the contrary, for PAO1 grown in LB and SCFM , it took 13-14 days for the death of 50% flies. While, by 13 days all flies fed with PAO1 grown in BMM were found dead (Fig. 6.3.1). Therefore, the BMM growth medium was selected for further studies.

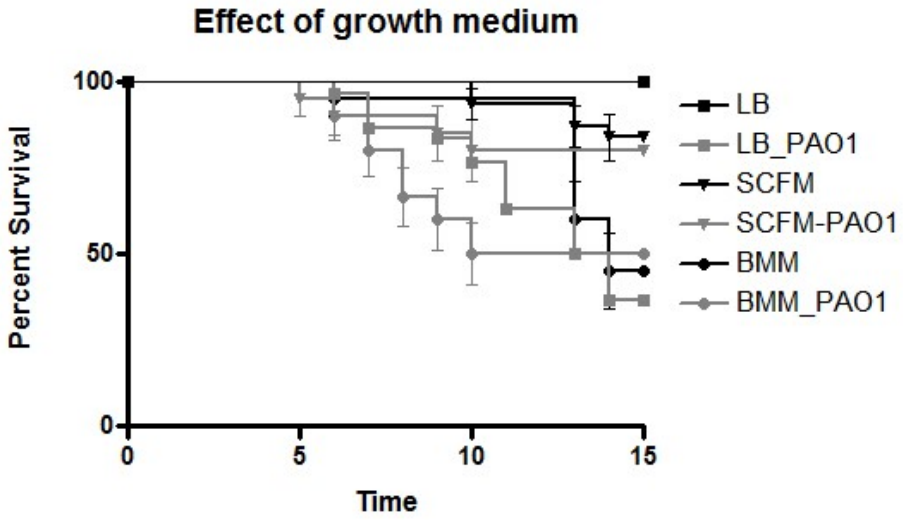

Figure 6.3.1: Effect fo Different medium on fruitfly killing by PAO1 infection. PAO1 was grown overnight for 12 hours at 37° C and 200 rpm in BMM, LB or SCFM media before the cells were harvested, normalized to an OD_{600} of 3.0 and resuspended in 5% sucrose solution. This cell supensions were added to the feeding assay vials on filter papers soaked with 5% sucrose solution. Age synchronized 10 male flies were added to each test vials. Vials containing sucrose solution (prepared into LB, BMM or SCFM medium) soaked filter paper without any bacterium were used as negative control of infection. Dead flies were scored every day for 15 days. At least 3 biological replicates were used.

Growth at 5 mM Ca^{2+} increases the death rate in flies caused by PAO1 infection

To elucidate the effect of Ca^{2+} on infectivity of PAO1 in fruit fly infection model, the cells were grown in BMM with or without 5 mM Ca^{2+}. The bacterial suspension to be added to the feeding vial was prepared in 5% sucrose with or without 5 mM Ca^{2+}. This allowed uptake of Ca^{2+} in the fly gut through feeding. We have deterimined that growth at 5 mM Ca^{2+} increased the *P. aeruginosa* infection mediated killing of fruit flies. Here we observed that, the LT_{50} for PAO1 grown with added Ca^{2+} was 9 days where after 15 days PAO1 grown in BMM without any added Ca^{2+} was unable to kill 50% of the fly population. However, variation in death rate was observed for the Bcaterium grown in BMM without added Ca^{2+} performed in different batches (Fig. 6.3.1and Fig. 6.3.2). This might reflect a possible limitation of such assay where individual experiment sets may not be compared due to the effect of external unknown variables (room temperature, humidity etc.) affecting the outcome of the event. Besides, another limitation of this experimentation was lack of evidence on the virulence factors which may contribute in the death of the flies.

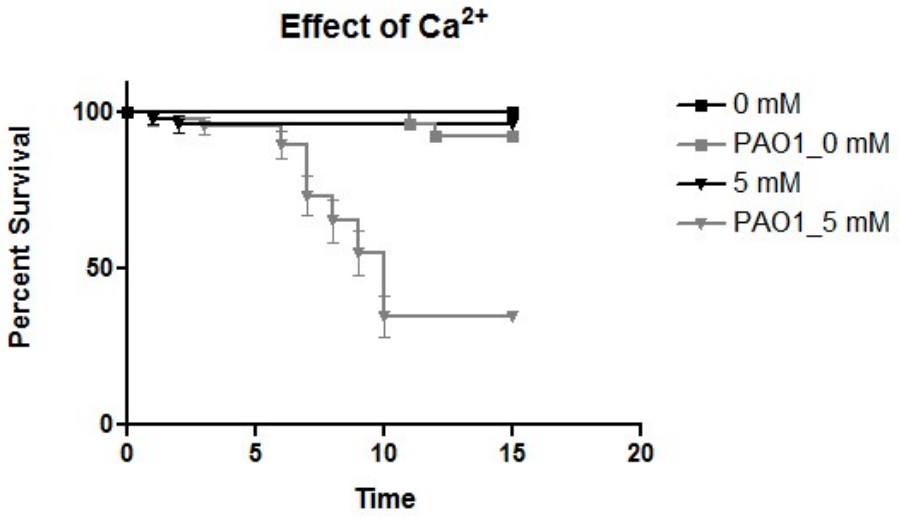

Fig. 6.3.2: Effect of Ca^{2+} on fruitfly killing by PAO1 infection. PAO1 was grown overnight for 12 hours at 37° C and 200 rpm in BMM with no added or 5 Mm Ca^{2+} prior to the cells harvested, normalized to an OD_{600} of 3.0 and resuspended in 5% sucrose solution with corresponding Ca^{2+} concentration. This cell supensions were added to the feeding assay vials on filter papers soaked with 5% sucrose solution and respective Ca^{2+}. Age synchronized 10 male flies were added to each test vials. Vials containing filter paper soaked with sucrose solution (prepared into BMM) with 0 Mm OR 5 Mm Ca^{2+} were used as negative control of infection. Dead flies were scored every day for 15 days. At least 3 biological replicates were used.

Ca^{2+} slows down the P. aeruginosa infection mediated killing of C. elegans

C. elegans assay has been widely used for studying the infectivity of *P. aeruginosa* and both the host factors and the pathogens virulence factors contribute to both fast killing assay and slow killing assay are identified (375, 376). We selected slow killing assay, as the medium for bacterial lawn preparation in this assay, NGM is defined and allows controling Ca^{2+} levels. We further optimized the assay by adding 5 mM Ca^{2+} to the NGM plates, and thus providing the conditions for inducing virulence in growing bacterial lawn, which the worms were fed on during the assay. Furthermore, to avoid progeny overlap during the slow killing assay, we used temperature sensitive sterile mutant of *C. elegans*.

Interestingly, killing of *C. elegans* was faster when *P. aeruginosa* cells were grown at no added Ca^{2+}. Under these conditions, the worms displayed a distinctively slow movement as early as after one day of observation. Although by the end of the fifth day most worms fed on PAO1 grown at both 0 mM and 5 mM Ca^{2+} were dead, the worms grown at no added Ca^{2+} showed more dramatic effect of *P. aeruginosa* infection with engorgement of the body as well as green pigments produced by the bacterium **(Fig 6.3.3)**. This may suggest that type III secretion-dependent toxins mediated killing of *C. elegans*. This secretion system is known to

be negatively regulated by Ca^{2+} (70, 73). Therefore, additional Ca^{2+} in the media may prevent faster killing of the worms by *C. elegans*.

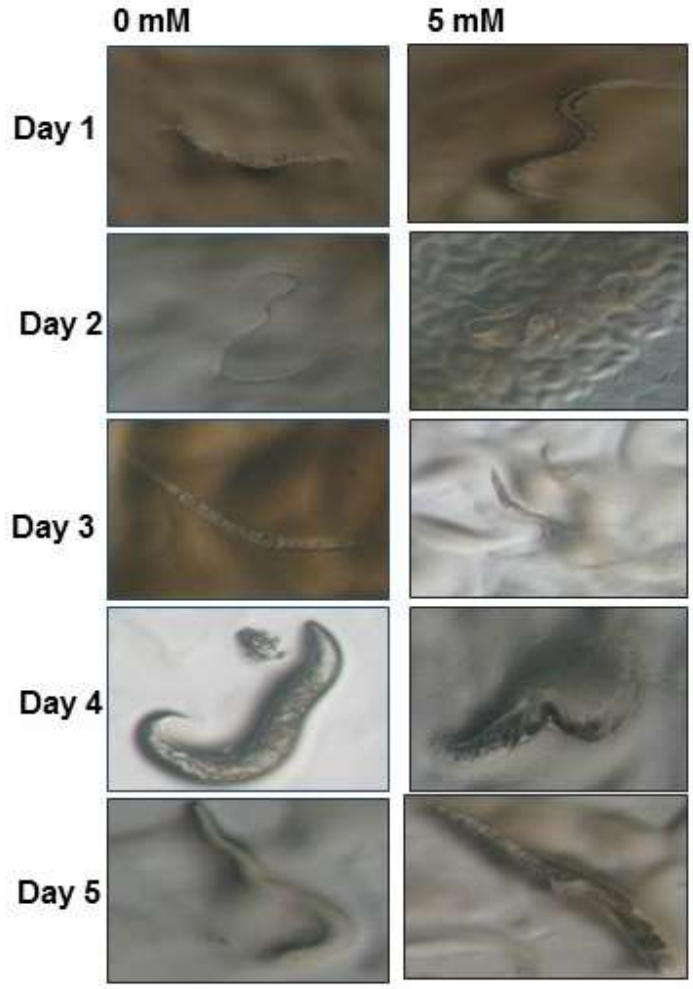

Fig. 6.3.3: Effect of Ca^{2+} on killing of *C. elega*ns mediated by *P. aeruginosa* infection. *P. aeruginosa* were grown in BMM with or without 5 mM Ca^{2+} for 12 hours prior to normalization of cell culture and inoculation onto NGM plates with corresponding Ca^{2+}. These plates were incubated at 37° C for 24 hours to grow bacterial lawn before adding age synchronized temperature sensitive sterile *C. elegans* strains. The worms were then observed under either dissection microscope

or fluorescence microscope at 400X magnification. Camera magnification were used often to get more detailed features of the worms. *C. elegans* fed with non-pathogenic *E. coli* OP50 were added as controls.

DISCUSSION AND CONCUSION

P. aeruginosa is highly virulent human pathogen, quite well known for its multi drug resistance (110, 117). Besides its remarkable antibiotic resistance, *P. aeruginosa* is highly adaptable (362). Considering its extreme versatility, it is essential to understand how this pathogen can adapt to a certain environment and become virulent. Among various animal models currently in use for studying the virulence of *P. aeruginosa*, the mouse ant rat models exemplifying the acute and chronic infection models of CF lung are most popular (383, 384). However, invertebrate models such as *D. melanogaster* (385), Galleria melonella (386), *C. elegans* (375) are often appreciated for their cost-and time-efficiency and overall usefulness in screening for factors contributing to the virulence of this pathogen. The goal of this study was to investigate the regulatory effect of Ca^{2+} on the infectivity of *P. aeruginosa* using invertebrate models, *D. melanogaster* and *C. elegans*.

Since Ca^{2+} is a host associated environmental factor (387) with a potential to be utilized by *P. aeruginosa* as a signaling molecule (47, 70, 71), it is essential to identify the molecular mechanisms of Ca^{2+} regulation of the pathogenic lifestyle of *P. aeruginosa*. Both fruitfly assay and *C. elegans* infection models are widely used to study virulence and infectivity of *P. aeruginosa*. However, one of the

greatest challenge in our studies is to generate diverse Ca^{2+} conditions during *P. aeruginosa* growth. We have optimized both assays to generate controlled conditions of no-added and elevated Ca^{2+} levels for bacterial growth. The fruit fly assay showed a potential to be useful for studying the mechanisms of Ca^{2+} regulated killing due to the positive effect of Ca^{2+} on killing of fruit flies by *P. aeruginosa*. However, further studies of the model are required. They include understanding of the environmental factors, such as temperature/ humidity, as well as the knowledge of the mechanisms involved in fruit fly killing by *Pseudomonas*, Furthermore, *C. elegans* killing by *P. aeruginosa* appeared to be downregulated in the presence of Ca^{2+}, likely due to the involvement of type III secretion system, which limits its usefulness for our studies. Therefore, for further studies of the regulatory role of Ca^{2+} on infectivity of *P. aeruginosa*, other animal models such as *Galleria mellonella*, rat, or mouse should be considered.

CHAPTER VII

MATERIALS AND METHODS

MATERIALS

Transposon insertion mutants were purchased from the University of Washington Two-Allele library (grant # NIH P30 DK089507) (98). All *Caenorhabditis elegans* strains were purchased from Caenorhabditis Genetic Center (CGC) (Grant# NIH P40 OD010440), University of Minnesota, USA (website: http://cbs.umn.edu/cgc/home). D. melanogaster OR strain was purchased from Carolina (website: http: //www.carolina.com Burlington, NC, USA). Antimicrobial strips for tobramycin, polymyxin-B, ceftazidin, ciprofloxacin and doripenem were purchased from Biomerieux (Biomerieux, USA). Coelenterazine was purchased from Life Technologies (California, USA). RNeasy Bacterial mini kits, ZR Fungal/Bacterial MiniPrepTm, High Pure RNA Isolation Kit were purchased from Qiagen (Valencia, CA), Zymo Research (Zymo, Irvine, USA) and Roche Diagnostics corporations (Roche, Indianapolis, USA) respectively. Transcriptor First Strand cDNA Synthesis Kit, LightCycler® 480 SYBR Green I Master, LightCycler® 480 Multiwell Plate 384, white, TriPure Isolation Reagent were purchased from Roche Diagnostics corporations (Roche, Indianapolis, USA). Gel red was purchased from Phoenix research. Deoxynucleotide (dNTP) and Taq polymerase were purchased from New England Biolabs (Ipswich, MA). 2 M MgCl2 solution, was purchased from Thermo Scientific (Pittsburgh, PA). QIAprep

Mini-spin kit, was purchased from Qiagen (Valencia, CA). Oligonucleotide primers were obtained from Integrated DNA Technologies (Coralville, IA). Ragent grade ingredients for LB-agar, cornmeal agar, and nematode agar were purchased from VWR (Atlanta, GA, USA) unless otherwise specified. All other reagent grade chemicals were purchased from Thermo-Fisher Scientific (Waltham, MA) or Sigma- Aldrich (St. Louis, MO), unless otherwise indicated.

Preparation of Buffers and Reagents

All buffers were made with ultrapure deionized water from Barnstead-thermolyne deionization system at resistance of 18.2 MΩ. See Appendix A for buffer compositions, media and other recipes. The pH of buffers and solutions were adjusted by concentrated hydrochloric acid (HCl) or 5N sodium hydroxide (NaOH) as required.

Bacterial strains, media, and growth conditions

All bacterial strains and plasmids used in this study are listed in the **table 7.1**.

Table 7.1: Strains and plasmids used in this study.

Strains/ Plasmids	Description	Ref.
E. coli DH5α	*fhuA2 Δ(argF-lacZ)U169 phoA glnV44 Φ80Δ (lacZ)M15 gyrA96 recA1 relA1 endA1 thi-1 hsdR17*	
P. aeruginosa PAO1	Wild type	(96)
PW1780[a] (*mexB:*Tn5[b])	PA0426 H01::ISlacZ/hah	(98)
PW8752 (*mexC:*Tn5)	PA4599E04::ISlacZ/hah	(98)
PW5233 (*muxC:* Tn5)	PA2526A07::ISlacZ/hah	(98)
PW8386 (*mexV:*Tn5)	PA4374D09::ISlacZ/hah	(98)
PW8137 (*mexI:*Tn5)	PA4207H08::ISlacZ/hah	(98)
PW5180 (*mexE:*Tn5)	PA2493H04::ISlacZ/hah	(98)
PW6963 (*mexQ:*Tn5)	PA3522H12::ISlacZ/hah	(98)
PW7220(*mexJ:*Tn5)	PA3677D11::ISlacZ/hah	(98)
PW4499 (*mexY:*Tn5)	PA2019D05::ISlacZ/hah	(98)
PW3609 (*mexM:*Tn5)	PA1435G06::ISlacZ/hah	(98)
PW1265 (*triA:*Tn5)	PA0156E03::ISlacZ/hah	(98)
PW5224 (*czcB:*Tn5)	PA2521B08::ISlacZ/hah	(98)
PW5099 (*PA2435*:Tn5)	PA2435A02::ISphoA/hah	(98)
PW7626 (*PA3920*:Tn5)	PA3920G01::ISphoA/hah	(98)
PW4602 (*PA2092*:Tn5)	PA2092F01::ISlacZ/hah	(98)

PW4772 (*PA4614*:Tn5)	PA4614B11::ISphoA/hah	(98)
PA5056::Tn5	PW9491 lacZbp03q3G11	(98)
PA5058::Tn5	PW9495 phoAwp10q1D06	(98)
PA5241::Tn5	PW9824 phoAwp03q3A10	(98)
PAO1:pMS402	PAO1 with promoterless pMS402	(82)
PAO1:PmexAB-oprM	PAO1 with PmexBA-orM	(82)
calC::Tn5:pMS402	calC::Tn5 with promoterless pMS402	This study
calC::Tn5: PmexAB-oprM	calC::Tn5 with PmexBA-orM	This study
ladS :: Tn5	PW7727 phoAwp05q1G04	(98)
ladS :: Tn5	PW7726 phoAwp03q1D01	(98)
ΔcarR	PAO1 with deletion of carS gene.	(70)
ΔcarP	PAO1 with deletion of carP gene.	(70)
ΔcarO	PAO1 with deletion of carO gene.	(70)
ΔefhP	PAO1 with deletion of efhP gene	(71)
ΔbfmR	PAO1 with deletion of bfmR gene.	(162)
ΔlasR (lasR:Gm)	PAO1 with deletion of lasR gene	(163)
ladS :: Tn5 / pMS402	ladS::Tn5 with promoterless pMS402	This study

ladS :: Tn5 / pSK-2604F	ladS::Tn5 with pSK2604F	This study
ΔcarR / pMS402	ΔcarS with promoterless pMS402	This study
ΔcarR / pSK2604F	ΔcarS with with pSK2604F	This study
ΔcarP / pMS402	ΔcarP with promoterless pMS402	This study
ΔcarP / pSK2604F	ΔcarP with with pSK2604F	This study
ΔcarO / pMS402	ΔcarO with promoterless pMS402	This study
ΔcarO / pSK2604F	ΔcarO with with pSK2604F	This study
ΔefhP / pMS402	ΔefhP with promoterless pMS402	This study
ΔefhP / pSK2604F	ΔefhP with with pSK2604F	This study
ΔbfmR / pMS402	ΔbfmR with promoterless pMS402	This study
ΔbfmR / pSK2604F	ΔbfmR with with pSK2604F	This study
ΔlasR / pMS402	ΔlasR with promoterless pMS402	This study
ΔlasR / pSK2604F	ΔlasR with with pSK2604F	This study
PAO1 / CTX6.1	PAO1 transformed with promoter activity reporter empty plasmid CTX6.1	(164)
PAO1 / CTX-rsmA	PAO1 electroporated with promoter activity reporter construct for *rsmA*	(164)
PAO1 / CTX-rsmZ	PAO1 electroporated with promoter activity reporter construct for *rsmZ*	(164)
calC::Tn5 / CTX6.1	*calC::Tn5* transformed with promoter activity reporter empty plasmid CTX6.1	(164)
calC::Tn5 / CTX-rsmA	*calC::Tn5* electroporated with promoter activity reporter construct for *rsmA*	(164)

calC::Tn5 / CTX-rsmZ	*calC::Tn5* electroporated with promoter activity reporter construct for *rsmZ*	(164)
CSK231	*calC::Tn5* mutant complemented with *calC* on mini-TN7 transposon inserted on the chromosome.	This study
E. coli DH5α	*fhuA2 Δ(argF-lacZ)U169 phoA glnV44 Φ80Δ (lacZ)M15 gyrA96 recA1 relA1 endA1 thi-1 hsdR17*	
P. aeruginosa PAO1	Wild type	(96)
PW3128 (phoP:Tn5)	PA1179F08::ISlacZ/hah	(98)
PW9024 (PmrB:Tn5)	PA4777A09::ISlacZ/hah	(98)
PW4167 (*parR:*Tn5)	PA1799G12::ISlacZ/hah	(98)
ΔcarR:Gm (*ΔPA2657)*	PAO1 with deletion of *carR* by replacing with Gm^R gene.	(70)
PW5693(PA2802:Tn5)	PA2802D02::ISlacZ/hah	(98)
PW5694(PA2803:Tn5)	PA2803A12::ISlacZ/hah	(98)
PW5696(PA2804:Tn5)	PA2804G06::ISlacZ/hah	(98)
PW6426(PA3237:Tn5)	PA3237F01::ISlacZ/hah	(98)
PW6427 (PA3238:Tn5)	PA3238A02::ISlacZ/hah	(98)
PW9960(PA5317:Tn5)	PA5317H12::ISlacZ/hah	(98)
PW5349(PA2590:Tn5)	PA2590H04::ISlacZ/hah	(98)
PAOH26NTG22.3	Selected Polymyxin-B sensitive PAO1 mutant of PAO1	This study

PAOH27NTG22.5	Selected Polymyxin-B sensitive PAO1 mutant of PAO1	This study
PAOH28NTG22.5	Selected Polymyxin-B sensitive PAO1 mutant of PAO1	This study
PAOH29NTG22.17	Selected Polymyxin-B sensitive PAO1 mutant of PAO1	This study
PAOH30	PAOH26NTG22.3 mutant with pDOH30	This study
PAOH31	PAOH27NTG22.5 mutant with pDOH31	This study
PAOH32	PAOH28NTG22.5 mutant with pDOH32	This study
PAOH33	PAOH29NTG22.17 mutant with pDOH33	Thisstudy
PA2803::pDOH30	PA2803:Tn5 containing pDH30 plasmid with the PA2802-PA2804 region	This study
PA3237:: pDOH31	PA3237:Tn5 containing pDH31 plasmid with the PA3237-PA3238 region	This study
PA5317:: pDOH33	PA5317:Tn5 containing pDH33 plasmid with the PA5317 region	This study
C elegans N2 bristol	Wild type C. elegans	(375, 381)
C. clegans, CF 512 (rrf-3(b26) II; fem-1(hc17) IV)	Temperature sensitive sterile mutant of *C. elegans*	(375)

Plasmids		
pMMB66EH-AEQ	pMMB66EH plasmid containing aequorin gene from Aequorea Victoria	(165)

pTNS1	Helper plasmid carrying transposase genes.	
pUC18T-miniTN7-GM-eyfP	pUC18 based mini TN7 delivery plasmid, GmR, YFP tagged, modified Plac promoter.	(388)
pSK231	PA2604 cloned into pUC18T-miniTN7-GM-eyfP, AmpR, GmR.	This study
pMS402	Expression reporter plasmid carrying promoterless luxCDABE gene, ori of pRO1615. KanR, TmpR.	(82)
pSK2604	Promoter region of PA2604 cloned upstream of lux operon on pMS402,	This study
CTX 6.1	Integration plasmid origins of plasmid mini-CTX-lux; Tcr	(164)
CTX-rsmA	Integration plasmid, CTX6.1 with a fragment of pKD-rsmY containing rsmA promoter region and luxCDABE gene; Kn, Tmp, Tc	(164)
CTX-rsmZ	Integration plasmid, CTX6.1 with a fragment of pKD-rsmY containing rsmZ promoter region and luxCDABE gene; KanR, TmpR, TcR.	(164)
pMS402	Reporter vector, luxCDABE; KanR TmpR	(82)
pKD-mexA	pMS402 carrying the promoter region of mexAB-oprM; KanR TmpR	(82)

pKD-mexX	pMS402 carrying the promoter region of mexXY-oprM; KanR TmpR	(82)
pKD-czcC	pMS402 carrying the promoter region of czcCBA; KanR TmpR	(82)
pSK-muxA	pMS402 carrying the promoter region of muxABC-opmB; KanR TmpR	This study
pSK-mexJ	pMS402 carrying the promoter region of mexJK-oprM; KanR TmpR	This study
pSK-mexE	pMS402 carrying the promoter region of mexEF-oprN; KanR TmpR	This study
pMF36	A broad range *trc* expression vector	(212)
pDOH30	pMF36 with PAO1 gene fragments containing part of PA2802- PA2804	This study
pDOH31	pMF36 with PAO1 gene fragments containing part of PA3237- PA3238	This study
pDOH32	pMF36 with PAO1 gene fragments containing part of PA2590	This study
pDOH33	pMF36 with PAO1 gene fragments containing Part of PA5317	This study

[a]The mutant identifier from UW transposon mutant library.

[b]The designated name of the mutant strain in this study.

Genomic DNA and Plasmid Isolation

All DNA manipulation procedures were performed according to manufacturar's protocol with a slight modification. Genomic DNA was isolated using DNA isolation kit (Promega, Fitchburg, WI). For Genomic DNA used for cloning, a thread of DNA was separated at the precipitation step and transferred to a new tube, washed with ethanol, air dried before adding the appropriate amount of nanopure water. This was to avoid fragmentation of DNA. Plasmid DNA was isolated using the QIAprep mini-spin kit. Concentration of both genomic DNA and plasmid DNA was determined spectrophotometrically (A260 nm) using Nanodrop 2000 spectrophotometer (Thermo Fischer Scientific, Waltham, MA). The genomic DNA or plasmid DNA samples with the 260/230 and 260/280 ratios within the range of 1.8-2.0 were used for experiments.

Colony PCR (Polymerase Chain Reaction). In order to perform colony PCR

Taq-polymerase based PCR was used. For this, the pipette tip or sterilized tooth pick tip was dipped into single isolated bacterial colony once or twice and the collected bacterial sample was mixed into 25µl sterilized nanopure water. The PCR tubes containing this cell mixture was incubated into heat block at 90°C- 100°C to boile open the cells to rescue exposed nucleotides. A 25 µl reaction was prepared by adding 15.5 µl of nuclease free water, 2.5 µl of 25 mM $MgCl_2$, 2 µl of 2.5 mM dNTP, 2 µl of 10 x PCR buffer, 0.5 µl of 10 µM forward primer, 0.5 µl of 10 µM

reverse primer, 0.5 µl of template (gDNA or colony template DNA), 1.5 µl of 100 % DMSO and 0.25 µl of Taq DNA polymerase. To carry out the reaction, T3 Thermocycler (Whatman Biometra, Gottingen, Germany) was used and programmed with following steps: **1.** Initial denaturation at 94 °C for 5 min (1 cycle), **2.** 30 cycles of denaturation at 94 °C for 45 s, annealing at temperature 5 °C lower than the lowest melting temperature of the primer pair for 40 s and extension at 72 °C for 1 min 30s (1 kb/min); **3.** Final extension at 72° C for 10 min and **4.** Incubation at 15° C prior to running the sample on agarose gel.

PCR with genomic DNA or plasmid DNA

The PCR reaction with genomic DNA was perfomed similarly as above except, gDNA or plasmid DNA was used as template instead of boiled bacterial cell lysate.

Gel electrophoresis

For agarose gel electrophoresis, any nucleotide sample with a size of 100-250 bp was run on 1.8% agarose gel and nucleotides larger in size were run on 1% agarose gel for better resolution of stained product. Agarose gel was prepared by adding 1% (W/V) of agarose to 1X TAE buffer (0.5 gm in 50 ml buffer) and microwaving the mixture until the agarose was completely dissolved (2-3 min). The liquid hot agarose solution was poured onto a gel-cast with gel-comb already palced

into the cast. Any bubble formed during pouring the agarose can be disrupted by poking the bubbles with pipette tip. Once solidified, the solidified gel on a cast was moved into the electrophoresis tank filled with 1X TAE buffer in such a way that the gel is merged under the buffer. The gel need to be placed in a way that the wells on the gel will be toward the anode and the rear end of the gel is toward the cathode. The PCR product is mixed with DNA loading dye at 1:6 ratio. The mixture is then inoculated into the wells very carefully avoiding any bubble formation or poking the neighboring wells. Molcular marker (DNA/RNA ladder) was added to at least one well as a reference for size determination. The cord connecting the gel tank then is connected to the voltage generator. The gel is run at 125-130 MV for 30-45 min.

Bacterial Growth Analysis

Growth analysis of PAO1 and each mutant were performed in BMM with no added or 5 mM Ca^{2+}. The growth rate was calculated according to (115). The growth of each mutant was compared to that of the PAO1 to identify any growth defect due to mutation. For this, bacterial cells were grown on LB agar plates with selective antibiotics when needed. Isolated individual colonies were inoculated into 3 ml of BMM with no or 5 mM Ca^{2+}, incubated at 37°C and 200 rpm for 12 hours. Upon collecting the cultures at 12^{th} hour, OD of each cultures were measured at 600nm wavelength using the Biomate 3 spectrophotometer (Fisher Scientific). The

cultures were then normalized by diluting the initial cultures in corresponding media in such a way that the final OD600 would be 0.1. These normalized cultures were then inoculated into 100 ml of corresponding media (BMM with no or 5 mM Ca^{2+}) at 1:1000 ratio into 250 ml ehrmyer flasks. The flasks were incubated at 37°C and 200 rpm and OD600 was measured every 2-4 hours until the bacteria reached to stationary phase. At least three biological replicates were used for each experimental set.

Antimicrobial Susceptibility Assay (E-strips)

Bacterial cultures were first grown on LB agar plates containing selective antibiotics. for PAO1 there was no antibiotic and for transposon mutants received from University of Washington genome center, tetracycline was added at the final concentration of 60µg/ml. Isolated individual colonies were inoculated into 3ml of BMM with no or 5 mM Ca^{2+}, incubated at 37°C and 200 rpm for 18 hours (early stationary). The OD_{600} of each bacterial cultures were measured. The bacterial cultures were then diluted into corresponding media in such a way that the final OD_{600} of cultures were 0.1. In parallel, BMM agar plates with no added or 5 mM Ca^{2+} were dried under UV (Hood) for 15 min prior to the experiment to dry up excess moisture on the plate.100 µL of the normalized culture were spread-plated onto BMM agar plates with Ca^{2+} concentrations corresponding to the growth media. Once the cultures were dried onto the plates (5-10 min after spreading), the

commercially available E-strips containing gradient of antibiotics on them, were placed on the middle of the plate. It is crucial to make sure no bubble has been formed in between the E-strip and the agar. Any resultant bubble would inhibit dispersion of the antibiotic from that part of the strip and provide incorrect concentration of antibiotic around that area of the plate. Also, once the strips touched the plate, it should not be moved to make a better placement. Moving the strips results into inappropriate dispersion of antibiotic onto the agar and might generate wrong experimental result. The plates were then incubated at 37°C for 24 hours. Then the minimum concentration of antibiotics that prevented the growth of bacteria around the strips was recorded for each bacterial strains grown at each condition. At least three replicates were used to assure the statistical significance of the result.

Antimicrobial Susceptibility assay (Plate dilution assay)

For plate dilution assay, isolated individual colonies from plates were inoculated into 3ml of BMM with no or 5 mM Ca^{2+}, incubated at 37°C and 200 rpm for 12 hours (middle log.) These middle log cultures grown in BMM with or without added Ca^{2+} were then diluted into corresponding media in such a way that the final OD600 is 0.3. The normalized cultures were then inoculated at 1:100 ratio into BMM with the corresponding Ca^{2+} concentration. For each tube 10µl of tobramycin was added at the final concentration of 0.25, 0.5, 0.75, 0.1, 1.5 µg/ml

to BMM without added Ca^{2+} and of 1.0, 1.5, 1.75, 2.0, 3.5 µg/ml to BMM supplemented with 5 mM Ca^{2+}. 200 µl of the final cultures were added to each well of 96 well clear plates with sterilized triton treated cover on it. For treating the covers, 5% triton solution (10 ml sterilized nanopure water, 2.5 ml 95% ethanol, and 5µl concentrated triton) was used to rinse the inside surface of the cover thoroughly. Then both the plate and the cover was UV treated under UV hood for 15 min before the experiment. Once aliquoted into 96 well plates, the cultures were incubated with fast shaking for 8 h, and OD600 was measured using the Synergy MS plate reader (Biotek). At least three replicates were tested. To determine the minimum concentration of antibiotic that inhibited growth of the bacteria, positive control for growth (without added antibiotic) and no growth (no bacteria added, non-inoculated control) were added to the plate. The OD_{600} of cultures containing antibiotics that was same as the non-inoculated control was considered as growth inhibited culture and the concentration of antibiotic in the corresponding well was recorded as MIC for that antibiotic.

Efflux inhibitor assay

For efflux inhibitor assay, a plate dilution technique was used. First, isolated individual colonies from plates were inoculated into 3ml of BMM with no or 5 mM Ca^{2+}, incubated at 37°C and 200 rpm for 12 hours (middle log.) These middle log cultures grown in BMM with or without added Ca^{2+} were then diluted into

corresponding media in such a way that the final OD600 is 0.3. The normalized cultures were then inoculated at 1:100 ratio into BMM with the corresponding Ca^{2+} concentration with or without PAβN. For each tube 10µl of PAβN was added at the final concentration of 10, 20, 30, 40, 50, 60, 70, 80, 90 and 100 µg/ml to both BMM without added Ca^{2+} or supplemented with 5 mM Ca^{2+}. 200 µl of the final cultures were added to each well of 96 well clear plates with sterilized triton treated cover on it. For treating the covers, .5% triton solution (10 ml sterilized nanopure water, 2.5 ml 95% ethanol, and 5µl concentrated triton) was used to rinse the inside surface of the cover thoroughly. Then both the plate and the cover was UV treated under UV hood for 15 min before the experiment. Once aliquoted into 96 well plates, the cultures were incubated with medium for 24 h, and OD600 was measured every 2 hours using the Synergy MS plate reader (Biotek). At least three replicates were tested. To determine the minimum concentration of PAβN that inhibited growth of the bacteria, positive control for growth (without added antibiotic) and no growth (no bacteria added, non-inoculated control) were added to the plate. The OD600 of cultures were then plotted on a connected scatter plot to visualize the growth curve. The growth curve performed for bacteria grown at BMM with no Ca2+ was compared to that of BMM with 5 mM Ca^{2+} to assess the effect of Ca^{2+} on the PAβN tolerance.

For plate assay, isolated individual colonies were inoculated into 3ml of BMM with no or 5 mM Ca^{2+}, incubated at 37°C and 200 rpm for 18 hours (early

stationary). The OD600 of each bacterial culture were measured. The bacterial cultures were then diluted into corresponding media in such a way that the final OD600 of cultures were 0.1. Before spreading the bacterial cultures, it was essential to get rid of excess moistures on the BMM agar plates to be used for this experiment. For this, plates were dried under UV (Hood) for 15 min prior to the experiment.100 µL of culture was spread-plated onto BMM agar plates with Ca^{2+} concentrations corresponding to the growth media. Once the cultures were dried onto the plates (5-10 min after spreading), sterilized dry 0.3 mm disks were placed onto the bacterial lawn and 15µl of PaβN were added onto the disks. For this assay PAβN were used at the concentration of 10, 20, 30, 40 and 50 µg/ml for each Ca^{2+} concentration. The plates were then incubated at 37° C in the table top incubator for 24 hours. This experiment was performed to determine the concentration at with PAβN had no effect on growth of PAO1 at both no added or 5 mM Ca^{2+}.

Primer Design and selection for RT-qPCR.

Primers for 12 RND transporter genes (*triA, mexB, muxC, mexI, mexC, mexE, mexJ, mexQ, mexV, mexX, czcB*, and *mexM*), three carbonic anhydrase genes PA2053, PA4614 and PA102, as well as PA2604 were designed using Primer3Plus or Primer BLAST and listed in Supplementary **Table 7.2**. For this the FASTA format gene sequence for each gene was copied from http://www.ncbi.nlm.nih.gov/ onto a word document. In order to design the primers, 1. On the primer3 plus home

(http://primer3plus.com/cgi-bin/dev/primer3plus.cgi) main page sequences were copied-pasted into the box or files were uploaded via "upload" tool on the right top of the box, 2. On "General settings tab , primer size was chosen to be 100-250 bp long with optimum size of 200, primer Tm was selected to be 50-65 with an optimum Tm of 60 and primer GC % was selected to be within the range of 45%-55% with an optimum GC content of 50%. Maximum Tm difference between two primers were selected to be 5° C. 3. Moving onto the Advanced settings, "Max poly-X" was set at 3, "number to return" set to 10 and "Max 3' stability" set to 8. 4. Besides this everything else was at default settings. 5. "Pick primer" tab on the top-right of the page was selected to derive the paired primers designed. 6. The output information was then copied to an excel file for further analysis.

To design primers in Primer BLAST, the same selective criteria were used.

These Primers were then tested in silico using OligoAnalyzer (IDT, https://www.idtdna.com/calc/analyzer) for their primer compatibility and stability. Each individual primer was copied-pasted on the toolbox and "analyze" tab was selected to generate the information on the primer melting Tm, GC content and these informations were compared to the paired primer to confirm their compatibility. Similarly, the individual primers were assessed for "Hairpin" analysis. Any primer with a $\Delta G \geq 0$ was automatically selected for further analysis.

Primers with $\Delta G \leq 0$ were only chosen if the ΔG value was found at a temperature much less than the annealing temperature of the pair.

Table 7.2: Primers used in this study

Primer name	Primer sequence (5′ - 3′)	Primer efficiency (%)	Reference
0576_F1	CTCAACTACCAGCGGCAGAA	97	(103)
0576_R1	CGCAGCTCGGTATAGGAAAG		(103)
0156_F1	CTCAACTACCAGCGGCAGAA	93	This study
0156_R1	CGCAGCTCGGTATAGGAAAG		This study
0426_F1	TACGAAAGCTGGTCGATTCC	100	This study
0426_R1	GCGAACTCCACGATGAGAAT		This study
2526_Fiv	AGGAACAGGAAGACCACCAG	100	This study
2526_Riv	TCAAGCTGAACGTGATGGAC		This study
4207 F1	GTCGAACCGAACAAGCTGAT	100	This study
4207 R1	TGTTGCCTTCCTGGGTGTAT		This study
4599_F2	TTCCGAACTCAGCGCCAG	97	This study
4599_R2	ATAGGAAGGATCGGGGCGTT		This study
2493_F1	TGGAACAGTCATCCCACTTC	93	This study
2493_R1	AATTCGTCCCACTCGTTCAG		This study
3677_F3	CGGTAGCTGTTCTGGATGTTC	96	This study
3677_R3	GAGCGGGTAAAGAAGGACCA		This study
3522_F3	CGACGGATAGCCGTTGTAGT	93	This study
3522_R3	TCGCACCTACAAGGTCACTG		This study
2019_F3	TTCTCGACGATCACCCACTC	97	This study
2019_R3	TCAAGGTGGTCAACCCAAAG		This study
4374_F3	AAGGTCTACTCCATCCGTCAG	96	This study
4374_R3	CCGGAAAGGAACAGTACGTC		This study

2521_F2	TGCCCAGTTCGGATTTGAGG	97	This study
2521_R2	CGAGGACGTGGTGTTCGTC		This study
1435_3rt F	GCACCGATCTCCGTAGTCTT	89	This study
1435_3rt R	GGTGGAACTGTCGATCTGGT		This study
muxA- f	AAC**CTCGAG**TTTCAACGGGTCG ATCATCT		(82)
muxA- r	CC**GGATCC**ATCACCAGGCCGAT CAC		(82)
mexJ- f	AAA**CTCGAG**GGCGATATTCAGC AGGAC		(82)
mexJ- r	CA**GGATCC**GGTACATGTGACAC CTTC		(82)
mexE- f	AAT**CTCGAG**CATGTTCATCGGCG ATCC		(82)
mexE- r	CA**GGATCC**AGGCGCTCAGGACC AGTA		(82)
49172F.f	GGAAGAGTCTCCCCTTCGAC		(98)
49172F.r	TAGAAGAACAGGCGGACGAT		(98)
Aeq-Forward	CTTACATCAGACTTCGACAACCC AAG		(72)
Aeq-reverse	CGTAGAGCTTCTTAGGGCACAG		(72)
PA2604-SH-F	**AGAGAGaagctt**ATGCAAGAACAG CAATATCAGC		This study
PA2604SH-R	**AGAGAGgagctc**TCAGTCGTCGCC GC		This study
PA2604F-F	AAC**CTCGAG**GGTGTGGGTACTC CTTAAC		This study
PA2604F-R	CC**GGATCC**GACCGTTGCCTTAAA CC		This study
TN7-seq-F	CTCCTCTTTAATTCTAGATGTGTG AAATTG		This study

TN7-SEQ-R	CACAGCATAACTGGACTGATTTC		This study
PTn7R	ATTAGCTTACGACGCTACACCC		(388)
PTn7L	ATTAGCTTACGACGCTACACCC		(388)
$P_{glmS\text{-}down}$	GCACATCGGCGACGTGCTCTC		(388)
$P_{glmS\text{-}up}$	CTGTGCGACTGCTGGAGCTGA		(388)
psCA1-F	AGAGAGCATATGCCAGACCGTATG	97	This study
psCA1-R	AGAGAGGGATCCTCACGAGCTCAG		This study
psCA2-F	AGAGAGCATATGCGTGACATCATCG	93	This study
psCA2-R	AGAGAGGGATCCTCAGGCGAC		This study
psCA3-F	AGAGAGCATATGAGCGACTTGCAG	94	This study
psCA3-R	AGAGAGGGATCCTCAGCAGCAAC		This study

Primer specificity and efficiency assessment

At First, The primer specificity was tested by BLAST alignment against *P. aeruginosa* genome available at www.pseudomonas.com. On http://pseudomonas.com/ page (Now, http://beta.pseudomonas.com/) under the sequence search section on the main toolbar, BLAST was selected. On the redirected page, under the BLASTN the primer sequence was copied to the sequence box. The primer sequence was then used to perform a BLAST against PAO1 reference genome. It was expected that the primer sequence will be 100% identical to the specific target only. As long as the second best hit showed less than 50% identity, the primers were selected for further analysis.

In vitro, Primer specificity of each pair of oligos was confirmed by gradient PCR. PCR master mix was prepared same way as the general PCR described in "PCR" section of methodology chapter. For PCR, gradient of annealing temperature were used. The range of temperature was based on the melting temperature of the primer pair. Lowest temperature for he gradient was 5° C below the lowest Tm of the oligo pair and highest temperature was maximum 5° C above the highest Tm of the pair, making sure the range between two temperature chosen was no more than 10° C. Gradient PCR also revealed the annealing temperature at which primers were mostly specific to the target gene. For this, genome DNA of PAO1 at the concentration of 5 ng/µl was used.

Also, RT-qPCR melt curve analysis using gDNA as a template was performed to confirm the primer specificity. RT-qPCR was performed following the manufacturer's protocols (Roche). For this, 5 µl of SYBR green master mix (Roche, Indianapolis, IN), 0.5 µM of each primer and 5 ng of RNA were added to a total volume of 10 µl of reaction mixture. RT-qPCR was run using 384 well plates sealed with LightCycler 480 Sealing Foil (Roche, Indianapolis, IN) in Roche LightCycler 480. At least three technical replicates were used. A no-template control was used as a negative control. The cycle included 10 min denaturation at 95° C followed by 35 cycles of 95° C for 10 s, specific annealing temperature (this was selected by gradient PCR) for 15 s, and 72° C for 10 s.

Prior to each experiment, the light cycler program was prepared for each set of experiment following the manufacturer's protocol. For this, the sample information as it is distributed on the plate was entered into the experiment file's plate template. All the technical replicates were selected and grouped under the specific category. For each set of experiment, housekeeping gene control and no template controls were also added. The step by step protocol for creating a new experiment to run on LightCycler480 is described in the machines instruction manual (http://plantbio.okstate.edu/resources/files/Roche_RT-PCR_Manual.pdf)

For primer efficiency, RT-qPCR was performed for each primer pair using 10 fold serial dilution of gDNA, and the obtained Cp values were plotted against the concentration of nucleotides. The plot generated the values for the following equation

$$\mathbf{Y} = -(\boldsymbol{mx}) + \boldsymbol{c}$$

Here, 'm' represents the slope. And the R^2 value for the plot was ≤ 1.

The efficiency was calculated using linear regression analysis using the equation $\mathbf{10^{(-1/slope)}-1.}$

Following the MIQE guidelines (100), the primers with an R2 value of 0.99 and an efficiency of (The efficiency of control gene primer pair) 97% ± 10 % were selected.

Selection of Housekeeping genes

At first, four tested housekeeping genes, rpoD, rpoS, proC and 16S rRNA were selected based on the current literatures on the field (103). The primers were previously designed in (103) and (389).These primers were also subjected to gradient PCR and RT-PCR melt curve analysis for primer efficiency calculation and determination of annealing temperature. Then the efficiency of the primers was measured by above method. Upon the qualitative assessment of the primers, these primers were further tested to assess the transcript abundance of corresponding genes for PAO1 grown at no added Ca^{2+} and 5 mM Ca^{2+} (The gene expression analysis protocols follows). The housekeeping genes which displayed no change in the transcript abundance due to exposure to elevated Ca^{2+} was (were) selected as a control.

RNA Isolation

Several RNA isolation techniques were used to optimize the standard protocol to be used in our lab. For all RNA extraction method 3 biological replicates for each type of bacterial cultures were used. The first step was starting bacterial culture in three ml BMM with no added or added 5 mM Ca^{2+}. After 12 hours of incubation the precultures were taken out and the cell density was measured by spectrophotometer. The cultures were then normalized to an OD600 of 0.1 and added to 100 ml of BMM with corresponding Ca^{2+} to a 1:1000 ratio in 250 ml

flasks. The cultures were grown at 37º C, 200rpm (using the floor shaker incubator) for 13 hours ± 15 min (for RNA extraction for RNA-seq and second batch of RNA extraction) with an OD reaching up to (0.23 ± 0.01- 0.03). Cultures were harvested into RNA later (prepared in lab)/ RNeasy RNA protect reagent (Qiagen)/ RNA later (Ambion) in 1:1 volume and mix well by inversion. It was kept at room temperature for 5 min prior to RNA extraction. **Each protocols were modified from manufacturer's protocol to get highest yield and good quality RNA.**

1. **HighpureRNA isolation Kit (Roche) based extraction.** For this bacterial cultures were transferred to a 50 ml falcon tubes and placed into ice before pelleting the cells by centrifugation at 4500 rpm for 15 min. 1 ml of TriPure isolation reagent (Roche) solution was added to resuspend the cells and was then transferred to RNase free screw-capped 2 ml microfuge tubes. This was incubated at room temperature for 6 min and 200 µl of chloroform was added to the tube followed by mixing with inversion. Three distinct layers were visible in the tube after centrifugation at 15,000 rpm for 5 min. Upper aqueous layer containing RNA was transferred into highpure tube and centrifuged at 11,000 rpm for 15 s. On column DNase treatment was performed with DNase (Roche). 20 µl of DNase was mixed with 90 µl of DNase incubation buffer in a RNase free PCR tube and transferred onto the column. The column was then incubated at room temperature for an hour. After DNase treatment the column was washed 500 µl of with wash buffer

I and wash buffer II at 11,000 rpm for 15 s. The final wash step was performed with 200 µl of wash buffer II. At 14,000 rpm for 2 min. 100 µl of elution buffer was added and the RNA was eluted at 11,000 rpm for 1 min. The RNA sample was transferred to a new RNase free tube.

2. **HighpureRNA isolation Kit (Roche) based extraction combined with Phenol-Chloroform extraction protocol.** For this bacterial cultures were transferred to a 50 ml falcon tubes and placed into ice before pelleting the cells by centrifugation at 4500 rpm for 15 min. 1 ml of TriPure isolation reagent (Roche) solution was added to resuspend the cells and was then transferred to RNase free screw-capped 2 ml microfuge tubes. This was incubated at room temperature for 6 min and 200 µl of chloroform was added to the tube followed by mixing with inversion. Three distinct layers were visible in the tube after centrifugation at 15,000 rpm for 5 min. Upper aqueous layer containing RNA was transferred into a new RNase free 2 ml tube already aliquoted with 500 µl of isopropanol followed by centrifugation at 15,000 rpm for 10 min. The supernatant was discarded and the pelleted nucleotides were washed with 1 ml of 75% ethanol at 15,000 rpm for 5 min. The pellets were air dried and was resuspended into 43 µl of RNase free water and incubated at 55º C on hot plate for 1 hour. For DNase treatment 2 µl of DNase and 5 µl of DNase buffer (Ambion) was added to this sample was kept at room temperature for 1 hour. After the DNase

treatment, 200 µl of RNase free water was added to the tube and the enzymes were precipitated by phenol-chloroform based extraction. For this low pH (4.3) phenol was added to the tube at 250 µl and was mixed by gentle inversion. This was centrifuged at 15,000 rpm for 6 min. 250 µl of upper phase (avoid the interphase) was transferred to a new RNase free tube and 250 µl of pheol-chloroform was mixed to it. A centrifugation at 15,000 rpm for 6 min, transfer of 250 µl of upper phase to another tube, addition of 25 µl of sodium acetate (3 mM) followed by addition of 625 µl of 100% ethanol was performed sequentially. The final solution was kept at -20 ºC for overnight. The next morning this solution was centrifuged at 15,000 rpm for 6 min and the supernatant was discarded. The pellet was washed with 75% ethanol at 15,000 rpm for 3 min and air dried after decanting the supernatant to get rid of residual ethanol The pelleted RNA was reconstituted into 50 µl of RNase free water.

3. **RNeasy Bacterial mini kit (Qiagen) based extraction.** A total volume of 30 ml solution of 15 ml bacterial culture and 15 ml of RNeasy protect solution (Qiagen) were centrifuged at 4500 rpm and 4º C for 10 min. The supernatant of eact tube was decanted and the tubes were dabbed on kimwipes to get rid of residual liquid leaving the cell pellet at the bottom of the tubes. 200 µl of lysozyme (1µg/ml) was used to resuspend the pellet and transferred to a sterile 1.5 ml RNase free tube, before adding 700 µl of the

cell lysis buffer RLT (1% β- markeptoethanol added to RLT right before it was added to the cell pellet). The mixture was then vortexed vigorously for 10 s. This mixture was centrifuged at 15,000 rpm for 6 min. The clear supernatant was transferred carefully (without touching the pellet) to a fresh RNase free 1.5 ml tube. 500 µl of 95% ethanol was added to the tube and was mixed by gentle pipetting (DNA may precipitate as white fiber like substance inside the tube). 700 µl of this lysate was then transferred to a column placed on 2 ml collection tube (Qiagen). The collection tube with the column was centrifuged briefly at 11,000 rpm for 15 s. If any residual lysate were left, this step was repeated. The columns were washed with 350 µl of RW1 buffer and then on column DNase treatment wqas performed using QDNase (Qiagen). For this 20 µl of DNase and 140 µl of buffer RDD (Qiagen) was mixed into a separate RNase free tube and transferred to the column. The columns were kept at room temperature for 2 hours to allow complete digestion of DNA and washed with 350 µl of buffer RW1 (Qiagen). Buffer RPE (Qiagen) was added to each column at a volume of 500 µl and centrifuged for 2 m. at 11,000 rpm. An additional centrifugation step for 30 s. was performed to get ridof residual buffer from the colums. The columns were tehn transferred to new collection tubes. 30 µl of RNase free water (Qiagen or DEPC treated at he lab) was added to the column. The RNA was eluted by centrifuging the columns at 15,000 rpm for 3 min. The

eluted RNA sample was transferred to a RNase free 500 µl snap-cap microfuge tube. An additional DNase treatment was performed using DNase treatment kit (Ambion).

4. **RNA extraction using combination of trizol (Roche) based and RNeasy bacteria mini kit (Qiagen).** For this bacterial cultures were transferred to prechilled 50 ml falcon tubes and placed into ice before pelleting the cells by centrifugation at 4500 rpm for 15 min. 1 ml of Trizol (Roche) solution was added to resuspend the cells and was then transferred to RNase free screw-capped 2 ml microfuge tubes.200 µl of chloroform was added to the tube and mixed by inversion. This solution was then centrifuged at 15,000 rpm for 15 min. at this point three distinct layers were created inside the tube with a clear aqueous layer at the top. This aqueous layer was carefully transferred to a new RNase free 2 ml microfuge tube and 500 µl of 95% ethanol was mixed by inversion. 700 µl of this lysate was then added to qia column (Qiagen) followed by a wash step with buffer RW1 (Qiagen). The rest of the steps are exactly same as described in the RNA extraction by **RNeasy Bacterial mini kit (Qiagen).**

5. **Direct-zol RNA kit based extraction.** For this, 15 ml of RNA later was added to 15 ml of culture and was centrifuged at 4500 rpm for 10 min. The pelleted cells were resuspended into 200µl of lysozyme (1mg/ml) followed

by adding 1 ml of Trizol (Roche) solution and incubated at room temperature for 5 min. This solution was centrifuged at 15,000 rpm for 10 min. The supernatant was then transferred to a new RNase free tube and equivolume 95% ethanol was added to the solution. This mixture was then transferred to zymospin column at the volume of 700 µl and was spun at 15,000 rpm for 15 s. once all lysates were spun down, 400 µl of RNA prewash buffer was added to the column and then centrifuged at 11,000 rpm for1 min. Then 700 µl of RNA wash buffer was added to the column and centrifuged at 11,000 rpm for 1 min. This step was further repeated without any addition of buffer to get rid of residual buffer from the column. The column was then transferred to a new collection tube. 25-30 µl of RNase free water was added tot eh column and kept at room temperature for 1 min prior to elute the RNA sample by centrifugation at 15,000 rpm for 3 min.

6. **Zymo Bacterial/Fungal RNA mini prep based extraction.** 15 ml RNA later (prepared in lab) aliquot was added to a 50 ml falcon tube, labeled with sample names prior to harvesting the middle log bacterial cells (the mid-log phase and OD_{600} was selected based on growth profile of the bacterium). Upon harvesting the cells, cultures were added to the corresponding tubes at a 1:1 ratio and incubated at room temperature no more than 10 min (for more than 10 min incubation, cells should be kept at ice; I consistently incubated for 6 min and then went for centrifugation). The cultures were

centrifuged at 42,00 rpm for 15 min at 4º C. Cell pellets can be stored at -20 for ~ 3 months to extract RNA later (I kept for couple of weeks only). Cell pellets were resuspended into 200 µl of lysozyme (1mg/ml) followed by adding 800 µl of RNA lysis buffer to the cell suspension. A very good mixing is necessary at this point to make sure no pellets are left unmixed. This solution was then added to the bashing bead tube and centrifuged at 13,000 rpm for 1 min. 800 µl of the solution was taken out carefully avoiding the beads (this step can be skipped and the solution can be added to the column directly) and transferred to the zymo spin IIIC column. The column was then centrifuged at 13,5000 rpm for 30 s. The flowthrough was collected into an RNase free 2 ml tube already aliquoted with equivolume of 95% ethanol and was mixed by inversion. This lysate was then transferred to zymo spin column at 700 µl volume at a time and spun down by 13,500 rpm for 30 s. The flowthrough was discarded. 400 µl of RNA prep buffer was added to the column and centrifuged at 13, 500 rpm for 30 s. The columns were then washed by 700 µl and 400 µl of RNA wash buffer consecutively with a 2 min. centrifugation at 13,500 rpm. An additional 1 min spin was performed at the end without adding any buffer to get rid of residual wash buffer. 40 µl of RNase free water was used to elute the RNA at 15,000 rpm for 3 min. This step was repeated with 10 µl of RNase free water to ensure complete elution of RNA sample.

DNase treatment of RNA samples

Upon isolation of RNA at first the RNA samples were measured by Nanodrop 2000 (Thermofischer) at the botany core facility. The samples with a 260/280 ratio of (1.8-2.2) and 260/230 ratio of 1.6-2.0 were selected and diluted to a concentration of 100 ng/µl with RNase free water. These samples were then subjected to general PCR using *rpoD* primers and genomic DNA as a positive control for presence of DNA. If DNA was present, the RNA samples were treated with Turbo DNase (Invitrogen). In a 25µl of RNA solution, 3 µl of Turbo DNase buffer and 1µl of DNase were added and were mixed thoroughly, spun down and incubated at 37° C for 2-4 hours. Then the tubes were cooled down at room temperature and moistures on the tube wall were spun down prior to adding the DNase inactivation buffer. The inactivation buffer has a tendency to settle down, so it was mixed occasionally (every 2 min) while incubating at room temperature for 10 min. The mixed solution was then centrifuged at 15000 rpm () for 4 min. The supernatant was transferred very carefully without touching the pellet. The RNA sampleas were then again measured by Nanodrop 200 and assessed for presence of residual DNA by general PCR. If DNA still remained, additional DNase treatment were carried out and the removal of DNA was confirmed by same PCR method.

Qualitative assessment of RNA by Gel electrophoresis

1% agarose gel electrophoresis of RNA samples followed by Bioanalyzer assay has been established to be an effective way of assessing the RNA integrity (100). For this, the RNA samples were linearized by incubating at 65° C for 10 min prior to running on the gel. 1% agarose gel was prepared by adding agarose to 1X TAE buffer at the ratio of 1% (W/V). The mixture was microwaved to dissolve the agarose into buffer. 5% of gel red (V/V) was added to the gel before pouring it to the cast. This minimizes the time of gel electrophoresis and chance of RNA degradation while staining after running the gel. For each gel electrophoresis 500 ng-1µg of RNA was used and gel loading dye was added to the RNA samples before loading onto the wells. 1 KB plus DNA ladder were used as a reference to assess the ribosomal RNA bands. The gels were visualized under UV (machine name). Also, a general PCR as well as RT-qPCR of RNA samples were performed using *rpoD* primers to confirm no DNA was present. For this genomic DNA was used as positive control and no template as negative control for amplification.

Bio-analyzer Assay

In combination with 1% agarose gele analysis, RNA bioanalyzer assay has been established and required to claim validation of transcriptional analysis. Upon selecting the RNA samples with very strong bands representing the 16S and 23S ibosomal RNAs on the 1% agarose gele, the samples were sent to OSU RNA core

facility for qualitative assessment by Agilent bionalyzer nano (Agilent technologies). The analyzed results were provided by the core facility in three format. 1. Diagrams of RNA samples with peaks for different RNA species 2. Image of RNA samples on gel with the ladder showing the bands for different RNA species. 3. Excell file containing detailed information about the RNA including the 16S:23S rRNAs, total RNA and most importantly calculated RNA integrity value. Any RNA samples with an RIN value ≤ 6 were rejected. Samples with RIN value within 5-6 were only accepted when the rRNA species were quite visible on the gel image (only when there were no other option).

cDNA Synthesis

For cDNA synthesis, Transcriptor first strand cDNA synthesis kit from Roche was used. The detailed protocol is as follows,

1. 1µg of total RNA was mixed with the following reagents at the defined volume in a sterile DNase-RNase free PCR tube to a final volume of 13µl:

I.	Anchored oligo dT	1.0 µl
II.	Random hexamer	2.0µl
III.	PCR grade water	0.5µl

At this point the mixture was incubated at 65°C for 10 min in a thermocycler. Immediately after this step the tubes were kept back into an ice block and 7 µl of a master mix consist of

I. Transcriptor reverse transcriptase reaction buffer (8mM MgCl2)

4µl

II. Protector Rnase inhibitor

.5µl

III. dNTPs

2.0µl

IV. Transcriptor reverse transcriptase

.5µl

Was added to the tube to make the final volume 20µl. This mixture was then run for one cycle with 25°C for 10 min, 55°C for 30 min and 85°C for 5 min. Once the cycle was completed the cDNA samples were stored at -20° C.

RT-qPCR

To characterize the transcription profiles of RND genes, RT-qPCR was performed following the manufacturer's protocols (Roche). For this, 5 µl of SYBR green master mix (Roche, Indianapolis, IN), 0.5 µM of each primer and 5 ng of RNA were added to a total volume of 10 µl of reaction mixture. RT-qPCR was run using 384 well plates sealed with LightCycler 480 Sealing Foil (Roche, Indianapolis, IN) in Roche LightCycler 480. At least five technical replicates for each biological replicate and a minimum of three biological replicates for every sample were analyzed. A no-template control was used as a negative control. The cycle included 10 min denaturation at 95 °C followed by 35 cycles of 95 °C for 10

s, 61 °C for 15 s, and 72 °C for 10 s. A fold change in gene transcription was calculated using 2-ΔΔCt method. Statistical analysis was performed by using two tailed T-test assuming equal variances.

RNA seq analysis

Library preparation and RNA seq.(The tables and gel picture was generated and provided by Vertis biotechnologies, Germany) RNA seq analysis was performed at Vertis Biotechnology AG, Germany. First, RNA samples were assessed by capillary gel electrophoresis using Shimadzu MultiNa microchip and RNA samples with a 16S/23S ratio of 1:1- 1:3 were selected for further analysis (Table 7.3 and Fig. 7.1).

Table 7.3: Sample information for RNA-seq (from Vertis technologies)

No.	Sample	Conc. (ng/µl)	Amount (µg)	Conc. (ng/µl)	Amount (µg)	Ratio 23S/16S	Yield Capable-seq enriched RNA (%)	Recovery after rRNA depletion (%)
		Customer-specified		Own measurements (see Fig.1)				
1	PAO1_0.1	535	16,1	443	12,9	1,1	0,1	0,4
2	PAO1_0.2	1.045	31,4	839	24,3	1,1	0,2	0,8
3	PAO1_5.2	753	22,6	595	17,3	1,3	0,7	3,8
4	PAO1_5.3	733	22,0	606	17,6	1,2	0,6	4,0
5	PA2604:IS_0.1	1.155	34,7	1.332	38,6	1,3	0,2	2,2
6	PA2604:IS_0.2	1.201	36,0	1.123	32,6	1,3	0,6	3,0
7	PA2604:IS_5.1	1.997	59,9	1.831	53,1	1,3	0,1	3,6
8	PA2604:IS_5.2	1.909	57,3	1.776	51,5	1,3	0,3	1,3

The RNA samples were analyzed by Capillary electrophoresis (Fig. 1)

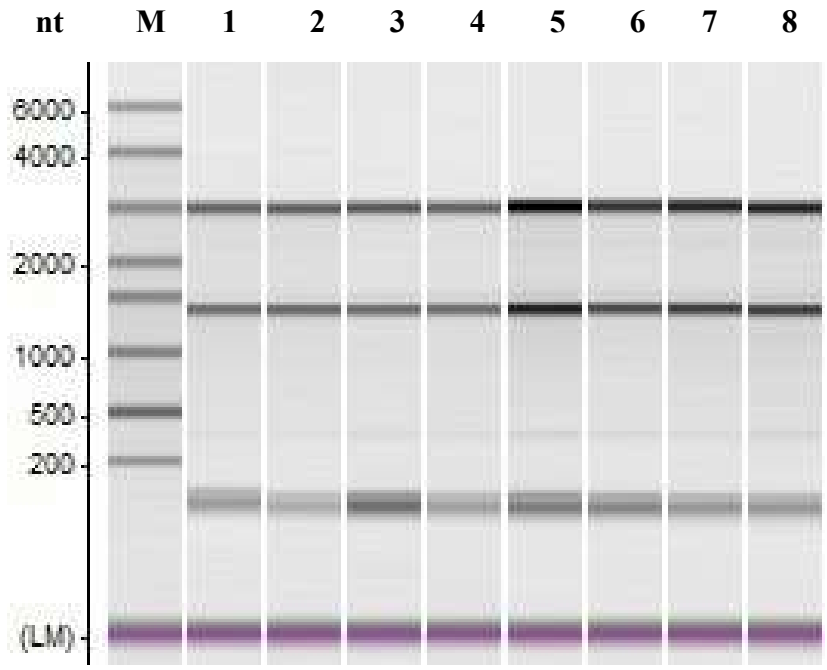

Figure 7.1: Analysis of the total RNA samples on a Shimadzu MultiNA microchip electrophoresis system. M = RNA marker

For capable RNA seq, first the RNA samples were enriched by capping the 5′ triphosphorylated RNA with 3′-desthiobiotin-TEG-guanosine 5′ triphosphate (DTBGTP) (NEB). For reversible binding of biotinylated RNA species to streptavidin vaccinia capping enzyme (VCE) (NEB) was used. And elution step was performed to capture the biotinylated species to streptavidin and obtain the 5' fragments of the primary transcripts.

Table: 7.4. Sample information for RNA-seq (from Vertis technologies)

Sample name	Barcode i5	Sequence file (R1/R2 in case of PE	Number of Read
PAO1-01-minusT	ATTAGACG	PAO1-01-Cap_S11_R1_001.fastq.gz	11.160.550
PAO1-02-minusT	CGGAGAGA	PAO1-02-Cap_S12_R1_001.fastq.gz	10.141.937
PAO1-52-minusT	CTAGTCGA	PAO1-52-Cap_S13_R1_001.fastq.gz	13.728.521
PAO1-53-minusT	CTTAATAG	PAO1-53-Cap_S14_R1_001.fastq.gz	17.115.224
PA2604-IS-01-minusT	ATAGCCTT	PA2604-IS-01-Cap_S15_R1_001.fastq.gz	7.618.125
PA2604-IS-02-minusT	TAAGGCTC	PA2604-IS-02-Cap_S16_R1_001.fastq.gz	21.756.300
PA2604-IS-51-minusT	TCGCATAA	PA2604-IS-51-Cap_S17_R1_001.fastq.gz	21.597.390
PA2604-IS-52-minusT	AGTCTTCT	PA2604-IS-52-Cap_S18_R1_001.fastq.gz	21.074.901

Summary of Sequencing run:
The NGS library pool was analysed on a Shimadzu MultiNA microchip electrophoresis system.
Cluster(PF) 405.827.653
% Index 94,9
Total Reads 457.487.654
Reads ident. 385.129.516
% Cluster 88,7

Table: 7.5. Sample information for RNA-seq (from Vertis technologies)

Sample name	Barcode i5	Sequence file (R1/R2 in case of PE	Number of Read
PAO1-01-Cap	ATTAGACG	PAO1-01-Cap_S11_R1_001.fastq.gz	17.653.416
PAO1-02-Cap	CGGAGAGA	PAO1-02-Cap_S12_R1_001.fastq.gz	20.556.173
PAO1-5.2-Cap	CTAGTCGA	PAO1-52-Cap_S13_R1_001.fastq.gz	21.059.039
PAO1-5.3-Cap	CTTAATAG	PAO1-53-Cap_S14_R1_001.fastq.gz	21.533.521
PA2604-IS-01-Cap	ATAGCCTT	PA2604-IS-01-Cap_S15_R1_001.fastq.gz	20.837.183
PA2604-IS-02-Cap	TAAGGCTC	PA2604-IS-02-Cap_S16_R1_001.fastq.gz	20.565.312
PA2604-IS-51-Cap	TCGCATAA	PA2604-IS-51-Cap_S17_R1_001.fastq.gz	18.083.533
PA2604-IS-52-Cap	AGTCTTCT	PA2604-IS-52-Cap_S18_R1_001.fastq.gz	19.552.189

Summary of Sequencing run:

The NGS library pool was analysed on a Shimadzu MultiNA microchip electrophoresis system.
Cluster(PF) 430.061.763
% Index 95,9
Total Reads 471.674.507
Reads ident. 412.355.367
% Cluster 91,2

Two different aliquots of RNA samples were then treated with Ribo-Zero rRNA kit for bacteria (Illumina) to deplete the ribosomal RNA. These RNA samples were then used for cDNA library preparation. In brief, the RNA sampleas were poly(A) tailed using poly(A) polymerase. The 5′ triphosphate or CAP were then removed by pyrophosphatase (Cellsript) and an RNA adapter was ligated to the 5′ monophosphate end of RNAs. cDNA synthesis was performed using the oligo (dT)-adapter primer and M-MLV reverse transcripase. The resultant cDNA was then PCR amplified by up to 13 cycle to yield about 10-20 nm/µl using high fidelity polymerase. The cDNA pool for Illumina NextSeq sequencing was generated by taking equimolar cDNA samples followed by elution of samples to a size range of 200-500 bp from preparative agarose gel. The size fractionation was confirmed by capilary gel electrophoresis. The True-seq primers designed following the illumine instructions were used for the sequencing. The cDNA pools were sequenced on an Illumina NextSeq 500 system using 75 bp read length.

Preparation of chemically competent cells (P. aeruginosa) cells using $MgCl_2$.

P. aeruginosa PAO1 cells were inoculated from frozen stock in LB agar (Appendix A) at 37ºC for 24 h. An overnight culture was started from isolated colony in 5 ml LB broth (Appendix A) at 37 °C for ~ 16hrs with shaking at 200 rpm. 1.25 ml of overnight culture was inoculated into the 250 ml LB in 500 ml Erlenmeyer flask and incubated at 37ºC with shaking at 200 rpm. After

approximately 3.5 – 4h at an A600 of 0.5-0.6, the culture was transferred to 250 ml centrifuge bottle and chilled on ice to 4 °C for 10 min. The cells were then centrifuged at 6,000 g for 5 min at 4 °C and supernatant was discarded completely. Cell pellet was washed twice with ice cold 150 mM $MgCl_2$, first with 250 ml and finally with 125 ml. Cell pellets were resuspended in 125 ml of ice cold 150 mM $MgCl_2$ followed by incubation on ice with gentle shaking for 1h. Cells were harvested by centrifugation at 6,000 g for 5 min at 4 ºC. Cell pellet was finally resuspended in 10 ml ice cold 150 mM $MgCl_2$ containing 15% glycerol and mixed gently. The cells were prepared as 500 µl aliquots in sterile microfuge tubes and incubated at 4 ºC for 12-24h. The competent cells were flash frozen by storing for 1h in pre-chilled ethanol -80 ºC. Cells were then stored at -80 ºC until use.

Preparation of electrocompetent cells (P. aeruginosa).

PAO1 cells were grown in 5 ml of LB broth (Appendix A) for ~ 14 hours. Cells were divided in four microcentrifuge tubes in 1.5 ml aliquots and harvested by centrifugation for 2 min at 13,000 rpm at room temperature. Each cell pellet was washed twice with 1 ml of 300 mM sucrose at room temperature (RT). Two pellets were combined in a total of 100 µl 300 mM sucrose. Competent cells were stored at RT until transformed with plasmid DNA (388)

Electroporation of electro-competent P. aeruginosa cells.

For electroporation, 300-500ng of non-replicative plasmid DNA was added to previously described 100 µl of electrocompetent cells and transfer to a 2 mm gap width electroporation cuvette kept at R.T. A pulse at settings: 25 µF; 200 Ohm; 2.5 kV (Setting EC2) was applied on to a Bio-Rad Gene Pulser X cell™.

Preparation of chemically competent cells (E. coli DH5α) using $CaCl_2$.

E. coli DH5α cells were inoculated in 5 ml of LB broth from a frozen glycerol stock and incubated for ~ 14 hours at 37 °C with shaking at 200 rpm. The main culture was inoculated in 1 liter Erlenmeyer flask containing 500 ml LB and incubated at 37 ^{0}C with shaking at 200 rpm. After approximately 3.5 – 4h at an A600 of 0.5-0.6, the culture was transferred to 2 x 500 ml centrifuge bottles and chilled on ice for 10 min with shaking. The cells were then centrifuged at 6,000 g for 5 min at 4 °C and supernatant was discarded completely. Each pellet was resuspended in 125 ml ice cold 0.1 M $CaCl_2$ and combined into a single 500 ml centrifuge bottle. The resuspended cells were centrifuged at 6,000 g for 5 min at 4 ^{0}C. Cell pellet was resuspended in 250 ml ice cold 0.1 M $CaCl_2$ and chilled on ice for 30 min. Cell pellet was harvested by centrifugation at 6,000 g for 5 min at 4 ^{0}C. Post centrifugation, cell pellet was resuspended in 20 ml of ice cold buffer containing 0.1 M $CaCl_2$ and 15% glycerol. 100 µl of cells suspension was aliquoted in each chilled sterile microfuge tubes and stored at -80 ^{0}C.

Heat-shock transformation of E. coli DH5α CC.

DH5α heat-shock competent cells (prepared in lab) were thawed in ice during the ligation period. The whole ligated product was added to a tube of HSCC and mixed by gentle pipetting. This mixture was tncubated for 30 minutes in ice. Then the cells were exposed to heat shock at 42° C using a hot plate (or hot water bath) for 1.30 minute. The tubes were kept back into ice immediately after and incubated for 10 minutes. 1 ml of warm (pre heated LB at 37 °C) LB were added to the cells and the mixtures were then transferred to individual 15 ml glass tubes and incubated at 37°C for 1 hour. 100 µl of the cultures were spread-plated onto LB agar plates containing selective antibiotics.

Promoter prediction and construction of promoter activity reporter plasmid.

The promoter regions were either already defined at the beta.pseudomonas.com or was predicted by using promoter prediction tool BPROM. Usually 200-300 bp around the predicted promoter region was selected to be cloned into promoter activity reporter plasmid. The promoter less lux based reporter plasmid pMS402 was used for this.

Primers for promoter activity reporter plasmids were constructed on the both end of the selected intergenic region. The primers were flanked by six basepair long sequence to facilitate the restriction of the ends with corresponding restriction enzymes. The flanked region had sequence specific for recongnition by specific

restriction enzymes and three-four basepair for landing of restriction enzymes on the sequence. Primers were analyzed for melting temperature, GC content (45%-55%) as well as secondary structure formation ($\Delta G \geq 0$) by using OligoAnalyzer (IDT).

The promoter regions were amplified using pfx polymerase (Life technologies). The reaction mixtures constitute of, 2.5 µl of Pfx buffer, 10 mM dNTPs 0.75 µl, 50 mM MgSO4 0.5 µl, primers (10 µM) 0.3 µl each, DNA 100 ng to a total voleme of 25 µl of PCR mixtrure. The PCR was programmed as, 94 °C for 5 min (1 time), 30 cycles of 94 °C for 45 sec, annealing temperature for 40 sec and 72 ° C for 1.30 min, then one time 72°C for 10 min and finally incubated at 4° C. Amplicons were column purified by ( ). The right amplicons as well as empty vector pMS402 were digested with BamHI and xhoI restriction enzymes either in separate tubes or in a single tube with the molar ratio of 1:3 of vector and insert. Restriction digestion was performed using manufacturars protocol, where 5 µl of restriction buffer and 1 µl of each enzyme were added to 1 µg (volume may vary) of vector or insert in a total volume of reaction of 50 µl obtained by adding sterilized nanopure water. This reaction mixture was then incubated at 37 °C for overnight for complete digestion. Upon completion of the digestion process, the enzymes were first inactivated by incubating at 80 °C for 15 min. The vector only reaction mixture was then exposed to diphosphatase treatment by TSAP (Promega) using manufacturar's protocol. The TSAP was then deactivated at 74° C for 15 min. The

digested samples were column purified by…. And the concentration of the purified samples was measured using nanodrop 2000 (Thermofischer). Vector and insert were ligated at the molar ratio of 1:3 using quick ligase. 10 µl of quick ligase buffer and 1 µl of quick ligase was added to the vector-insert and the total volume was brought up to 20 µl by adding sterilized nanopure water. This mixture was incubated at room temperature for 15 min and the transformation was performed right after. The transformed cells after 1 hour of incubation at 37 °C was spread-plated onto LB agar with kanamycin (50µg/ml). These plates were incubated at 37° C for 12-16 hours. Only heat shock competenct cells and the cells transformed with digested-dephosphorylated (not ligated) vectors were spread-plated on LB agar plates containing kanamycin (50µg/ml) as negative controls for transformation. Isolated colonies on the transformant plates were selected and target gene (insert) specific colony PCR was performed to identify the transformant carrying the plasmid with successfully cloned insert. DH5α cells transformed with empty vector were used as a negative control, PAO1 was used as positive control and a non-inoculated control was included in the group to confirm the purity of the PCR ingredients.

Promoter activity assessment

pMS402 with a promoterless *luxCDABE* (82) reporter and pMSO4 with *luxABCDE* reporter under the specific promoters to be tested were transformed into

PAO1 as well as other bacterial strains (eg. PA2604:Tn5). To select the successfully transformed clones, trimethoprim resistant individual clones were tested for light production using 96 well clear bottom plates (Grenier bio one). For promoter activity assay, bacterial pre-cultures were grown for 12 hours in biofilm minimal media (BMM) with no added Ca^{2+} or 5mM Ca^{2+}. Normalized precultures (OD_{600} 0.3) were then inoculated at 1:100 ratio making the final OD_{600} of the starting culture to 0.003into 1 ml of BMM containing corresponding Ca^{2+} and with or without tobramycin at final concentration of 2.5 µg/ml of. 200µl of this solution was added to each well of 96 well clear bottom plates. Both cell density and the luminescence level were measured every 2 hours at 37°C, continuous shaking at fast shaking mode for 24 hours using Synergy MS microplate reader (Biotek). To measure the promoter activity of individual RND systems, luminescence readings were normalized by the absorbance of corresponding cultures and the luminescence produced by empty vector was subtracted from the luminescence produced by the vector containing corresponding RND promoter. At least 4 biological replicates were used for each strains used.

The data analyses followed the steps: 1) the averaged luminescence reading of non-inoculated controls was subtracted; 2) the luminescence at time 0 was subtracted from subsequent readings. The obtained luminescence readings were 3) normalized by the corresponding cell density and 4) averaged. 5) averaged normalized luminescence of the promoterless vector controls was subtracted from

that of the promoter carrying constructs, 6) fold change was calculated versus the condition when no Ca^{2+} or tobramycin were added. At each steps of data normalization, any negative values were replaced by the basal luminescence reading of empty vector at that point. At least 3 biological replicates in each experiment and 2 independent experiments were used.

Plant Infectivity Assay. Lettuce Leaf Assay.

The assay was performed with modification to the described method by (106).Fresh organic Romaine lettuce leaves from market (Walmart/ Food Pyramid) were purchased and healthy looking leaves from the core (do not use very young looking leaves) were detached. The leaves were then washed with 0.1% bleach and rinsed with distilled water (**Note: wear gloves during this step and during subsequent steps when handling leaves**). The excess leaf material was trimmed using scissors flamed with ethanol, from around the midrib and the midribs were placed in petri dish containing piece of Whatman no. 1 filter paper soaked in 10 mM $MgSO_4$ (**Note: one petri dish can contain up to two midribs if desired**). For Bacterial inoculation, bacteria were grown in 3 mL BMM at 37° for 16 hours at appropriate Ca^{2+} concentrations for 12 hours. The cultures were then harvested and 1.5 mL of culture was centrifuged at 13000X for 6 min. (add volume if pellet is not easily visible) The pellet was then washed with 10mM $MgSO_4$ of corresponding Ca^{2+} concentration. The cultures were resuspended in 10mM $MgSO_4$ (of

appropriate Ca^{2+} concentration) and diluted to an OD_{600} of 0.1. These cultures were then inoculated into the midribs with 10 µL of culture ~15 mm from one end and 10 µL of $MgSO_4$ ~15 mm from the other end (at appropriate Ca^{2+} concentration). The petri dishes containing inoculated midribs were kept at room temperature in the sunlight in clear plastic bins with water added to the bottom. The zone of necrosis was recorded for each midrib, measuring length and width of the zone. The following color intensity value was assigned to the necrosis zone.

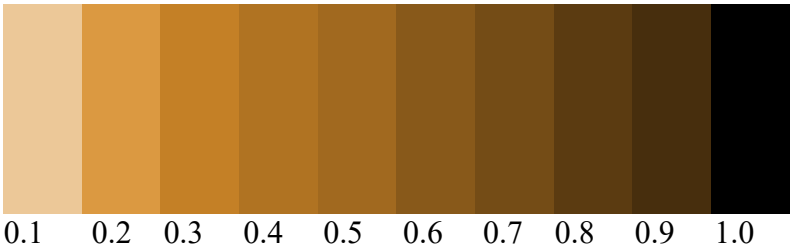

C. elegans Killing Assay

Maintenance: *C elegans* N2 bristol wild type strain was received on a NGM plates. Worms supplied were fed on E coli OP50 strain. The bacteria from the monoxenic C elegans culture were streaked onto an LB plate and one single clone was inoculated into LB broth over -night culture. 100 µl of the overnight culture was inoculated(seeded) onto NGM plates and were left to grow overnight at 37°C (The plates were dried before putting into 37°C incubator. The plates after 24 hours of growth of bacteria on to it, were then supplied with chunk of agar from the original NGM plates containing the worms. 5 plates were inoculated and the

plates were kept at RT (upside-up position) for the spread and growth of *C elegans* worms.

Frogen stock preparation: According to the literature (Maintenance of *C elegans*,wormbook.org) the L1 and L2 stage of larvae are the best one to keep at -80°C freezer for longer period. An NGM plate with hatched L1, L2 larvae of C elegans was selected. The plates were rinsed superficially with S buffer and the solute were collected into cryovials containing 50% of 30%glycerol (500µl S buffer containing larvae+ 500µl of 30% glycerol). The cryovials then were placed into container box inside a sterofoam box. The stereofoam box was kept in -80 to allow gradual freezing. The container box was taken out of the sterofoam box after 7 days and kept on the shelf of -80 freezer.

Slow Killing assay

Slow killing assay was performed using *C elegans* wild tpe N2 bristol strain and temperature sensitive sterile mutant CF-512 (fer-15(b26) II (CGC). In order to identify the role of Ca2+ in virulence of *Pseudomonas aeruginosa*, PAO1, bacterial lawn was grown on NGM agar plates with no added Ca^{2+} and 5 mM Ca2+. Previously well grown adult gravid worms were used for worm synchronization. Gravid worms were washed off the worm plate with M9W buffer and 100µl of 5N NaOH and 400µl of household bleach were added to the worms to lyse open the worms and release the eggs. The mixture was vigorously vortexed for no more than

4 min and 14ml of M9W buffer was added to the solution after 4 min. The eggs were washed three times with M9W buffer and resuspended into 5 ml of M9W buffer. The 15 ml falcon tubes containing the eggs were placed in a shaker at 200 rpm and room temperature (25°C) for 12 hours. Synchronized L1 stage larvae were transferred to NGM agar plates provided with E coli OP50. The worms were grown for 34 hours until they reach the young adult stage. 30-40 Young adult worms were then seeded in to the slow killing assay plates; NGM agar with bacterial lawn on it at 0mM and 5mM Ca2+. Dead worms were scored every 12 hours.

Fruit fly Maintenance

D. melanogaster (OR) flies were maintained in foam plugged plastic 250 mL Erlenmeyer flasks (VWR). Standard cornmeal fly medium (28 g dried brewer's yeast, 77 g cornmeal (Sigma), 27 g sucrose, 53 g glucose, 3.5 mL propionic acid, 0.3 mL 85 % phosphoric acid and 6 g select agar (VWR) per liter) was used for regular maintenance of the fly. The adult flies were transferred to new vials containing fresh medium every 5-7 days to allow continuation of progeny with healthy and viable fruitflies.

Fruitfly Killing assay

To assess the role of Ca^{2+} in virulence caused by *P. aeruginosa*, *Drosophyla melanogaster* infection models was used. For fly feeding assays, sucrose agar (1.2

g Bacto-agar (Difco), 14 mL 20% sucrose and 41 mL sterile distilled water) was used. Fly synchronization was done prior to each feeding assay was performed (382, 385). In brief, the adult flies from fly maintenance vial were transferred at least twice at two days interval and the same age larvae were left to grow. 2 day old synchronized flies were finally transferred to a new fly maintenance vial and left overnight. The flies were separated into polystyrene fly vials (Applied Scientific) and starved for 6 hours before separating and transferring the synchronized male flies to the assay vials. Simultaneously, the bacterial precultures were harvested at the 16th hour and the OD_{600of} the culture was normalized to 3.0 by resuspending the bacterial pellet into 200 µl of 5% sucrose prepare with the corresponding media at which the bacteria was grown. The normalized culture was then inoculated onto fly vials containing 2.3 cm whatman filter disk placed on top of sucrose agar (5% sucrose and 2.2% select agar). The assay vials inoculated with only 5% sucrose were used as negative controls. Starved synchronized male flies were transferred to the sucrose feeding vials containing the bacterial suspensions and incubated at 25ºC. Dead flies were scored daily for 14 days.

Data analysis for Fly Killing assay (PRISM).

The survival curve for fruitfly infection model was performed by Kaplan Meyer analysis of the data was performed using PRISM 3.0.

Gene complementation

For Genetic complementation, mini TN7-GM-eyfP was used and the cloning, transformation and transformed bacteria selection was perfomed according to (388). At first, primers were designed flanking the start and end site of PA2604 gene. Forward primer and reverse primer was had six bp long overhangs with sequence specific for HindIII and SacI restriction sites respectively along with extra 3-4 bases to facilitate landing of the restriction enzymes. Primers were analyzed for compatibility, secondary structure formation as well as GC content (as described in the promoter activity reporter plasmid construction section). It was made sure that the primers had no more than 5° C temperature difference between them. Also, for gene tic complementation, it was essential to amplify and clone the sequence "in frame" to keep the genetic signature intact.

To amplify the product gradient PCR using phusion polymerase (NEB) was used. The amplicons of correct size were restricted from gel and purified by QIAquick Gel extraction kit (Qiagen). The purified amplicons as well as vector containing the mini TN7 plasmid, pUC18T-miniTN7-GM-e*yfP* were subjected to restriction digestion, dephosphorylation of vector, inactivation of enzymes, column purification as well as 15 min ligation by quick ligase (NEB) as described before in promoter activity reporter construct section of the methodology. The ligated plasmids were then transformed into *E. coli* DH5α competent cells by heat shock transformation and transformants were selected on LB agar plates with 100 µg/ ml

of ampicillin. Colony PCR was performed to identify individual clones carrying the insert for PA2604 gene. For this plasmid specific primer **(Table 7.2.)** right up and down of the insert was used to confirm the presence of the gene was in the transposon.

Upon successful identification of individual colonies with PA2604 insert in them, the plasmids were purified and exposed to restriction analysis where the purified plasmids were digested with HindIII and SacI. Presence of two bands corresponding to the vector and insert further confirmed the successful cloning of the insert into the vector. Empty vector was used as a control.

The plasmid construct was then sent to OSU sequencing core facility to sequence the insert using the plasmid specific primer (table…). The received sequence was then aligned to the original FASTA sequence of the gene using Clustal Omega tool available online (website: http://www.ebi.ac.uk/Tools/msa/clustalo/). The plasmid construct with the insert aligning to the original sequence 100% was then finalized for incorporation into *P. aeruginos*a genome.

The finalized plasmid construct pUC18T-GM-PA2604-*eyfP* (pSK231) combined with pTNS1 (total 1 µg maximum) were electroporated into PAO1 electrocompetent cells as described in (ref). pTNS1 carries the gene for transposase that enables the miniTN7 plamid jump into *P. aeruginosa* genome in a site directed

manner up of *glmS* gene. The transformants were selected on LB agar plates containing gentamycin at the concentration of 30 µg/ml. The final individual clones (15- 20 of them) were then transferred to LB agar plates containing 30 µg/ml of gentamycin and 5% of sucrose to get rid of the plasmid since the mini TN7 was expected to be incorporated into P. aeruginosa genome. pUC18T-GM-eyfP plasmid has the sacB gene which makes the transformant P. aeruginosa intolerant to sucrose, thus adding sucrose as a carbon source on the agar plate help removal of the plasmid once but having gentamycin as a selective antimicrobial on the plate will allow the growth of the transformants those had minTN7-GM-PA2604-eyfP already incorporated into the genome. The gene was cloned into the transposon in frame and under the constitutively active modified promoter $P_{A1/04/03}$.

Sequence analysis for complemented gene.

CLUSTAL multiple sequence alignment by MUSCLE (3.8)

PA2604cl3. ----------ATGGAACTTCCGGCCGTTCGCGG-ACAGCGTGAAGTCAGC

gb|AE004091.2|:2947803-2948471|P ATGCAAGAACAGCAATATCAGCTGAACT--CCGCCG-

TCGCGGAACAGCGTGAAGTCAGC

PA2604cl19. ----------AGTTGAAACTCCCGCCG-TCGCGG-ACAGCGTG-AGTCAGC

*** * **** ****** ******** *******

PA2604cl3.

GGCGTTCTGCGCAATACCTACGGCCTGCTGGCACTCACCCTGGCCTTCAGCGGCCTGGTG

gb|AE004091.2|:2947803-2948471|P

GGCGTTCTGCGCAATACCTACGGCCTGCTGGCACTCACCCTGGCCTTCAGCGGCCTGGTG

PA2604cl19.

GGCGTTCTGCGCAATACCTACGGCCTGCTGGCACTCACCCTGGCCTTCAGCGGCCTGGTG

****

PA2604cl3.

GCCTACGTTTCGCAGCAGATGCGCCTGCCCTATCCGAACGTGTTCGTGGTGCTGATCGGC

gb|AE004091.2|:2947803-2948471|P

GCCTACGTTTCGCAGCAGATGCGCCTGCCCTATCCGAACGTGTTCGTGGTGCTGATCGGC

PA2604cl19.

GCCTACGTTTCGCAGCAGATGCGCCTGCCCTATCCGAACGTGTTCGTGGTGCTGATCGGC

****

PA2604cl3.

TTCTACGGCCTGTTCTTCCTCACCGTGAAGCTGCGCAACAGCGCCTGGGGTCTGGTCAGC

gb|AE004091.2|:2947803-2948471|P

TTCTACGGCCTGTTCTTCCTCACCGTGAAGCTGCGCAACAGCGCCTGGGGTCTGGTCAGC

PA2604cl19.

TTCTACGGCCTGTTCTTCCTCACCGTGAAGCTGCGCAACAGCGCCTGGGGTCTGGTCAGC

****

PA2604cl3.

ACTTTCGCCCTGACCGGCTTCATGGGCTACACGCTCGGCCCGATCCTCAACATGTACCTC

gb|AE004091.2|:2947803-2948471|P

ACTTTCGCCCTGACCGGCTTCATGGGCTACACGCTCGGCCCGATCCTCAACATGTACCTC

PA2604cl19.

ACTTTCGCCCTGACCGGCTTCATGGGCTACACGCTCGGCCCGATCCTCAACATGTACCTC

****

PA2604cl3.

GGCCTGCCCAACGGCGGCAGCGTCATCACTTCGGCGTTCGCCATGACCGCCCTGGTGTTC

gb|AE004091.2|:2947803-2948471|P

GGCCTGCCCAACGGCGGCAGCGTCATCACTTCGGCGTTCGCCATGACCGCCCTGGTGTTC

PA2604cl19.

GGCCTGCCCAACGGCGGCAGCGTCATCACTTCGGCGTTCGCCATGACCGCCCTGGTGTTC

****

PA2604cl3.

TTCGGCCTGTCCGCCTATGTGCTGACCACCCGCAAGGACATGAGCTTCCTGTCCGGCTTC

gb|AE004091.2|:2947803-2948471|P

TTCGGCCTGTCCGCCTATGTGCTGACCACCCGCAAGGACATGAGCTTCCTGTCCGGCTTC

PA2604cl19.

TTCGGCCTGTCCGCCTATGTGCTGACCACCCGCAAGGACATGAGCTTCCTGTCCGGCTTC

****

PA2604cl3.

ATCACCGCCGGCTTCTTCGTCCTGCTGGGCGCCGTGCTGGTATCGCTGTTCTTCCAGATC

gb|AE004091.2|:2947803-2948471|P

ATCACCGCCGGCTTCTTCGTCCTGCTGGGCGCCGTGCTGGTATCGCTGTTCTTCCAGATC

PA2604cl19.

ATCACCGCCGGCTTCTTCGTCCTGCTGGGCGCCGTGCTGGTATCGCTGTTCTTCCAGATC

****

PA2604cl3.

AGTGGCCTGCAACTGGCGATCAGCGCCGGCTTCGTCCTGTTCTCCTCGGCGATGATCCTC

gb|AE004091.2|:2947803-2948471|P

AGTGGCCTGCAACTGGCGATCAGCGCCGGCTTCGTCCTGTTCTCCTCGGCGATGATCCTC

PA2604cl19.

AGTGGCCTGCAACTGGCGATCAGCGCCGGCTTCGTCCTGTTCTCCTCGGCGATGATCCTC

****

PA2604cl3.

TACCAGACCAGCGCGATCATCCACGGCGGCGAACGCAACTACATCATGGCCACCATCAGC

gb|AE004091.2|:2947803-2948471|P

TACCAGACCAGCGCGATCATCCACGGCGGCGAACGCAACTACATCATGGCCACCATCAGC

PA2604cl19.

TACCAGACCAGCGCGATCATCCACGGCGGCGAACGCAACTACATCATGGCCACCATCAGC

****

PA2604cl3.

CTGTACGTGTCGATCTACAACCTGTTCATCAGCCTGTTGCAGATCTTCGGCATCGCCGGC

gb|AE004091.2|:2947803-2948471|P

CTGTACGTGTCGATCTACAACCTGTTCATCAGCCTGTTGCAGATCTTCGGCATCGCCGGC

PA2604cl19.

CTGTACGTGTCGATCTACAACCTGTTCATCAGCCTGTTGCAGATCTTCGGCATCGCCGGC

****

PA2604cl3.

GGCGACGACTGAGAGCTCATGCATGATCGAATTAGCTTCAAAAGCGCTCTGAAGTTCCTA

gb|AE004091.2|:2947803-2948471|P GGCGACGACTGA----------

PA2604cl19.

GGCGACGACTGAGAGCTCATGCATGATCGAATTAGCTTCAAAAGCGCTCTGAAGTTCCTA

****

PA2604cl3.

TACTTTCTAGAGAATAGGAACTTCGGAATAGGAACTTCAAGATCCCCTGATTCCCTTTGT

gb|AE004091.2|:2947803-2948471|P ----------

PA2604cl19.

TACTTTCTAGAGAATAGGAACTTCGGAATAGGAACTTCAAGATCCCCTGATTCCCTTTGT

PA2604cl3.

CAACAGCAATGGATCGAATTGACATAAGCCTGTTCGGTTCGTAAACTGTAATGCAAGTAG

gb|AE004091.2|:2947803-2948471|P ----------

PA2604cl19.

CAACAGCAATGGATCGAATTGACATAAGCCTGTTCGGTTCGTAAACTGTAATGCAAGTAG

PA2604cl3.

CGTATGCGCTCACGCAACTGGTCCAGAAACCTTGACCGAACGCAGCGGTGGTAACGGCGC

gb|AE004091.2|:2947803-2948471|P ----------

PA2604cl19. CGTATGCGCTCACGCAACTGGTCCAG-

AACCTTGACCGAACGCAGCGGTGGTAACGGCGC

PA2604cl3.

AGTGGCGGTTTTCATGGCTTGTTATGACTGTTTTTTTTGTACAGTCTATGCCTCGGGCAT

gb|AE004091.2|:2947803-2948471|P ----------

PA2604cl19. AGTGGCGGTTTTCATGGCTTGTTATGACTG-

TTTTTTTGTACAGTCTATGCCCTCGGGCA

PA2604cl3.

CCCAAGCAGCAAGCGCGTTACGCCGTGGGTCGATGTTTGATGTTATGGGAGCAGCAACGA

gb|AE004091.2|:2947803-2948471|P ----------

PA2604cl19. TCCAAGCAGCAAGCGCGTTACGCCGT-

GGTCGATGTTTGATGTTTTGGAAGCAGCACGAT

PA2604cl3. TGTTACGCAGCAGCCAACGATGTTACGCCAGCAAGGCAAGTCGCCCTTAAAA--

CAAAGT

gb|AE004091.2|:2947803-2948471|P ----------

PA2604cl19. GTTTACGCAGCAG-

CAACGATGTTTACGCAAGCAGGCAGTCGGCCCTTAAAAACAAAGGT

PA2604cl3. TAGTTGCTTCAAAGTTATGGGCATCATTTCGCACCATGTAG--

CTCGGACCTGACCAAAG

gb|AE004091.2|:2947803-2948471|P ----------

PA2604cl19. TAGGTGGCTCAAGGT--

ATGGCATCATTTCGGCACATGGTAGCCTCGGTCCCTTGACCAG

PA2604cl3. TCCAATCC--

ATGCGGCCTTGCTCCTTGATCTTTTCGGTCGTGAAGTTCCGGAGACGTAA

gb|AE004091.2|:2947803-2948471|P ----------

PA2604cl19. TCAAATTCCAATGCGGACTGCTCTTTGAATCTTTTCGGTCTGGAG---

TCGGAAACGTAG

PA2604cl3. -CCACCTACTTCCAAAATCAGTGCGTAC--

CCGATATCCTCGGGGAACTCTTGGTCCTAC

gb|AE004091.2|:2947803-2948471|P ----------

PA2604cl19.

CCCACCTACCTCCCAACTCCATCAGTACCTCCGATAACCTTCCGGAAACCTTGGCCTCTC

PA2604cl3. GTTA-

gb|AE004091.2|:2947803-2948471|P -----

PA2604cl19. CCGGT

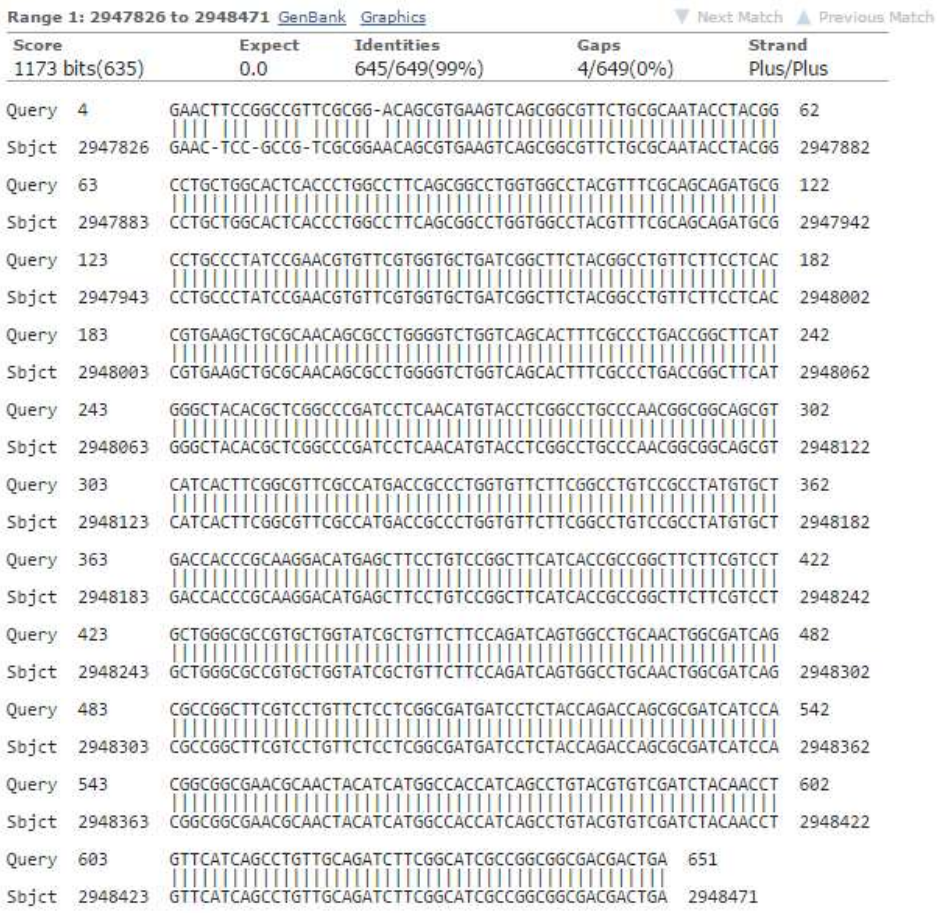

The co-ordinates in Pseudomonas.com: 2947803 – 2948471

LUSTAL multiple sequence alignment by MUSCLE (3.8)

PA2604cl19R. CCGAATGCCA----GTGCGAGACTTG--------CACAGGCTGATG-ACAGGTTGTAGAT

gb|AE004091.2|:2947803-2948471|P

TCAGTCGTCGCCGCCGGCGATGCCGAAGATCTGCAACAGGCTGATGAACAGGTTGTAGAT

PA2604cl3R. CCCGGGGCCA-----GGCGAGACTG---------CACAGGCTGATGAACAGGTTGTAGAT

* * * **** * *********** ************

PA2604cl19R.

CGACACGTACAGGCTGATGGTGGCCATGATGTAGTTGCGTTCGCCGCCGTGGATGATCGC

gb|AE004091.2|:2947803-2948471|P

CGACACGTACAGGCTGATGGTGGCCATGATGTAGTTGCGTTCGCCGCCGTGGATGATCGC

PA2604cl3R.

CGACACGTACAGGCTGATGGTGGCCATGATGTAGTTGCGTTCGCCGCCGTGGATGATCGC

****

PA2604cl19R.

GCTGGTCTGGTAGAGGATCATCGCCGAGGAGAACAGGACGAAGCCGGCGCTGATCGCCAG

gb|AE004091.2|:2947803-2948471|P

GCTGGTCTGGTAGAGGATCATCGCCGAGGAGAACAGGACGAAGCCGGCGCTGATCGCCAG

PA2604cl3R.

GCTGGTCTGGTAGAGGATCATCGCCGAGGAGAACAGGACGAAGCCGGCGCTGATCGCCAG

****

PA2604cl19R.

TTGCAGGCCACTGATCTGGAAGAACAGCGATACCAGCACGGCGCCCAGCAGGACGAAGAA

gb|AE004091.2|:2947803-2948471|P

TTGCAGGCCACTGATCTGGAAGAACAGCGATACCAGCACGGCGCCCAGCAGGACGAAGAA

PA2604cl3R.

TTGCAGGCCACTGATCTGGAAGAACAGCGATACCAGCACGGCGCCCAGCAGGACGAAGAA

****

PA2604cl19R.

GCCGGCGGTGATGAAGCCGGACAGGAAGCTCATGTCCTTGCGGGTGGTCAGCACATAGGC

gb|AE004091.2|:2947803-2948471|P

GCCGGCGGTGATGAAGCCGGACAGGAAGCTCATGTCCTTGCGGGTGGTCAGCACATAGGC

PA2604cl3R.

GCCGGCGGTGATGAAGCCGGACAGGAAGCTCATGTCCTTGCGGGTGGTCAGCACATAGGC

****

PA2604cl19R.

GGACAGGCCGAAGAACACCAGGGCGGTCATGGCGAACGCCGAAGTGATGACGCTGCCGCC

gb|AE004091.2|:2947803-2948471|P

GGACAGGCCGAAGAACACCAGGGCGGTCATGGCGAACGCCGAAGTGATGACGCTGCCGCC

PA2604cl3R.

GGACAGGCCGAAGAACACCAGGGCGGTCATGGCGAACGCCGAAGTGATGACGCTGCCGCC

****

PA2604cl19R.

GTTGGGCAGGCCGAGGTACATGTTGAGGATCGGGCCGAGCGTGTAGCCCATGAAGCCGGT

gb|AE004091.2|:2947803-2948471|P

GTTGGGCAGGCCGAGGTACATGTTGAGGATCGGGCCGAGCGTGTAGCCCATGAAGCCGGT

PA2604cl3R.

GTTGGGCAGGCCGAGGTACATGTTGAGGATCGGGCCGAGCGTGTAGCCCATGAAGCCGGT

****

PA2604cl19R.

CAGGGCGAAAGTGCTGACCAGACCCCAGGCGCTGTTGCGCAGCTTCACGGTGAGGAAGAA

gb|AE004091.2|:2947803-2948471|P

CAGGGCGAAAGTGCTGACCAGACCCCAGGCGCTGTTGCGCAGCTTCACGGTGAGGAAGAA

PA2604cl3R.

CAGGGCGAAAGTGCTGACCAGACCCCAGGCGCTGTTGCGCAGCTTCACGGTGAGGAAGAA

****

PA2604cl19R.

CAGGCCGTAGAAGCCGATCAGCACCACGAACACGTTCGGATAGGGCAGGCGCATCTGCTG

gb|AE004091.2|:2947803-2948471|P

CAGGCCGTAGAAGCCGATCAGCACCACGAACACGTTCGGATAGGGCAGGCGCATCTGCTG

PA2604cl3R.

CAGGCCGTAGAAGCCGATCAGCACCACGAACACGTTCGGATAGGGCAGGCGCATCTGCTG

****

PA2604cl19R.

CGAAACGTAGGCCACCAGGCCGCTGAAGGCCAGGGTGAGTGCCAGCAGGCCGTAGGTATT

gb|AE004091.2|:2947803-2948471|P

CGAAACGTAGGCCACCAGGCCGCTGAAGGCCAGGGTGAGTGCCAGCAGGCCGTAGGTATT

PA2604cl3R.

CGAAACGTAGGCCACCAGGCCGCTGAAGGCCAGGGTGAGTGCCAGCAGGCCGTAGGTATT

****

PA2604cl19R.

GCGCAGAACGCCGCTGACTTCACGCTGTTCCGCGACGGCGGAGTTCAGCTGATATTGCTG

gb|AE004091.2|:2947803-2948471|P

GCGCAGAACGCCGCTGACTTCACGCTGTTCCGCGACGGCGGAGTTCAGCTGATATTGCTG

PA2604cl3R.

GCGCAGAACGCCGCTGACTTCACGCTGTTCCGCGACGGCGGAGTTCAGCTGATATTGCTG

****

PA2604cl19R.

TTCTTGCATAAGCTTATTACTTGTACAGCTCGTCCATGCCGAGAGTGATCCCGGCGGCGG

gb|AE004091.2|:2947803-2948471|P TTCTTGCAT----------

PA2604cl3R.

TTCTTGCATAAGCTTATTACTTGTACAGCTCGTCCATGCCGAGAGTGATCCCGGCGGCGG

****

PA2604cl19R.

TCACGAACTCCAGCAGGACCATGTGATCGCGCTTCTCGTTGGGGTCTTTGCTCAGGGCGG

gb|AE004091.2|:2947803-2948471|P ----------

PA2604cl3R.

TCACGAACTCCAGCAGGACCATGTGATCGCGCTTCTCGTTGGGGTCTTTGCTCAGGGCGG

PA2604cl19R.

ACTGGTAGCTCACGTAGTGGTTGTCGGGCAGCAGCACGGGGCCGTCGCCGATGGGGGTGT

gb|AE004091.2|:2947803-2948471|P ----------

PA2604cl3R.

ACTGGTAGCTCAGGTAGTGGTTGTCGGGCAGCAGCACGGGGCCGTCGCCGATGGGGGTGT

PA2604cl19R.

TCTGCTGGTAGTGGTCGGCGAGCTGCACGCTGCCGTCCTCGATGTTGTGGCGGATCTTGA

gb|AE004091.2|:2947803-2948471|P ----------

PA2604cl3R.

TCTGCTGGTAGTGGTCGGCGAGCTGCACGCTGCCGTCCTCGATGTTGTGGCGGATCTTGA

PA2604cl19R.

AGTTCACCTTGATGCCGTTCTTCTGCTTGTCGGCCATGATATAGACGTTGTGGCTGTTGT

gb|AE004091.2|:2947803-2948471|P ----------

PA2604cl3R.

AGTTCACCTTGATGCCGTTCTTCTGCTTGTCGGCCATGATATAGACGTTGTGGCTGTTGT

PA2604cl19R. AGTTGTACTCCAGCTTGTGCCCC-

AGGATGTTGCCGTCCTCCTTGAAGTCGATGCCCTTC

gb|AE004091.2|:2947803-2948471|P ----------

PA2604cl3R.

AGTTGTACTCCAGCTTGTGCCCCAAGGATGTTGCCGTCCTCCTTGAAGTCGATGCCCTTC

PA2604cl19R. AGCTCGATGCGGTTCACCA--

GGTGTCGCCCCTCGAACTTCACTTCGGCGCGGGTCTTTG

gb|AE004091.2|:2947803-2948471|P ----------

PA2604cl3R.

AGCTCGATGCGGGTCACCAAGGGTGTCGCCCCTCGAACTTCACCTCGGCCGCGGGTCCTG

PA2604cl19R. TAGTGCC--GTCGTCTTGA--GAAGATGCTGCGCTCCTGACGTAGCTCCGGCATG---

CG

gb|AE004091.2|:2947803-2948471|P ----------

PA2604cl3R.

TAGTGCCCGTTCGTCCTGAAGAAAGATGTTGCGCTCTGAACGTAGCTCCGGCAATGGCCG

PA2604cl19R. GACTTGAAGA--GTCATGCTGCCTCATG-----TGGCTCAGTAGCGTCCAGCACTGCAGG

gb|AE004091.2|:2947803-2948471|P ----------

PA2604cl3R.

AACCTGAAGAAGGTCCTGCCTGCTCATGGTCATCGGGTAGCCGATCGAAGGCACTGCAGG

PA2604cl19R. --CGTAGCGAAAGGGTGGTCCACAC----AATG

gb|AE004091.2|:2947803-2948471|P ----------

PA2604cl3R. ACCGTAGACGAAAGCTGGCTCACACACGAAATG

Membrane permeability assay

In order to assess the effect of Ca^{2+} in modification of outermembrane , membrane permeability assay was performed according to loh *et al* (390) with modifications. Fort his first Bacterial cells were grown in 3 ml of BMM without any added Ca^{2+} for 12 hours at 37º C and 200 rpm using the floor shaker incubator. At 12^{th} hour the OD_{600} of the culture was measured and normalized to 0.1. 100µl

od normalized culture was added to 100 ml of corresponding media (1:1000) in ehrlmyer flasks and was incubated at 37º C and 200 rpm till middle log (Both time and OD_{600} was considered). 40 ml of this culture was taken into 50 ml falcon tubes and was washed with HEPES buffer (pH 7.2) at 4200 rpm for 5 min at room temperature. The cell pellets were resuspended into 3ml of the buffer. OD_{600} of this cell suspension was measured and normalized to OD600 of 0.5. 100 µl of normalized cell suspension was added to each well of 96 well clear bottom black plates. 4 replicates of non-inoculated buffer controls were also added to the wells. Then the cell density was measured at 600nm and fluorescence was measured at 350/420 excitation/ emission. Then 50 ml of 30 µM 1-N-Phenylenaphthylamine, NPN (sigma) was added to each well including the non-inoculated controls followed by cell density and fluorescence measurement. Finally, 50 µl of 20 mM Ca2+ or 1 µg/ml polymyxin-B was added to the wells to determine the effect of the added molecules on change in fluorescence level. The cell density as well as fluorescence was measured the same way as above. Data analysis was performed as follows: 1. The average readings of non-inoculated samples were subtracted from each set of readings for the experimental. 2. The fluorescent readings were divided by the OD_{600} of corresponding wells. 3. Normalized fluorescence of cells only (before adding NPN to the solution) was subtracted from the fluorescence reading of the cells after adding NPN as well as that of the cells after adding the Ca^{2+} or Pol-B. The changes in the fluorescence was observed by plotting the

fluorescence level before and after adding the Ca^{2+} and Pol-B. A students T-test on Microsoft excel was performed to confirm the statistical validation.

Reference List

1. Deva AK, Adams WP, Jr., Vickery K. 2013. The Role of Bacterial Biofilms in Device-Associated Infection. Plastic and Reconstructive Surgery 132:1319-1328.
2. Emerson J, Rosenfeld M, McNamara S, Ramsey B, Gibson RL. 2002. Pseudomonas aeruginosa and other predictors of mortality and morbidity in young children with cystic fibrosis. Pediatric Pulmonology 34:91-100.
3. Hassen AF, Ben Khalifa S, Daiki M. 2014. Epidemiological and bacteriological profiles in children with burns. Burns 40:1040-1045.
4. Turner KH, Everett J, Trivedi U, Rumbaugh KP, Whiteley M. 2014. Requirements for Pseudomonas aeruginosa Acute Burn and Chronic Surgical Wound Infection. Plos Genetics 10.
5. Aggarwal A, Ritter N, Reddy L, Lingutla D, Nasar F, El-Daher N, Hsi D. 2012. Recurrent Pseudomonas aortic root abscess complicating mitral valve endocarditis. Heart & Lung 41:181-183.
6. Bicanic TA, Eykyn SJ. 2002. Hospital-acquired, native valve endocarditis caused by Pseudomonas aeruginosa. Journal of Infection 44:137-139.
7. Breidenstein EBM, de la Fuente-Nunez C, Hancock REW. 2011. Pseudomonas aeruginosa: all roads lead to resistance. Trends in Microbiology 19:419-426.
8. Tam VH, Rogers CA, Chang K-T, Weston JS, Caeiro J-P, Garey KW. 2010. Impact of Multidrug-Resistant Pseudomonas aeruginosa Bacteremia on Patient Outcomes. Antimicrobial Agents and Chemotherapy 54:3717-3722.
9. Goncalves-de-Albuquerque CF, Silva AR, Burth P, Macedo Rocco PR, Castro-Faria MV, Castro-Faria-Neto HC. 2016. Possible mechanisms of Pseudomonas aeruginosa-associated lung disease. International Journal of Medical Microbiology 306:20-28.
10. Rello J, Ausina V, Ricart M, Castella J, Prats G. 2009. Impact of previous antimicrobial therapy on the etiology and outcome of ventilator-associated pneumonia. 1993. Chest 136:e30-e30.
11. Williams BJ, Dehnbostel J, Blackwell TS. 2010. Pseudomonas aeruginosa: Host defence in lung diseases. Respirology 15:1037-1056.
12. Poole K. 2011. Pseudomonas aeruginosa: resistance to the max. Frontiers in Microbiology 2.
13. Lister PD, Wolter DJ, Hanson ND. 2009. Antibacterial-Resistant Pseudomonas aeruginosa: Clinical Impact and Complex Regulation of Chromosomally Encoded Resistance Mechanisms. Clinical Microbiology Reviews 22:582-+.
14. Driscoll JA, Brody SL, Kollef MH. 2007. The epidemiology, pathogenesis and treatment of Pseudomonas aeruginosa infections. Drugs 67:351-368.
15. Setoguchi M, Iwasawa E, Hashimoto Y, Isobe M. 2013. A Patient with Infective Endocarditis Caused by Community-acquired Pseudomonas aeruginosa Infection. Internal Medicine 52:1259-1262.

16. Fernandes M, Vira D, Medikonda R, Kumar N. 2016. Extensively and pan-drug resistant Pseudomonas aeruginosa keratitis: clinical features, risk factors, and outcome. Graefes Archive for Clinical and Experimental Ophthalmology 254:315-322.
17. Strateva T, Yordanov D. 2009. Pseudomonas aeruginosa - a phenomenon of bacterial resistance. Journal of Medical Microbiology 58:1133-1148.
18. Masuda N, Sakagawa E, Ohya S. 1995. Outer-membrane proteins responsible for multiple-drug resistance in Pseudomonas aeruginosa. Antimicrobial Agents and Chemotherapy 39:645-649.
19. Parr TR, Moore RA, Moore LV, Hancock REW. 1987. ROLE OF PORINS IN INTRINSIC ANTIBIOTIC-RESISTANCE OF PSEUDOMONAS-CEPACIA. Antimicrobial Agents and Chemotherapy 31:121-123.
20. Zgurskaya HI, Lopez CA, Gnanakaran S. 2015. Permeability Barrier of Gram-Negative Cell Envelopes and Approaches To Bypass It. Acs Infectious Diseases 1:512-522.
21. Aghazadeh M, Hojabri Z, Mahdian R, Nahaei MR, Rahmati M, Hojabri T, Pirzadeh T, Pajand O. 2014. Role of efflux pumps: MexAB-OprM and MexXY(-OprA), AmpC cephalosporinase and OprD porin in non-metallo-beta-lactamase producing Pseudomonas aeruginosa isolated from cystic fibrosis and burn patients. Infection Genetics and Evolution 24:187-192.
22. Fernandez L, Gooderham WJ, Bains M, McPhee JB, Wiegand I, Hancock REW. 2010. Adaptive Resistance to the "Last Hope" Antibiotics Polymyxin B and Colistin in Pseudomonas aeruginosa Is Mediated by the Novel Two-Component Regulatory System ParR-ParS. Antimicrobial Agents and Chemotherapy 54:3372-3382.
23. McPhee JB, Bains M, Winsor G, Lewenza S, Kwasnicka A, Brazas MD, Brinkman FSL, Hancock REW. 2006. Contribution of the PhoP-PhoQ and PmrA-PmrB two-component regulatory systems to Mg2+-induced gene regulation in Pseudomonas aeruginosa. Journal of Bacteriology 188:3995-4006.
24. Nicas TI, Hancock REW. 1983. Alteration of susceptibility to EDTA, polymyxin-B and gentamycin by divalent cation regulation of outer membrane protein H1. Journal of General Microbiology 129:509-517.
25. Needham BD, Trent MS. 2013. Fortifying the barrier: the impact of lipid A remodelling on bacterial pathogenesis. Nature Reviews Microbiology 11:467-481.
26. Chuchalin A, Amelina E, Bianco F. 2009. Tobramycin for inhalation in cystic fibrosis: Beyond respiratory improvements. Pulmonary Pharmacology & Therapeutics 22:526-532.
27. Young DC, Zobell JT, Stockmann C, Waters CD, Ampofo K, Sherwin CMT, Spigarelli MG. 2013. Optimization of Anti-Pseudomonal Antibiotics for Cystic Fibrosis Pulmonary Exacerbations: V. Aminoglycosides. Pediatric Pulmonology 48:1047-1061.

28. Poole K. 2005. Aminoglycoside resistance in Pseudomonas aeruginosa. Antimicrobial Agents and Chemotherapy 49:479-487.
29. Li X-Z, Nikaido H. 2009. Efflux-Mediated Drug Resistance in Bacteria An Update. Drugs 69:1555-1623.
30. Nikaido H. 2011. Structure and mechanism of RND-type multidrug efflux pumps. Advances in enzymology and related areas of molecular biology 77:1-60.
31. Li Y, Mima T, Komori Y, Morita Y, Kuroda T, Mizushima T, Tsuchiya T. 2003. A new member of the tripartite multidrug efflux pumps, MexVW-OprM, in Pseudomonas aeruginosa. Journal of Antimicrobial Chemotherapy 52:572-575.
32. Mima T, Joshi S, Gomez-Escalada M, Schweizer HP. 2007. Identification and characterization of TriABC-OpmH, a Triclosan efflux pump of pseudomonas aeruginosa requiring two membrane fusion proteins. Journal of Bacteriology 189:7600-7609.
33. Hocquet D, Vogne C, El Garch F, Vejux A, Gotoh N, Lee A, Lomovskaya O, Plesiat P. 2003. MexXY-OprM efflux pump is necessary for adaptive resistance of Pseudomonas aeruginosa to aminoglycosides. Antimicrobial Agents and Chemotherapy 47:1371-1375.
34. Morita Y, Tomida J, Kawamura Y. 2015. Efflux-mediated fluoroquinolone resistance in the multidrug-resistant Pseudomonas aeruginosa clinical isolate PA7: identification of a novel MexS variant involved in upregulation of the mexEF-oprN multidrug efflux operon. Frontiers in Microbiology 6.
35. Poonsuk K, Tribuddharat C, Chuanchuen R. 2014. Simultaneous overexpression of multidrug efflux pumps in Pseudomonas aeruginosa non-cystic fibrosis clinical isolates. Canadian Journal of Microbiology 60:437-443.
36. Kai T, Tateda K, Kimura S, Ishii Y, Ito H, Yoshida H, Kimura T, Yamaguchi K. 2009. A low concentration of azithromycin inhibits the mRNA expression of N-acyl homoserine lactone synthesis enzymes, upstream of lasI or rhlI, in Pseudomonas aeruginosa. Pulmonary Pharmacology & Therapeutics 22:483-486.
37. Anderson GG, Moreau-Marquis S, Stanton BA, O'Toole GA. 2008. In vitro analysis of tobramycin-treated Pseudomonas aeruginosa Biofilms on cystic fibrosis-derived airway epithelial cells. Infection and Immunity 76:1423-1433.
38. Aendekerk S, Diggle SP, Song Z, Hoiby N, Cornelis P, Williams P, Camara M. 2005. The MexGHI-OpmD multidrug efflux pump controls growth, antibiotic susceptibility and virulence in Pseudomonas aeruginosa via 4-quinolone-dependent cell-to-cell communication. Microbiology-Sgm 151:1113-1125.
39. Llanes C, Kohler T, Patry I, Dehecq B, van Delden C, Plesiat P. 2011. Role of the MexEF-OprN Efflux System in Low-Level Resistance of Pseudomonas aeruginosa to Ciprofloxacin. Antimicrobial Agents and Chemotherapy 55:5676-5684.
40. Nies DH. 1995. THE COBALT, ZINC, AND CADMIUM EFFLUX SYSTEM CZCABC FROM ALCALIGENES-EUTROPHUS FUNCTIONS AS A CATION-PROTON ANTIPORTER IN ESCHERICHIA-COLI. Journal of Bacteriology 177:2707-2712.

41. Rensing C, Pribyl T, Nies DH. 1997. New functions for the three subunits of the CzcCBA cation-proton antiporter. Journal of Bacteriology 179:6871-6879.
42. Evans K, Passador L, Srikumar R, Tsang E, Nezezon J, Poole K. 1998. Influence of the MexAB-OprM multidrug efflux system on quorum sensing in Pseudomonas aeruginosa. Journal of Bacteriology 180:5443-5447.
43. Sharmily Khanam MG, Dirk L. Lenaburg, Ryan Kubat, Marianna A. Patrauchan. Jan 2017. Calcium induces tobramycin resistance in Pseudomonas aeruginosa by regulating RND efflux pumps. Cell Calcium 61:32-43.
44. Jeannot K, Elsen S, Koeher T, Attree I, van Delden C, Plesiat P. 2008. Resistance and virulence of Pseudomonas aeruginosa clinical strains overproducing the MexCD-OprJ efflux pump. Antimicrobial Agents and Chemotherapy 52:2455-2462.
45. Linares JF, Lopez JA, Camafeita E, Albar JP, Rojo F, Martinez JL. 2005. Overexpression of the multidrug efflux pumps MexCD-OprJ and MexEF-OprN is associated with a reduction of type III secretion in Pseudomonas aeruginosa. Journal of Bacteriology 187:1384-1391.
46. Sakhtah H, Koyama L, Zhang Y, Morales DK, Fields BL, Price-Whelan A, Hogan DA, Shepard K, Dietrich LE. 2016. The Pseudomonas aeruginosa efflux pump MexGHI-OpmD transports a natural phenazine that controls gene expression and biofilm development. Proceedings of the National Academy of Sciences 113:E3538-E3547.
47. Dominguez DC, Guragain M, Patrauchan M. 2015. Calcium binding proteins and calcium signaling in prokaryotes. Cell Calcium 57:151-165.
48. Kipnis E, Sawa T, Wiener-Kronish J. 2006. Targeting mechanisms of Pseudomonas aeruginosa pathogenesis. Medecine Et Maladies Infectieuses 36:78-91.
49. Houang ET, Greenwood D. 1977. AMINOGLYCOSIDE CROSS-RESISTANCE PATTERNS OF GENTAMICIN-RESISTANT BACTERIA. Journal of Clinical Pathology 30:738-744.
50. Barclay ML, Begg EJ, Chambers ST, Peddie BA. 1996. The effect of aminoglycoside-induced adaptive resistance on the antibacterial activity of other antibiotics against Pseudomonas aeruginosa in vitro. Journal of Antimicrobial Chemotherapy 38:853-858.
51. Karlowsky JA, Zelenitsky SA, Zhanel GG. 1997. Aminoglycoside adaptive resistance. Pharmacotherapy 17:549-555.
52. Gorgani N, Ahlbrand S, Patterson A, Pourmand N. 2009. Detection of point mutations associated with antibiotic resistance in Pseudomonas aeruginosa. International Journal of Antimicrobial Agents 34:414-418.
53. Poole K, Tetro K, Zhao QX, Neshat S, Heinrichs DE, Bianco N. 1996. Expression of the multidrug resistance operon mexA-mexB-oprM in Pseudomonas aeruginosa: mexR encodes a regulator of operon expression. Antimicrobial Agents and Chemotherapy 40:2021-2028.

54. Poole K, Gotoh N, Tsujimoto H, Zhao QX, Wada A, Yamasaki T, Neshat S, Yamagishi JI, Li XZ, Nishino T. 1996. Overexpression of the mexC-mexD-oprJ efflux operon in nfxB-type multidrug-resistant strains of Pseudomonas aeruginosa. Molecular Microbiology 21:713-724.
55. Sanchez P, Linares JF, Ruiz-Diez B, Campanario E, Navas A, Baquero F, Martinez JL. 2002. Fitness of in vitro selected Pseudomonas aeruginosa nalB and nfxB multidrug resistant mutants. Journal of Antimicrobial Chemotherapy 50:657-664.
56. Pan YP, Xu YH, Wang ZX, Fang YP, Shen JL. 2016. Overexpression of MexAB-OprM efflux pump in carbapenem-resistant Pseudomonas aeruginosa. Archives of Microbiology 198:565-571.
57. Mah TF, Pitts B, Pellock B, Walker GC, Stewart PS, O'Toole GA. 2003. A genetic basis for Pseudomonas aeruginosa biofilm antibiotic resistance. Nature 426:306-310.
58. Boles BR, Singh PK. 2008. Endogenous oxidative stress produces diversity and adaptability in biofilm communities. Proceedings of the National Academy of Sciences of the United States of America 105:12503-12508.
59. Arakawa Y, Murakami M, Suzuki K, Ito H, Wacharotayankun R, Ohsuka S, Kato N, Ohta M. 1995. A NOVEL INTEGRON-LIKE ELEMENT CARRYING THE METALLO-BETA-LACTAMASE GENE BLA(IMP). Antimicrobial Agents and Chemotherapy 39:1612-1615.
60. Hoyle BD, Wong CKW, Costerton JW. 1992. Disparate Efficacy of Tobramycin on Ca2+-Treated, Mg2+-Treated, and Hepes-Treated Pseudomonas-Aeruginosa Biofilms. Canadian Journal of Microbiology 38:1214-1218.
61. Chambonnier G, Roux L, Redelberger D, Fadel F, Filloux A, Sivaneson M, de Bentzmann S, Bordi C. 2016. The Hybrid Histidine Kinase LadS Forms a Multicomponent Signal Transduction System with the GacS/GacA Two-Component System in Pseudomonas aeruginosa. Plos Genetics 12.
62. Beceiro A, Tomas M, Bou G. 2013. Antimicrobial Resistance and Virulence: a Successful or Deleterious Association in the Bacterial World? Clinical Microbiology Reviews 26:185-230.
63. Berlutti F, Morea C, Battistoni A, Sarli S, Cipriani P, Superti F, Ammendolia MG, Valenti P. 2005. Iron availability influences aggregation, biofilm, adhesion and invasion of Pseudomonas aeruginosa and Burkholderia cenocepacia. International Journal of Immunopathology and Pharmacology 18:661-670.
64. Berridge MJ. 2016. The Inositol Trisphosphate/Calcium Signaling Pathway in Health and Disease. Physiological Reviews 96:1261-1296.
65. Feske S. 2007. Calcium signalling in lymphocyte activation and disease. Nature Reviews Immunology 7:690-702.
66. Liu LX, Ridefelt P, Hakansson L, Venge P. 1999. Regulation of human eosinophil migration across lung epithelial monolayers by distinct calcium signaling mechanisms in the two cell types. Journal of Immunology 163:5649-5655.

67. Lorin MI, Gaerlan PF, Mandel ID, Denning CR. 1976. Composition of nasal secretion in patients with cystic fibrosis. J Lab Clin Med 88:114-7.
68. Ribeiro CMP, Paradiso AM, Carew MA, Shears SB, Boucher RC. 2005. Cystic fibrosis airway epithelial Ca-i(2+) signaling. Journal of Biological Chemistry 280:10202-10209.
69. Damato RF, Thornsberry C, Baker CN, Kirven LA. 1975. Effect of Calcium and Magnesium-Ions on Susceptibility of Pseudomonas Species to Tetracycline, Gentamicin Polymyxin-B, and Carbenicillin. Antimicrobial Agents and Chemotherapy 7:596-600.
70. Guragain M, King MM, Williamson KS, Perez-Osorio AC, Akiyama T, Khanam S, Patrauchan MA, Franklin MJ. 2016. The Pseudomonas aeruginosa PAO1 Two-Component Regulator CarSR Regulates Calcium Homeostasis and Calcium-Induced Virulence Factor Production through Its Regulatory Targets CarO and CarP. Journal of Bacteriology 198:951-963.
71. Sarkisova SA, Lotlikar SR, Guragain M, Kubat R, Cloud J, Franklin MJ, Patrauchan MA. 2014. A Pseudomonas aeruginosa EF-Hand Protein, EfhP (PA4107), Modulates Stress Responses and Virulence at High Calcium Concentration. Plos One 9.
72. Guragain M, Lenaburg DL, Moore FS, Reutlinger I, Patrauchan MA. 2013. Calcium homeostasis in Pseudomonas aeruginosa requires multiple transporters and modulates swarming motility. Cell Calcium 54:350-361.
73. Patrauchan MA, Sarkisova SA, Franklin MJ. 2007. Strain-specific proteome responses of Pseudomonas aeruginosa to biofilm-associated growth and to calcium. Microbiology-Sgm 153:3838-3851.
74. Sarkisova S, Patrauchan MA, Berglund D, Nivens DE, Franklin MJ. 2005. Calcium-induced virulence factors associated with the extracellular matrix of mucoid Pseudomonas aeruginosa biofilms. Journal of Bacteriology 187:4327-4337.
75. Lau CH-F, Hughes D, Poole K. 2014. MexY-Promoted Aminoglycoside Resistance in Pseudomonas aeruginosa: Involvement of a Putative Proximal Binding Pocket in Aminoglycoside Recognition. Mbio 5:e01068-14.
76. Fraud S, Poole K. 2011. Oxidative Stress Induction of the MexXY Multidrug Efflux Genes and Promotion of Aminoglycoside Resistance Development in Pseudomonas aeruginosa. Antimicrobial Agents and Chemotherapy 55:1068-1074.
77. Fetar H, Gilmour C, Klinoski R, Daigle DM, Dean CR, Poole K. 2011. mexEF-oprN Multidrug Efflux Operon of Pseudomonas aeruginosa: Regulation by the MexT Activator in Response to Nitrosative Stress and Chloramphenicol. Antimicrobial Agents and Chemotherapy 55:508-514.
78. Lamarche MG, Deziel E. 2011. MexEF-OprN Efflux Pump Exports the Pseudomonas Quinolone Signal (PQS) Precursor HHQ (4-hydroxy-2-heptylquinoline). Plos One 6.

79. Kohler T, van Delden C, Curty LK, Hamzehpour MM, Pechere JC. 2001. Overexpression of the MexEF-OprN multidrug efflux system affects cell-to-cell signaling in Pseudomonas aeruginosa. Journal of Bacteriology 183:5213-5222.
80. Join-Lamberti OF, Michea-Hamzehpour M, Kohler T, Chau F, Faurisson F, Dautrey S, Vissuzaine C, Carbon C, Pechere JC. 2001. Differential selection of multidrug efflux mutants by trovafloxacin and ciprofloxacin in an experimental model of Pseudomonas aeruginosa acute pneumonia in rats. Antimicrobial Agents and Chemotherapy 45:571-576.
81. Hirakata Y, Srikumar R, Poole K, Gotoh N, Suematsu T, Kohno S, Kamihira S, Hancock REW, Speert DP. 2002. Multidrug efflux systems play an important role in the invasiveness of Pseudomonas aeruginosa. Journal of Experimental Medicine 196:109-118.
82. Yang L, Chen L, Shen L, Surette M, Duan K. 2011. Inactivation of MuxABC-OpmB Transporter System in Pseudomonas aeruginosa Leads to Increased Ampicillin and Carbenicillin Resistance and Decreased Virulence. Journal of Microbiology 49:107-114.
83. Carafoli E. 2002. Calcium signaling: A tale for all seasons. Proceedings of the National Academy of Sciences of the United States of America 99:1115-1122.
84. Chattopadhyay N, Brown EM. 2000. Cellular "sensing" of extracellular calcium (Ca-o(2+)): emerging roles in regulating diverse physiological functions. Cellular Signalling 12:361-366.
85. Ishiwada N, Niwa K, Tateno S, Yoshinaga M, Terai M, Nakazawa M, Japanese Soc Pediat Cardiology C. 2005. Causative organism influences clinical profile and outcome of infective endocarditis in pediatric patients and adults with congenital heart disease. Circulation Journal 69:1266-1270.
86. Eicher JC, De Nadai L, Soto FX, Falcon-Eicher S, Dobsak P, Zanetta G, Petit JM, Portier H, Louis P, Wolf JE. 2004. Bacterial endocarditis complicating mitral annular calcification: A clinical and echocardiographic study. Journal of Heart Valve Disease 13:217-227.
87. Halmerbauer G, Arri S, Schierl M, Strauch E, Koller DY. 2000. The relationship of eosinophil granule proteins to ions in the sputum of patients with cystic fibrosis. Clinical and Experimental Allergy 30:1771-1776.
88. Martins LO, Brito LC, Sacorreia I. 1990. Roles of Mn-2+, Mg-2+ and Ca-2+ on Alginate Biosynthesis by Pseudomonas-Aeruginosa. Enzyme and Microbial Technology 12:794-799.
89. Hameiste.W, Wahlig H. 1971. Influence of Mg++ and Ca++ Ions on Efficacy of Gentamycin against Pseudomonas-Aeruginosa in Agar Diffusion Test. Arzneimittel-Forschung 21:1658-&.
90. Davis SD, Iannetta A. 1972. Influence of serum and calcium on the bactericidal activity of gentamicin and carbenicillin on Pseudomonas aeruginosa. Applied Microbiology 23:775-9.

91. Irvin JE, Ingram JM. 1982. Divalent-Cation Regulation of Chloramphenicol Resistance in Pseudomonas-Aeruginosa. Fems Microbiology Letters 13:63-67.
92. Zimelis VM, Jackson GG. 1973. Activity of aminoglycoside antibiotics against Pseudomonas aeruginosa specificity and site of Calcium and magnesium antagonism. Journal of Infectious Diseases 127:663-669.
93. Hancock REW. 1998. Resistance mechanisms in Pseudomonas aeruginosa and other nonfermentative gram-negative bacteria. Clinical Infectious Diseases 27:S93-S99.
94. Nicas TI, Hancock REW. 1980. Outer membrane protein H-1 of Pseudomona saeruginosa : involvement in adaptive and mutational resistance to Ethylenediaminetetraacetate, polymyxin-B and Gentamycin. Journal of Bacteriology 143:872-878.
95. Mao WM, Warren MS, Lee A, Mistry A, Lomovskaya O. 2001. MexXY-OprM efflux pump is required for antagonism of aminoglycosides by divalent cations in Pseudomonas aeruginosa. Antimicrobial Agents and Chemotherapy 45:2001-2007.
96. Stover CK, Pham XQ, Erwin AL, Mizoguchi SD, Warrener P, Hickey MJ, Brinkman FSL, Hufnagle WO, Kowalik DJ, Lagrou M, Garber RL, Goltry L, Tolentino E, Westbrock-Wadman S, Yuan Y, Brody LL, Coulter SN, Folger KR, Kas A, Larbig K, Lim R, Smith K, Spencer D, Wong GKS, Wu Z, Paulsen IT, Reizer J, Saier MH, Hancock REW, Lory S, Olson MV. 2000. Complete genome sequence of Pseudomonas aeruginosa PAO1, an opportunistic pathogen. Nature 406:959-964.
97. Jacobs MA, Alwood A, Thaipisuttikul I, Spencer D, Haugen E, Ernst S, Will O, Kaul R, Raymond C, Levy R, Chun-Rong L, Guenthner D, Bovee D, Olson MV, Manoil C. 2003. Comprehensive transposon mutant library of Pseudomonas aeruginosa. Proc Natl Acad Sci U S A 100:14339-44.
98. Jacobs MA, Alwood A, Thaipisuttikul I, Spencer D, Haugen E, Ernst S, Will O, Kaul R, Raymond C, Levy R, Liu CR, Guenthner D, Bovee D, Olson MV, Manoil C. 2003. Comprehensive transposon mutant library of Pseudomonas aeruginosa. Proceedings of the National Academy of Sciences of the United States of America 100:14339-14344.
99. Nouwens AS, Cordwell SJ, Larsen MR, Molloy MP, Gillings M, Willcox MD, Walsh BJ. 2000. Complementing genomics with proteomics: the membrane subproteome of Pseudomonas aeruginosa PAO1. Electrophoresis 21:3797-809.
100. Huggett JF, Foy CA, Benes V, Emslie K, Garson JA, Haynes R, Hellemans J, Kubista M, Mueller RD, Nolan T, Pfaffl MW, Shipley GL, Vandesompele J, Wittwer CT, Bustin SA. 2013. The Digital MIQE Guidelines: Minimum Information for Publication of Quantitative Digital PCR Experiments. Clinical Chemistry 59:892-902.
101. Rozen S, Skaletsky H. 2000. Primer3 on the WWW for general users and for biologist programmers. Methods in molecular biology (Clifton, NJ) 132:365-86.

102. Ye J, Coulouris G, Zaretskaya I, Cutcutache I, Rozen S, Madden TL. 2012. Primer-BLAST: A tool to design target-specific primers for polymerase chain reaction. Bmc Bioinformatics 13:13-134.
103. Savli H, Karadenizli A, Kolayli F, Gundes S, Ozbek U, Vahaboglu H. 2003. Expression stability of six housekeeping genes: a proposal for resistance gene quantification studies of Pseudomonas aeruginosa by real-time quantitative RT-PCR. Journal of Medical Microbiology 52:403-408.
104. Lenz AP, Williamson KS, Pitts B, Stewart PS, Franklin MJ. 2008. Localized gene expression in Pseudomonas aeruginosa Biofilms. Applied and Environmental Microbiology 74:4463-4471.
105. Schmittgen TD, Livak KJ. 2008. Analyzing real-time PCR data by the comparative C-T method. Nature Protocols 3:1101-1108.
106. Starkey M, Rahme LG. 2009. Modeling Pseudomonas aeruginosa pathogenesis in plant hosts. Nature Protocols 4:117-124.
107. Sala-Newby G, Kendall J, Jones H, Taylor K, Badminton M, Llewellyn D, Campbell A. 1999. Bioluminescent and chemiluminescent indicators for molecular signalling and function in living cells. Fluorescent and Luminescent Probes for Biological Activity 2.
108. Irani VR, Rowe JJ. 1997. Enhancement of transformation in Pseudomonas aeruginosa PAO1 by Mg2+ and heat. Biotechniques 22:54-6.
109. Jones HE, Holland IB, Baker HL, Campbell AK. 1999. Slow changes in cytosolic free Ca2+ in Escherichia coli highlight two putative influx mechanisms in response to changes in extracellular calcium. Cell Calcium 25:265-274.
110. Flume PA, Mogayzel PJ, Robinson KA, Goss CH, Rosenblatt RL, Kuhn RJ, Marshall BC, Clinical Practice Guidelines P. 2009. Cystic Fibrosis Pulmonary Guidelines Treatment of Pulmonary Exacerbations. American Journal of Respiratory and Critical Care Medicine 180:802-808.
111. Hennig S, Norris R, Kirkpatrick CMJ. 2008. Target concentration intervention is needed for tobramycin dosing in paediatric patients with cystic fibrosis - a population pharmacokinetic study. British Journal of Clinical Pharmacology 65:502-510.
112. Lam W, Tjon J, Seto W, Dekker A, Wong C, Atenafu E, Bitnum A, Waters V, Yau Y, Solomon M, Ratjen F. 2007. Pharmacokinetic modelling of a once-daily dosing regimen for intravenous tobramycin in paediatric cystic fibrosis patients. Journal of Antimicrobial Chemotherapy 59:1135-1140.
113. Kashuba ADM, Nafziger AN, Drusano GL, Bertino JS. 1999. Optimizing aminoglycoside therapy for nosocomial pneumonia caused by Gram-negative bacteria. Antimicrobial Agents and Chemotherapy 43:623-629.
114. Shawar RM, MacLeod DL, Garber RL, Burns JL, Stapp JR, Clausen CR, Tanaka SK. 1999. Activities of tobramycin and six other antibiotics against Pseudomonas aeruginosa isolates from patients with cystic fibrosis. Antimicrobial Agents and Chemotherapy 43:2877-2880.

115. Widdel F. 2010. Theory and Measurement of Bacterial Growth. University Bremen,
116. Goldberg M, Pribyl T, Juhnke S, Nies DH. 1999. Energetics and topology of CzcA, a cation/proton antiporter of the resistance-nodulation-cell division protein family. Journal of Biological Chemistry 274:26065-26070.
117. Zobell JT, Young DC, Waters CD, Ampofo K, Stockmann C, Sherwin CMT, Spigarelli MG. 2013. Optimization of anti-pseudomonal antibiotics for cystic fibrosis pulmonary exacerbations: VI. Executive summary. Pediatric Pulmonology 48:525-537.
118. Dean CR, Visalli MA, Projan SJ, Sum PE, Bradford PA. 2003. Efflux-mediated resistance to tigecycline (GAR-936) in Pseudomonas aeruginosa PAO1. Antimicrobial Agents and Chemotherapy 47:972-978.
119. Srikumar R, Li XZ, Poole K. 1997. Inner membrane efflux components are responsible for beta-lactam specificity of multidrug efflux pumps in Pseudomonas aeruginosa. Journal of Bacteriology 179:7875-7881.
120. Minagawa S, Inami H, Kato T, Sawada S, Yasuki T, Miyairi S, Horikawa M, Okuda J, Gotoh N. 2012. RND type efflux pump system MexAB-OprM of pseudomonas aeruginosa selects bacterial languages, 3-oxo-acyl-homoserine lactones, for cell-to-cell communication. Bmc Microbiology 12.
121. Morita Y, Tomidaand J, Kawamura Y. 2012. MexXY multidrug efflux system of Pseudomonas aeruginosa. Frontiers in Microbiology 3.
122. Vogne C, Aires JR, Bailly C, Hocquet D, Plesiat P. 2004. Role of the multidrug efflux system MexXY in the emergence of moderate resistance to aminoglycosides among Pseudomonas aeruginosa isolates from patients with cystic fibrosis. Antimicrobial Agents and Chemotherapy 48:1676-1680.
123. Wolter DJ, Smith-Moland E, Goering RV, Hanson ND, Lister PD. 2004. Multidrug resistance associated with mexXY expression in clinical isolates of Pseudomonas aeruginosa from a Texas hospital. Diagnostic Microbiology and Infectious Disease 50:43-50.
124. Chuanchuen R, Gaynor JB, Karkhoff-Schweizer R, Schweizer HP. 2005. Molecular characterization of MexL, the transcriptional repressor of the mexJK multidrug efflux operon in Pseudomonas aeruginosa. Antimicrobial Agents and Chemotherapy 49:1844-1851.
125. Hassan MET, van der Lelie D, Springael D, Romling U, Ahmed N, Mergeay M. 1999. Identification of a gene cluster, czr, involved in cadmium and zinc resistance in Pseudomonas aeruginosa. Gene 238:417-425.
126. Li XZ, Zhang L, Poole K. 2000. Interplay between the MexA-MexB-OprM multidrug efflux system and the outer membrane barrier in the multiple antibiotic resistance of Pseudomonas aeruginosa. Journal of Antimicrobial Chemotherapy 45:433-436.
127. Riou M, Avrain L, Carbonnelle S, El Garch F, Pirnay JP, De Vos D, Plesiat P, Tulkens PM, Van Bambeke F. 2016. Increase of efflux-mediated resistance in

Pseudomonas aeruginosa during antibiotic treatment in patients suffering from nosocomial pneumonia. International Journal of Antimicrobial Agents 47:77-83.
128. Nies DH. 1992. Resistance to Cadmium, Cobalt, Zinc and Nickel in Microbes. Plasmid 27:17-28.
129. Caille O, Rossier C, Perron K. 2007. A copper-activated two-component system interacts with zinc and imipenem resistance in Pseudomonas aeruginosa. Journal of Bacteriology 189:4561-4568.
130. Chang W, Small DA, Toghrol F, Bentley WE. 2005. Microarray analysis of Pseudomonas aeruginosa reveals induction of pyocin genes in response to hydrogen peroxide. Bmc Genomics 6:1-14.
131. Teitzel GM, Geddie A, De Long SK, Kirisits MJ, Whiteley M, Parsek MR. 2006. Survival and growth in the presence of elevated copper: Transcriptional profiling of copper-stressed *Pseudomonas aeruginosa*. Journal of Bacteriology 188:7242-7256.
132. Muller C, Plesiat P, Jeannot K. 2011. A Two-Component Regulatory System Interconnects Resistance to Polymyxins, Aminoglycosides, Fluoroquinolones, and beta-Lactams in Pseudomonas aeruginosa. Antimicrobial Agents and Chemotherapy 55:1211-1221.
133. Wang D, Seeve C, Pierson LS, III, Pierson EA. 2013. Transcriptome profiling reveals links between ParS/ParR, MexEF-OprN, and quorum sensing in the regulation of adaptation and virulence in Pseudomonas aeruginosa. Bmc Genomics 14.
134. Perez A, Poza M, Fernandez A, del Carmen M, Mallo FS, Merino M, Rumbo-Feal S, Cabral MP, Bou G. 2012. Involvement of the AcrAB-TolC Efflux Pump in the Resistance, Fitness, and Virulence of Enterobacter cloacae. Antimicrobial Agents and Chemotherapy 56:2084-2090.
135. Webber MA, Bailey AM, Blair JMA, Morgan E, Stevens MP, Hinton JCD, Ivens A, Wain J, Piddock LJV. 2009. The Global Consequence of Disruption of the AcrAB-TolC Efflux Pump in Salmonella enterica Includes Reduced Expression of SPI-1 and Other Attributes Required To Infect the Host. Journal of Bacteriology 191:4276-4285.
136. Bialek S, Lavigne JP, Chevalier J, Marcon E, Leflon-Guibout V, Davin A, Moreau R, Pages JM, Nicolas-Chanoine MH. 2010. Membrane Efflux and Influx Modulate both Multidrug Resistance and Virulence of Klebsiella pneumoniae in a Caenorhabditis elegans Model. Antimicrobial Agents and Chemotherapy 54:4373-4378.
137. Von Ruecker AA, Bertele R, Harms HK. 1984. Calcium metabolism and cystic fibrosis: mitochondrial abnormalities suggest a modification of the mitochondrial membrane. Pediatric research 18:594-599.
138. Halmerbauer G, Arri S, Schierl M, Strauch E, Koller DY. 2000. The relationship of eosinophil granule proteins to ions in the sputum of patients with cystic fibrosis. Clin Exp Allergy 30:1771-6.
139. Dominguez DC. 2004. Calcium signalling in bacteria. Mol Microbiol 54:291-7.

140. Herbaud ML, Guiseppi A, Denizot F, Haiech J, Kilhoffer MC. 1998. Calcium signalling in Bacillus subtilis. Biochim Biophys Acta 1448:212-26.
141. Borriello G, Werner E, Roe F, Kim AM, Ehrlich GD, Stewart PS. 2004. Oxygen limitation contributes to antibiotic tolerance of Pseudomonas aeruginosa in biofilms. Antimicrob Agents Chemother 48:2659-64.
142. Leganes F, Forchhammer K, Fernandez-Pinas F. 2009. Role of calcium in acclimation of the cyanobacterium Synechococcus elongatus PCC 7942 to nitrogen starvation. Microbiology 155:25-34.
143. Zhao Y, Shi Y, Zhao W, Huang X, Wang D, Brown N, Brand J, Zhao J. 2005. CcbP, a calcium-binding protein from Anabaena sp. PCC 7120, provides evidence that calcium ions regulate heterocyst differentiation. Proceedings of the National Academy of Sciences of the United States of America 102:5744-5748.
144. Straley SC, Plano GV, Skrzypek E, Haddix PL, Fields KA. 1993. Regulation by Ca2+ in the Yersinia low-Ca2+ response. Mol Microbiol 8:1005-10.
145. Tisa L, Olivera BM, Adler J. 1993. Inhibition of Escherichia coli chemotaxis by omega-conotoxin, a calcium ion channel blocker. Journal of bacteriology 175:1235-1238.
146. Sarkisova S, Patrauchan MA, Berglund D, Nivens DE, Franklin MJ. 2005. Calcium-induced virulence factors associated with the extracellular matrix of mucoid Pseudomonas aeruginosa biofilms. J Bacteriol 187:4327-37.
147. Hu Y, Zhang X, Shi Y, Zhou Y, Zhang W, Su XD, Xia B, Zhao J, Jin C. 2011. Structures of Anabaena calcium-binding protein CcbP: insights into Ca2+ signaling during heterocyst differentiation. J Biol Chem 286:12381-8.
148. Rosch JW, Sublett J, Gao G, Wang YD, Tuomanen EI. 2008. Calcium efflux is essential for bacterial survival in the eukaryotic host. Molecular microbiology 70:435-444.
149. Campbell AK, Naseem R, Holland IB, Matthews SB, Wann KT. 2007. Methylglyoxal and other carbohydrate metabolites induce lanthanum-sensitive Ca 2+ transients and inhibit growth in E. coli. Archives of biochemistry and biophysics 468:107-113.
150. Falagas ME, Bliziotis IA. 2007. Pandrug-resistant Gram-negative bacteria: the dawn of the post-antibiotic era? International journal of antimicrobial agents 29:630-636.
151. Kaye KS, Kanafani ZA, Dodds AE, Engemann JJ, Weber SG, Carmeli Y. 2006. Differential effects of levofloxacin and ciprofloxacin on the risk for isolation of quinolone-resistant Pseudomonas aeruginosa. Antimicrobial agents and chemotherapy 50:2192-2196.
152. Bicanic T, Eykyn S. 2002. Hospital-acquired, native valve endocarditis caused by Pseudomonas aeruginosa. Journal of Infection 44:137-139.
153. Ishiwada N, Niwa K, Tateno S, Yoshinaga M, Terai M, Nakazawa M. 2005. Causative organism influences clinical profile and outcome of infective

endocarditis in pediatric patients and adults with congenital heart disease. Circulation journal 69:1266-1270.
154. Komshian SV, Tablan OC, Palutke W, Reyes MP. 1990. Characteristics of left-sided endocarditis due to Pseudomonas aeruginosa in the Detroit Medical Center. Review of Infectious Diseases 12:693-702.
155. Jesaitis AJ, Franklin MJ, Berglund D, Sasaki M, Lord CI, Bleazard JB, Duffy JE, Beyenal H, Lewandowski Z. 2003. Compromised host defense on Pseudomonas aeruginosa biofilms: characterization of neutrophil and biofilm interactions. The Journal of Immunology 171:4329-4339.
156. Walters MC, Roe F, Bugnicourt A, Franklin MJ, Stewart PS. 2003. Contributions of antibiotic penetration, oxygen limitation, and low metabolic activity to tolerance of Pseudomonas aeruginosa biofilms to ciprofloxacin and tobramycin. Antimicrobial agents and chemotherapy 47:317-323.
157. Sarkisova SA, Lotlikar SR, Guragain M, Kubat R, Cloud J, Franklin MJ, Patrauchan MA. 2014. A *Pseudomonas aeruginosa* EF-hand protein, EfhP (PA4107), modulates stress responses and virulence at high calcium concentration. PLoS One 9:e98985.
158. Guragain M, King MM, Williamson KS, Perez-Osorio AC, Akiyama T, Khanam S, Patrauchan MA, Franklin MJ. 2016. The Pseudomonas aeruginosa PAO1 Two-Component Regulator CarSR Regulates Calcium Homeostasis and Calcium-Induced Virulence Factor Production through Its Regulatory Targets CarO and CarP. J Bacteriol 198:951-63.
159. Bultynck G, Kiviluoto S, Methner A. 2014. Bax inhibitor-1 is likely a pH-sensitive calcium leak channel, not a H+/Ca2+ exchanger. Science signaling 7:pe22-pe22.
160. Chang Y, Bruni R, Kloss B, Assur Z, Kloppmann E, Rost B, Hendrickson WA, Liu Q. 2014. Structural basis for a pH-sensitive calcium leak across membranes. Science 344:1131-5.
161. Stover CK, Pham XQ, Erwin AL, Mizoguchi SD, Warrener P, Hickey MJ, Brinkman FS, Hufnagle WO, Kowalik DJ, Lagrou M, Garber RL, Goltry L, Tolentino E, Westbrock-Wadman S, Yuan Y, Brody LL, Coulter SN, Folger KR, Kas A, Larbig K, Lim R, Smith K, Spencer D, Wong GK, Wu Z, Paulsen IT, Reizer J, Saier MH, Hancock RE, Lory S, Olson MV. 2000. Complete genome sequence of *Pseudomonas aeruginosa* PAO1, an opportunistic pathogen. Nature 406:959-64.
162. Cao Q, Wang Y, Chen FF, Xia YJ, Lou JY, Zhang X, Yang NN, Sun XX, Zhang Q, Zhuo C, Huang X, Deng X, Yang CG, Ye Y, Zhao J, Wu M, Lan LF. 2014. A Novel Signal Transduction Pathway that Modulates rhl Quorum Sensing and Bacterial Virulence in Pseudomonas aeruginosa. Plos Pathogens 10.
163. Popat R, Crusz SA, Messina M, Williams P, West SA, Diggle SP. 2012. Quorum-sensing and cheating in bacterial biofilms. Proceedings of the Royal Society B: Biological Sciences doi:10.1098/rspb.2012.1976.
164. Kong WN, Chen L, Zhao JQ, Shen T, Surette MG, Shen LX, Duan KM. 2013. Hybrid sensor kinase PA1611 in Pseudomonas aeruginosa regulates transitions between

acute and chronic infection through direct interaction with RetS. Molecular Microbiology 88:784-797.
165. Watkins NJ, Knight MR, Trewavas AJ, Campbell AK. 1995. Free calcium transients in chemotactic and non-chemotactic strains of Escherichia coli determined by using recombinant aequorin. Biochem J 306 (Pt 3):865-9.
166. Overhage J, Lewenza S, Marr AK, Hancock RE. 2007. Identification of genes involved in swarming motility using a *Pseudomonas aeruginosa* PAO1 mini-Tn5-lux mutant library. J Bacteriol 189:2164-9.
167. Hoegy F, Mislin GL, Schalk IJ. 2014. Pyoverdine and pyochelin measurements. Pseudomonas Methods and Protocols:293-301.
168. Cox CD, Adams P. 1985. Siderophore activity of pyoverdin for Pseudomonas aeruginosa. Infection and immunity 48:130-138.
169. Qi Q, Rehm BH, Steinbüchel A. 1997. Synthesis of poly (3-hydroxyalkanoates) in Escherichia coli expressing the PHA synthase gene phaC2 from Pseudomonas aeruginosa: comparison of PhaC1 and PhaC2. FEMS microbiology letters 157:155-162.
170. Miyake T, Shiba T, Kameda A, Ihara Y, Munekata M, Ishige K, Noguchi T. 1999. The gene for an exopolyphosphatase of Pseudomonas aeruginosa. DNA Research 6:103-108.
171. Ishige K, Kameda A, Noguchi T, Shiba T. 1998. The polyphosphate kinase gene of Pseudomonas aeruginosa. DNA Research 5:157-162.
172. Haddad A, Jensen V, Becker T, Häussler S. 2009. The Pho regulon influences biofilm formation and type three secretion in Pseudomonas aeruginosa. Environmental microbiology reports 1:488-494.
173. Lamarche MG, Wanner BL, Crépin S, Harel J. 2008. The phosphate regulon and bacterial virulence: a regulatory network connecting phosphate homeostasis and pathogenesis. FEMS microbiology reviews 32:461-473.
174. Petrova OE, Sauer K. 2009. A novel signaling network essential for regulating Pseudomonas aeruginosa biofilm development. PLoS Pathog 5:e1000668.
175. Typas A, Banzhaf M, Gross CA, Vollmer W. 2012. From the regulation of peptidoglycan synthesis to bacterial growth and morphology. Nature Reviews Microbiology 10:123-136.
176. Stewart GC. 2005. Taking shape: control of bacterial cell wall biosynthesis. Molecular microbiology 57:1177-1181.
177. Broder UN, Jaeger T, Jenal U. 2016. LadS is a calcium-responsive kinase that induces acute-to-chronic virulence switch in Pseudomonas aeruginosa. Nature Microbiology 2:16184.
178. Chang Y, Bruni R, Kloss B, Assur Z, Kloppmann E, Rost B, Hendrickson WA, Liu Q. 2014. Structural basis for a pH-sensitive calcium leak across membranes. Science 344:1131-1135.

179. Smith EE, Sims EH, Spencer DH, Kaul R, Olson MV. 2005. Evidence for diversifying selection at the pyoverdine locus of Pseudomonas aeruginosa. Journal of bacteriology 187:2138-2147.
180. Lamont IL, Beare PA, Ochsner U, Vasil AI, Vasil ML. 2002. Siderophore-mediated signaling regulates virulence factor production in Pseudomonas aeruginosa. Proceedings of the National Academy of Sciences 99:7072-7077.
181. Banin E, Vasil ML, Greenberg EP. 2005. Iron and Pseudomonas aeruginosa biofilm formation. Proceedings of the National Academy of Sciences of the United States of America 102:11076-11081.
182. Vaara M. 1992. Agents that increase the permeability of the outer membrane. Microbiological reviews 56:395-411.
183. Asbell MA, Eagon R. 1966. Role of multivalent cations in the organization, structure, and assembly of the cell wall of Pseudomonas aeruginosa. Journal of bacteriology 92:380-387.
184. Sawyer JG, Martin NL, Hancock R. 1988. Interaction of macrophage cationic proteins with the outer membrane of Pseudomonas aeruginosa. Infection and immunity 56:693-698.
185. Whiteley M, Bangera MG, Bumgarner RE, Parsek MR. 2001. Gene expression in Pseudomonas aeruginosa biofilms. Nature 413:860.
186. Richards MJ, Edwards JR, Culver DH, Gaynes RP, Natl Nosocomial Infections S. 2000. Nosocomial infections in combined medical-surgical intensive care units in the United States. Infection Control and Hospital Epidemiology 21:510-515.
187. Falagas ME, Koletsi PK, Bliziotis IA. 2006. The diversity of definitions of multidrug-resistant (MDR) and pandrug-resistant (PDR) Acinetobacter baumannii and Pseudomonas aeruginosa. Journal of Medical Microbiology 55:1619-1629.
188. Hancock REW, Lehrer R. 1998. Cationic peptides: a new source of antibiotics. Trends in Biotechnology 16:82-88.
189. Edgar W, Dickinson K. 1962. A TRIAL OF COLISTIN METHANE SULPHONATE IN URINARY INFECTION WITH: Pseudomonas pyocyanea. The Lancet 280:739-740.
190. Falagas ME, Michalopoulos A. 2006. Polymyxins: old antibiotics are back. The Lancet 367:633.
191. Li J, Nation RL, Turnidge JD, Milne RW, Coulthard K, Rayner CR, Paterson DL. 2006. Colistin: the re-emerging antibiotic for multidrug-resistant Gram-negative bacterial infections. Lancet Infectious Diseases 6:589-601.
192. Zavascki AP, Goldani LZ, Li J, Nation RL. 2007. Polymyxin B for the treatment of multidrug-resistant pathogens: a critical review. Journal of Antimicrobial Chemotherapy 60:1206-1215.
193. Dean ACR. 1971. ADAPTIVE DRUG RESISTANCE IN GRAM-NEGATIVE BACTERIA. Proceedings of the Royal Society of Medicine-London 64:534-&.
194. Gilleland HE, Murray RGE. 1976. ULTRASTRUCTURAL STUDY OF POLYMYXIN-RESISTANT ISOLATES OF PSEUDOMONAS-AERUGINOSA. Journal of Bacteriology 125:267-281.

195. Skiada A, Markogiannakis A, Plachouras D, Daikos GL. 2011. Adaptive resistance to cationic compounds in Pseudomonas aeruginosa. International Journal of Antimicrobial Agents 37:187-193.
196. Wang X, Quinn PJ. 2010. Lipopolysaccharide: Biosynthetic pathway and structure modification. Progress in Lipid Research 49:97-107.
197. Ernst RK, Moskowitz SM, Emerson JC, Kraig GM, Adams KN, Harvey MD, Ramsey B, Speert DP, Burns JL, Miller SI. 2007. Unique lipid A modifications in Pseudomonas aeruginosa isolated from the airways of patients with cystic fibrosis. Journal of Infectious Diseases 196:1088-1092.
198. Li JD, Dohrman AF, Gallup M, Miyata S, Gum JR, Kim YS, Nadel JA, Prince A, Basbaum CB. 1997. Transcriptional activation of mucin by Pseudomonas aeruginosa lipopolysaccharide in the pathogenesis of cystic fibrosis lung disease. Proceedings of the National Academy of Sciences of the United States of America 94:967-972.
199. Ernst RK, Hajjar AM, Tsai JH, Moskowitz SM, Wilson CB, Miller SI. 2003. Pseudomonas aeruginosa lipid A diversity and its recognition by Toll-like receptor 4. Journal of Endotoxin Research 9:395-400.
200. Ciornei CD, Novikov A, Beloin C, Fitting C, Caroff M, Ghigo J-M, Cavaillon J-M, Adib-Conquy M. 2010. Biofilm-forming Pseudomonas aeruginosa bacteria undergo lipopolysaccharide structural modifications and induce enhanced inflammatory cytokine response in human monocytes. Innate Immunity 16:288-301.
201. Kulshin VA, Zahringer U, Lindner B, Jager KE, Dmitriev BA, Rietschel ET. 1991. STRUCTURAL CHARACTERIZATION OF THE LIPID-A COMPONENT OF PSEUDOMONAS-AERUGINOSA WILD-TYPE AND ROUGH MUTANT LIPOPOLYSACCHARIDES. European Journal of Biochemistry 198:697-704.
202. Zhou ZM, Ribeiro AA, Lin SH, Cotter RJ, Miller SI, Raetz CRH. 2001. Lipid A modifications in polymyxin-resistant Salmonella typhimurium - PMRA-dependent 4-amino-4-deoxy-L-arabinose, and phosphoethanolamine incorporation. Journal of Biological Chemistry 276:43111-43121.
203. Raetz CRH, Reynolds CM, Trent MS, Bishop RE. 2007. Lipid a modification systems in gram-negative bacteria, p 295-329, Annual Review of Biochemistry, vol 76.
204. King JD, Kocincova D, Westman EL, Lam JS. 2009. Lipopolysaccharide biosynthesis in Pseudomonas aeruginosa. Innate Immunity 15:261-312.
205. Miller AK, Brannon MK, Stevens L, Johansen HK, Selgrade SE, Miller SI, Hoiby N, Moskowitz SM. 2011. PhoQ Mutations Promote Lipid A Modification and Polymyxin Resistance of Pseudomonas aeruginosa Found in Colistin-Treated Cystic Fibrosis Patients. Antimicrobial Agents and Chemotherapy 55:5761-5769.
206. Poole K. 2011. Pseudomonas aeruginosa: resistance to the max. Frontiers in microbiology 2:65-65.
207. Olaitan AO, Morand S, Rolain J-M. 2014. Mechanisms of polymyxin resistance: acquired and intrinsic resistance in bacteria. Frontiers in microbiology 5:643.

208. Macfarlane EL, Kwasnicka A, Ochs MM, Hancock RE. 1999. PhoP–PhoQ homologues in Pseudomonas aeruginosa regulate expression of the outer-membrane protein OprH and polymyxin B resistance. Molecular microbiology 34:305-316.
209. McPhee JB, Lewenza S, Hancock RE. 2003. Cationic antimicrobial peptides activate a two-component regulatory system, PmrA-PmrB, that regulates resistance to polymyxin B and cationic antimicrobial peptides in Pseudomonas aeruginosa. Molecular microbiology 50:205-217.
210. Moskowitz SM, Ernst RK, Miller SI. 2004. PmrAB, a two-component regulatory system of Pseudomonas aeruginosa that modulates resistance to cationic antimicrobial peptides and addition of aminoarabinose to lipid A. Journal of Bacteriology 186:575-579.
211. Gutu AD, Sgambati N, Strasbourger P, Brannon MK, Jacobs MA, Haugen E, Kaul RK, Johansen HK, Høiby N, Moskowitz SM. 2013. Polymyxin resistance of Pseudomonas aeruginosa phoQ mutants is dependent on additional two-component regulatory systems. Antimicrobial agents and chemotherapy 57:2204-2215.
212. Franklin MJ, Ohman DE. 1993. Identification of algF in the alginate biosynthetic gene cluster of Pseudomonas aeruginosa which is required for alginate acetylation. Journal of bacteriology 175:5057-5065.
213. Kuroda A, Kumano T, Taguchi K, Nikata T, Kato J, Ohtake H. 1995. Molecular cloning and characterization of a chemotactic transducer gene in Pseudomonas aeruginosa. Journal of bacteriology 177:7019-7025.
214. Mindich L, Cohen J, Weisburd M. 1976. Isolation of nonsense suppressor mutants in Pseudomonas. Journal of Bacteriology 126:177-182.
215. Yang J, Yan R, Roy A, Xu D, Poisson J, Zhang Y. 2015. The I-TASSER Suite: protein structure and function prediction. Nature methods 12:7-8.
216. Roy A, Kucukural A, Zhang Y. 2010. I-TASSER: a unified platform for automated protein structure and function prediction. Nature protocols 5:725-738.
217. Zhang Y. 2008. I-TASSER server for protein 3D structure prediction. BMC bioinformatics 9:40.
218. Schrödinger L. The PyMOL Molecular Graphics System, version 1.8; Schrödinger, LLC, 2015. There is no corresponding record for this reference.
219. Marchler-Bauer A, Bo Y, Han L, He J, Lanczycki CJ, Lu S, Chitsaz F, Derbyshire MK, Geer RC, Gonzales NR. 2017. CDD/SPARCLE: functional classification of proteins via subfamily domain architectures. Nucleic acids research 45:D200-D203.
220. Krogh A, Larsson B, Von Heijne G, Sonnhammer EL. 2001. Predicting transmembrane protein topology with a hidden Markov model: application to complete genomes. Journal of molecular biology 305:567-580.
221. D'Amato RF, Thornsberry C, Baker CN, Kirven LA. 1975. Effect of calcium and magnesium ions on the susceptibility of Pseudomonas species to tetracycline,

gentamicin polymyxin B, and carbenicillin. Antimicrobial agents and chemotherapy 7:596-600.
222. Reller LB, Schoenknecht FD, Kenny MA, Sherris JC. 1974. Antibiotic susceptibility testing of Pseudomonas aeruginosa: selection of a control strain and criteria for magnesium and calcium content in media. Journal of Infectious Diseases 130:454-463.
223. Davis SD, Iannetta A, Wedgwood RJ. 1971. Activity of colistin against Pseudomonas aeruginosa: inhibition by calcium. Journal of Infectious Diseases 124:610-612.
224. Kenward M, Brown M, Fryer J. 1979. The Influence of Calcium or Manganese on the Resistance to EDTA, Polymyxin B or Cold Shock, and the Composition of Pseudomonas aeruginosa Grown in Glucose-or Magnesium-depleted Batch Cultures. Journal of Applied Bacteriology 47:489-503.
225. Gunn JS, Miller SI. 1996. PhoP-PhoQ activates transcription of pmrAB, encoding a two-component regulatory system involved in Salmonella typhimurium antimicrobial peptide resistance. Journal of Bacteriology 178:6857-6864.
226. Gooderham WJ, Bains M, McPhee JB, Wiegand I, Hancock RE. 2008. Induction by cationic antimicrobial peptides and involvement in intrinsic polymyxin and antimicrobial peptide resistance, biofilm formation, and swarming motility of PsrA in Pseudomonas aeruginosa. Journal of bacteriology 190:5624-5634.
227. Kuznetsova E. 2009. Activity-based functional annotation of unknown proteins: HAD-like hydrolases from E. coli and S. cerevisiaeDepartment of Medical Biophysics, University of Toronto.
228. Kuznetsova E, Proudfoot M, Gonzalez CF, Brown G, Omelchenko MV, Borozan I, Carmel L, Wolf YI, Mori H, Savchenko AV. 2006. Genome-wide analysis of substrate specificities of the Escherichia coli haloacid dehalogenase-like phosphatase family. Journal of Biological Chemistry 281:36149-36161.
229. Rudbeck ME, Blomberg MR, Barth A. 2013. Hydrolysis of the E2P Phosphoenzyme of the Ca2+-ATPase: A Theoretical Study. The Journal of Physical Chemistry B 117:9224-9232.
230. Winsor GL, Griffiths EJ, Lo R, Dhillon BK, Shay JA, Brinkman FS. 2016. Enhanced annotations and features for comparing thousands of Pseudomonas genomes in the Pseudomonas genome database. Nucleic acids research 44:D646-D653.
231. Pletzer D, Lafon C, Braun Y, Köhler T, Page MG, Mourez M, Weingart H. 2014. High-throughput screening of dipeptide utilization mediated by the ABC transporter DppBCDF and its substrate-binding proteins DppA1-A5 in Pseudomonas aeruginosa. PloS one 9:e111311.
232. Abouhamad W, Manson M, Gibson M, Higgins C. 1991. Peptide transport and chemotaxis in Escherichia coli and Salmonella typhimurium: characterization of the dipeptide permease (Dpp) and the dipeptide-binding protein. Molecular microbiology 5:1035-1047.

233. Felder CB, Graul RC, Lee AY, Merkle H-P, Sadee W. 1999. The Venus flytrap of periplasmic binding proteins: an ancient protein module present in multiple drug receptors. The AAPS Journal 1:7-26.
234. Li J, Nation RL, Turnidge JD, Milne RW, Coulthard K, Rayner CR, Paterson DL. 2006. Colistin: the re-emerging antibiotic for multidrug-resistant Gram-negative bacterial infections. The Lancet infectious diseases 6:589-601.
235. Evans ME, Feola DJ, Rapp RP. 1999. Polymyxin B sulfate and colistin: old antibiotics for emerging multiresistant gram-negative bacteria. Annals of Pharmacotherapy 33:960-967.
236. Barrow K, Kwon DH. 2009. Alterations in two-component regulatory systems of phoPQ and pmrAB are associated with polymyxin B resistance in clinical isolates of Pseudomonas aeruginosa. Antimicrobial agents and chemotherapy 53:5150-5154.
237. Gunn JS, Lim KB, Krueger J, Kim K, Guo L, Hackett M, Miller SI. 1998. PmrA-PmrB-regulated genes necessary for 4-aminoarabinose lipid A modification and polymyxin resistance. Molecular Microbiology 27:1171-1182.
238. Ternan NG, Mc Grath JW, Mc Mullan G, Quinn JP. 1998. Review: organophosphonates: occurrence, synthesis and biodegradation by microorganisms. World Journal of Microbiology and Biotechnology 14:635-647.
239. Dumora C, Marche M, Doignon F, Aigle M, Cassaigne A, Crouzet M. 1997. First characterization of the phosphonoacetaldehyde hydrolase gene of Pseudomonas aeruginosa. Gene 197:405-412.
240. Tamae C, Liu A, Kim K, Sitz D, Hong J, Becket E, Bui A, Solaimani P, Tran KP, Yang H. 2008. Determination of antibiotic hypersensitivity among 4,000 single-gene-knockout mutants of Escherichia coli. Journal of bacteriology 190:5981-5988.
241. Han X, Dorsey-Oresto A, Malik M, Wang J-Y, Drlica K, Zhao X, Lu T. 2010. Escherichia coli genes that reduce the lethal effects of stress. BMC microbiology 10:35.
242. Yu X, Doroghazi JR, Janga SC, Zhang JK, Circello B, Griffin BM, Labeda DP, Metcalf WW. 2013. Diversity and abundance of phosphonate biosynthetic genes in nature. Proceedings of the National Academy of Sciences 110:20759-20764.
243. Bredenbruch F, Geffers R, Nimtz M, Buer J, Häussler S. 2006. The Pseudomonas aeruginosa quinolone signal (PQS) has an iron-chelating activity. Environmental microbiology 8:1318-1329.
244. Tremblay J, Déziel E. 2010. Gene expression in Pseudomonas aeruginosa swarming motility. BMC genomics 11:587.
245. Backhed F, Normark S, Schweda EKH, Oscarson S, Richter-Dahlfors A. 2003. Structural requirements for TLR4-mediated LPS signalling: a biological role for LPS modifications. Microbes and Infection 5:1057-1063.
246. Mikkelsen H, McMullan R, Filloux A. 2011. The Pseudomonas aeruginosa reference strain PA14 displays increased virulence due to a mutation in ladS. PLoS One 6:e29113.

247. Cai XJ, Wang XB, Patel S, Capham DE. 2015. Insights into the early evolution of animal calcium signaling machinery: A unicellular point of view. Cell Calcium 57:166-173.
248. Clapham DE. 2007. Calcium signaling. Cell 131:1047-1058.
249. Marchadier E, Oates ME, Fang H, Donoghue PCJ, Hetherington AM, Gough J. 2016. Evolution of the Calcium-Based Intracellular Signaling System. Genome Biology and Evolution 8:2118-2132.
250. Plattner H, Verkhratsky A. 2015. Evolution of calcium signalling. Cell Calcium 57:121-122.
251. Dominguez DC. 2004. Calcium signalling in bacteria. Molecular microbiology 54:291-297.
252. Nowycky MC, Thomas AP. 2002. Intracellular calcium signaling. Journal of cell science 115:3715-3716.
253. Shuai J, Jung P. 2002. Optimal intracellular calcium signaling. Physical review letters 88:068102.
254. Putney JW. 2005. Capacitative calcium entry sensing the calcium stores. The Journal of cell biology 169:381-382.
255. Ramsey IS, Delling M, Clapham DE. 2006. An introduction to TRP channels. Annu Rev Physiol 68:619-647.
256. Yáñez M, Gil-Longo J, Campos-Toimil M. 2012. Calcium binding proteins, p 461-482, Calcium Signaling. Springer.
257. Gangola P, Rosen B. 1987. Maintenance of intracellular calcium in Escherichia coli. Journal of Biological Chemistry 262:12570-12574.
258. Knight MR, Campbell AK, Smith SM, Trewavas AJ. 1991. Recombinant aequorin as a probe for cytosolic free Ca2+ in Escherichia coli. FEBS letters 282:405-408.
259. Raeymaekers L, Wuytack E, Willems I, Michiels C, Wuytack F. 2002. Expression of a P-type Ca 2+-transport ATPase in Bacillus subtilis during sporulation. Cell calcium 32:93-103.
260. Seufferheld M, Lea CR, Vieira M, Oldfield E, Docampo R. 2004. The H+-pyrophosphatase of Rhodospirillum rubrum is predominantly located in polyphosphate-rich acidocalcisomes. Journal of Biological Chemistry 279:51193-51202.
261. Seufferheld M, Vieira MC, Ruiz FA, Rodrigues CO, Moreno SN, Docampo R. 2003. Identification of organelles in bacteria similar to acidocalcisomes of unicellular eukaryotes. Journal of Biological Chemistry 278:29971-29978.
262. van Asselt EJ, Dijkstra BW. 1999. Binding of calcium in the EF-hand of Escherichia coli lytic transglycosylase Slt35 is important for stability. FEBS letters 458:429-435.
263. Bilecen K, Yildiz FH. 2009. Identification of a calcium-controlled negative regulatory system affecting Vibrio cholerae biofilm formation. Environmental microbiology 11:2015-2029.

264. Lu D, Shang G, Zhang H, Yu Q, Cong X, Yuan J, He F, Zhu C, Zhao Y, Yin K. 2014. Structural insights into the T6SS effector protein Tse3 and the Tse3–Tsi3 complex from Pseudomonas aeruginosa reveal a calcium-dependent membrane-binding mechanism. Molecular microbiology 92:1092-1112.
265. Wolfgang MC, Lee VT, Gilmore ME, Lory S. 2003. Coordinate regulation of bacterial virulence genes by a novel adenylate cyclase-dependent signaling pathway. Developmental cell 4:253-263.
266. Kenny MA, Pollock HM, Minshew BH, Casillas E, Schoenknecht FD. 1980. Cation components of Mueller-Hinton agar affecting testing of Pseudomonas aeruginosa susceptibility to gentamicin. Antimicrob Agents Chemother 17:55-62.
267. Long F, Su CC, Lei HT, Bolla JR, Do SV, Yu EW. 2012. Structure and mechanism of the tripartite CusCBA heavy-metal efflux complex. Philosophical Transactions of the Royal Society B-Biological Sciences 367:1047-1058.
268. Sobel ML, McKay GA, Poole K. 2003. Contribution of the MexXY multidrug transporter to aminoglycoside resistance in Pseudomonas aeruginosa clinical isolates. Antimicrobial Agents and Chemotherapy 47:3202-3207.
269. Kulaev I, Kulakovskaya T. 2000. Polyphosphate and phosphate pump. Annual Reviews in Microbiology 54:709-734.
270. Reusch RN. 1992. Biological complexes of poly-β-hydroxybutyrate. FEMS microbiology reviews 9:119-129.
271. Reusch R. 1999. Polyphosphate/poly-(R)-3-hydroxybutyrate) ion channels in cell membranes, p 151-182, Inorganic Polyphosphates. Springer.
272. Jones HE, Holland I, Baker HL, Campbell AK. 1999. Slow changes in cytosolic free Ca2+ inEscherichia colihighlight two putative influx mechanisms in response to changes in extracellular calcium. Cell calcium 25:265-274.
273. Macfarlane ELA, Kwasnicka A, Hancock REW. 2000. Role of Pseudomonas aeruginosa PhoP-PhoQ in resistance to antimicrobial cationic peptides and aminoglycosides. Microbiology-Uk 146:2543-2554.
274. Coornaert A, Lu A, Mandin P, Springer M, Gottesman S, Guillier M. 2010. MicA sRNA links the PhoP regulon to cell envelope stress. Molecular Microbiology 76:467-479.
275. Zhao GJ, Hong GL, Liu JQ, Lu Y, Lu ZQ. 2014. Septic shock due to community-acquired *Pseudomonas aeruginosa* necrotizing fasciitis: A case report and literature review. Experimental and Therapeutic Medicine 7:1545-1548.
276. Lakkis C, Fleiszig SM. 2001. Resistance of *Pseudomonas aeruginosa* isolates to hydrogel contact lens disinfection correlates with cytotoxic activity. J Clin Microbiol 39:1477-86.
277. Silby MW, Winstanley C, Godfrey SA, Levy SB, Jackson RW. 2011. Pseudomonas genomes: diverse and adaptable. FEMS Microbiol Rev 35:652-80.
278. Gooderham WJ, Hancock RE. 2009. Regulation of virulence and antibiotic resistance by two-component regulatory systems in *Pseudomonas aeruginosa*. FEMS Microbiol Rev 33:279-94.

279. Guragain M, Lenaburg DL, Moore FS, Reutlinger I, Patrauchan MA. 2013. Calcium homeostasis in *Pseudomonas aeruginosa* requires multiple transporters and modulates swarming motility. Cell Calcium 54:350-61.
280. Anderson S, Appanna VD, Huang J, Viswanatha T. 1992. A novel role for calcite in calcium homeostasis. FEBS Lett 308:94-6.
281. Glunk C, Dupraz C, Braissant O, Gallagher KL, Verrecchia EP, Visscher PT. 2011. Microbially mediated carbonate precipitation in a hypersaline lake, Big Pond (Eleuthera, Bahamas). Sedimentology 58:720-738.
282. Steinhorst L, Kudla J. 2013. Calcium - a central regulator of pollen germination and tube growth. Biochim Biophys Acta 1833:1573-81.
283. Bose J, Pottosin, II, Shabala SS, Palmgren MG, Shabala S. 2011. Calcium efflux systems in stress signaling and adaptation in plants. Front Plant Sci 2:85.
284. Robertson WG, Marshall RW, Bowers GN. 1981. Ionized calcium in body-fluids. Crc Critical Reviews in Clinical Laboratory Sciences 15:85-125.
285. Blomfiel.J, Warton KL, Brown JM. 1973. Flow-rate and inorganic components of submandibular saliva in cystic-fibrosis. Archives of Disease in Childhood 48:267-274.
286. Berg JM, Tymoczko, J. L., and Stryer, L. 2002. Biochemistry, vol 5. W. H. Freeman.
287. Vitolo MR, Valente Soares LM, Carvalho EB, Cardoso CB. 2004. Calcium and magnesium concentrations in mature human milk: influence of calcium intake, age and socioeconomic level. Arch Latinoam Nutr 54:118-22.
288. Lorin MI, Gaerlan PF, Mandel ID, Denning CR. 1976. COMPOSITION OF NASAL SECRETION IN PATIENTS WITH CYSTIC-FIBROSIS. Journal of Laboratory and Clinical Medicine 88:114-117.
289. Sanders NN, Franckx H, De Boeck K, Haustraete J, De Smedt SC, Demeester J. 2006. Role of magnesium in the failure of rhDNase therapy in patients with cystic fibrosis. Thorax 61:962-8.
290. Smith DJ, Anderson GJ, Bell SC, Reid DW. 2014. Elevated metal concentrations in the CF airway correlate with cellular injury and disease severity. J Cyst Fibros 13:289-95.
291. Patrauchan MA, Sarkisova SA, Franklin MJ. 2007. Strain-specific proteome responses of *Pseudomonas aeruginosa* to biofilm-associated growth and to calcium. Microbiology 153:3838-51.
292. Stock AM, Robinson VL, Goudreau PN. 2000. Two-component signal transduction. Annual review of biochemistry 69:183-215.
293. Hoch JA. 2000. Two-component and phosphorelay signal transduction. Curr Opin Microbiol 3:165-70.
294. McPhee JB, Bains M, Winsor G, Lewenza S, Kwasnicka A, Brazas MD, Brinkman FS, Hancock RE. 2006. Contribution of the PhoP-PhoQ and PmrA-PmrB two-component regulatory systems to Mg2+-induced gene regulation in *Pseudomonas aeruginosa*. J Bacteriol 188:3995-4006.

295. McPhee JB, Lewenza S, Hancock REW. 2003. Cationic antimicrobial peptides activate a two-component regulatory system, PmrA-PmrB, that regulates resistance to polymyxin B and cationic antimicrobial peptides in *Pseudomonas aeruginosa*. Molecular Microbiology 50:205-217.
296. Moskowitz SM, Ernst RK, Miller SI. 2004. PmrAB, a two-component regulatory system of *Pseudomonas aeruginosa* that modulates resistance to cationic antimicrobial peptides and addition of aminoarabinose to lipid A. J Bacteriol 186:575-9.
297. Miller AK, Brannon MK, Stevens L, Johansen HK, Selgrade SE, Miller SI, Hoiby N, Moskowitz SM. 2011. PhoQ mutations promote lipid A modification and polymyxin resistance of *Pseudomonas aeruginosa* found in colistin-treated cystic fibrosis patients. Antimicrob Agents Chemother 55:5761-9.
298. Gooderham WJ, Gellatly SL, Sanschagrin F, McPhee JB, Bains M, Cosseau C, Levesque RC, Hancock RE. 2009. The sensor kinase PhoQ mediates virulence in *Pseudomonas aeruginosa*. Microbiology 155:699-711.
299. Brinkman FSL, MacFarlane ELA, Warrener P, Hancock REW. 2001. Evolutionary relationships among virulence-associated histidine kinases. Infection and Immunity 69:5207-5211.
300. Kwon DH, Lu CD. 2006. Polyamines induce resistance to cationic peptide, aminoglycoside, and quinolone antibiotics in *Pseudomonas aeruginosa* PAO1. Antimicrobial Agents and Chemotherapy 50:1615-1622.
301. Perron K, Caille O, Rossier C, van Delden C, Dumas JL, Kohler T. 2004. CzcR-CzcS, a two-component system involved in heavy metal and carbapenem resistance in *Pseudomonas aeruginosa*. Journal of Biological Chemistry 279:8761-8768.
302. Rahme LG, Ausubel FM, Cao H, Drenkard E, Goumnerov BC, Lau GW, Mahajan-Miklos S, Plotnikova J, Tan MW, Tsongalis J, Walendziewicz CL, Tompkins RG. 2000. Plants and animals share functionally common bacterial virulence factors. Proc Natl Acad Sci U S A 97:8815-21.
303. Whitchurch CB, Alm RA, Mattick JS. 1996. The alginate regulator AlgR and an associated sensor FimS are required for twitching motility in *Pseudomonas aeruginosa*. Proc Natl Acad Sci U S A 93:9839-43.
304. Carterson AJ, Morici LA, Jackson DW, Frisk A, Lizewski SE, Jupiter R, Simpson K, Kunz DA, Davis SH, Schurr JR, Hassett DJ, Schurr MJ. 2004. The transcriptional regulator AlgR controls cyanide production in *Pseudomonas aeruginosa*. J Bacteriol 186:6837-44.
305. Lizewski SE, Lundberg DS, Schurr MJ. 2002. The transcriptional regulator AlgR is essential for *Pseudomonas aeruginosa* pathogenesis. Infection and Immunity 70:6083-6093.
306. Reimmann C, Beyeler M, Latifi A, Winteler H, Foglino M, Lazdunski A, Haas D. 1997. The global activator GacA of *Pseudomonas aeruginosa* PAO positively controls the production of the autoinducer N-butyryl-homoserine lactone and the

formation of the virulence factors pyocyanin, cyanide, and lipase. Mol Microbiol 24:309-19.
307. Linares JF, Gustafsson I, Baquero F, Martinez JL. 2006. Antibiotics as intermicrobial signaling agents instead of weapons. Proceedings of the National Academy of Sciences of the United States of America 103:19484-19489.
308. Whitchurch CB, Erova TE, Emery JA, Sargent JL, Harris JM, Semmler ABT, Young MD, Mattick JS, Wozniak DJ. 2002. Phosphorylation of the *Pseudomonas aeruginosa* response regulator AlgR is essential for type IV fimbria-mediated twitching motility. Journal of Bacteriology 184:4544-4554.
309. Morici LA, Carterson AJ, Wagner VE, Frisk A, Schurr JR, Bentrup KHZ, Hassett DJ, Iglewski BH, Sauer K, Schurr MJ. 2007. *Pseudomonas aeruginosa* AlgR represses the Rhl quorum-sensing system in a biofilm-specific manner. Journal of Bacteriology 189:7752-7764.
310. Ritchings BW, Almira EC, Lory S, Ramphal R. 1995. Cloning and Phenotypic Characterization of Fles and Fler, New Response Regulators of *Pseudomonas aeruginosa* Which Regulate Motility and Adhesion to Mucin. Infection and Immunity 63:4868-4876.
311. Breidenstein EBM, Khaira BK, Wiegand I, Overhage J, Hancock REW. 2008. Complex Ciprofloxacin Resistome Revealed by Screening a *Pseudomonas aeruginosa* Mutant Library for Altered Susceptibility. Antimicrobial Agents and Chemotherapy 52:4486-4491.
312. Hurley BP, Goodman AL, Mumy KL, Murphy P, Lory S, McCormick BA. 2010. The two-component sensor response regulator RoxS/RoxR plays a role in *Pseudomonas aeruginosa* interactions with airway epithelial cells. Microbes Infect 12:190-8.
313. Damron FH, McKenney ES, Schweizer HP, Goldberg JB. 2013. Construction of a broad-host-range Tn7-based vector for single-copy PBAD-controlled gene expression in Gram-negative bacteria. Applied and environmental microbiology 79:718-721.
314. Hoang TT, Karkhoff-Schweizer RR, Kutchma AJ, Schweizer HP. 1998. A broad-host-range Flp-FRT recombination system for site-specific excision of chromosomally-located DNA sequences: application for isolation of unmarked *Pseudomonas aeruginosa* mutants. Gene 212:77-86.
315. Liu L, Ridefelt P, Håkansson L, Venge P. 1999. Regulation of Human Eosinophil Migration Across Lung Epithelial Monolayers by Distinct Calcium Signaling Mechanisms in the Two Cell Types. The Journal of Immunology 163:5649-5655.
316. Clapham DE. 2007. Calcium signaling. Cell 131:1047-58.
317. Halmerbauer G, Arri S, Schierl M, Strauch E, Koller DY. 2000. The relationship of eosinophil granule proteins to ions in the sputum of patients with cystic fibrosis. Clinical & Experimental Allergy 30:1771-1776.

318. Lorin MI GP, Mandel ID, Denning CR. 1976. Composition of nasal secretion in patients with cystic fibrosis. The Journal of laboratory and clinical medicine 88:114-117.
319. Sabanayagam C SA. 2011. Serum calcium levels and hypertension among U.S. adults. Journal of Clinical Hypertension 13:716-21. .
320. Rolf Jorde JS, Patrick Fitzgerald, and Kaare H. Bønaa. 1999. Serum Calcium and Cardiovascular Risk Factors and Diseases: The Tromsø Study. Hypertension 34.
321. Kholová I, Dragneva G, Čermáková P, Laidinen S, Kaskenpää N, Hazes T, Čermáková E, Šteiner I, Ylä-Herttuala S. 2011. Lymphatic vasculature is increased in heart valves, ischaemic and inflamed hearts and in cholesterol-rich and calcified atherosclerotic lesions. European Journal of Clinical Investigation 41:487-497.
322. Shanahan CM, Crouthamel MH, Kapustin A, Giachelli CM. 2011. Arterial Calcification in Chronic Kidney Disease: Key Roles for Calcium and Phosphate. Circulation Research 109:697-711.
323. Gilardini L, Pasqualinotto L, Di Matteo S, Caffetto K, Croci M, Girola A, Invitti C. 2011. Factors Associated With Early Atherosclerosis and Arterial Calcifications in Young Subjects With a Benign Phenotype of Obesity. Obesity 19:1684-1689.
324. Naruhiko Ishiwada KN, Shigeru Tateno; Masao Yoshinaga,, Masaru Terai MN. 2005. Causative Organism Influences Clinical Profile and Outcome of Infective Endocarditis in Pediatric Patients and Adults With Congenital Heart Disease. Circulation journal 69:1266 – 1270.
325. Von Ruecker AA, Bertele, Rosemarie, Karsten Harms, H. 1984. Calcium metabolism and cystic fibrosis: mitochondrial abnormalities suggest a modification of the mitochondrial membrane. Pediatric research 18:594-599.
326. Minardi G, Pino P, Sordi M, Pavaci H, Manzara C, Pulignano G, Natale E, Gaudio C. 2009. Infective endocarditis on mitral annular calcification: a case report. Cases Journal 2:9072.
327. Stewart VL, Herling P, Dalinka MK. 1983. CAlcification in soft tissues. JAMA 250:78-81.
328. Black AS KI. 1985. A review of soft tissue calcifications. The Journal of Foot Surgery 24:243-250.
329. Ojemann JG, Grubb RL, Kyriakos M, Baker KB. 1997. Calcium carbonate apatite deposition in the cervical spine with associated vertebral destruction. Journal of Neurosurgery 86:1022-1026.
330. Keefe WE. 1976. Formation of crystalline deposits by several genera of the family *Enterobacteriaceae.* Infection and Immunity 14:590-592.
331. Carson DA. 1998. An infectious origin of extraskeletal calcification. Proc Natl Acad Sci USA 95:7846–7847.
332. Hofbauer LC, Brueck CC, Shanahan CM, Schoppet M, Dobnig H. 2007. Vascular calcification and osteoporosis—from clinical observation towards molecular understanding. Osteoporosis International 18:251-259.

333. Li Q, Brodsky JL, Conlin LK, Pawel B, Glatz AC, Gafni RI, Schurgers L, Uitto J, Hakonarson H, Deardorff MA, Levine MA. 2014. Mutations in the ABCC6 Gene as a Cause of Generalized Arterial Calcification of Infancy: Genotypic Overlap with Pseudoxanthoma Elasticum. J Invest Dermatol 134:658-665.
334. Nelsen DA. 2002. Gluten-Sensitive Enteropathy (Celiac Disease): More Common Than You Think. American Family Physician 66:2259-2266.
335. Young JMaJD-E. 2008. Purported nanobacteria in human blood as calcium carbonate nanoparticles. Proceedings of the National Academy of Sciences 105:5549-5554.
336. Rodriguez-Navarro C, Jroundi F, Schiro M, Ruiz-Agudo E, González-Muñoz MT. 2012. Influence of Substrate Mineralogy on Bacterial Mineralization of Calcium Carbonate: Implications for Stone Conservation. Applied and Environmental Microbiology 78:4017-4029.
337. Hammes F, Verstraete, Willy. 2002. Key roles of pH and calcium metabolism in microbial carbonate precipitation. Reviews in Environmental Science and Biotechnology 1:3-7.
338. Reddy MS. 2013. Biomineralization of calcium carbonates and their engineered applications: a review. Frontiers in Microbiology 4.
339. Fortin D, F. G. Ferris, and T. J. Beveridge. 1997. Surface-mediated mineral development by bacteria. Reviews in Mineralogy and Geochemistry 35:161-180.
340. Douglas S, and T. J. Beveridge. . 1998. Mineral formation by bacteria in natural microbial communities. FEMS Microbiology Ecology 26:79-88.
341. Bäuerlein E. 2003. Biomineralization of unicellular organisms: an unusual membrane biochemistry for the production of inorganic nano- and microstructures. . Angewandte Chemie International Edition 42:614-641.
342. Castanier S, Le Métayer-Levrel,G., Jean-Pierre Perthuisot, J.-P. 1999. Ca-carbonates precipitation and limestone genesis — the microbiogeologist point of view. . Sedimentary Geology 126:9-23.
343. Castanier S, Le Métayer-Levrel G, Orial G, Loubière J-F, Perthuisot J-P. 2000. Bacterial Carbonatogenesis and Applications to Preservation and Restoration of Historic Property, p 203-218. *In* Ciferri O, Tiano P, Mastromei G (ed), Of Microbes and Art doi:10.1007/978-1-4615-4239-1_14. Springer US.
344. Anderson S AV, Huang J, Viswanatha T. 1992. A novel role for calcite in calcium homeostasis. FEBS letters 308:94-96.
345. Zamarreño DV IR, May E. 2009. Carbonate crystals precipitated by freshwater bacteria and their use as a limestone consolidant. Applied and Environmental Microbiology 75:5981-5990.
346. Barabesi C, Galizzi A, Mastromei G, Rossi M, Tamburini E, Perito B. 2007. *Bacillus subtilis* Gene Cluster Involved in Calcium Carbonate Biomineralization. Journal of Bacteriology 189:228-235.
347. Smith KS, Ferry JG. 2000. Prokaryotic carbonic anhydrases. FEMS Microbiol Rev 24:335-66.

348. Favre N, Christ ML, Pierre AC. 2009. Biocatalytic capture of CO2 with carbonic anhydrase and its transformation to solid carbonate. Journal of Molecular Catalysis B: Enzymatic 60:163-170.
349. Gaume B, Fouchereau-Peron M, Badou A, Helléouet M-N, Huchette S, Auzoux-Bordenave S. 2011. Biomineralization markers during early shell formation in the European abalone Haliotis tuberculata, Linnaeus. Marine Biology 158:341-353.
350. Tohse H, Ando H, Mugiya Y. 2004. Biochemical properties and immunohistochemical localization of carbonic anhydrase in the sacculus of the inner ear in the salmon Oncorhynchus masou. Comparative Biochemistry and Physiology Part A: Molecular & Integrative Physiology 137:87-94.
351. Aurélie Moya ST, Anthony Bertucci, Eric Tambutté, Séverine Lotto, Daniela Vullo, Claudiu T. Supuran, Denis Allemand, and Didier Zoccola. 2008. Carbonic Anhydrase in the Scleractinian Coral *Stylophora pistillata*: Characterization, Localization, And Role In Biomineralization. Journal of Biological Chemistry 283:25475-25484.
352. Wei Li L-PL, Peng-Peng Zhou, Long Cao, Long-Jiang Yu, and Shi-Yun Jiang. 2011. Calcite precipitation induced by bacteria and bacterially produced carbonic anhydrase Current Science 100.
353. Ramanan R, Kannan K, Sivanesan S, Mudliar S, Kaur S, Tripathi A, Chakrabarti T. 2009. Bio-sequestration of carbon dioxide using carbonic anhydrase enzyme purified from *Citrobacter freundii*. World Journal of Microbiology and Biotechnology 25:981-987.
354. Lotlikar SR, Hnatusko S, Dickenson NE, Choudhari SP, Picking WL, Patrauchan MA. 2013. Three functional β-carbonic anhydrases in Pseudomonas aeruginosa PAO1: role in survival in ambient air. Microbiology 159:1748-1759.
355. Hai-Bo Jiang H-MC, Kun-Shan Gao, and Bao-Sheng Qiu. 2013. Inactivation of Ca^{2+}/H^{+} Exchanger in *Synechocystis sp.* Strain PCC 6803 Promotes Cyanobacterial Calcification by Upregulating CO_2-Concentrating Mechanisms. Applied and Environmental Microbiology 79:4048-4055.
356. Son MS, Matthews WJ, Kang Y, Nguyen DT, Hoang TT. 2007. In Vivo Evidence of *Pseudomonas aeruginosa* Nutrient Acquisition and Pathogenesis in the Lungs of Cystic Fibrosis Patients. Infection and Immunity 75:5313-5324.
357. Bielecki P, Komor U, Bielecka A, Müsken M, Puchałka J, Pletz MW, Ballmann M, Martins dos Santos VAP, Weiss S, Häussler S. 2013. Ex vivo transcriptional profiling reveals a common set of genes important for the adaptation of *Pseudomonas aeruginosa* to chronically infected host sites. Environmental Microbiology 15:570-587.
358. Bury-Mone S, Mendz GL, Ball GE, Thibonnier M, Stingl K, Ecobichon C, Ave P, Huerre M, Labigne A, Thiberge JM, De Reuse H. 2008. Roles of alpha and beta carbonic anhydrases of *Helicobacter pylori* in the urease-dependent response to acidity and in colonization of the murine gastric mucosa. Infection and immunity 76:497-509.

359. Valdivia RH, Falkow S. 1997. Fluorescence-based isolation of bacterial genes expressed within host cells. Science (New York, NY 277:2007-11.
360. Burghout P, Cron LE, Gradstedt H, Quintero B, Simonetti E, Bijlsma JJE, Bootsma HJ, Hermans PWM. 2010. Carbonic Anhydrase Is Essential for Streptococcus pneumoniae Growth in Environmental Ambient Air. Journal of Bacteriology 192:4054-4062.
361. Covarrubias AS, Larsson AM, Högbom M, Lindberg J, Bergfors T, Björkelid C, Mowbray SL, Unge T, Jones TA. 2005. Structure and Function of Carbonic Anhydrases from *Mycobacterium tuberculosis*. Journal of Biological Chemistry 280:18782-18789.
362. Folkesson A, Jelsbak L, Yang L, Johansen HK, Ciofu O, Hoiby N, Molin S. 2012. Adaptation of Pseudomonas aeruginosa to the cystic fibrosis airway: an evolutionary perspective. Nature Reviews Microbiology 10:841-851.
363. Spiers AJ, Buckling A, Rainey PB. 2000. The causes of Pseudomonas diversity. Microbiology-Uk 146:2345-2350.
364. Silby MW, Winstanley C, Godfrey SAC, Levy SB, Jackson RW. 2011. Pseudomonas genomes: diverse and adaptable. Fems Microbiology Reviews 35:652-680.
365. Grosso-Becerra M-V, Santos-Medellin C, Gonzalez-Valdez A, Mendez J-L, Delgado G, Morales-Espinosa R, Servin-Gonzalez L, Alcaraz L-D, Soberon-Chavez G. 2014. Pseudomonas aeruginosa clinical and environmental isolates constitute a single population with high phenotypic diversity. Bmc Genomics 15.
366. Mathee K, Narasimhan G, Valdes C, Qiu X, Matewish JM, Koehrsen M, Rokas A, Yandava CN, Engels R, Zeng E, Olavarietta R, Doud M, Smith RS, Montgomery P, White JR, Godfrey PA, Kodira C, Birren B, Galagan JE, Lory S. 2008. Dynamics of Pseudomonas aeruginosa genome evolution. Proceedings of the National Academy of Sciences of the United States of America 105:3100-3105.
367. Burrows LL. 2012. Pseudomonas aeruginosa Twitching Motility: Type IV Pili in Action, p 493-520. *In* Gottesman S, Harwood CS, Schneewind O (ed), Annual Review of Microbiology, Vol 66, vol 66.
368. Saiman L, Prince A. 1993. PSEUDOMONAS-AERUGINOSA PILI BIND TO ASIALOGM1 WHICH IS INCREASED ON THE SURFACE OF CYSTIC-FIBROSIS EPITHELIAL-CELLS. Journal of Clinical Investigation 92:1875-1880.
369. Govan JRW, Deretic V. 1996. Microbial pathogenesis in cystic fibrosis: Mucoid Pseudomonas aeruginosa and Burkholderia cepacia. Microbiological Reviews 60:539-+.
370. Soberon-Chavez G, Lepine F, Deziel E. 2005. Production of rhamnolipids by Pseudomonas aeruginosa. Applied Microbiology and Biotechnology 68:718-725.
371. Zulianello L, Canard C, Kohler T, Caille D, Lacroix JS, Meda P. 2006. Rhamnolipids are virulence factors that promote early infiltration of primary human airway epithelia by Pseudomonas aeruginosa. Infection and Immunity 74:3134-3147.
372. Filloux A. 2011. Protein secretion systems in Pseudomonas aeruginosa: an essay on diversity, evolution, and function. Frontiers in Microbiology 2.

373. Lau GW, Hassett DJ, Ran HM, Kong FS. 2004. The role of pyocyanin in Pseudomonas aeruginosa infection. Trends in Molecular Medicine 10:599-606.
374. Newton K, Dixit VM. 2012. Signaling in innate immunity and inflammation. Cold Spring Harbor perspectives in biology 4:a006049.
375. Mahajan-Miklos S, Tan M-W, Rahme LG, Ausubel FM. 1999. Molecular mechanisms of bacterial virulence elucidated using a Pseudomonas aeruginosa–Caenorhabditis elegans pathogenesis model. Cell 96:47-56.
376. Tan M-W, Ausubel FM. 2000. Caenorhabditis elegans: a model genetic host to study Pseudomonas aeruginosa pathogenesis. Current opinion in microbiology 3:29-34.
377. Apidianakis Y, Rahme LG. 2009. Drosophila melanogaster as a model host for studying Pseudomonas aeruginosa infection. Nature protocols 4:1285-1294.
378. Lutter EI, Faria MM, Rabin HR, Storey DG. 2008. Pseudomonas aeruginosa cystic fibrosis isolates from individual patients demonstrate a range of levels of lethality in two Drosophila melanogaster infection models. Infection and immunity 76:1877-1888.
379. Lutter EI, Purighalla S, Duong J, Storey DG. 2012. Lethality and cooperation of Pseudomonas aeruginosa quorum-sensing mutants in Drosophila melanogaster infection models. Microbiology 158:2125-2132.
380. Palmer KL, Aye LM, Whiteley M. 2007. Nutritional cues control Pseudomonas aeruginosa multicellular behavior in cystic fibrosis sputum. Journal of bacteriology 189:8079-8087.
381. Brenner S. 1974. The genetics of Caenorhabditis elegans. Genetics 77:71-94.
382. Lutter EI, Purighalla S, Duong J, Storey DG. 2012. Lethality and cooperation of Pseudomonas aeruginosa quorum-sensing mutants in Drosophila melanogaster infection models. Microbiology-Sgm 158:2125-2132.
383. Cash H, Woods D, McCullough B, Johanson Jr W, Bass J. 1979. A Rat Model of Chronic Respiratory Infection with Pseudomonas aeruginosa 1, 2. American Review of Respiratory Disease 119:453-459.
384. Stotland PK, Radzioch D, Stevenson MM. 2000. Mouse models of chronic lung infection with Pseudomonas aeruginosa: models for the study of cystic fibrosis. Pediatric pulmonology 30:413-424.
385. Lutter EI, Faria MMP, Rabin HR, Storey DG. 2008. Pseudomonas aeruginosa cystic fibrosis isolates from individual patients demonstrate a range of levels of lethality in two Drosophila melanogaster infection models. Infection and Immunity 76:1877-1888.
386. Miyata S, Casey M, Frank DW, Ausubel FM, Drenkard E. 2003. Use of the Galleria mellonella caterpillar as a model host to study the role of the type III secretion system in Pseudomonas aeruginosa pathogenesis. Infection and immunity 71:2404-2413.
387. Shiner EK, Terentyev D, Bryan A, Sennoune S, Martinez-Zaguilan R, Li G, Gyorke S, Williams SC, Rumbaugh KP. 2006. Pseudomonas aeruginosa autoinducer

modulates host cell responses through calcium signalling. Cellular Microbiology 8:1601-1610.
388. Choi K-H, Schweizer HP. 2006. Mini-Tn7 insertion in bacteria with single attTn7 sites: example Pseudomonas aeruginosa. Nature Protocols 1:153-161.
389. Xu KD, Stewart PS, Xia F, Huang C-T, McFeters GA. 1998. Spatial physiological heterogeneity inPseudomonas aeruginosa biofilm is determined by oxygen availability. Applied and environmental microbiology 64:4035-4039.
390. Loh B, Grant C, Hancock REW. 1984. USE OF THE FLUORESCENT-PROBE 1-N-PHENYLNAPHTHYLAMINE TO STUDY THE INTERACTIONS OF AMINOGLYCOSIDE ANTIBIOTICS WITH THE OUTER-MEMBRANE OF PSEUDOMONAS-AERUGINOSA. Antimicrobial Agents and Chemotherapy 26:546-551.

APPENDICES

Appendix A: Recipes

Antibiotics:

Ampicillin stock solution (100 mg/ml)

1 g Ampicillin
10 ml Nano-pure water
Sterilize using 0.22 μm pore-size filter. Store in 1 ml aliquots at -20 °C.

Carbenicillin stock solution (300 mg/ml)

3 g Carbenicillin
10 ml Nano-pure water
Sterilize using 0.22 μm pore-size filter. Store in 1 ml aliquots at -80 °C.

Gentamycin stock solution (30 mg/ml)

300 mg Gentamycin
10 ml Nano-pure water
Sterilize using 0.22 μm pore-size filter. Store in 1 ml aliquots at -20 °C.

Gentamycin stock solution (100 mg/ml)

1 g Gentamycin
10 ml Nano-pure water
Sterilize using 0.22 μm pore-size filter. Store in 1 ml aliquots at -20 °C.

Tetracycline hydrochloride stock solution (20mg/ml)

200 mg Tetracycline
10 ml Nano-pure water
Sterilize using 0.22 μm pore-size filter. Store in 1 ml aliquots at -20 °C.

Note: Solubility limit of Tetracycline hydrochloride in water is 20 mg/ml.

Trimethoprim stock solution (50mg/ml)

500 mg Trimethoprim
10 ml of chloroform:ethanol = 1:1
Sterilize using 0.22 μm pore-size filter. Store in 1 ml aliquots at -20 °C, dark.

Note: Trimethoprim is hard to dissolve. Solubility can be enhanced by vortexing and
leaving at room temperature for 15 -30 min.

Kanamycin stock solution (50mg/ml)

500 mg Kanamycin
10 ml Nano-pure water
Sterilize using 0.22 µm pore-size filter. Store in 1 ml aliquots at -20 °C, dark.

Buffers:

Discharge buffer (5 ml)

12.5 mM $CaCl_2$
62.5 µl CaCl2 (1M)

2% NP40 (70%)
143 µl NP40 (70%)

Coelenterazine (50mM)

250 µg coelenterazine
1.136 ml ethanol (95%)

HEPES buffer (1000ml)

25 mM HEPES
5.96 g HEPES
125 mM NaCl
7.3 g NaCl
1mM MgCl2
0.0952 g MgCl2

Adjust pH to 7.2 with 1M NaOH
Add CCCP to a final concentration of 5µM and Glucose to a final concentration of 5 mM. (This is used for membrane permeability assay and CCP and glucose was added on the day of the experiment each time)

Potassium Phosphate buffer (20mM)

Solution 1:
620 mM K2HPO4
107.99 g K2HPO4
Q.S to 1 L
Solution 2:
620 mM KH2PO4
84.37g KH2PO4
Q.S to 1 L

Mix 615 ml of solution 1 and 385 ml of solution 2

The ratio ensures that the pH of the buffer is pH 7.0.

Phosphate-Buffered Saline (PBS)

130 mM NaCl
10 mM Na_2HPO_4
1.5 mM K_2HPO_4
30 mM KCl
pH – 7.4
Q.S to 1 L

50 X TAE (running buffer for agarose gel DNA electrophoresis)

242 g Trisma base
57.1 ml Glacial acetic acid
100 ml 0.5 M EDTA, pH – 8.0
Q.S. to 1 L
Dilute to 1X for running DNA-agarose gel.

Media:

1x Biofilm Minimal Media (BMM)

This bacterial growth medium is well defined and supports excellent growth of *P. aeruginosa.*

9mM Monosodium Glutamate
50mM Glycerol (w/v)
0.15 mM Sodium Phosphate Monobasic
0.34 mM Dipotassium phosphate
145 mM Sodium Chloride
pH: 7
Q.S. to 1 L and Autoclave

After cooling down add the following:
1 ml of Vitamin solution
200 µl of Trace Metal Solution
0.02 Mm (20 µl) of Magnesium sulfate solution

1X BMM agar medium (for antibiotic susceptibility assay)

9mM Monosodium Glutamate
50mM Glycerol (w/v)
0.15 mM Sodium Phosphate Monobasic

0.34 mM Dipotassium phosphate
145 mM Sodium Chloride
15 g of Becto agar
pH: 7

Q.S. to 1 L and Autoclave

After cooling down add the following:
1 ml of Vitamin solution
200 µl of Trace Metal Solution
0.02 Mm (20 µl) of Magnesium sulfate solution

~ 20 ml media poured onto the each 16 mm petridishes under UV hood and dried 15 minuite after the plates solidified

Luria-Bertani (LB) Broth

10 g Bacto-Tryptone
5 g Yeast Extract
5 g Sodium Chloride
Q.S. to 1 L. Autoclave.

LB Agar

10 g Bacto-Tryptone
5 g Yeast Extract
5 g Sodium Chloride
15 g Agar
Q.S. to 1 L. Autoclave.

LB Agar with 10% sucrose

10 g Bacto-Tryptone
5 g Yeast Extract
15 g Agar
Q.S. to 800 ml. Autoclave
Add 200 ml of filter sterilized 50 % sucrose stock solution.

Nematode growth medium

Nanopure water	975 ml
Nacl	3g
Agar	17g
Peptone	2.5g

Autoclave, cool afterward and add following:

1M $CaCl_2$	1ml
etOH solublized Cholestrol(5mg/ml)	1ml
1M MgSO4	1ml
1M KPO4 buffer	25ml

Pour the medium onto NGM plates (petridishes, 3 mM)

Brain Heart Infusion Broth (BHI)

37 g BHI (ready-made mix)
Q.S to 1 L. Autoclave.

Brain Heart Infusion agar (BHI agar)

37 g BHI (ready-made mix)
15 g of Becto agarose
Q.S to 1 L. Autoclave.

Cornmeal agar

28 g dried brewer's yeast
77 g cornmeal (Sigma)
27 g sucrose, 53 g glucose
3.5 mL propionic acid
0.3 mL 85 % phosphoric acid
6 g select agar (Invitrogen)

Q.S. to 1 L and bring to boil slowly on magnetic hot plate by continuous stirring.

Sucrose agar

1.2 g Bacto-agar (Difco)
14 mL 20% sucrose
41 mL sterile distilled water

Microwave and pour 6 ml into each fly vial.

<u>Stock Solutions:</u>

Biotin Stock Solution (BSS)

1 mg Biotin

Q.S. to 10 ml
Filter Sterilize

Vitamin Solution for BMM (100 ml)

50 mg Thiamine
1 ml BSS
Q.S. to 100 ml
Filter Sterilize

Trace Metal Solution for BMM (100 ml)

0.5g Copper (II) sulfate pentahydrate
0.5 g Zinc sulfate heptahydrate
0.5 g Ferrous sulfate heptahydrate
0.2 g Manganese chloride tetrahydrate
0.83 M Hydrochloric acid (10 ml)
Q.S to 100 ml
Filter sterilize

1 M Magnesium Sulfate Solution for BMM

24.65 g of Magnesium sulfate heptahydrate
Q.S. to 100 ml
Filter Sterilize

1 M Calcium chloride solution ($CaCl_2.2H_2O$)

11.098 g Calcium chloride
Q.S. to 100 ml

500 mM IPTG stock solution (isopropyl β-D-1- thiogalactpyranoside)

1.19 g IPTG
10 ml diH2O
Filter through 0.22 µm filter. Store at -20 °C in 1 ml aliquots.

50% Sucrose stock solution

100 g Sucrose
Q.S to 200 ml.
Sterilize using 0.22 µm pore-size filter. Store at 4 °C.

10% Glucose stock solution

10 g Glucose
Q.S to 100 ml.
Sterilize using 0.22 µm pore-size filter. Store at 4 °C.

50% DMSO stock solution

2.5 ml DMSO
2.5 ml Nanopure water
Sterilize using 0.22 µm pore-size filter. Store at 4 °C.

Saline solution (0.85 % NaCl)

8.5 g NaCl
Q.S to 1 L
Autoclave. Store at R.T

1N Sodium hydroxide (NaOH) solution

40 g NaOH
Q.S to 1 L

Ethylenediaminetetraacetic acid (EDTA) solution (0.5 M)

73. 06 g EDTA
Add 300 ml of water
Adjust pH to 8 with 1N NaOH
Q.S to 500 ml

300 mM Sucrose stock solution

51.34 g Sucrose
Q.S to 500 ml.
Sterilize using 0.22 µm pore-size filter. Store at 4 °C.

Recipe for an RNAlater-like buffer solution: For 1.5 liters:

935 ml of autoclaved, MilliQ water
700 g Ammonium sulfate
Stir until dissolved.

Add 25 ml of 1 M Sodium Citrate
And 40 ml of 0.5 M EDTA
Adjust to pH 5.2 using concentrated H_2SO_4 (about 20 drops= 1 ml) Store at RT

DEPC treated water (DNase and RNase free water)

Add 100 µl of Diethyle Pyrocarbonate (sigma) to 1L water.
Incubate at 37° C for overnight.
Autoclave for 1 Hr.

Other receipes:

Agarose gel for DNA electrophoresis

50 ml 1 X TAE
0.5 g agarose (electrophoresis grade)
Final concentration of agarose (1 % w/v)

VITA

Sharmily S Khanam

Candidate for the Degree of

Doctor of Philosophy

Thesis: CALCIUM REGULATED ANTIBIOTIC RESISTANCE IN *PSEUDOMONAS AERUGINOSA*.

Major Field: Microbiology and Molecular Genetics

Biographical:

Education:
Completed the requirements for the Doctor of Philosophy in Microbiology and Molecular Genetics at Oklahoma State University, Stillwater, Oklahoma in May, 2017.

Completed the requirements for the M.Sc. in Molecular Medical Microbiology, University of Nottingham, Nottingham, UK. Degree Conferred: 2009.

Completed the requirements for the M.S. in Zoology (Specialization: Parasitology), University of Dhaka, Dhaka, Bangladesh. Degree Conferred: 2008.

Completed the requirements for the B.Sc. in Zoology (Specialization: Parasitology), University of Dhaka, Dhaka, Bangladesh. Degree Conferred: 2007.

Experience and Selected Awards:
Two published peer-reviewed manuscripts (one first-author)
Ten awards for excellence in research, presentation, or academics.
Three presentations at national professional meetings.
Nineteen presentations at regional/local professional meetings.
Graduate Research Assistant at Oklahoma State University 2012-2015
Graduate Teaching Assistant at Oklahoma State University Fall 20011, Summer, 2017.

Professional Memberships:
American Society for Microbiology
American Society for Microbiology Missouri Valley Branch